Electro-weak Corrections to Top Decay; and the Upsilon Inclusive J/Psi Decay Width in Perturbative Q.C.D.

Blake A. Irwin

Physics Department

Mc Gill University, Montreal

November, 1991

A Thesis submitted to the Faculty of Graduate Studies and Research

in partial fulfillment of the requirements for the degree of

Doctor of Philosophy

To my parents, and C◇W◇N.

Abstract

The order $G_F m_t^2$ electro-weak corrections to the decay $t \to bW^+$ are calculated, arising essentially from virtual radiation of the Higgs boson. For large m_t these represent the dominant effect serving to shift the top lifetime from its tree level value. In practice, for $m_t < 240\,GeV$ these corrections are typically 0.1%. A comparison with recent calculations of the complete electro-weak and strong effects is made.

Several contributions to the branching ratio for the inclusive decay $\Upsilon \to J/\psi X$ are calculated using perturbative Q.C.D. to lowest order in the relative quark momentum and the strong coupling α_s. In addition to the direct transition, decay to J/ψ through the states ψ' and χ_1 is also considered. The following results are obtained: $Br(\Upsilon \to \psi' X) = (0.26 \pm 0.13) \times 10^{-3}$, $Br(\Upsilon \to \chi_1 X) \leq 0.17 \times 10^{-3}$, and $Br(\Upsilon \to J/\psi X) = (0.44 \pm 0.15) \times 10^{-3}$. The latter may just be consistent with the experimental result $(1.1 \pm 0.4 \pm 0.2) \times 10^{-3}$ where the first error is statistical and the second systematic.

Résumé

Les corrections électro-faibles à la désintégration $t \to bW^+$ sont calculées à l'ordre $G_F m_t^2$, résultant essentiellement de la radiation virtuelle d'un boson de Higgs. Pour des valeurs de m_t assez larges, celles-ci réprésentent l'effet dominant servant à déplacer la demi-vie du quark t de sa valeur au niveau arborescant. En practique, pour $m_t \leq 240\, GeV$ ces corrections sont de l'ordre de 0.1 %. Ceci est comparé avec des résultats récents qui considèrent les effets électro-faibles et forts.

Plusieures contributions au rapport de branchement pour la désintégration $\Upsilon \to J/\psi X$ sont calculées en utilisant la chromodynamique quantique perturbative au plus bas ordre dans la quantité de mouvement rélative du quark et dans la constante de couplage forte α_s. En plus de la transition directe, les désintégrations à travers des états ψ' et χ_1 sont aussi calculées. Les résultats suivants sont obtenus: $RB(\Upsilon \to \psi' X) = (0.26 \pm 0.13) \times 10^{-3}$, $RB(\Upsilon \to \chi_1 X) \leq 0.17 \times 10^{-3}$, et $RB(\Upsilon \to J/\psi X) = (0.44 \pm 0.15) \times 10^{-3}$. Ce dernier pourrait être consistant avec la valeur expérimentale de $(1.1 \pm 0.4 \pm 0.2) \times 10^{-3}$ où la première erreur est statistique et la deuxième systématique.

Acknowledgements

Most of what I learned in graduate school came from other people. I would like to acknowledge that each of the following persons has shown me a new type of problem or a new type of solution: Dr. B. Margolis, Howard Trottier, David Atwood, Cliff Burgess, Gerry Robinson, Harry Lam, Doug Stairs, Cherif Hamzoui, Francois Begin, Eric Therrien, Pierre St. Hilaire, Ralf Brunning, Russ Letkemen, Kavita Murty, Ken McLean, Noureddine Hambli, Juan Gallego, Pierre Valin, Jean-Francios Malouin, Ivan Macsyniuk, Alan Carre, Pat Saull, Sandy Bultena, Rejean Girard, Paul Sitarski, Scott Hagan, Hubert Deguise, Charles Hooge, Laurel Sinclair, Roberto Mendel, Arlen Anderson, James Anglin, David Gilkinson, Catrina Charlesworth, Bao Nguyen, Martin Phipps, Sean Punch, Hachemi Benaoum, Eric Hyatt, Noureddine Mebarki, Alain Legault, Raymond Nadeau, George Tsipolitis, .

I would like to thank David Gilkinson for suggesting that I perform an error analysis, and Juan for a generous supply of cigarettes without which this thesis could not have been written. I also thank Noureddine for assisting me in preparing the figures, Lynda for help with the labels, Juan again for tasks to numerous too mention, and Paul for keeping the system going and my files intact despite a suspiciously large number of power failures.

Mostly I would like to say that I found McGill a wonderful environment in which to study and learn and do physics.

Statement of Originality

This thesis is divided into two parts. In the first part I have included a review of the evidence for the existence of the top quark. With the exception of a discussion on the extraction of the b quark total weak iso-spin from an analysis of the charged current coupling matrix, the material of this section has been obtained from the existing literature. The remnant of the first part is concerned with certain electro weak corrections to the top decay width. This is original research and has been published in Physics Letters **256B** 533 (1991). The idea to study this problem was my own, and the calculation was initially performed by myself. My collaborator Howard Trottier and my advisor Dr. B. Margolis then found several errors in my calculation, and through many discussions we arrived at the best choice of renormalization scheme for this particular problem.

The second part of the thesis, the analysis of the inclusive J/ψ width of the Υ in perturbative Q.C.D., also constitutes original research. I am in the process of preparing it for publication, resolving some of the questions that are mentioned inside. The decision to study this particular problem was mine, though it was known to both Howard Trottier and Dr. Margolis that this would be an interesting though potentially tedious problem. All of the calculations presented in this section were performed by myself. The method of computing loop integrals that have singularities related to absorptive cuts was originally developed by H. Trottier and B. Margolis. My contributions to this method are a criterion for choosing the routing of the loop momenta such that the number of such singularities is minimized, and a method for determining the minimum number of Feynman diagrams that must be added to obtain an infra-red finite result. It was at Dr. Margolis' suggestion that I undertook the study of the indirect production of J/ψ's.

Contents

Chapter 1

Preface

This thesis describes the results of two essentially unrelated studies in standard model phenomenology.

In the first part, the order $G_F m_t^2$ corrections to the top lifetime are calculated, which are essentially due to the virtual radiation of the Higgs boson. To motivate the reader as to the usefulness of this exercise, I have included in the first chapter a mini-review on why we believe the top exists, what bounds we can put on its mass in the standard model, and what can be said about the Higgs in the standard model. During the discussion I also comment on the origin of $G_F m_t^2$ effects in general, and the seeming violation of the decoupling theorem. The new research is contained in the second chapter of part 1, and is essentially self contained.

In the second part, the inclusive J/ψ width of the Υ is calculated using perturbative Q C D. Our ignorance of the meson wave functions is circumvented by working to lowest order in the relative quark momenta. Integral to this approach is the assumption that the Υ and J/ψ are non relativistic systems. This postulate has been extensively discussed in the literature. Further, this calculation scheme originates historically in the study of positronium like systems, which may be found in many standard textbooks. For these reasons, and the fact that as it stands the presentation of the calculation is already somewhat long, only a very brief discussion of the historical context of the study is presented in the second part.

Part I

Top Decay

Chapter 2

Introduction

2.1 The Standard Model

The standard model[1, 2] of high energy physics is a Yang-Mills[3] theory based on the group $SU(3)_c \times SU(2) \times U(1)_Y$. The fermions fall into three families, each containing 15 hyper-charged fields, which transform in the following representations of $SU(3)_c \times SU(2)$: a (3,2) and a (1,2) of left-handed fields, and two (3,1)'s and a (1,1) of right-handed fields. The $SU(3)$ triplets are called quarks, the singlets leptons.

It also contains exactly one $SU(2)$ doublet of color singlet, hyper-charged scalars (which makes four real fields). These are assumed to possess (renormalizable) non-linear self-interactions such that the ground state of the theory prefers a non-zero vacuum expectation value (v.e.v.) for the scalar field. This simultaneously serves two purposes:

1. Three of four gauge bosons of the electro-weak sector acquire mass via the Higgs[4] mechanism.

2. Mass terms for the fermions may be generated. The left- and right-handed parts of the fermion fields transform differently under SU(2), preventing any Dirac mass terms for them. Since they are (hyper-)charged, Majorana mass terms are also excluded. But a coupling between a left handed and a right handed field and a scalar doublet is fully lorentz and gauge invariant, and becomes a Dirac mass term it the scalar acquires a v.e.v.

As a result of the scalar sector performing these two functions, the spectrum of physical states of the standard model ends up containing exactly one, neutral, spin-0 field which couples to every particle in the model (fermion, gauge boson, even the Higgs itself) in proportion to the particle's mass.

The standard model has been tested extensively and seems to be able to account for a wide variety of phenomena via the tuning of its 15 or so free parameters (particle masses, mixing angles, coupling constants, etc.). However, two of the fermions in the model, the top quark and neutrino of the third generation have yet to be observed directly, though there is much indirect evidence for both. Further, there is essentially no evidence, direct or indirect for the existence of the single scalar boson discussed above

(The best indirect evidence for the third generation neutrino consists of the LEP Z-width measurement.)

2.2 Theoretical "Evidence" for the Top

We wish to generate the standard model by gauging a global $SU(3)_c \times SU(2) \times U(1)_Y$ symmetry. However, it turns out the global $U(1)_Y$ symmetry is broken by quantum mechanical corrections. A gauge theory based on a broken symmetry is mathematically inconsistent, it is non-renormalizable and possibly meaningless Thus this global symmetry must somehow be maintained if we are to believe the standard model [6].

The simplest way to see that the $U(1)_Y$ symmetry is broken is to note that its associated noether current is not conserved. Pictorially, the lowest order feynman diagram causing the effect is given in figure 2 1 (higher order diagrams do not change the situation [5]) where each wavy line represents the current associated with a symmetry. The contribution of this diagram to the divergence of the $U(1)_Y$ noether current is given by:

$$\partial_\mu J^\mu_Y \;\propto\; tr\{Y\{T_1, T_2\}\} \;\equiv\; A(Y12)$$

where "Y" is the $U(1)_Y$ hypercharge coupling matrix, and T_1, T_2 are the coupling matrices of the other currents There are four possibilities for the two other currents that result in problems:

- {current 1, current 2} = {SU(3) current, SU(3) current}
- {current 1, current 2} = {SU(2) current, SU(2) current}
- {current 1, current 2} = {U(1) current, U(1) current}
- {current 1, current 2} = {lorentz current, lorentz current}

If we allow each of the fermions from one generation to circulate through the loop, the anomalous divergences in the hypercharge current are proportional to:

$$\begin{aligned}
A(Y33) &= 2Y_Q + Y_{u^c} + Y_{d^c} \\
A(Y22) &= 3Y_Q + Y_L \\
A(Y11) &= 6Y_Q^3 + 3Y_{u^c}^3 + 3Y_{d^c}^3 + 2Y_L^3 + Y_{e^c}^3 \\
A(YLL) &= 6Y_Q + 3Y_{u^c} + 3Y_{d^c} + 2Y_L + Y_{e^c}
\end{aligned} \tag{2.1}$$

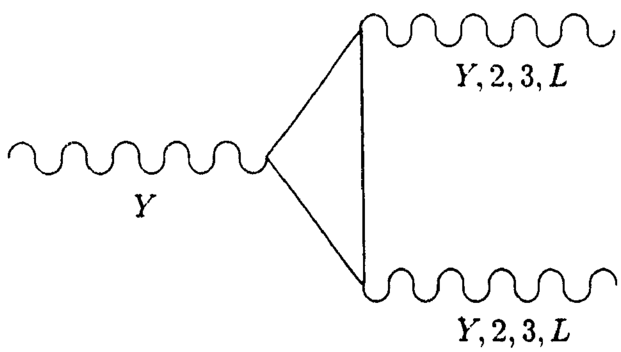

Figure 2.1: Diagram leading to anomalous non-conservation of hypercharge

where {Q,u,d,L,e} represent the {quark doublet, up quark singlet, down quark singlet, lepton doublet, lepton singlet} respectively.

Amazingly, the standard model assignments for the quarks and leptons in each generation lead to all four of these equations fortuitously vanishing. If any one fermion in a generation is removed, one or more of the above equations becomes non-zero, and the standard model becomes inconsistent; thus the theoretical argument for top quark existence. Note that this relies on our belief that the τ, b quark, and presumably ν_τ each fall into exactly their expected positions in the third generation.

I do not find this argument very compelling, because it relies on a number of assumptions which themselves imply the existence of something very much like a top quark. For example, suppose the third generation contains all the usual fermions, but has in addition a coloured field whose left- and right-handed parts are SU(2) singlets, and whose hypercharge (= electric charge) = -1/3. Then the contribution of the "normal" fermions to the anomaly coefficients above still vanishes, and the extra effect of the new "D" quark field is:

$$
\begin{aligned}
\Delta A(Y33) &= Y_D + Y_{D^c} = 0 \\
\Delta A(Y22) &= 0 \\
\Delta A(Y11) &= Y_D^3 + Y_{D^c}^3 = 0 \\
\Delta A(YLL) &= Y_D + Y_{D^c} = 0
\end{aligned}
\tag{2.2}
$$

Thus this is also a consistent model from the anomaly standpoint. Now suppose that the b-quark we have *observed* is this extra SU(2) singlet field, and the other quark fields in the third generation are very heavy and have not yet been seen. The "top" quark that resides in the third generation could now have mass in excess of a TeV or more; in fact, we might never see it.

This model is ruled out by phenomenological studies of the b, which demonstrate that the b-quark is almost surely *not* a weak iso-singlet. Once we have made this assumption, however, the anomaly argument is completely superfluous: if the b-quark transforms non-trivially under SU(2), it *must* have a charge $+2/3$ partner, which is just the top quark. Thus, as claimed, one of the underlying assumptions of the anomaly discussion is on its own sufficient to imply top existence. These more basic arguments are the subject of the next section.

2.3 Evidence for the Top from b Quark Analysis

Herein I will review a *somewhat* model independent argument that the top quark exists[7] So for the rest of this section, by the "standard model" I will mean the theory described in the section 2.1 with the exception of the assertion that the third family is a copy of the first two. We will try to deduce precisely how the b extends the two generation standard model. We will conclude that the only way to add b onto the existing model is to include a charge $+2/3$ partner with it.

As we go along, I will try to identify any model dependence which does arise. Of course some assumptions have to be made somewhere along the way, and here I list the more important ansatzes upon which our conclusions will rest:

1. The W^- is a gauge boson introduced to localize a global SU(2) symmetry of the model, with a similar claim concerning a part of the Z^0
2. The global SU(2) symmetry is not *explicitly* broken i.e. the complete lagrangian of all matter is an SU(2) scalar
3. The light quarks (d,u,s,c) lie in their standard model SU(2) multiplet positions as described in section 2.1

Assumptions #1,3 essentially summarize a vast body of experimental data. The remaining one, #2, is very much the weak link and its justification requires subtler arguments. We return to this point later.

On the basis of assumptions # 1-3, the argument for the top quark existence goes like:

- Experimentally, it is inferred that the b quark couples to the W^- or the SU(2) part of the Z^0.
- By # 1 above, the b must therefore have non-trivial values of the SU(2) "weak isospin" quantum numbers i.e. of T^2 and T_3.
- So by # 2, the b must actually be part of a not-trivial SU(2) multiplet.

- But we have assumed in # 3 that the other known quarks are already all paired up with each other in the weak iso-doublets and singlets of the two generation standard model (Alternately, if the b was paired with a lighter quark, its decay rate would be 400 times that observed [8])

- Therefore the b-quark must have one or more so far unobserved partners, which is essentially the statement that a top quark must exist

- From that point, a more detailed analysis of phenomena yields the specific weak iso-spin values T_L, T_{3L}, T_R, T_{3R} of b_L and b_R

Let us discuss assumption # 2 for a moment. Its analogue in the effective theory [9] of the light mesons based on chiral $SU(3) \times SU(3)$ global symmetry would forbid the inclusion of a term transforming like the generator "T_8", an integral part of the model necessary to give masses to the the pseudoscalar mesons and generate the Gell-Mann Okubo relation The difference here is that our $SU(2)$ symmetry is *gauged*, so that assumption 2 is seemingly absolutely necessary from the standpoint of mathematical consistency: a gauge theory based on an explicitly broken symmetry is not renormalizable.

However, suppose we discard the requirement that the standard model be renormalizable. Specifically, it could merely be an effective theory obtained by integrating out the heavy degrees of freedom of some other, finite, theory. The existence of a sector in this effective theory violating assumption 2, like an iso-doublet b quark without its t quark partner, would result in large corrections to any observable in the standard model which is finite only because of delicate cancelations between several amplitudes related by global or local SU(2) invariance. There would exist an upper cut-off for which the model would be phenomenologically invalid, indicating that new physics would have to be included. Whether this physics is the top quark or not is another question The point is that in principle model independent bounds could be placed on the existence of explicit $SU(2)$ breaking.

I am not familiar with any such generic study However, an analysis of the standard model in the limit $m_t \to \infty$ should give us an idea of what kind of bounds are to be expected. This will been reviewed in section 2.4.

2.3.1 Determining That b Interacts with W

The argument that the b_L or b_R ($\equiv b$) must couple to the W^- proceeds by contradiction First note that quarks can only decay by coupling to a lighter species of quark; i e only if there exist flavour non-diagonal couplings between the quarks. In the first two generations of the standard model, the only flavour non-diagonal couplings at tree level occur in the charged current sector, in the couplings of the quarks to the W bosons. This is required to accomodate stringent limits on flavour changing neutral currents So now suppose that the (weak-eigenstate) b quark is an SU(2) singlet. Since there are no other charge

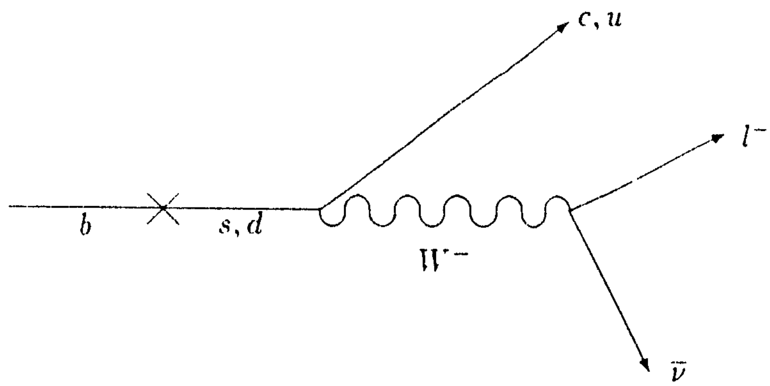

Figure 2.2: Charged current decay of a weak iso-singlet b

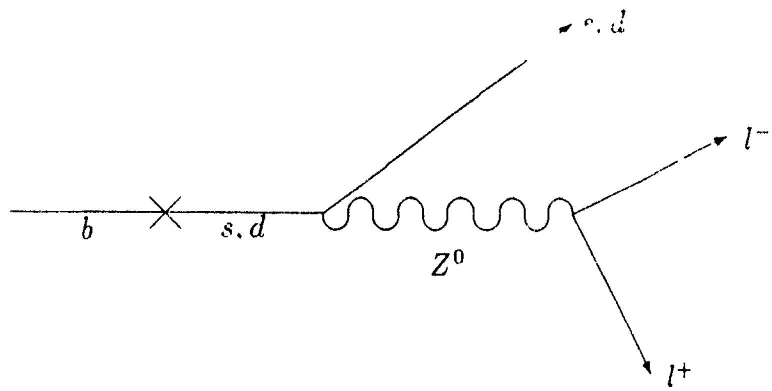

Figure 2.3: Neutral current decay of a weak iso-singlet b

-1 bosons in the model, the b quark cannot couple to the charge $+2/3$ quarks u and c. This does not mean it cannot decay however, since the mass eigenstate b', which is what we observe in our experiments, will in general be some mixture of the charge $-1/3$ weak eigenstates d,s,b. Thus the mass eigenstate b' will effectively have couplings to the W^- via its s or d component. This leads to the diagram of figure 2.2 for the observed decay of $b' \rightarrow cl^-\bar{\nu}$. The prediction for this rate depends on the magnitude of the unknown b-s, b-d mixings. Now the problem is that it is also possible for the b' to decay as in figure 2.3, $b' \rightarrow sl^-l^+$. In the ratio of these rates the dependence of the unknown mixing angles either disappears or may be constrained. (The ratio is not simply "1" because of complications arising from the fact that the parameters of the mixing must be fine tuned to eliminate FCNC's in the light quark sector.) Different authors[10] estimate:

$$\frac{\Gamma(b \to l^- l^+ X)}{\Gamma(b \to l^- \overline{\nu} X)} \geq 1\%$$

Experimentally[11], the branching ratio for this mode is less than .1%. This establishes that b is not an SU(2) singlet

A few points should be made. One is that this discussion exactly parallels the analysis[12] of $Br(\tau^- \to \mu^- X)$ used to exclude a singlet assignment for the τ^- lepton. Another is that we should not be surprised to see that the final contradiction involved properties of flavour changing neutral currents. Such problems always arise when quarks of *like* charge obtain their masses via two or more different mechanisms[13]. In the above case, the first two generations of quarks are chiral and can only get their masses from S S B involving an SU(2) doublet of scalars while the singlet b quark admits only "direct" gauge invariant Dirac mass terms or spontaneously generated masses from SU(2) singlet scalars. Figures 1 and 2 are essentially graphical illustrations of the theorem of [13]

Further, if extra charge -1 bosons exist then $\Gamma(b \to c l^- \overline{\nu})$ can occur via the analogue of the usual SM W^- exchange decay, with no implications on the existence of FCNC's. This is one feature of the canonical "topless" model[14] based on the group E_6, wherein b *is* a singlet under the SM SU(2), and there is an extra W^- is associated with a new gauge symmetry $SU(2)_2$ under which b_R transforms as a doublet. This model has many problems in explaining a host of other phenomena, especially the precision LEP data as discussed in [15], wherein it is pronounced ruled out.

2.3.2 Determining the b's Weak Iso-spin: General

Having argued that the either b_L or b_R must be part of a non trivial SU(2) representation, we now turn to trying to determine exactly *which* representation. Put another way, now that we believe that there must be other quarks in the universe other than the five we have observed, we want to find out exactly how many such fields the existence of the weakly interacting b quark implies. This information is contained in the coupling matrices of the W gauge bosons to the b quarks. Essentially, since SU(2) is a simple non-abelian group the generators obey the following non-linear relation:

$$[T_i, T_j] = i c_{ijk} T_k \tag{2.3}$$

where the c_{ijk} are anti-symmetric and not *all* zero for any fixed value of "i", say. This non-linearity means that the relative size of the coupling of a given gauge boson to fermions within the same multiplet, *and* the relative size of the coupling of the *different* gauge bosons to the same multiplet, are fixed and determinable solely by group theoretic means. The non-linearity of 2.3 fixes the relative normalization of the interaction strengths and removes much of the arbitrariness from the model.

So, suppose b_L, b_R belong to T_L, T_R SU(2) representations, and consider the gauge part of the kinetic energy term for the left-handed multiplet ($\equiv f$).

$$\begin{aligned} L_{int} &\equiv \bar{f}[g\vec{\not{W}}\cdot\vec{T} + g'\not{B}Y]P_L f \\ &= \frac{g}{\sqrt{2}}\bar{f}[\not{W}^+T_+ + \not{W}^-T_-]P_L f + \bar{f}[g\not{W}^3T_3 + g'\not{B}Y]P_L f \\ &\equiv L_L^{CC} + L_L^{NC} \end{aligned} \tag{2.4}$$

where:

$$\begin{aligned} \not{B} &\equiv B_\mu\gamma^\mu \\ W^\pm &\equiv (W^1 \mp iW^2)/\sqrt{2} \\ T_\pm &\equiv (T_1 \pm iT_2) \end{aligned} \tag{2.5}$$

Recall [16]:

$$\begin{aligned} T_\pm f^{T,T_3} &\equiv C_\pm(T,T_3)f^{T,T_3\pm 1} \\ C_\pm(T,T_3) &= \sqrt{T(T+1) - T_3(T_3 \pm 1)} \end{aligned} \tag{2.6}$$

Thus:

$$\begin{aligned} L_L^{CC} &= \frac{g}{\sqrt{2}}\sum_{m=-T_L}^{T_L}\bar{f}_{m+1}[C_+(T_L,m)\not{W}^+ + C_-(T_L,m)\not{W}^-]P_L f_m \\ L_L^{NC} &= \sum_{m=-T_L}^{T_L}\bar{f}_m[gm\not{W}^3 + g'Y_L\not{B}]P_L f_m \end{aligned} \tag{2.7}$$

The multiplet f contains the fields $(\cdots, U, t, b, D, \ldots)$, where U,D, etc. are exotically charged quarks. Picking out only the non-exotic terms containing the b quark from equation 2.7 yields:

$$\begin{aligned} L_{tb,L}^{CC} &= \frac{g}{\sqrt{2}}C_+(T_L,T_{3L}^b)\bar{t}\not{W}^+P_L b + h.c. \\ L_L^{NC} &= \bar{b}[gT_{3L}^b\not{W}^3 + g'Y_L\not{B}]P_L b \end{aligned} \tag{2.8}$$

We see that L^{NC} is sensitive to the T_{3L} and T_{3R} values of the b quark, while L_{tb}^{CC} "knows" about T_L and T_R also. However, the extraction of these quantities is complicated by the fact that all like charged fields in the theory can mix after the S.S.B. We first analyze L^{NC}

2.3.3 T_3 Values of the b: Neutral Current Analysis

We must assume the gauge group of the non-color sector is just $SU(2) \times U(1)$ in order to extract T_{3L}, T_{3R} without ambiguity from experimental data. Under this assumption, the spin-one mass eigenstates Z^0 and A can only be combinations of W_3 and B:

$$\begin{aligned} W_3 &\equiv \cos\theta_w Z^0 + \sin\theta_w A \\ B &\equiv -\sin\theta_w Z^0 + \cos\theta_w A \end{aligned} \qquad (2.9)$$

so that L_L^{NC} becomes ($s_w \equiv \sin\theta_w$, etc. :

$$L_L^{NC} = \bar{b}\,[g c_w T_{3L}^b - g' s_w Y_L]\not{Z}^0 P_L b \;+\; \bar{b}\,[g s_w T_{3L}^b + g' c_w Y_L]\not{A} P_L b$$

There is exactly one known massless color singlet neutral spin-one boson, namely the photon. Supposing without loss of generality that this is the "A" field in 2.9, we must therefore identify the A coupling matrix with eQ:

$$eQ \equiv g s_w T_{3L} + g' c_w Y_L$$

This relation may be solved by considering the $(\nu_e, e^-)_L$ doublet. The representation of Q on these fields is $diag(0,-1)$. Since $[T_k, Y] = 0$, we have that Y is proportional to the unit matrix on any irreducible representation of the T_k. Thus: (the Δ operation subtracts neighbouring diagonal matrix elements)

$$\begin{aligned} e\Delta Q &= g\sin\theta_W \Delta T_3 \quad \Longrightarrow \quad e = g\sin\theta_W \\ \Rightarrow Q &= T_{3L} + \frac{c_w}{e} g' Y_L \end{aligned} \qquad (2.10)$$

The relative normalization of g' and Y is completely free since the $U(1)$ group is abelian[17]. A common convention is to set $g' c_w = e$. Then:

$$Q = T_{3L} + Y_L \;=\; T_{3R} + Y_R$$

This leads to the expression for the whole (i.e. left plus right) neutral current:

$$\begin{aligned} L^{NC} &= \frac{g}{c_w}\,\bar{b}\not{Z}^0 (Q_L^b P_L + Q_R^b P_R) b \;+\; e\,\bar{b} Q^b \not{A} b \\ Q_{L,R} &\equiv T_{3L,R} - s_w^2 Q \end{aligned} \qquad (2.11)$$

The parameters e, θ_w are known from a studies of the two generation model. Q^b has been deduced [18] from the magnitude of "R" in $e^+e^- \rightarrow$ *hadrons* above threshold for "b" production where the photon exchange is dominant The quantities T_{3L}^b and T_{3R}^b may be extracted from two appropriately chosen Z^0 experiments. One is just the Z^0 partial b width [19]:

$$\Gamma(Z^0 \rightarrow b\bar{b}) = 664\,Mev \times [(Q_L^b)^2 + (Q_R^b)^2] = (360 \pm 50)\,Mev \qquad (2.12)$$

where the last number is the experimental result.

The other experiment must involve a search for parity violation. This is because all parity even observables in the theory will be functions of $(Q_L^2 +$

Q_R^2), whose value we already know from 2.12. We choose $A_{FB}(e^+e^- \to b\bar{b})$ as measured at the Z^0 peak. This is the difference between the number of b quarks coming out in a forward direction (with respect to the e^+e^- beam) from the number coming out in a backward direction, divided by the sum of the same; a "forward direction" pierces the hemisphere about the e^- beam. A simple argument yields the formula for this quantity in the centre of momentum frame on the Z^0 pole where the contribution of the photon can be neglected for our purposes.

Setting all fermion masses to zero, the initial e^+e^- can only annihilate into a Z^0 if they are in a $|1, \pm 1>$ total angular momentum state with respect to the e^+e^- axis. This follows from the chirality conservation of the standard Z^0 interactions[20], and from the fact that the Z^0 is spin one. The +/- sign corresponds to right/left handed electrons. Similarly, the final $b\bar{b}$ is in a $|1, \pm 1>$ total angular momentum state with respect to the b-$\bar{b}$ axis. The amplitude must be proportional to the Z^0 -charges of the left- or right-handed fields that annihilate or are produced, and the spin one representation of the rotation matrices:

$$D^1_{1,\pm1}(\theta) = (1 \pm \cos\theta)/2$$

$$D^1_{\pm1,1}(\theta) = (1 \pm \cos\theta)/2$$

where θ is the angle between the e^- and b axes. Thus [21]

$$\begin{aligned}
\frac{d\sigma}{d\cos\theta} &\propto [(Q_{Le}Q_{Lb})^2 + (Q_{Re}Q_{Rb})^2](1+\cos\theta)^2 \\
&\quad + [(Q_{Le}Q_{Rb})^2 + (Q_{Re}Q_{Lb})^2](1-\cos\theta)^2 \\
A_{FB} &\equiv \left[\int_0^1 \frac{d\sigma}{d\cos\theta}d(\cos\theta) - \int_{-1}^0 \frac{d\sigma}{d\cos\theta}d(\cos\theta)\right] / \int_{-1}^1 d\sigma \\
&= \frac{3}{4}\frac{(Q_{Le}Q_{Lb})^2 + (Q_{Re}Q_{Rb})^2 - (Q_{Le}Q_{Rb})^2 - (Q_{Re}Q_{Lb})^2}{(Q_{Le}Q_{Lb})^2 + (Q_{Re}Q_{Rb})^2 + (Q_{Le}Q_{Rb})^2 + (Q_{Re}Q_{Lb})^2} \\
&= \frac{3}{4}\frac{Q_{Le}^2 - Q_{Re}^2}{Q_{Le}^2 + Q_{Re}^2}\frac{Q_{Lb}^2 - Q_{Rb}^2}{Q_{Lb}^2 + Q_{Rb}^2} \\
&= (-13.3 \pm 9.9)\% \qquad (2.13)
\end{aligned}$$

The number in the final line is the observed value [22]. Combining equations 2.11, 2.12, and 2.13:

$$\begin{aligned}
Q_{Lb}^2 + Q_{Rb}^2 &= 0.53 \pm 0.08 \\
Q_{Lb}^2 - Q_{Rb}^2 &= 0.65 \pm 0.57 \\
|T_{3L}| &= 0.69 \pm 0.16 \\
|T_{3R}| &= 0.17 \pm 0.16
\end{aligned}$$

These results are consistent with the values $|T_{3L}| = 1/2$ and $T_{3R} = 0$. Unfortunately the sign of T_{3L} may not be determined from this experiment, because

$$A_{FB} \quad \propto \quad (Q_{Lb} - Q_{Rb})(Q_{Lb} + Q_{Rb})$$

$$= \quad (T_{3L} - T_{3R})(T_{3L} + T_{3R} + 2s_w^2/3)$$
$$\stackrel{T_{3R}=0}{=} \quad T_{3L}(T_{3L} + 2s_w^2/3) > 0 \quad for\ T_{3L} = \pm 1/2$$

since $2s_w^2/3 \approx 1/6$. Thus the sign of A_{FB} on the Z^0 peak is not sensitive to the sign of T_{3L}.

At lower energies where the interference of the Z^0 and photon exchange graphs is more significant, A_{FB} does depend on the sign of T_{3L}. The formulae are more complicated, and the analysis has been performed by several groups [23] with the typical result $2T_{3L} = -(1.15 \pm .41)$ (deduced by setting $T_{3R} \equiv 0$). In conclusion:

$$T_{3L}^b = -\frac{1}{2} \qquad T_{3R}^b = 0 \tag{2.14}$$

2.3.4 T Values of the b: Charged Current Analysis

We now return to the charged current portion of the electro-weak b-quark interactions. Recall equation 2.8.

$$L_{tb,L}^{CC} = \frac{g}{\sqrt{2}} C_+(T_L, T_{3L}^b)\, \bar{t}\, \not{W}^+ P_L\, b \quad + \ h.c$$

In light of the conclusions 2.14, let us make the simplifying assumption that $T_R = 0$, so that that $L_{tb,R}^{CC} \equiv 0$, but leave T_L general:

$$\begin{aligned} C_+(T_L, T_{3L}^b) &= \sqrt{T_L(T_L+1) + 1/4} = T_L + \frac{1}{2} \\ L_{tb}^{CC} &= \frac{g}{\sqrt{2}}(T_L + 1/2)\, \bar{t}\, \not{W}^+ P_L b \quad + \ h.c. \end{aligned} \tag{2.15}$$

Naively, if we could observe the t-b transition we could deduce immediately into what representation of SU(2) the b quark falls, and thus what extra fields the existence of the b necessarily implies. For example, for $T = 1/2$ corresponding to the standard model scenario, the W^+ would couple to the b with the same strength we have seen it couple to the e^-, while for $T = 3/2, 5/2$ ... it couples with 2, 3, ... times that strength, making the transition rate 4, 9, ... larger.

Unfortunately, such a simple analysis is not possible due to the existence of mixing between like charge quarks. This complicates the discussion just as the mixing between the like charge gauge bosons W^3 and B complicated the analysis of the neutral current data. Since SU(2) is spontaneously broken and its generators do not commute with the hamiltonian appropriate to our vacuum, the quark mass eigenstates will in general be linear combinations of the weak eigenstates. Specifically, though the T_L value of the b is currently arbitrary while the d and s certainly are in $T = 1/2$ multiplets, all have charge $-1/3$ and can mix. Similarly the charge of the t quark is $-1/3 + 1 = 2/3$ and can combine with the u and c. Letting q, q', denote the quark weak, mass, eigenstates, we allow for generic mixing:

$$
\begin{aligned}
b'_i \equiv (d',s',b')_i &\equiv U^{D}_{ij}(d,s,b)_j \\
t'_i \equiv (u',c',t')_i &\equiv U^{U}_{ij}(u,c,t)_j
\end{aligned}
$$

$$
\begin{aligned}
L^{CC}_{tot} &= \frac{g}{\sqrt{2}}(\bar{u},\bar{c},\bar{t})\begin{pmatrix} 1 & & \\ & 1 & \\ & & C_+ \end{pmatrix} \not{W}^{+} P_L \begin{pmatrix} d \\ s \\ b \end{pmatrix} \quad + h.c. \\
&= \frac{g}{\sqrt{2}}(\bar{u}',\bar{c}',\bar{t}')(U^{U})^{\dagger}\begin{pmatrix} 1 & & \\ & 1 & \\ & & C_+ \end{pmatrix} \not{W}^{+} P_L\, U^{D} \begin{pmatrix} d' \\ s' \\ b' \end{pmatrix} \quad + h.c. \\
&\equiv \frac{g}{\sqrt{2}} V^{eff}_{ij} \cdot \bar{t}'_i \not{W}^{+} P_L b'_j \quad + h.c. \qquad (2.16)
\end{aligned}
$$

Evidently the T, T_3 information becomes absorbed in the effective charged current coupling matrix

$$
\begin{aligned}
V^{eff}_{ij} &\equiv \sum_k U^{U*}_{ki} U^{D}_{kj}(1 + a\delta_{k3}) \qquad (2.17) \\
a &= T_L - \frac{1}{2}
\end{aligned}
$$

One outstanding feature of 2.18 is that the coupling matrix is not unitary except for the case $T = 1/2$ corresponding to the standard model scenario of the C.K.M. [24] mechanism. It is not immediately obvious what the best phenomenological implications of this are. However, this effect is in principle distinguishable from those produced by the existence of a fourth generation. For suppose that at some point in the future all *nine* coupling matrix elements have been independently determined, including their phases i.e. with no assumption of unitarity. Then consider the following observable in the three scenarios, KM, 4^{th} generation, and the general three generation case above:

$$
\begin{aligned}
\sum_{ij} \left|V^{km}_{ij}\right|^2 &= 3 \\
\sum_{ij} \left|V^{4g}_{ij}\right|^2 &< 3 \\
\sum_{ij} \left|V^{eff}_{ij}\right|^2 &= 3 + 2a + a^2 \geq 6 > 3 \qquad (2.18)
\end{aligned}
$$

Admittedly, this is a very poor observable from the point of view of it ever being measured, or measured accurately. A search for subtler implications of the type of non-unitarity displayed above is currently being undertaken.

2.4 Constraints on m_t in the Standard Model

2.4.1 Lower Bound on m_t

Within the context of the standard model the production rate of the top quark at hadron colliders can be accurately predicted [25]. For example, the cross section at FNAL for the process $gg \to t\bar{t}$ is about 0.1 n-barn for $m_t = 100$ GeV. Further, the standard model allows essentially only one decay mechanism for the top:

- $t \to be^+\nu$ for $m_t < m_W + m_b$
- $t \to bW^+$ for $m_t > m_W + m_b$

These two facts allow the absence of a top signal at FNAL to be translated [26] into a 90% confidence level lower bound on m_t:

$$m_t > 89\,GeV \tag{2.19}$$

If the standard model is extended to include certain types of new physics, the bound drops. The idea is that the top could really be lighter than 89 GeV and is in fact being "copiously" produced at FNAL, but is simply escaping detection there. This could happen if the top decays predominantly through an exotic mode that the experiments do not search for or are not sensitive to. Two examples [7] are:

- $t \to bH^+$ in models with extra scalars. [27]
- $t \to \tilde{t}\tilde{\gamma}$ in supersymmetric extensions.

Since these are two body decays, they would dominate the three body mode $t \to be^+\nu$ appropriate for $m_t < m_W + m_b$.

A slightly less model dependent bound on m_t comes from a measurement of the W^+ width. For a top quark with mass sufficiently below m_W so that phase space suppression can be ignored, the top quark makes a 25% contribution to Γ_W. This is of course independent of whether the top is decaying through the "invisible" modes described above or not. The idea here is similar to that of counting the number of neutrinos by measuring the Z^0 width. An analysis [28] of data coming from CDF at FNAL yields the 90% confidence limit of:

$$m_t > 41\,GeV \tag{2.20}$$

2.4.2 Upper Bound on m_t

The are several phenomena involving only light particles whose standard model predictions are very sensitive to m_t. This sensitivity arises from the fact that radiative corrections introduce into the standard model formulae pieces that are proportional to:

$$G_F m_t^2 \;\propto\; g^2 \frac{m_t^2}{m_W^2} \;\propto\; \left(\frac{m_t}{v}\right)^2 \;\propto\; g_t^2 \;\propto\; \alpha_t \tag{2.21}$$

where g_t is the Yukawa coupling of the scalar doublet to the third family fermions:

$$g_t \bar{t}_R \tilde{\phi}^\dagger \begin{pmatrix} t \\ b \end{pmatrix} + h.c. \quad \equiv \quad g_t \bar{t}_R \begin{pmatrix} \frac{1}{\sqrt{2}}(v + H + i\phi^0) \\ -\phi^+ \end{pmatrix} \begin{pmatrix} t \\ b \end{pmatrix} + h.c. \tag{2.22}$$

Note that as $\alpha_t \equiv g_t^2/4\pi$ becomes as large as 1, these radiative corrections can rival the tree terms. This is a signal that the perturbative technique used to compute the corrections is breaking down; i.e. for $\alpha_t \approx 1$ the scalar-fermion sector of the standard model has entered a strong coupling regime. This occurs for:

$$m_t \approx \sqrt{4\pi}\, v/\sqrt{2} \quad = 617\, GeV$$

If we want a "nice" perturbative theory, this gives us our first upper bound on the top quark mass (see also [29]). In actuality, precision measurements we will review below are currently accurate enough to place significantly better constraints on the top mass:

$$m_t < 240 GeV \tag{2.23}$$

This is equivalent to a coupling constant of $\alpha_t < 0.11$ so that the use of perturbation theory in the derivation of the formulae is consistent.

Violation of Decoupling Theorem

The existence on phenomena whose standard model formulae diverge as $m_t \to \infty$ would seem to violate the decoupling theorem [30]. The latter concerns renormalizable theories containing particles with widely separated masses. Roughly speaking, the argument goes as follows. Consider a process involving virtual heavy particle exchange. If all subgraphs containing the heavy particles are convergent, then the process is suppressed by inverse powers of M (up to logarithms). If, on the other hand, the heavy particle occurs in a primitively divergent subgraph, then its effect can absorbed into the counterterm associated with this subgraph. In this way, all effects of the heavy particle are either suppressed by its mass or absorbed into renormalizations of couplings involving only light particles.

In the standard model, there is an important limitation to this reasoning. Gauge invariance my forbid counterterms corresponding to certain primitively divergent graphs. The finiteness of the theory results from delicate cancellations between different graphs, sometimes between graphs containing heavy virtual

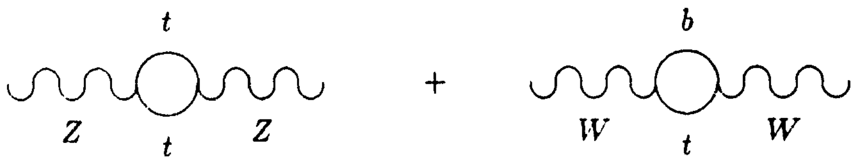

Figure 2.4: Diagrams generating m_t^2 corrections to gauge boson masses.

particles and graphs containing only light virtual particles. In this situation, the heavy particles certainly do not decouple; on the contrary we should expect effects which *grow* with the heavy-particle mass.

What makes the violation of the decoupling theorem especially significant in the case of the top is that these effects diverge *quadratically*. There are essentially two sources of this type of behaviour:

1. Universal effects due to large mass splitting between the third generation $T_3 = +\frac{1}{2}$ and $T_3 = -\frac{1}{2}$ isospin members. These upset the relation between the W^+ and Z^0 masses and $\sin\theta_w$ as determined in the neutral current coupling to any light fermion. ("ρ parameter")

2. Non-universal effects due to the top quark as the iso-spin partner of the b quark, as in the Z^0-b-$\bar{b}$ vertex [31].

It is from the first of these that the bound 2.23 is extracted. The second has not yet been measured to enough accuracy to be sensitive to m_t^2 effects, but I discuss it because it is illustrative of the calculation performed in this thesis.

ρ Parameter Analysis

A shift of the Higgs field in the standard model lagrangian yields the terms:

$$2g_0^2 v_0^2 \, W_\mu^- W^{+\mu} \;+\; \left(g_0^2 + g_0'^2\right) v_0^2 \, Z_\mu^0 Z^{0\mu} \tag{2.24}$$

which leads to the tree level relation:

$$\rho \equiv \frac{M_W}{M_Z \cos\theta_w} = 1. \tag{2.25}$$

The diagrams in figure 2.4 generate corrections to the W^+ and Z^0 masses that are proportional to m_t^2. This induces a change in 2.25 [32]:

$$\Delta^{(t)}\rho = \frac{3}{16\sqrt{2}\pi^2} G_F m_t^2 \tag{2.26}$$

It is essentially this equation that leads to the bound 2.23.

The decoupling theorem is violated here because we cannot just absorb the radiative corrections into arbitrary gauge boson mass counterterms, for example like:

$$\delta m_w^2 W_\mu^- W^{+\mu} \; + \; \delta m_z^2 Z_\mu^0 Z^{0\mu}$$

The gauge boson mass terms in the standard model arise in the very specific fashion of 2.24, and adding these arbitrary extra mass terms in will typically destroy the (hidden) SU(2) gauge invariance.

Though it is not apparent in 2.26 which was derived setting $m_b = 0$, it turns out that if if $m_t = m_b$ then the fermionic corrections to ρ will vanish. This is linked to the existence of a spurious extra symmetry exhibited by the standard model scalar sector. The SU(2) doublet Higgs field has the most general potential:

$$V(\phi) \;=\; \lambda\left(2\phi^\dagger\phi - v^2\right)^2 \tag{2.27}$$

and $\phi^\dagger\phi$ can be written as:

$$\phi^\dagger\phi \equiv \phi^\dagger \begin{pmatrix} \phi_1 + i\phi_2 \\ \phi_3 + i\phi_0 \end{pmatrix} \;=\; \phi_0^2 + \phi_1^2 + \phi_2^2 + \phi_3^2 \tag{2.28}$$

Thus $V(\phi)$ is invariant under the group of $SO(4)$ rotations. SO(4) = SU(2) × SU(2), and one of these SU(2)'s is the original weak SU(2) that all terms in the standard model lagrangian must be invariant under, while the other is an extra, spurious, symmetry. It arises because the constraint of renormalizability does not allow us to write more complicated terms in the scalar potential. The three fields which are absorbed by the gauge bosons,

$$\phi_0, \phi_1, \phi_2$$

transform as a triplet under the extra symmetry, and:

$$\phi_3 \;\equiv\; \frac{1}{\sqrt{2}}(v \;+\; H) \tag{2.29}$$

transforms as a singlet. In the usual way, this global symmetry would lead to a degeneracy in the eigenstates of the hamiltonian. Specifically, the diagonal elements of the gauge-boson mixing matrix generated by spontaneous symmetry breaking that correspond to the three fields:

$$W^3, W^1, W^2$$

are all equal. It is easy to show that this statement is equivalent to the relation 2.26.

Let us now include one generation of quarks [33]:

$$\begin{aligned} &g_t\left(\bar{t},\bar{b}\right)_L \begin{pmatrix} \varphi^{0*} \\ -\phi^- \end{pmatrix} t_R \;+\; g_b\left(\bar{t},\bar{b}\right)_L \begin{pmatrix} \phi^+ \\ \varphi^0 \end{pmatrix} t_R \\ &= g_t\left(\bar{t},\bar{b}\right)_L \begin{pmatrix} \varphi^{0*} & \phi^+ \\ -\phi^- & \varphi^0 \end{pmatrix} \begin{pmatrix} t \\ b \end{pmatrix}_R \qquad + \; O(g_t - g_b) \end{aligned} \tag{2.30}$$

where $\varphi \equiv \phi_3 + i\phi_0$ Thus for $g_t = g_b$ (and ignoring the quarks hypercharge for a moment), the fermion-scalar sector *also* has the SO(4) symmetry, since the transformation:

$$\Phi \equiv \begin{pmatrix} \varphi^{0*} & \phi^{+} \\ -\phi^{-} & \varphi^{0} \end{pmatrix} \rightarrow U_L \Phi U_R^{\dagger}$$

causes the four fields $(\phi_0, \phi_1, \phi_2, \phi_3)$ to transform as a vector representation of SO(4), as above. So for $m_t = m_b$, we have a symmetry which keeps the ρ parameter equal to 1. This is the origin of the m_t^2, or more accurately

$$(g_t - g_b)^2 \propto (m_t - m_b)^2$$

corrections to the relation 2 25. Essentially, $g_t - g_b$ behaves as the order parameter for the custodial symmetry that would otherwise keep relation 2.25 true to all orders. Recalling the quarks' different charges, a similar statement applies to the fine structure constant α.

The Z^0 - b - $\bar{b}$ Vertex

The radiative corrections to the $Z^0 - b - \bar{b}$ vertex involves a piece proportional [31] to m_t^2:

$$\begin{aligned} \Gamma^{\mu}_{zbb} &\propto g_0 \gamma^{\mu} \left[(a - \frac{1}{2}) P_L + \frac{1}{3} s_w^2 \right] \\ a &= \frac{\alpha}{16\pi^2 s_w^2} \frac{m_t^2}{m_w^2} \end{aligned} \tag{2.31}$$

(This is the asymptotic, large m_t, limit.) Again, the decoupling theorem is violated because of the bad behaviour of "a" as $m_t \rightarrow \infty$. We cannot simply absorb "a" into a redefinition of the left handed Z^0-b-$\bar{b}$ tree level coupling strength, because this would destroy gauge invariance: the gauge bosons must couple to all fields with the same strength at tree level, up to group-theoretic factors.

It will be instructive for later purposes to identify the particular feynman diagrams that lead to the formula 2 31. We perform the gauge fixing using the ξ class of gauges[34], in particular setting $\xi = 1$ (feynman-t'Hooft gauge [35]). Under such a scheme the would-be goldstone bosons appear explicitly in the lagrangian, and the propagators for them and the W^{+} bosons are:

$$G_{\phi}^{(2)}(p) = -i \left(p^2 - m_w^2\right)^{-1}$$
$$G_{w}^{(2)}(p) = -i g^{\mu\nu} \left(p^2 - m_w^2\right)^{-1}$$

(Note the negative residue of the ϕ propagator indicating it cannot be an asymptotic state.) The two diagrams shown in figure 2.5 are the source of the $G_F m_t^2$

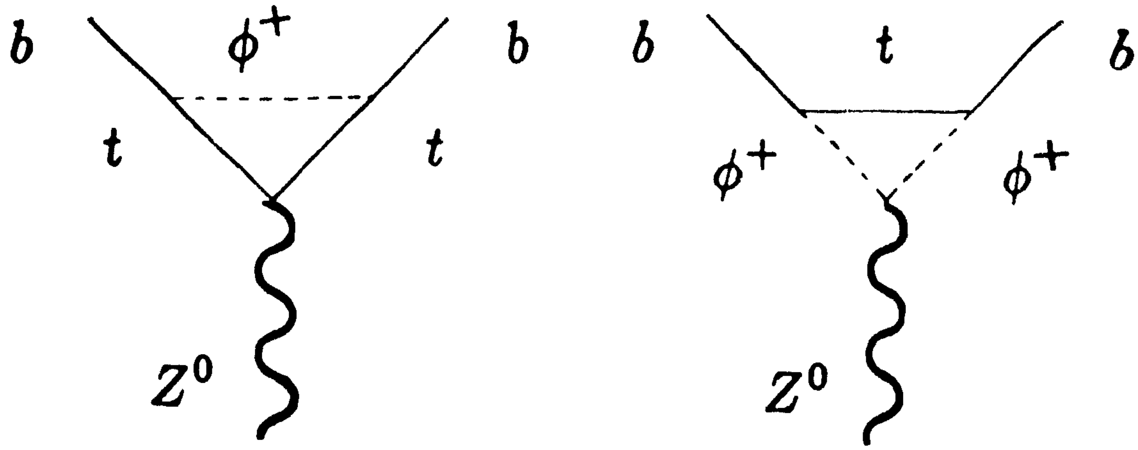

Figure 2.5: Diagrams generating m_t^2 corrections to Z^0 decay.

dependence. The first diagram, for example, generates the amplitude:

$$\sim g_0 \cdot g_t^2 \cdot \int \frac{d^4 l}{(\not{l} - m_t)^2 (l^2 - m_w^2)}$$

By power counting, this integral can only yield either $\log(m_t)$ or $\frac{1}{m_t^2}$ pieces. Thus for large m_t, the amplitude behaves as:

$$\sim g_0 \cdot g_t^2 \cdot \log(m_t)$$

This is the promised $g_t^2 = G_F m_t^2$ dependence.

In general, by power counting the only radiative corrections to dimension four operators going as m_t^2 must involve the coupling of a would-be goldstone boson.

2.5 Indirect Evidence for the Higgs boson

2.5.1 Lower Bound on the Higgs Mass

LEP has recently obtained [36] the following lower limit for the mass of a standard model Higgs:

$$M_H > 40\, GeV \tag{2.32}$$

The production mechanism is $Z^0 \to H f \bar{f}$, where "f" is any fermion. Note that there are some ambiguities in the arguments that rule out a a very light Higgs, $M_H < 1\, GeV$, so that this may also be a possibility.

2.5.2 Sensitivity of Radiative Corrections to the Higgs

As for the top, there exist Higgs phenomena which violate the decoupling theorem. These are associated with primitively divergent diagrams containing the Higgs whose effects we cannot simply absorb into parameter redefinitions, because of gauge invariance.

In the case of the top, there were two asymptotic forms:

1. $\log(m_t)$

2. $\frac{m_t^2}{v^2} = g_t^2$

It was the second type of behaviour which was responsible for the stringent limits on the top mass. In the case of the Higgs, the situation is entirely different. Now the bad large m_H behaviour has the forms:

1. $\log(m_h^2)$

2. $\alpha\frac{m_H^2}{v^2} = \alpha\lambda$

λ is the scalar quartic interaction constant, and is the analogue of g_t above. We see that even in the case of a strongly coupled scalar sector corresponding to $\lambda = 1$, the second form of behaviour only produces corrections of order α. Thus the mechanism that led to such abundant information on the top breaks down in the scalar sector. This is the screening theorem [37]. for large Higgs mass, we have a strongly coupled theory screened off from observation by a factor α.

Here I describe two observables whose radiative corrections depend on m_H:

1. Corrections to the ρ parameter, as for the top.

2. Corrections to the anomalous magnetic moment of the muon.

ρ Parameter

The ρ parameter gave us our best information about the top because of the quadratic dependence of the radiative corrections, which was due to the fact that $(m_t - m_b)$ functioned as an order parameter for the global custodial symmetry. However, the physical Higgs is a singlet (see 2.29) under the extra SU(2) symmetry, so that the custodial symmetry is preserved as $m_H \to \infty$. Thus we should not expect m_H^2 behaviour, which is consistent with the screening theorem.

The correction to the ρ parameter coming from figure 2.6 is [38]:

$$\begin{aligned}\Delta\rho_H &= \frac{3\alpha}{16\pi s_w^2}\left[\frac{M_H^2}{M_H^2 - M_W^2}\log\frac{M_H^2}{M_W^2} - \frac{M_H^2}{c_w^2(M_H^2 - M_W^2)}\log\frac{M_H^2}{M_Z^2}\right] \\ &\to \frac{-3\alpha}{16\pi c_w^2}\log\frac{M_H^2}{M_W^2} \qquad as\ M_H \to \infty \end{aligned} \tag{2.33}$$

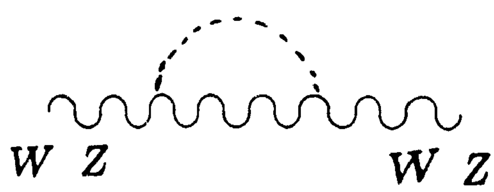

Figure 2.6: Diagrams generating Higgs dependence of the gauge boson masses

which has the promised $\log(m_h)$ dependence, with an additional suppression of α. A recent fit to a host of neutral and charged current precision data leads to the following constraint [39]:

$$M_h < 1.6\, TeV$$

Muon Anomalous Magnetic Moment

The muon anomalous magnetic moment "a_μ" is defined by:

$$\Gamma^\alpha_{\gamma\mu\mu}(q^2_\gamma = 0, p^2_e = m^2_e) \equiv ie\gamma^\alpha + a_\mu \frac{\sigma^{\alpha\beta} q_\beta}{4m_\mu}$$

The Higgs boson contributes to a_μ through the diagram of figure 2.7, yielding (where $r = m_h^2/m_\mu^2$):

$$\begin{aligned} a_\mu^H &= \frac{G_F m_\mu^2}{8\pi^2\sqrt{2}} \int_0^1 dx \frac{x^2(2-x)}{x^2 + r(1-x)} \\ &\to \frac{G_F m_\mu^2}{4\pi^2\sqrt{2}} \frac{m_\mu^2}{m_h^2} \log\left(\frac{m_\mu^2}{m_h^2}\right) \quad as \quad m_h \to \infty \end{aligned} \tag{2.34}$$

The factor:

$$G_F m_\mu^2 \propto \frac{m_\mu^2}{v^2}$$

originates in the Higgs-muon couplings, while the:

$$\frac{m_\mu^2}{m_h^2}$$

part represents an *additional* suppression that can be explained by power counting and the fact that an anomalous magnetic moment is generated by a dimension six operator. This extra suppression is less important for a light Higgs:

$$a_\mu = (2 - 300) \times 10^{-11} \qquad for \ m_h < 3\, GeV$$

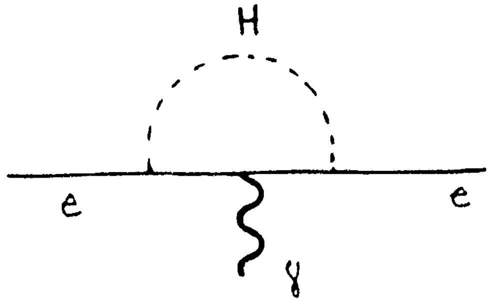

Figure 2.7: Diagram generating Higgs dependence of the muon magnetic moment

The W^+ and Z^0 make contributions of 200×10^{-11}, and new experiments should probe a_μ to order 40×10^{-11}. Thus this experiment is sensitive to a light Higgs, though such a scenario is probably ruled out.

In this case, the extreme accuracy to which this observable can be measured offsets the ubiquitous mass-suppression factor coming from the Higgs-muon coupling.

Chapter 3

Electro-weak Corrections to the Top Decay

The research presented in this chapter has been published in Physics Letters **256B**, 533 (1991). (reference [40])

3.1 Motivation

There is little evidence for the standard model physical Higgs boson. As we have seen, this mostly stems from the fact that the Higgs couples to particles in proportion to their mass. However, the screening theorem [37] must also be used to fully understand the smallness of the radiative corrections, as we now review:

1. In the case of observables involving light external fermions, the radiative Higgs corrections are proportional to $g_f^2 = 2\frac{m_f^2}{v^2}$, by the mass-coupling rule.

2. In the case of observables with gauge bosons as the external particles, naive application of the mass-coupling principle would lead us to guess that the radiative Higgs corrections are proportional to $g^2 = 4\frac{m_W^2}{v^2}$. However, since the gauge bosons contain the would-be goldstone scalars it is possible that the radiative corrections could be proportional to $\lambda = \frac{m_h^2}{v^2}$, and thus be large for large m_h. This is where the screening theorem comes in; there are no such effects. Thus the naive estimate is correct.

I propose another observable which is naively much more sensitive to the Higgs than any process with light external fermions or gauge bosons, namely the t-b-W^+ vertex. For consider the Feynman diagram in figure 3.1. By mass

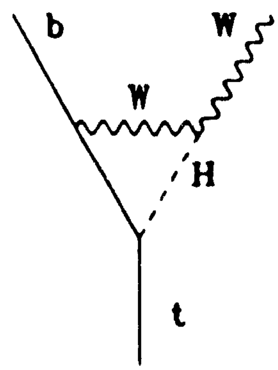

Figure 3.1: Higgs correction to top decay in unitary gauge

coupling arguments, this is suppressed relative to the tree level diagram by:

$$\frac{m_t}{v}\frac{m_w}{v} \sim g_t g$$

However, this estimate is complicated by the momentum dependence in the numerator of the W^+ propagator, which also introduces ambiguities into the renormalization procedure. Thus, consider the description of this process in terms of the ξ-gauge fixed Lagrangian [34], for the particular choice $\xi = 1$ (Feynman-t'Hooft gauge [35]). The Feynman diagram associated with figure 3.1 in the new $\xi = 1$ language is depicted in figure 3 2. Now it is easy to see that the "suppression" of this radiative correction relative to the tree level vertex is typically:

$$\frac{m_t^2}{v^2}$$

Since m_t can be as large as 240 GeV (see 2.23), *this is really no suppression at all.* However, since figure 3.2 is a loop diagram, its contribution is down relative to tree level by an additional $\frac{1}{16\pi^2}$. Thus a first estimate of the correction to the t-b-W^+ vertex due to figure 3.2 is:

$$\frac{1}{16\pi^2}\frac{m_t^2}{v^2} \sim \frac{1}{2}\%$$

This is the typical size of other electro-weak corrections in the standard model. This in itself is quite surprising from the point of view of our experience with Higgs corrections to light fermion processes, where its effects could always be ignored. Nevertheless, a full calculation of all strong and electro-weak

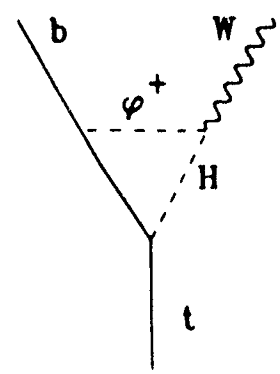

Figure 3.2: Higgs correction to top decay in Feynman-t'Hooft gauge

contributions would have to be performed if we ever wanted to disentangle the effects of the virtual radiation of all the standard model bosons. The purpose of the research presented in this thesis was to study only the magnitude of the "unsuppressed" Higgs radiative corrections, to see if they really are as large as naively suspected.

The context in which this study would be phenomenologically interesting is the following. Suppose that the top quark has been discovered, but that the Higgs boson has not. It could be that either the Higgs is very heavy or that perhaps it does not exist at all — something else is breaking the electro-weak gauge symmetries. Then we will find that the measurement of the top width to an accuracy of less that a per-cent will yield information distinguishing these two scenarios. It has been estimated [41] that top production at the SSC will exceed 10^8 pairs, so that such an accurate measurement of its width is not obviously out of the question. By contrast, at a TeV linear e^+e^- collider it has been estimated [42] that the top width could be known to no better than 25%.

Lastly, the final number we compute will represent a well defined, gauge invariant, portion of the complete set of corrections to the decay width. This follows from the fact that gauge invariance is satisfied order by order in perturbation theory: gauge dependence in the coefficient of the g_t^2 term cannot be cancelled by other gauge dependence in the coefficient of the g^2 term, for example, because both g_t and g are free parameters of the model.

The ensuing discussion is organized as follows. First I will describe the on-shell renormalization prescription as it applies to fixing the values of the field rescalings. I will spend some time deriving the formulae for the rescalings because I could not find a proof in the literature. Then we will go on to find the general expression for the decay width in terms of a general t-b-W^+ vertex function. Lastly, the Feynman diagrams are presented and computed, and our results summarized. An appendix is included to discuss how the deviation in the top width can be distinguished from the effects of a KM matrix, until that point, we shall always set $V_{tb} = 1$.

3.2 The Renormalized Lagrangian

3.2.1 S-matrix, Greens functions

Our goal is to describe the on-shell renormalization prescription. It will be useful to review the relationship between Greens functions and the S-matrix. For this purpose it will suffice to work within the context of scalar field theory.

The S-matrix for n particle scattering is given in the Heisenberg picture by:

$$S = < q_1 \cdots q_l, out | q_{l+1} \cdots q_n; in > \tag{3.1}$$

$|in>$ and $|out>$ are in and out asymptotic states which are eigenstates of the total hamiltonian and the other conserved charges. They contain a definite number of particles. They are constructed from the vacuum $|0>$ by creation operators, $\phi_{as}(x)$, which satisfy.

$$(\Box + m^2)\phi_{as}(x) = 0 \tag{3.2}$$

Here m is the physical, measured, mass of the field. The asymptotic field is related to the fields ϕ in the Lagrangian according to:

$$\phi(x) \longrightarrow \tilde{Z}^{1/2}\, \phi_{as}(x) \quad as\ t \rightarrow \pm\infty \tag{3.3}$$

(This is actually the so-called weak limit, or LSZ asymptotic condition.) The factor $\tilde{Z}^{1/2}$ is just the amplitude that the operator $\phi(x)$ create a single particle state out of the vacuum. Since in general in an interacting theory $\phi(x)$ can create many other states in addition to just the single particle one, we have:

$$\tilde{Z}^{1/2} < 1 \tag{3.4}$$

Further analysis using a spectral representation of the propagator or two point function for the ϕ field tells us that $\tilde{Z}^{1/2}$ can be calculated: it is the pole residue of the ϕ propagator $G^{(2)}$ at $p^2 = m^2$.

$$G^{(2)}(p^2) = \frac{i\tilde{Z}}{p^2 - m^2 - i\epsilon} + \int_{thresh}^{\infty} d\sigma \rho(\sigma) \frac{1}{p^2 - \sigma^2 - i\epsilon} \tag{3.5}$$

The S-matrix is related to the Greens functions $G^{(k)}$ via the reduction formula:

$$G^{(k)}(x_l) \quad \equiv \quad < 0|T\phi(x_1)\cdots\phi(x_l)|0 > \equiv F.T. \left[G^{(k)}(p_l)\Delta\right] \tag{3.6}$$

$$
\begin{aligned}
S &= i^n \tilde{Z}^{-n/2} \int \prod_i^n d^4x_i(\Box_i + m^2) \cdot G^{(n)}(x_1, \ldots, x_n) \\
&= i^n \tilde{Z}^{-n/2} \prod_i^n (m^2 - p_i^2) \cdot G^{(n)}(p_k) \cdot \Delta \\
&= i^n \tilde{Z}^{n/2} \cdot G_{tr}^{(n)}(p_k) \cdot \Delta \qquad (3.7)
\end{aligned}
$$

where $\Delta \equiv (2\pi)^4 \delta^4(\Sigma p_i)$, and we have introduced the truncated Greens functions:

$$
G_{tr}^{(n)}(p_k) = \prod_{j=1}^{n} [G^{(2)}(p_j)]^{-1} G^{(n)}(p_k) \qquad (3.8)
$$

The perturbative expansion of the truncated Greens functions proceeds in the usual way, *with the exception that the associated diagrams have no self energy bubbles on the external lines.*

In future, all Greens functions used will be functions of momentum, so we will henceforth not explicitly display that momentum dependence.

3.2.2 Wave Function Renormalization

Now we discuss renormalization conditions concerning the field rescalings or wave function renormalizations. These conditions are necessary to compute Greens functions, but they have no effect on the value of the S-matrix, which only depends on the fields and the well defined $\tilde{Z}^{1/2}$ factors. In particular, we could proceed without ever rescaling the fields, so long as we remember to compute the $\tilde{Z}^{1/2}$ factors to the same order in perturbation theory that we compute the Greens functions, and insert our results in the complete equation 3.7 for the S-matrix. This approach is discussed in [43].

However, it is convenient to work with Greens functions that are themselves finite. This can be accomplished by rescaling the fields:

$$
\phi(x) \equiv Z^{1/2} \phi_r(x) \qquad (3.9)
$$

This leads to new quantities, namely Greens functions of the rescaled fields (see 3.6 and 3.8):

$$
\begin{aligned}
G^{(k)} &= Z^{k/2} G_r^{(k)} \\
G_{tr}^{(k)} &= Z^{-k/2} G_{r,tr}^{(k)} \qquad (3.10)
\end{aligned}
$$

where:

$$
\begin{aligned}
G_r^{(k)} &\equiv \langle 0 | T\phi_r(x_1) \cdots \phi_r(x_k) | 0 \rangle \\
G_{r,tr}^{(k)} &= \prod_1^n [G_r^{(2)}]^{-1} G_r^{(k)} \qquad (3.11)
\end{aligned}
$$

Finally, the S-matrix 3.7 becomes:

$$S = i^n \left(\frac{\tilde{Z}}{Z}\right)^{n/2} G^{(n)}_{r,tr} \cdot \Delta \tag{3.12}$$

Obviously, a particular choice for the rescaling cries out:

$$Z = \tilde{Z} \tag{3.13}$$

With this identification, we have chosen a renormalization scheme. It is characterized by the equality of the rescalings and the well-defined $\tilde{Z}$ factors, which we know are the particle propagator residues about their mass poles. This scheme is simple and convenient since we have to calculate the $\tilde{Z}$ factors anyway to obtain the S-matrix elements.

There is one more constraint to discuss. We shall shift each mass parameter in the Lagrangian such that each is equal to the physical mass of the asymptotic state i.e. the pole of the full propagator. The effect of this will be evident in what follows.

These two prescriptions may be neatly summarized in terms of the behaviour of the each re-scaled field's two-point function near its pole (see 3.5):

$$\begin{aligned} G^{(2)}_r(p^2) &= Z^{-1}G^{(2)}(p^2) \longrightarrow \frac{1}{Z}\frac{i\tilde{Z}}{p^2 - m^2 - i\epsilon} \quad as \quad p^2 \to m^2 \\ &= \frac{i}{p^2 - m^2 - i\epsilon} \end{aligned} \tag{3.14}$$

In other words:

> *In the on-shell renormalization scheme the particle propagators have poles at the observed particle masses, and the residue about each of these poles is "i" times the unit.*

The mass parameters in the Lagrangian are just the masses of the asymptotic states, and the field operators create states containing asymptotic states normalized to "1"; in terms of the LSZ limit 3.3, the field operators create the asymptotic states. When we turn to the more general case of a field theory containing different fermions and bosons, it is these expressions of the renormalization scheme that we will use.

3.2.3 Formulae for the Field Rescalings

We now have to translate the prescriptions of the last section into formulae for the Z. This is not quite so straight-forward if the fields are fermions, which is the case we have to consider in this thesis.

Let us concentrate on just the kinetic energy and mass terms for a fermion field ψ.

$$L = \overline{\psi}_0(\not\partial - m_0)\psi_0 \quad + \lambda L_{int} \tag{3.15}$$

We have introduced the subscript "0" on the initial fields to avoid excessive occurrences of "r" subscripts later. In a theory with parity violating interactions, the left and right handed parts of the field are differently related to the left and right handed parts of the asymptotic field. Thus it is necessary to rescale each part separately:

$$\begin{aligned} \psi_{0L} &\equiv Z_L^{1/2}\psi_L \\ \psi_{0R} &\equiv Z_R^{1/2}\psi_R \\ m_0 &\equiv m + \delta m \end{aligned} \tag{3.16}$$

The following combinations will occur frequently:

$$\begin{aligned} \delta Z_{L/R} &\equiv Z_{L/R} - 1 \\ \delta Z_v &\equiv (\delta Z_R + \delta Z_L)/2 \\ \delta Z_a &\equiv (\delta Z_R - \delta Z_L)/2 \end{aligned} \tag{3.17}$$

Substituting 3.16 into 3.15:

$$\begin{aligned} L &= \overline{\psi}(\not\partial - m)\psi + \delta L + \lambda L_{int} \\ \delta L &\equiv \delta Z_v \overline{\psi}(\not\partial - m)\psi + \delta Z_a \overline{\psi}\not\partial\gamma_5\psi - \delta m\, Z_v \overline{\psi}\psi \end{aligned} \tag{3.18}$$

We will see below that the piece δL is proportional to the small parameter λ in the on-shell prescription. More accurately, we will first assume that we can calculate Greens functions by using δL and λL to perturb about the free particle solutions, and under this assumption deduce the aforementioned relation. Thus our approach is consistent, in the sense of mean field theory.

Inspecting this new form for L, we see that we have gained a term with a new lorentz structure not present in the initial Lagrangian, namely $\overline{\psi}\not\partial\gamma_5\psi$. However, 3.18 still does not have the most general form possible, due to the absence of expressions like:

$$\overline{\psi}\gamma_5\psi \tag{3.19}$$

The reason such terms were not generated under the shifts and rescalings in 3.16 is:

1. the term in 3.19 is odd under CP transformations,

2. the free field part of the initial Lagrangian 3.15 is CP even;

3. and the transformations of 3.16 preserve CP.

$G^{(2)}(p) \;=$

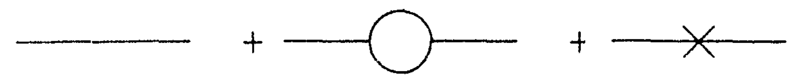

Figure 3.3: The two-point Greens function

Had we allowed $Z_L^{1/2}$, $Z_R^{1/2}$ to have imaginary parts, the term 3.19 *would* have arisen. Such a procedure would be necessary if there were CP violating interactions in the theory, so that the asymptotic left and right handed pieces acquire a relative phase difference. In the standard model, electro-weak CP violation only arises in processes that involve all three families of quarks, which is not a characteristic of our problem. Thus we have left the rescaling factors real. Another way to know if the more general procedure is necessary is if terms of the form 3.19 appear in the self energy function as computed in perturbation theory.

We return to the problem of obtaining formulae for the Z. The final statement of the on-shell prescription was that $G_r^{(2)}$ must have a pole at m and a residue of "1" about that pole. So we must compute $G_r^{(2)}$. Diagramatically, this is done in figure 3.3. The diagrams containing the "cross" and the "blob" represent the contributions of the δL and λL_{int} pieces of 3.18 respectively. We will see that it is consistent to assume that the δL terms are of the same order as λL_{int}. We represent the formula for the blob by $\Sigma(p)$.

$$\begin{aligned} G_r^{(2)} &= (\not{p} - m)^{-1} \\ &+ (\not{p} - m)^{-1}\left[\Sigma(p) + \delta Z_v(\not{p} - m) + \delta Z_a \not{p}\gamma_5 - \delta m\right](\not{p} - m)^{-1} \quad + O(\lambda^2) \end{aligned} \tag{3.20}$$

In the absence of CP violation, $\Sigma(p)$ has the most general form:

$$\begin{aligned} \Sigma(p) &\equiv \Sigma_v(p^2)\not{p} + \Sigma_a(p^2)\not{p}\gamma_5 + m\Sigma_s(p^2) \\ &\equiv \Sigma_L(p^2)\not{p}P_L + \Sigma_R(p^2)\not{p}P_R + m\Sigma_s(p^2) \end{aligned} \tag{3.21}$$

where in the case of massless particles, "m" may have to be replaced with the mass parameter of some other particle in the theory. Note that p^μ is the only four-vector in the problem, so that other terms with $\sigma^{\mu\nu}$ etc. in them are absent or may be transformed to this form using dirac algebra. A term proportional to just γ_5 has opposite CP transformation properties from those above and will not occur in our problem as discussed.

We are now going to taylor expand $\Sigma(p)$ about $p^2 = m^2$. Due to our parametrization 3.21 of $\Sigma(p)$ this turns out to be somewhat messy. Surprisingly, *we will find that it is not necessary to expand Σ_a; the higher order terms* *in its expansion affect neither the pole nor the residue.*

$$\Sigma'_x \equiv \left.\frac{\partial}{\partial p^2}\right|_{m^2} \Sigma_x$$

$$\begin{aligned}\Sigma_s &= \Sigma_s + \Sigma'_s(p^2 - m^2) \quad + O(p^2 - m^2)^2 \\ &= \Sigma_s + 2m\Sigma'_s(\not p - m) \quad + O(\not p - m)^2 \end{aligned} \qquad (3.22)$$

$$\begin{aligned}\Sigma_v \not p &= \left[\Sigma_v(m^2) + \Sigma'_v(p^2 - m^2) + O(p^2 - m^2)^2\right] \times [m + (\not p - m)] \\ &= m\Sigma_v(m^2) + \Sigma_v(m^2)(\not p - m) + m\Sigma'_v(\not p + m)(\not p - m) \quad + O(\not p - m)^2 \\ &= m\Sigma_v(m^2) + \left[\Sigma_v(m^2) + 2m^2\Sigma'_v\right](\not p - m) \quad + O(\not p - m)^2 \end{aligned} \qquad (3.23)$$

$$\begin{aligned}\Sigma_a \not p \gamma_5 &= \left\{m\Sigma_a(m^2) + \Sigma_a(m^2)(\not p - m) + m\Sigma'_a(\not p - m)(\not p + m)\right\}\gamma_5 \quad + O(\not p - m)^2 \\ &= \left\{m\Sigma_a(m^2) + \Sigma_a(m^2)(\not p - m)\right\}\gamma_5 - m\Sigma'_a(\not p - m)\gamma_5(\not p - m) \end{aligned} \qquad (3.24)$$

We now substitute all this into equation 3 20 for $G_r^{(2)}$:

$$G_r^{(2)} \equiv (\not p - m)^{-1} + (\not p - m)^{-1}[\Sigma_{ren}](\not p - m)^{-1} \quad + O(1) \quad + O(\lambda^2) \qquad (3.25)$$

$$\begin{aligned}\Sigma_{ren} &= [m(\Sigma_s + \Sigma_v)_{m^2} - \delta m] + \left[\Sigma_v + 2m^2\Sigma'_s + 2m^2\Sigma'_v + \delta Z_v\right](\not p - m) \\ &\quad + m\left[\Sigma_a(m^2) + \delta Z_a\right]\gamma_5 + \left[\Sigma_a(m^2) + \delta Z_a\right](\not p - m)\gamma_5 \\ &\quad - (\not p - m)\left[m\Sigma'_a\gamma_5\right](\not p - m) \end{aligned} \qquad (3.26)$$

No matter what happens, we do not want any γ_5's to infect the propagator near its pole. This leads to the first condition:

$$\delta Z_a = -\Sigma_a(m^2) \qquad (3.27)$$

The piece in 3.26 involving Σ'_a represents a correction of $O(1)$ near the pole, so the further condition $\Sigma'_a = 0$ is not implied. It is surprising that the one condition 3.27 simultaneously eliminates the γ^5 dependencies to zeroth and first order in $\not p$. This only happens because we are neglecting CP violating effects. By contrast, the implications of the on-shell prescription to the non-γ_5 parts will yield *two* such constraints.

$$\begin{aligned}G_r^{(2)} &= \frac{1}{\not p - m} + \frac{1}{\not p - m}\left\{m(\Sigma_s + \Sigma_v)_{m^2} - \delta m\right\}\frac{1}{\not p - m} \\ &\quad + \frac{1}{\not p - m}\left\{\Sigma_v + 2m^2\Sigma'_s + 2m^2\Sigma'_v + \delta Z_v\right\} - m\Sigma'_a\gamma_5 \\ &\equiv \frac{1 + B}{\not p - m - A} \quad + O(1) \quad + O(\lambda^2) \end{aligned} \qquad (3.28)$$

The on-shell scheme demands that the A and B pieces be zero:

$$\begin{aligned} A &\equiv m(\Sigma_s + \Sigma_v)_{m^2} - \delta m = 0 \\ B &\equiv \Sigma_v + 2m^2\Sigma_s' + 2m^2\Sigma_v' + \delta Z_v = 0 \end{aligned} \tag{3.29}$$

Thus we see that δZ_v, δZ_a, and δm are each proportional to the Σ functions, which represent the effects of λL_{int} Thus δZ etc. are proportional to λ, as promised. Finally, we obtain the formulae for Z_L, Z_R, and δm, returning to the more convenient second form for $\Sigma(p)$ in 3.21:

$$\begin{aligned} Z_L &= 1 - \left\{\Sigma_L + m^2\frac{\partial}{\partial p^2}[\Sigma_L + \Sigma_R + 2\Sigma_s]\right\}_{m^2} \\ Z_R &= 1 - \left\{\Sigma_R + m^2\frac{\partial}{\partial p^2}[\Sigma_L + \Sigma_R + 2\Sigma_s]\right\}_{m^2} \\ \delta m &= m + \{\Sigma_s + (\Sigma_L + \Sigma_R)/2\}_{m^2} \end{aligned} \tag{3.30}$$

Recall that the Z's were purely real; but what if the self energy functions have imaginary parts? We now address this issue.

Comments on Absorptive Phases

The self energy function $\Sigma(p)$ can have an imaginary part if the associated field is unstable. It is possible to demonstrate from unitarity that this imaginary part is essentially the particle width, up to kinematic factors. Since the imaginary part of the self energy is therefore an observable, it can never be regulator dependent and we do not need to renormalize it. It is only the real part of the self-energy whose regulator dependence has to be eliminated by the field re scalings (if we want regulator independent Greens functions that is). Thus the appropriate formulae for the Z's and δm should really be:

$$\begin{aligned} Z_L &= 1 - Re\left\{\Sigma_L + m^2\frac{\partial}{\partial p^2}[\Sigma_L + \Sigma_R + 2\Sigma_s]\right\}_{m^2} \\ Z_R &= 1 - Re\left\{\Sigma_R + m^2\frac{\partial}{\partial p^2}[\Sigma_L + \Sigma_R + 2\Sigma_s]\right\}_{m^2} \\ \delta m &= m + Re\{\Sigma_s + (\Sigma_L + \Sigma_R)/2\}_{m^2} \end{aligned} \tag{3.31}$$

3.2.4 Effects of Wave Function Renormalization

I would like to comment on the mechanisms by which our re-scalings, etc. will affect the outcome of a calculation. At this point, the only effect of our manipulations has been the generation of extra terms in the Lagrangian 3.18, and the rule that we no longer have to divide the truncated Greens functions by the propagator residues to obtain the S-matrix (see 3.14 and 3.13). Since the latter

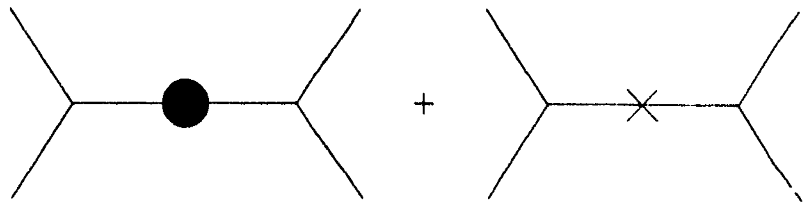

Figure 3.4: Manifest effect of wave function renormalization

on its own manifestly produces a change, there must be Feynman diagrams to which those extra terms contribute so that final result remains the same.

One class of problems in which the extra terms appear are processes described by Feynman diagrams that admit self energy bubbles on *internal* lines (Diagrams with self-energy bubbles on external lines are irrelevant since the S-matrix depends solely on the truncated Greens functions 3.8). Such a situation is depicted in figure 3.4, where the extra terms have been depicted by a cross. The sum of the two diagrams will be of the form:

$$\cdots\ (\Sigma(p) + \delta A)\ \cdots$$

This combination will be regulator independent, which is a convenient but not necessary property for a Greens function to have.

What about a Greens function that does not have these types of diagrams? Such is the case for the three point function $G^{(3)}$ in Q.E.D. and many other theories. Since the extra terms do not enter in the formulae, where is the compensating effect effect postulated above? The answer lies the L_{int} part of the Lagrangian 3 18 that we have so far ignored. In the example of Q.E.D. we have:

$$\lambda L_{int} = e_0 \overline{\psi}_0 A\!\!\!/_0 \psi_0 = e_0 Z_e Z_A^{1/2}\, \overline{\psi} A\!\!\!/ \psi$$

The effective coupling of the interaction has become:

$$\lambda_r \equiv e_0 Z_e Z_A^{1/2}$$

Using this everywhere in place of λ, we will obtain the same answers as if we had done no field re-scalings at all. The situation is complicated, however, by the convention of replacing this combination with the measured quantity "e", which is the coefficient of the "γ^μ" part of the e-e-γ form factor measured at $q^2 = 0$:

$$e \equiv B \times e_0 Z_e Z_A^{1/2}$$

"B" is customarily denoted "$1/Z_1$". The situation is further complicated in Q.E.D. by the subtlety that the gauge invariance of the theory results in "B"

being, to all orders in perturbation theory, equal to:

$$B = \frac{1}{Z_e}$$

Thus, in Q.E.D., use of the coupling $e = e_0 Z_A^{1/2}$ everywhere yields the same answers as if no rescalings had been done at all. Thus, *in the computation of the three point function of Q.E.D. to one loop order, the fermion field rescaling factor never appears.*

In this sense, our calculation is less subtle. We are computing one loop corrections to the t-b-W^+ vertex, so consider:

$$\lambda L_{int} = \frac{g_0}{\sqrt{2}}\bar{t}_{0L}\not{W}_0 b_{0L} = \frac{g_0}{\sqrt{2}}(Z_{tL}Z_{bL}Z_W)^{1/2}\,\bar{t}_L\not{W}b_L$$

The SU(2) gauge invariance is broken so the fermion field rescalings bear no simple relation to the gauge boson rescaling $Z_W^{1/2}$, no matter what convention we choose to define a new coupling constant "g", the analogue of "e" discussed above. The Z_{tL} and Z_{bL} will occur all over the place in our final formula. Their presence there reflects the fact that we have cleverly removed the propagator residue factors from the formula for the S-matrix.

3.2.5 The Renormalized Lagrangian

We will only have to renormalize the portion of the standard model Lagrangian containing the fields that are present at tree level in the process under study, namely t,b, and W^+. Also, recall two simplifying assumptions that have been made:

1. $m_b \equiv 0$
2. $V_{tb} \equiv 1$

The relevant Lagrangian is thus:

$$L = \bar{t}_0(\not{\partial} - m_0)t_0 + \bar{b}_0\not{\partial}b_0 + \frac{g_0}{\sqrt{2}}\bar{t}_0\not{W}b_0 \quad + h.c. \tag{3.32}$$

We perform the following re-scalings and shifts:

$$\begin{aligned} t_{0L} &\equiv Z_{tL}^{1/2}t_L \\ t_{0R} &\equiv Z_{tR}^{1/2}t_R \\ b_{0L} &\equiv Z_{bL}^{1/2}b_L \\ b_{0R} &\equiv Z_{bR}^{1/2}b_R \\ W_0^+ &\equiv Z_W^{1/2}W^+ \\ m_{t0} &\equiv m_t + \delta m_t \end{aligned} \tag{3.33}$$

Given that the interaction part of the Lagrangian 3.32 only involves the left handed fields, it is impossible for a b-quark mass to be radiatively generated. Thus we do not perform any renormalizations to keep it zero. 3.32 now becomes.

$$\begin{aligned} L &= \bar{t}(\not\partial - m_t)t + \bar{b}\not\partial b + \frac{g_0}{\sqrt{2}}(Z_{tL}Z_{bL}Z_W)^{1/2}\,\bar{t}\not W^- b \quad + \delta L_{tb} \quad + h.c. \\ \delta L_{tb} &\equiv \delta Z_{tv}\bar{t}(\not\partial - m_t)t + \delta Z_{ta}\bar{t}\not\partial\gamma_5 t - \delta m_t\bar{t}t + \delta Z_{bv}\bar{b}\not\partial b + \delta Z_{ba}\bar{b}\not\partial\gamma_5 b \end{aligned} \tag{3.34}$$

As we will discuss, it will also be necessary to know the renormalized portion of the standard model Lagrangian containing e and ν, which is:

$$L = \bar{e}\not\partial e + \bar{\nu}_e\not\partial\nu_e + \frac{g_0}{\sqrt{2}}(Z_{eL}Z_{\nu L}Z_W)^{1/2}\,\bar{\nu}\not W^- e + \delta L_{e\nu} \quad + h.c. \tag{3.35}$$

3.3 Comparison with $W^+ \to e^+\nu$

3.3.1 Why We Compare to $W^+ \to e^+\nu$

We are going to compute the standard model prediction for the top width Γ_t to beyond lowest order in the scalar top coupling g_t. If that were *all* we were going to calculate, we would have two problems.

1. Our result would be regulator dependent i.e. meaningless
2. The study would be non-predictive. we have one unknown parameter, g_t, and one experimental result Γ_t.

The fundamental idea of renormalization is that these two problems have a common solution. We must use the model to compute *another* formula for a second observable to the same perturbation order. After eliminating the unknown parameter between these two formulae, we have left an unambiguous prediction for the relative outcome of two experiments, which must be independent of any regulator introduced in the intermediate steps. Given the results of the experiments, the model may then be accepted or discarded.

To be more specific, our final result will be a formula expressing the top lifetime as a function of the following Lagrangian parameters:

$$m_W, m_Z, m_t, m_H, g_0$$

In our renormalization prescription, the mass parameters appearing in the Lagrangian are the actual masses of the asymptotic states: they already represent the results of experiment. However the parameter g_0 stands in a complicated relation to physical phenomena. This is where $W^+ \to e^+\nu$ comes in. It is from this experiment that we will extract g_0, and use the value to make predictions for $t \to bW^+$ as a function of m_H, etc. In fact, parametrizing the W-e-ν vertex as measured in this decay by:

$$\Gamma^{\mu}_{We\nu}(q^2 = m_W^2, p_e^2 = 0) \equiv i\frac{g^{e\nu}}{\sqrt{2}}\gamma^{\mu}P_L + f_2\sigma^{\mu\nu}q_{\nu} + \cdots \tag{3.36}$$

we will compute a formula for the top width as a function of:

$$m_W, m_Z, m_t, m_H, g^{e\nu} \tag{3.37}$$

The viability of this approach relies entirely on the fact that the underlying model is a gauge theory based on a non-abelian group. This means that the W must couple *universally* to all matter with the same bare coupling strength g_0, up to group-theoretically determined factors. (Note that we have deferred considerations involving mixing between like sign quarks till section 3.7).

It might be argued that $W^+ \to e^+\nu$ is a crude source of information about the electro-weak coupling, since this decay is poorly known. This is not important to our study for the following reasons:

1. By the time the top decay width is known to sufficient accuracy to be sensitive to radiative corrections, $W^+ \to e^+\nu$ and thus $g^{e\nu}$ will also be known to great accuracy.

2. There already exist [44] detailed standard model calculations that predict what value of $g^{e\nu}$ will be measured in $W^+ \to e^+\nu$, using existing precision information like α_{em}, G_μ, M_Z, etc. as input. Were we so inclined, we could insert these predicted values into our formulae and thus obtain a prediction of the top width as a function of that input data.

An alternate calculation working directly from the precision data mentioned in 2 would be extremely complicated, entailing as it would a careful study of the neutral current sector of the standard model. On the one hand, this would obliterate the simplicity of the study. More importantly, in that approach the zeroth order top width is computed using g_0 as determined from tree level relations between parameters like α_{em} measured at very low energy scales. Going to the next order, many of the radiative corrections would produce large logarithms of the ratio of the top mass and the low energy scale, in essence describing just the running of α_{em} up to the top quark scale. (There may also be terms proportional to m_t^2). Even at LEP energies such effects are known to be about 8%, which would dwarf the 1% corrections that we expect. These sort of renormalization phenomena, the running of coupling constants, are well understood and thus boring. In our scheme all the inputs are measured at the same scale, and the contributions we find will thus involve only the "interesting" physics.

3.3.2 Summary of Renormalization Scheme

We use an on-shell renormalization scheme, characterized by:

1. The mass parameter for each field identically equals the mass of the corresponding asymptotic field.

2. The two point function of each fermion field must satisfy

$$G^{(2)}(p) = \frac{i}{\not p - m - i\epsilon} \quad as \quad p^2 \to m^2 \tag{3.38}$$

where m is the mass of the asymptotic fermion field.

3. The two point function of each physical boson field must satisfy

$$G^{(2)}(p^2) = \frac{i}{p^2 - m^2 - i\epsilon} \quad as \quad p^2 \to m^2 \tag{3.39}$$

where m is the mass of the asymptotic boson field

4. The primary, input, phenomena that we will express all other observables in terms of are:

$$m_W, m_Z, m_t, m_H, g^{e\nu} \tag{3.40}$$

where the masses all refer to the asymptotic fields, and $g^{e\nu}$ is defined in terms of the W^+-e-ν vertex function at the point where the W^+, e^+, and ν are all on-shell:

$$\Gamma^{\mu}_{We\nu}(q^2 = m_W^2, p_e^2 = 0) \equiv i\frac{g^{e\nu}}{\sqrt{2}}\gamma^{\mu}P_l + \cdots \tag{3.41}$$

3.4 The Formula

3.4.1 Matrix Element and Vertex Function

The invariant amplitude for $t \to bW^+$ is given in terms of the vertex function Γ^{μ}_{tbw}:

$$M^{\mu} = \bar{u}_{\alpha}(p_b)(\Gamma^{\mu}_{tbw})^{\alpha\beta}\, u_{\beta}(p_t) \tag{3.42}$$

The transition starts with a t quark. The b-quark can only be obtained from this initial state via a charged current interaction. Such interactions only produce *left-handed* quarks. Further, we are everywhere assuming $m_b \equiv 0$. This means that the produced left-handed b-quark can never oscillate into a right-handed b-quark. Thus we know that the outgoing b-quark produced in the top decay is completely left-handed. Thus we can make the replacement:

$$u(p_b) \to P_L u(p_b) \tag{3.43}$$

in the previous equation.

$$M^{\mu} = \bar{u}_{\alpha}(p_b)(P_R\Gamma^{\mu}_{tbw})^{\alpha\beta}\, u_b(p_t) \tag{3.44}$$

The most general form for the vertex function that does not vanish when projected on from the left by P_R is:

$$\Gamma^{\mu}_{tbw} = a\gamma^{\mu}P_L \,+\, b'\left(\frac{p_t^{\mu}}{m_t}\right)P_R \,+\, c'\left(\frac{p_b^{\mu}}{m_t}\right)P_R \tag{3.45}$$

where we have used the usual Gordan [45] decomposition to convert possible $\sigma^{\mu\nu}p_{\nu}$ terms into the forms above. We can throw away terms proportional to q^{μ}, the W^+ four-momentum, appearing in Γ^{μ}_{tbw}. There are two cases to consider:

1. Decay to a real W^+. The amplitude is $M_{\mu}\epsilon^{\mu}_{w}$, but for a massive on shell vector boson, $q_{\mu}\epsilon^{\mu}_{w}$ is identically zero by the equations of motion.

2. Decay through a virtual W^+ to light particles. The amplitude is proportional to:

   $$M_{\mu}(g^{\mu\nu} - q^{\mu}q^{\nu}/M_w^2)J_L^{\nu}$$

   where J_L^{ν} is the left-handed current of the light particles to which the W^+ couples. A q^{μ} piece in M^{μ} thus makes a contribution to the amplitude proportional to $q_{\nu}J_L^{\nu}$, which is in turn proportional to the light particle masses that we are neglecting.

Thus the most general form for the vertex function becomes:

$$\Gamma^{\mu}_{tbw} = a\gamma^{\mu}P_L \,+\, b\left(\frac{p_t^{\mu}}{m_t}\right)P_R \tag{3.46}$$

3.4.2 Decay Rate and Spectrum

Here we present formulae for the decay rate and spectrum in terms of the most general vertex function derived in the last section. Combining 3.44 and 3.46:

$$\begin{aligned}\frac{1}{2}\sum_{q\,pol} M_\mu^\dagger M_\nu &= a^2\left[p_t^\mu p_b^\nu + p_t^\nu p_b^\mu - p_t\cdot p_b g^{\mu\nu}\right] + ab\left[p_t^\mu p_b^\nu + p_t^\nu p_b^\mu\right] \quad + O(b^2) \\ &= a^2\left[2p_t^\mu p_t^\nu - p_t\cdot p_b g^{\mu\nu}\right] + 2ab p_t^\mu p_t^\nu \quad + O(b^2) \qquad (3.47)\end{aligned}$$

The second line follows from the first by discarding q^μ pieces, as discussed.

Decay Rate for $t \to bW^+$

Recalling that:

$$\sum_{W\,pol} \epsilon_w^\mu \epsilon_w^\nu = -g^{\mu\nu} + \frac{q^\mu q^\nu}{M_W^2} \qquad (3.48)$$

we obtain:

$$\frac{1}{2}\sum_{pol}|M_\mu \epsilon_w^\mu|^2 = (m_t^2 - m_w^2)\left[a^2(2+\frac{m_t^2}{m_w^2}) + ab(\frac{m_t^2}{m_w^2}-1)\right] \quad + O(b^2) \quad (3.49)$$

The rate for a two-body decay is given in terms of $|M|^2$ by [46]:

$$\Gamma = \frac{1}{8\pi}\frac{p_f}{m^2}\cdot\frac{1}{2}\sum_{pol}|M|^2$$

and so:

$$\Gamma_t = \frac{1}{32\pi}m_t\left(1-\frac{m_w^2}{m_t^2}\right)^2\left[a^2(2+\frac{m_t^2}{m_w^2}) + ab(\frac{m_t^2}{m_w^2}-1)\right] \qquad (3.50)$$

Decay Spectrum for $t \to be^+\nu$

Now we turn to the decay $t \to be^+\nu$. We will consider this since the lepton spectrum for this decay is probably a more easily measured quantity than the t width. Graphically, it is given in figure 3.5. The amplitude for this process is:

$$\begin{aligned} A(t\to be^+\nu) &= M_\mu D_w^{\mu\alpha} J_{L\alpha} \\ D_w^{\mu\alpha} &= \frac{-g^{\mu\alpha} + q^\mu q^\alpha/m_w^2}{q^2 - m_w^2 - i\Gamma_w m_w} \\ J_{L\alpha} &= \overline{u}(p_\nu)\gamma_\alpha P_L v(p_e) \qquad (3.51)\end{aligned}$$

Squaring and summing over polarizations:

$$\begin{aligned}\sum_{pol}|A(t\to be^+\nu)|^2 &= \sum_{q\,pol} M_\mu^\dagger M_\nu \cdot D_w^{*\mu\alpha} D_w^{\nu\beta}\cdot L_{\alpha\beta}(p_\nu, p_e) \\ L^{\alpha\beta}(k,l) &= 2\left[k^\alpha l^\beta + k^\beta l^\alpha - g^{\alpha\beta} k\cdot l + i\epsilon^{\alpha\beta\rho\eta}k_\rho l_\eta\right]\end{aligned}$$

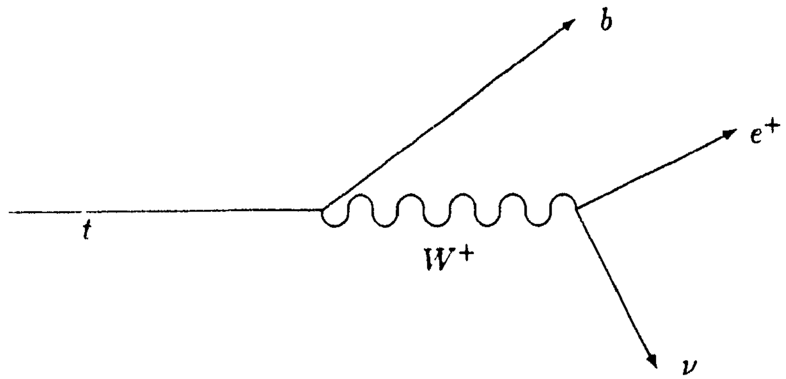

Figure 3.5: The decay $t \to b e^+ \nu$

Inserting 3.47 for $M^\dagger M$ into this:

$$
\begin{aligned}
\sum_{pol} |A(tbe\nu)|^2 &= C_1 \cdot x_e(1 - x_e) \left\{ (1 + 2a + 2b) - \frac{2b}{x_e} \hat{m}^2_{e\nu} \right\} |D_w(\hat{m}^2_{e\nu})|^2 \\
|D_w(\hat{m}^2_{e\nu})| &= \left[(\hat{m}^2_{e\nu} - \hat{m}^2_w)^2 + \Gamma^2_w \hat{m}^2_w \right]^{-1} \\
x_e &= 2E_e/m_t \\
m_{e\nu} &= (p_e + p_\nu)^2 \qquad (3.52)
\end{aligned}
$$

where "$\hat{m}$" denotes "m/m_t" for each m, and C_1 is a numerical constant that does not concern us. The decay width is obtained by multiplying 3.52 by the three body phase space [46] (see also section 6.5):

$$
\begin{aligned}
d^3\Gamma_{tbe\nu} &= \sum_{pol} |A(x_e, \hat{m}^2_{e\nu})|^2 d(3BPS, p_b, p_e, p_\nu) \\
\frac{d^3\Gamma_{tbe\nu}}{d^3 p_e/2E_e} &= C_2 \sum_{pol} \int_0^{x_e} |A(x_e, \hat{m}^2_{e\nu})|^2 d(\hat{m}^2_{e\nu}) \qquad (3.53)
\end{aligned}
$$

where we have neglected all final particle masses in 3.53, and C_2 is another inconsequential numerical constant.

3.4.3 $\Gamma_t^{(0)}$ and the Equivalence Theorem

Let us now discuss the top width at tree level. To lowest order, we may extract the parameters "a" and "b" in 3.46 from the non-renormalized Lagrangian 3.32:

$$
a = \frac{g_0}{\sqrt{2}} \qquad b = 0 \qquad (3.54)
$$

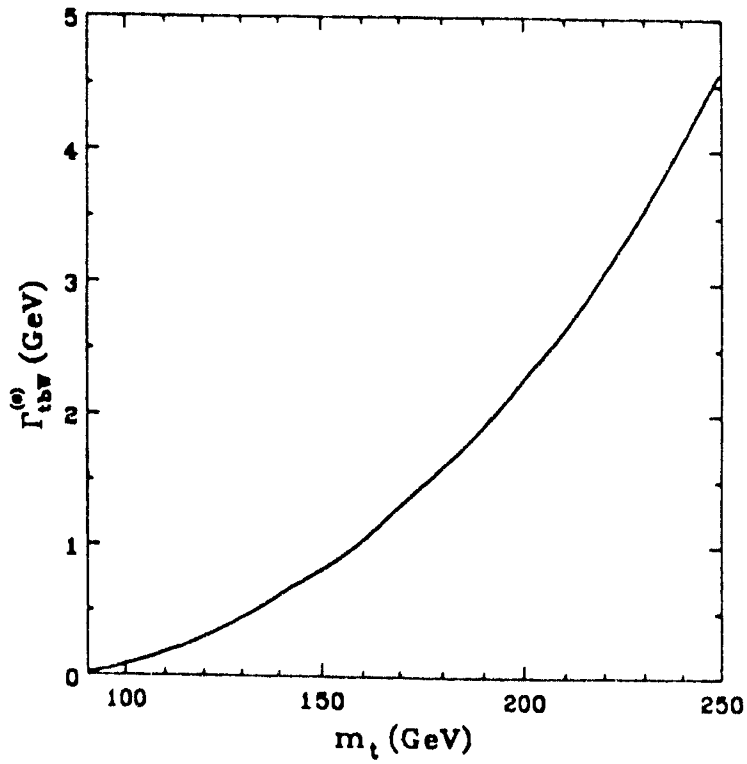

Figure 3.6: The top width to lowest order

The general formula 3.50 thus becomes:

$$\Gamma_t^{(0)} = \frac{1}{16} m_t \frac{\alpha_{em}}{s_w^2} \left(1 - \frac{m_w^2}{m_t^2}\right)^2 \left(\frac{m_t^2}{m_w^2} + 2\right) \tag{3.55}$$

where we have used the zeroth order, tree, relation:

$$\epsilon = g \sin\theta_w$$

This zeroth order width for the decay $t \rightarrow bW^+$ is graphed in figure 3.6. Evidently, the top width becomes very large.

For m_t large in comparison to m_w, $\Gamma_t^{(0)}$ in equation 3.55 becomes:

$$\Gamma_t^{(0)} = \frac{1}{16} \frac{\alpha_{em}}{s_w^2} \cdot \frac{m_t^3}{m_w^2} \tag{3.56}$$

As a decaying particle mass becomes larger that all other masses in the problem we expect on the basis of dimensional analysis that the particle width behave as:

$$\Gamma \sim \alpha M$$

where α is the coupling strength of the interaction mediating the decay. So what is going on here, where the decay width is going as m_t^3 rather than m_t?

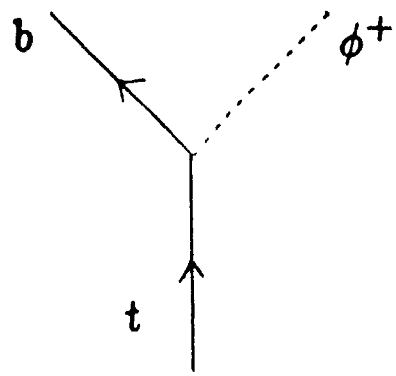

Figure 3.7: Equivalence theorem view of top decay

This behaviour may be understood [47] by recalling the equivalence theorem of spontaneously broken gauge theories [48]. It asserts that any process involving longitudinally polarized gauge bosons is well approximated by replacing these bosons with the associate would-be Goldstone bosons that they mix with, *in the limit that the energy of the gauge boson is large compared to the mass of the gauge boson* For large m_t, the W^+ energy E_w approaches $m_t/2$, so that the E_w/m_w does indeed become much larger than 1.

Toward an equivalence theorem calculation of the top width, recall how t and b couple to ϕ^+ and the Higgs (see 2 22)

$$g_t\phi^+\bar{t}b + g_t\left(\frac{H+v}{\sqrt{2}}\right)\bar{t}t \tag{3.57}$$

Thus (recalling the analogous formula for m_w):

$$m_t = \frac{1}{\sqrt{2}}g_t v \qquad m_w = \frac{1}{2}gv \tag{3.58}$$

We now use 3.57 to compute the rate for the decay $t \to b\phi^+$, depicted in figure 3.7:

$$\begin{aligned}\frac{1}{2}\sum_{pol}|M_{tb\phi}|^2 &= g_t^2\,\frac{1}{2}tr\{(\not{p}_t + m_t)\not{p}_b\} \\ &= g_t^2\,2p_t\cdot p_b \quad = g_t^2 m_t^2 + O(\frac{m_w^2}{m_t^2})\end{aligned} \tag{3.59}$$

By comparison, the large m_t limit of equation 3.49 for the zero order (see equation 3.54) $t \to bW^+$ decay amplitude squared is:

$$\frac{1}{2}\sum_{pol}|M_{tbW}|^2 = \frac{g^2}{2}m_t^2\frac{m_t^2}{m_w^2}$$

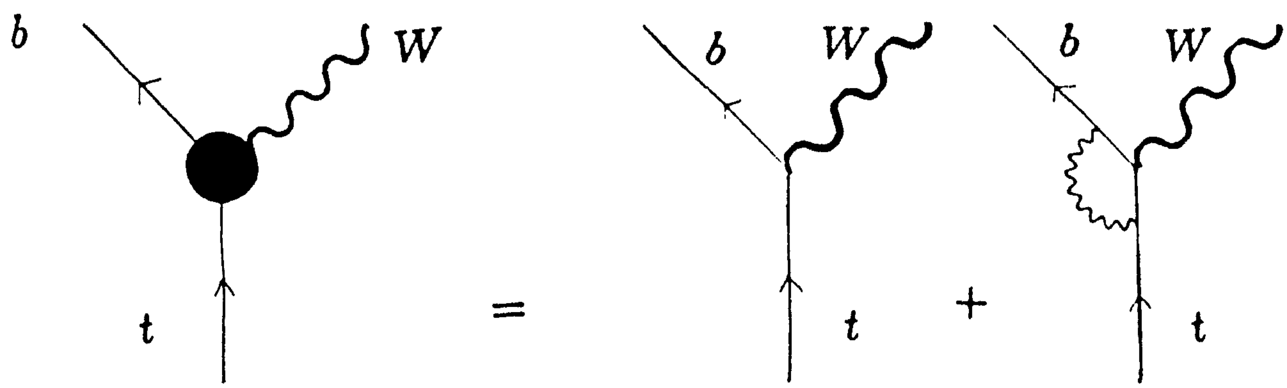

Figure 3.8: The t-b-W^+ vertex to first order

$$= m_t^2 \frac{g^2}{2} \frac{m_t^2}{g^2 v^2/4} \quad = g_t^2 m_t^2 \tag{3.60}$$

These two equations are identical. Thus the m_t^3 behaviour of the top width makes sense in the context of the equivalence theorem, if we assume that the decay width for a heavy top is dominated by longitudinally polarized W^+'s in the final state.

3.4.4 Vertex Function to First Order

t-b-W^+ Vertex Function

The t-b-W^+ vertex to first order is depicted in figure 3.8. The particular 1-loop vertex correction diagram shown there is generic; the precise combination of such diagrams relevant to our process will be presented in the next chapter. Right now I only want to write a general expression for the second diagram(s) to the right of the "=" sign in figure 3.8. Anticipating the results of the next chapter, each of these loop diagrams which generate the leading m_t^2 dependence is proportional to:

$$\frac{g_0}{\sqrt{2}} \cdot g_t^2$$

Combining this with the discussion of section 3.4.1 wherein we deduced the most general form of the vertex function, we can say that expressions associated with these one-loop diagrams will always have the form:

$$\Lambda^\mu \equiv \frac{g_0}{\sqrt{2}}\left[\lambda\gamma^\mu P_L + \alpha\frac{p_t^\mu}{m_t}P_R\right] \tag{3.61}$$

where

$$\lambda, \alpha \sim g_t^2$$

Now consider the first diagram to the left of the "=" sign in figure 3.8. It represents the tree level t-b-W coupling obtained from the renormalized Lagrangian 3.34 of the last chapter:

$$L_r^{tb} = \bar{t}(\not{\partial} - m_t)t + \bar{b}\not{\partial}b + \frac{g_0}{\sqrt{2}}(Z_{tL}Z_{bL}Z_W)^{1/2}\,\bar{t}\not{W}b$$

We will require formulae for the Z's beyond zeroth order, where they were $\equiv 1$. This will be done using equations 3.31, in the next chapter. For now, we need only note:

$$Z^{1/2} = (1+\delta Z)^{1/2} = 1 + \delta Z/2 + \quad O(\delta Z^2) \tag{3.62}$$

where:

$$\delta Z \sim g_t^2$$

Putting all this together, we obtain an expression for the vertex function from the diagrams of figure 3.8.

$$\begin{aligned}\Gamma^{(1)\mu}_{tbw} &= \frac{g_0}{\sqrt{2}}(Z_{tL}Z_{bL}Z_w)^{1/2}\gamma^\mu P_L + \frac{g_0}{\sqrt{2}}\left[\lambda\gamma^\mu P_L + \alpha\frac{p_t^\mu}{m_t}P_R\right]\\ &= \frac{g_0 Z_w^{1/2}}{\sqrt{2}}\left[1 + \frac{\delta Z_{tL}+\delta Z_{bL}}{2} + \lambda\right]\gamma^\mu P_L + \frac{g_0}{\sqrt{2}}\alpha\frac{p_t^\mu}{m_t}P_R + \quad O(\delta Z^2)\end{aligned} \tag{3.63}$$

(see equation 3.69). This contains the annoying bare parameter g_0, whose elimination we now discuss.

W^+-e-ν Vertex Function

To proceed further, we must compute $W^+ \to e^+\nu$ decay to the same order in perturbation theory, since this is one of the input experiments in our renormalization scheme (see 3.40). More precisely, in equation 3.41, we defined the quantity $g^{e\nu}$ via:

$$\Gamma^\mu_{We\nu}(q^2 = m_W^2, p_e^2 = 0) \equiv i\frac{g^{e\nu}}{\sqrt{2}}\gamma^\mu P_L + f_2\sigma^{\mu\nu}q_\nu + \cdots \tag{3.64}$$

The right hand side represents the experimental data, and we assume it known (see section 3.3.1). The left hand side is the W^+-e-ν vertex function, which is described in our model to first order by the diagrams in figure 3.9.

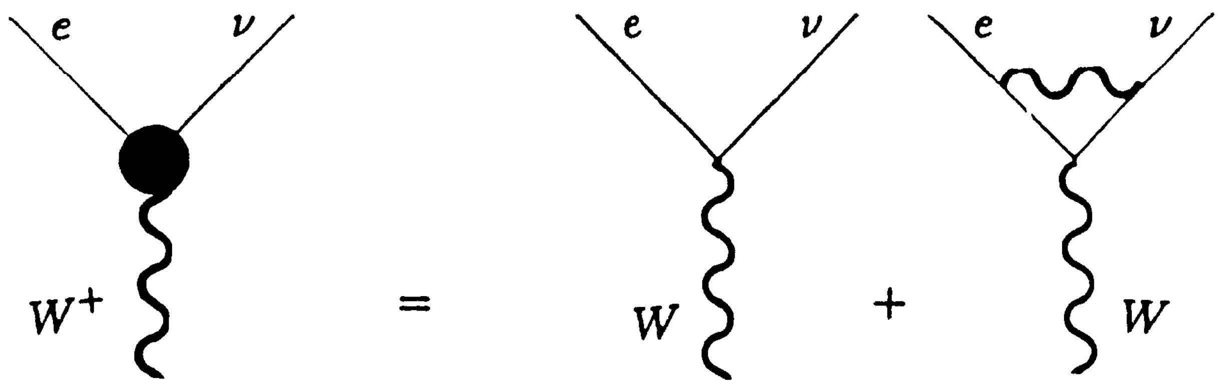

Figure 3.9: The W^+-e^+-ν vertex to first order

Proceeding analogously to the t-b-W^+ case above, we recall the renormalized W^+-e-ν Lagrangian (3.35):

$$L_r^{e\nu} = \bar{e}\not{\partial}e + \bar{\nu}_e\not{\partial}\nu_e + \frac{g_0}{\sqrt{2}}(Z_{eL}Z_{\nu L}Z_W)^{1/2}\,\bar{\nu}\not{W}e$$

Also, the arguments of section 3.4.1 for the general form of the vertex function are applicable here, so we obtain:

$$\Gamma^{(1)\mu}_{we\nu} = \frac{g_0}{\sqrt{2}}(Z_{\nu L}Z_{eL}Z_w)^{1/2}\gamma^\mu P_L + \frac{g_0}{\sqrt{2}}\left[\lambda^{(e\nu)}\gamma^\mu P_L + \alpha^{(e\nu)}\frac{p_\nu^\mu}{m_t}P_R\right] \quad (3.65)$$

$\lambda^{(e\nu)}$ and $\alpha^{(e\nu)}$ represent the results of a one loop calculation, but there are no irreducible one loop feynman diagrams for the W^+-e-ν vertex that even contain the top quark. Hence they can have *no* m_t dependence and must be proportional to:

$$\lambda^{(e\nu)}, \alpha^{(e\nu)} \sim g_0^2$$

Similarly, the lepton self-energies to one loop order cannot be functions of m_t so that δZ_e, δZ_ν are also of order:

$$\delta Z_{eL}, \delta Z_{\nu L} \sim g_0^2$$

Hence the vertex function becomes:

$$\Gamma^{(1)\mu}_{we\nu} = i\frac{g_0 Z_w^{1/2}}{\sqrt{2}}\gamma^\mu P_L + O(g_0^2) \quad (3.66)$$

Comparison with equation 3.64 yields the relation between g_0 and the observable $g^{e\nu}$:

$$g^{e\nu} = g_0 Z_w^{1/2} \quad + \quad O(g_0^2) \tag{3.67}$$

Final Formula for t-b-W^+ Vertex

Using 3.67 to eliminate g_0 from 3.63 we finally obtain:

$$\Gamma^{(1)\mu}_{tbw} = \frac{g^{e\nu}}{\sqrt{2}}\left[1 + \frac{\delta Z_{tL} + \delta Z_{bL}}{2} + \lambda\right]\gamma^\mu P_L + \frac{g^{e\nu}}{\sqrt{2}}\alpha\left(\frac{p_t}{m_t}\right)P_R \tag{3.68}$$

where we used the fact that

$$g^{e\nu} = g_0 \quad + O(\delta Z_w) \tag{3.69}$$

to replace g_0 by $g^{e\nu}$ in the terms already of order g_t^2, even if g_0 *isn't* accompanied by the factor $Z_w^{1/2}$. Equation 3.68, when combined with 3.50 for Γ_t, tells us almost everything we need to know. All that remains is to compute the feynman diagrams.

As an aside, I would like to point out the Z_w *does* have an m_t^2 dependent part, coming from the diagram in figure 2.4. Its contribution drops out in our scheme, though, because in both our decay and the reference experiment, the W^+ is on-shell.

3.4.5 Deviations from Tree Level

Decay Rate Deviation

Using our expression 3.68 for the vertex function, and equations 3.50, 3.55 for the first and zeroth order $t \to bW^+$ decay widths respectively, we obtain:

$$\begin{aligned}\Gamma_t^{(1)} - \Gamma_t^{(0)} &= \frac{1}{32\pi}m_t\left(1 - \frac{m_w^2}{m_t^2}\right)^2\left(\frac{g_{e\nu}^2}{2}\right) \\ &\quad \times\left[(2\lambda + \delta Z_{tL} + \delta Z_{bL})(\frac{m_t^2}{m_w^2} + 2) + \alpha(\frac{m_t^2}{m_w^2} - 1)\right]\end{aligned} \tag{3.70}$$

$$\begin{aligned}\frac{\Gamma_t^{(1)} - \Gamma_t^{(0)}}{\Gamma_t^{(0)}} &= 2\lambda + \delta Z_{tL} + \delta Z_{bL} + \left(\frac{m_t^2 - m_w^2}{m_t^2 + 2m_w^2}\right)\alpha \\ &= 2\lambda + \alpha + \delta Z_{tL} + \delta Z_{bL} \quad + O(\frac{m_w^2}{m_t^2})\end{aligned} \tag{3.71}$$

Decay Spectrum Deviation

We now consider deviations in the lepton energy spectrum produced by radiative corrections. Note that we may set:

$$d^3p_e/2E_e \ = \ 2\pi E_e dE_e$$

since the e^+ solid angle just describes the overall orientation of the decay plane, and we are averaging over the top polarizations. Thus we may write:

$$\begin{aligned}
\frac{d\Delta\Gamma_{tbe\nu}/dx_e}{d\Gamma^{(0)}_{tbe\nu}/dx_e} &\equiv \frac{d\Gamma^{(1)}_{tbe\nu}/dx_e - d\Gamma^{(0)}_{tbe\nu}/dx_e}{d\Gamma^{(0)}_{tbe\nu}/dx_e} \\
&= \left[\frac{d^3\Gamma^{(1)}_{tbe\nu}}{d^3p_e/2E_e} - \frac{d^3\Gamma^{(0)}_{tbe\nu}}{d^3p_e/2E_e}\right] \Bigg/ \frac{d^3\Gamma^{(0)}_{tbe\nu}}{d^3p_e/2E_e} \qquad (3.72)
\end{aligned}$$

We can now use our equations 3.53 and 3.68 to obtain:

$$\frac{d\Delta\Gamma_{tbe\nu}/dx_e}{d\Gamma^{(0)}_{tbe\nu}/dx_e} = \frac{\int_0^{x_e} d(\hat{m}^2_{e\nu})|D_w(\hat{m}^2_{e\nu})|^2 \left[\lambda + \alpha + (\delta Z_{tL} + \delta Z_{bL})/2 - \alpha/x_e\right]}{\int_0^{x_e} d(\hat{m}^2_{e\nu})|D_w(\hat{m}^2_{e\nu})|^2} \qquad (3.73)$$

Further making the "narrow width" approximation:

$$\begin{aligned}
|D_w(\hat{m}^2_{e\nu})| &= \left[(\hat{m}^2_{e\nu} - \hat{m}^2_w)^2 + \hat{\Gamma}^2_w \hat{m}^2_w\right]^{-1} \\
&= \frac{\pi}{\hat{\Gamma}_w}\delta(\hat{m}^2_{e\nu} - \hat{m}^2_w) \quad + O(1) \qquad (3.74)
\end{aligned}$$

(which just asserts the majority of the time the W^+ is on-shell), we obtain:

$$\frac{d\Delta\Gamma_{tbe\nu}/dx_e}{d\Gamma^{(0)}_{tbe\nu}/dx_e} = \left[\lambda + \alpha + \frac{\delta Z_{tL} + \delta Z_{bL}}{2} - \frac{\alpha}{x_e}\right] \cdot \theta\left(x_e - \frac{m^2_w}{m^2_t}\right) \qquad (3.75)$$

3.5 Feynman Diagrams

We have obtained formulae 3.71,3.75 for the observable quantities in terms of δZ_{tL}, δZ_{bL}, λ, and α. These are in turn expressed in terms of Feynman diagrams via equations 3.31 and 3.40:

$$\begin{aligned} Z_L &= 1 - Re\left\{\Sigma_L + m^2 \frac{\partial}{\partial p^2}\left[\Sigma_L + \Sigma_R + 2\Sigma_s\right]\right\}_{m^2} \\ Z_R &= 1 - Re\left\{\Sigma_R + m^2 \frac{\partial}{\partial p^2}\left[\Sigma_L + \Sigma_R + 2\Sigma_s\right]\right\}_{m^2} \end{aligned}$$

$$\Lambda^\mu \equiv \frac{ig_0}{\sqrt{2}}\left[\lambda\gamma^\mu P_L + \alpha\left(\frac{p_t^\mu}{m_t}\right)P_R\right]$$

These quantities are in turn computed perturbatively using Feynman diagram techniques.

3.5.1 Leading m_t Dependence

The identification of the Feynman diagrams which are leading order in:

$$g_t^2 = g^2\frac{m_t^2}{2m_w^2}$$

is simplest in the Feynman-t'Hooft, or $\xi = 1$ gauge, where the degree of divergence of a diagram may be determined by naive power counting. As discussed in the decoupling theorem [30], the large mass behaviour of an amplitude "A" is in general related to its degree of divergence "d" by:

$$\begin{aligned} A &\propto m^d && for\ d \neq 0 \\ A &\propto \log(m) && for\ d = 0 \end{aligned} \qquad (3.76)$$

However, the above neglects the possibility of couplings proportional to the heavy particle mass. Thus in the case of the standard model with m_t also being essentially the scalar-top coupling, we finally obtain the following rule:

> *The leading m_t dependence originates in the most divergent Feynman diagrams containing the most scalar bosons coupled to top quarks.*

In our problem, we will have two types of diagrams:

1. fermion self energy diagrams
2. vertex correction diagrams

Simple analysis reveals that in both cases, the associated amplitudes can be at most logarithmically divergent. Thus our problem is now reduced to finding and computing the logarithmically divergent diagrams containing the most number of scalar-top vertices.

3.5.2 Feynman Rules

With the following choice of parameters:

1. $V_{tb} \equiv 1$
2. $m_b \equiv 0$

here are the standard model tree level vertex functions [49] that we will need.

- H-t-$\bar{t}$: $\dfrac{-ig_t}{\sqrt{2}}$
- ϕ^0-t-$\bar{t}$: $\dfrac{-g_t}{\sqrt{2}}\gamma_5$
- ϕ^--t-$\bar{b}$: $ig_t P_L$
- ϕ^+-$\bar{t}$-b: $ig_t P_R$
- W^+-$\bar{t}$-b: $i\dfrac{g}{\sqrt{2}}\gamma^\mu P_L$
- W^+-ϕ^--H: $\dfrac{ig}{2}(p_{\phi^-} - p_h)^\mu$
- W^+-ϕ^--ϕ^0: $\dfrac{g}{2}(p_{\phi^-} - p_{\phi^0})^\mu$

3.5.3 Self Energy Diagrams

Define the two functions "A, B" [50]:

$$
\begin{aligned}
A(p^2, m_f^2, m_s^2) &\equiv \int \frac{d^4 l}{(2\pi)^4} \frac{1}{(p-l)^2 - m_f^2 - i\epsilon} \frac{1}{l^2 - m_f^2 - i\epsilon} \\
&= \frac{1}{16\pi^2}\left\{C_{UV} - \int_0^1 dx \cdot \log[D_2(p^2, m_f^2, m_s^2)/\mu^2]\right\} \\
B(p^2, m_f^2, m_s^2)p^\mu &\equiv \int \frac{d^4 l}{(2\pi)^4} \frac{(p-l)^\mu}{(p-l)^2 - m_f^2 - i\epsilon} \frac{1}{l^2 - m_f^2 - i\epsilon} \\
B(p^2, m_f^2, m_s^2) &= \frac{1}{16\pi^2}\left\{\frac{1}{2}C_{UV} - \int_0^1 dx\,(1-x) \cdot \log[D_2(p^2, m_f^2, m_s^2)/\mu^2]\right\} \\
D_2(p^2, m_f^2, m_s^2) &= m_f^2 x + m_s^2(1-x) - p^2 x(1-x) - i\epsilon \\
C_{UV} &= \frac{1}{\varepsilon} - \gamma_E + \log(4\pi)
\end{aligned}
$$

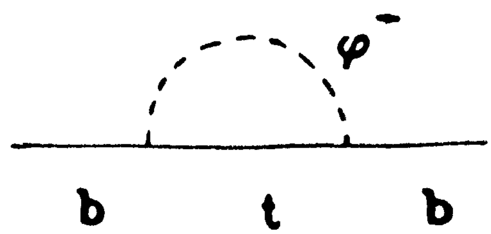

Figure 3.10: m_t^2 contribution to b quark self energy

Thus we have:

$$
\begin{aligned}
\frac{\partial}{\partial p^2} A(p^2, m_f^2, m_s^2) &= \frac{1}{16\pi^2} \int_0^1 dx \frac{-x(1-x)}{D_2(p^2, m_f^2, m_s^2)} \\
\frac{\partial}{\partial p^2} B(p^2, m_f^2, m_s^2) &= \frac{1}{16\pi^2} \int_0^1 dx \frac{-x(1-x)^2}{D_2(p^2, m_f^2, m_s^2)}
\end{aligned}
$$

b-quark Self Energy

There is only one b-quark self energy diagram that is of order g_t^2, shown in figure 3.10. Using the couplings in section 3.5.2:

$$
\begin{aligned}
\Sigma^b(p) &= (ig_t)^2 \int \frac{d^4 l}{(2\pi)^4} \frac{P_R(\not{p} - \not{l} + m_t) P_L}{[(p-l)^2 - m_t^2]\,[l^2 - m_w^2]} \\
&= -g_t^2 B(p^2, m_t^2, m_w^2) \not{p} P_L
\end{aligned}
$$

t-quark Self Energy

There are three t-quark self-energy diagrams of order g_t^2, shown in figure 3.11.

$$
\Sigma^t(p) = \Sigma^{tH}(p) + \Sigma^{tz}(p) + \Sigma^{tw}(p)
$$

where, using the couplings in section 3.5.2, we obtain:

$$
\begin{aligned}
\Sigma^{th}(p) &= \left(\frac{-ig_t}{\sqrt{2}}\right)^2 \int \frac{d^4 l}{(2\pi)^4} \frac{(\not{p} - \not{l} + m_t)}{[(p-l)^2 - m_t^2]\,[l^2 - m_h^2]} \\
&= -\frac{1}{2} g_t^2 B(p^2, m_t^2, m_h^2) \not{p} \; - \; \frac{1}{2} g_t^2 A(p^2, m_t^2, m_h^2) m_t
\end{aligned}
$$

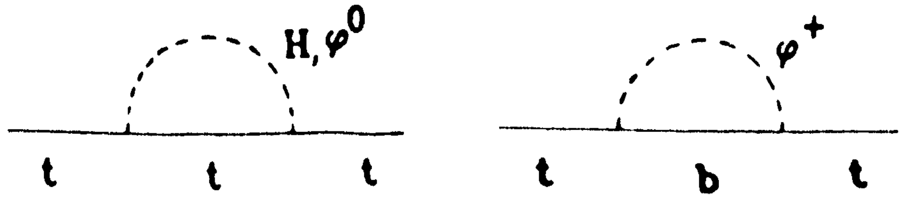

Figure 3.11: m_t^2 contribution to t quark self energy

$$\begin{aligned}\Sigma^{tz}(p) &= \left(\frac{-g_t}{\sqrt{2}}\right)^2 \int \frac{d^4l}{(2\pi)^4} \frac{\gamma_5(\not p - \not l + m_t)\gamma_5}{[(p-l)^2 - m_t^2][l^2 - m_z^2]} \\ &= -\frac{1}{2} g_t^2 B(p^2, m_t^2, m_z^2)\not p + \frac{1}{2} g_t^2 A(p^2, m_t^2, m_z^2) m_t\end{aligned}$$

$$\begin{aligned}\Sigma^{tw}(p) &= (-ig_t)^2 \int \frac{d^4l}{(2\pi)^4} \frac{P_L(\not p - \not l + m_t)P_R}{[(p-l)^2 - m_b^2][l^2 - m_w^2]} \\ &= -g_t^2 B(p^2, 0, m_w^2)\not p P_R\end{aligned}$$

Collecting these results and writing them in the form 3.21:

$$\begin{array}{lll} \Sigma_L^b = -g_t^2 B(p^2, m_t^2, m_w^2) & \Sigma_R^b = 0 & \Sigma_s^b = 0 \\ \Sigma_L^{th} = -\frac{1}{2} g_t^2 B(p^2, m_t^2, m_h^2) & \Sigma_R^{th} = \Sigma_L^{th} & \Sigma_s^{th} = -\frac{1}{2} g_t^2 A(p^2, m_t^2, m_h^2) \\ \Sigma_L^{tz} = -\frac{1}{2} g_t^2 B(p^2, m_t^2, m_z^2) & \Sigma_R^{tz} = \Sigma_L^{tz} & \Sigma_s^{tz} = +\frac{1}{2} g_t^2 A(p^2, m_t^2, m_z^2) \end{array}$$

$$\Sigma_L^{tw} = 0 \quad \Sigma_R^{tw} = -g_t^2 B(p^2, 0, m_w^2) \quad \Sigma_s^{tw} = 0$$

3.5.4 Computation of Z_{tL}, Z_{bL}

We now compute the δZ's, using equations 3 31 quoted at the beginning of this section.

$$\begin{aligned}\delta Z_{bL} + \delta Z_{tL} &= -\left[\Sigma_L^{th} + \Sigma_L^{tz} + \Sigma_L^b + Re\,E\right] \\ &= \frac{1}{2} g_t^2 \left[B(m_t^2, m_t^2, m_h^2) + B(m_t^2, m_t^2, m_z^2) + 2B(0, m_t^2, m_w^2)\right] - Re\,E \\ &= \frac{g_t^2}{16\pi^2}\left[C_{UV} - \int_0^1 dx(1-x)\log\left(F/\mu^4\right)\right] - Re\,E \qquad (3\ 77)\end{aligned}$$

$$F(x) = \left[D_2(m_t^2, m_t^2, m_h^2) D_2(m_t^2, m_t^2, m_z^2)\right]^{1/2} D_2(0, m_t^2, m_w^2)$$

$$\begin{aligned}
E &= 2m_t^2 \frac{\partial}{\partial p^2}\left[\Sigma_L^{th} + \Sigma_s^{th} + \Sigma_L^{tz} + \Sigma_s^{tz} + \frac{1}{2}\Sigma_R^{tw}\right]_{m_t^2} \\
&= -g_t^2 m_t^2 \frac{\partial}{\partial p^2}\left[B(p^2, m_t^2, m_h^2) + A(m_h^2) + B(m_z^2) - A(m_z^2) + B(p^2, 0, m_w^2)\right] \\
&= \frac{g_t^2}{16\pi^2}\int_0^1 dx\, x(1-x)\left[\frac{1-x+1}{D_2(1,1,\hat{m}_h^2)} + \frac{1-x-1}{D_2(1,1,\hat{m}_z^2)} + \frac{1-x}{D_2(1,0,\hat{m}_w^2)}\right]
\end{aligned}$$

Note that:

$$\begin{aligned}
D_2(1,1,\hat{m}_s^2) &= x^2 + \hat{m}_s^2(1-x) \\
D_2(1,0,\hat{m}_w^2) &= (1-x)(\hat{m}_w^2 - x) - i\epsilon
\end{aligned}$$

The first is positive definite for $0 \le x \le 1$, but the second has a zero within the integration interval. Using:

$$\frac{1}{x - i\epsilon} = P\left(\frac{1}{x}\right) + i\pi\delta(x)$$

we obtain:

$$\begin{aligned}
Re\,E &= \frac{g_t^2}{16\pi^2}\int_0^1 x(1-x)\left[\frac{2-x}{D_2(1,1,\hat{m}_h^2)} + \frac{-x}{D_2(1,1,\hat{m}_z^2)}\right] \\
&+ \frac{g_t^2}{16\pi^2}\left[-\frac{1}{2} + \hat{m}_w^2 + \hat{m}_w^2(\hat{m}_w^2 - 1)\log(1 - \hat{m}_w^{-2})\right] \qquad (3.78)
\end{aligned}$$

3.5.5 Vertex Correction Diagrams

There are only two vertex correction diagrams that are proportional to g_t^2, shown in figure 3.12. All other diagrams are either manifestly convergent by power counting and thus $\propto \frac{1}{m_t^2}$, or are proportional to g_0^2 or $g_b \equiv 0$.

From "H" part of diagram 3.12 we obtain:

$$\begin{aligned}
\Lambda_h^\mu &= \frac{-ig_t}{\sqrt{2}}(ig_t)\frac{ig_t}{2}\int\frac{d^4l}{(2\pi)^4}\frac{P_R(\not{l} + m_t)\cdot 2(l-p_t)^\mu}{(l^2 - m_t^2)[(l-p_t)^2 - m_h^2][(l-p_b^2) - m_w^2]} \\
&= \frac{ig}{\sqrt{2}}\left[\lambda_h\gamma^\mu P_L + \alpha_h\left(\frac{p_t^\mu}{m_t}\right)P_R\right] \\
\lambda_h &= \frac{g_t^2}{32\pi^2}\left\{-\frac{1}{2}C_{UV} + \int_0^1\int_0^1 dx\,dy\,y\log\left(D_3(m_h^2)/\mu^2\right)\right\} \\
\alpha_h &= \frac{g_t^2}{16\pi^2}\int_0^1\int_0^1 dx\,dy\,\frac{y(1-y)(xy-y-1)}{D_3(m_h^2)/m_t^2} \qquad (3.79)
\end{aligned}$$

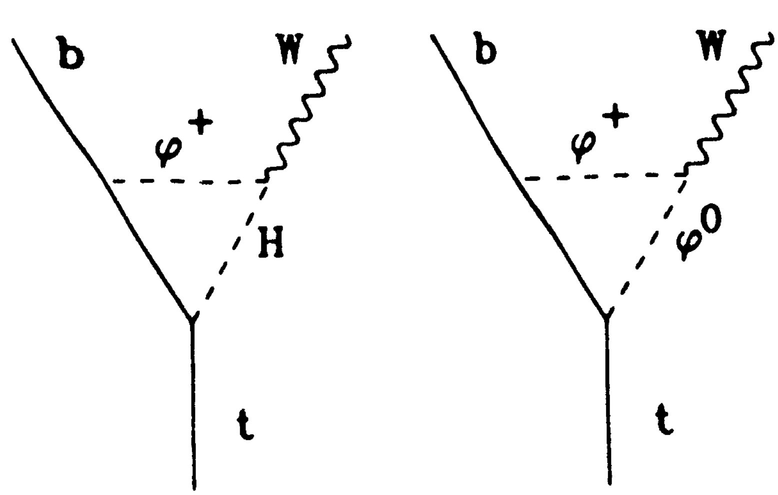

Figure 3.12: m_t^2 contributions to t-b-W^+ vertex

From ϕ^0 part of diagram 3.12 we obtain:

$$
\begin{aligned}
\Lambda^\mu &= \frac{-g_t}{\sqrt{2}}(ig_t)\frac{g_t}{2}\int \frac{d^4 l}{(2\pi)^4}\frac{P_R(\not{l}+m_t)\gamma_5\cdot 2(l-p_t)^\mu}{(l^2-m_t^2)[(l-p_t)^2-m_h^2][(l-p_b^2)-m_w^2]} \\
&= \frac{ig}{\sqrt{2}}\left[\lambda_z\gamma^\mu P_L + \alpha_z\left(\frac{p_t^\mu}{m_t}\right)P_R\right] \\
\lambda_z &= \frac{-g_t^2}{32\pi^2}\left\{-\frac{1}{2}C_{UV} + \int_0^1\int_0^1 dx\,dy\,y\log\left(D_3(m_z^2)/\mu^2\right)\right\} \\
\alpha_z &= \frac{g_t^2}{16\pi^2}\int_0^1\int_0^1 dx\,dy\,\frac{y(1-y)(xy-y+1)}{D_3(m_z^2)/m_t^2}
\end{aligned}
\tag{3.80}
$$

where:

$$
\begin{aligned}
m_t^{-2}D_3^{(s)} \equiv D_3(m_s^2)/m_t^2 &= (1-y) + y^2(1-x) - y^2x(1-x)\hat{q}_w^2 \\
&\quad + xy\hat{m}_w^2 + y(1-x)(\hat{m}_s^2 - 1)
\end{aligned}
$$

Finally, λ, α of 3.61 are given by:

$$
\begin{aligned}
\lambda &= \lambda_h + \lambda_z \\
\alpha &= \alpha_h + \alpha_z
\end{aligned}
\tag{3.81}
$$

3.6 Results

3.6.1 Cutoff Independence

Inspection of the formulae of the last section reveals that some of the quantities λ, α, δZ_{tL}, δZ_{bL} contain the regulator:

$$C_{UV} = \frac{1}{\varepsilon} - \gamma_E + \log(4\pi)$$

and the meaningless scale parameter μ^2. We will now see that both of these disappear in the expressions for the observables. To do so, first note that α_h and α_z in 3.79 and 3 80 are already free of such dependence. Next, observe that both of the observables 3.71 and 3.75 are functions of only the combination:

$$X \equiv 2\lambda + \delta Z_{tL} + \delta Z_{bL}$$

whose regulator dependent parts we now study.

$$\begin{aligned}
\lambda_h + \lambda_z &= \frac{g_t^2}{32\pi^2}\left[-C_{UV} + \int_0^1\int_0^1 dx\,dy\,y\log\left(D_3^{(h)}D_3^{(z)}/\mu^4\right)\right] \\
\delta Z_{bL} + \delta Z_{tL} &= \frac{g_t^2}{16\pi^2}\left[C_{UV} - \int_0^1 dx(1-x)\log\left(F(x)/\mu^4\right) - ReE\right]
\end{aligned}$$

Therefore:

$$\begin{aligned}
X &= \frac{g_t^2}{16\pi^2}\left[\int_0^1\int_0^1 dx\,dy\,y\log\left\{D_3^{(h)}D_3^{(z)}/\mu^4\right\} - \int_0^1 dyy\log\left\{F(1-y)/\mu^4\right\} - ReE\right] \\
&= \frac{g_t^2}{16\pi^2}\left[\int_0^1\int_0^1 dx\,dy\,y\log\left\{D_3^{(h)}D_3^{(z)}/F(1-y)\right\} - ReE\right] \qquad (3.82)
\end{aligned}$$

Thus, as claimed, the regulator C_{UV} and the scale μ^2 will completely drop out of the final formulae.

3.6.2 The Final Result

We now make the replacement:

$$\frac{g_t^2}{16\pi^2} = \frac{g_{ev}^2}{32\pi^2}\frac{m_t^2}{m_w^2} \qquad (3.83)$$

in all our formulae: 3.71, 3.75, 3.77, 3.78, 3.79, 3.80, 3.81 3.82, to obtain the summary:

$$\frac{\Delta\Gamma_{tbw}}{\Gamma_{tbw}^{(0)}} = \frac{g_{ev}^2}{32\pi^2}\frac{m_t^2}{m_w^2}\left[\tilde{X} + \left(\frac{m_t^2 - m_w^2}{m_t^2 + 2m_w^2}\right)\tilde{\alpha}\right]$$

$$
\begin{aligned}
\frac{d\Delta\Gamma_{tbe\nu}/dx_e}{d\Gamma^{(0)}_{tbe\nu}/dx_e} &= \frac{g_{e\nu}^2}{32\pi^2}\frac{m_t^2}{m_w^2}\left[\frac{\tilde{X}}{2} + \left(1-\frac{1}{x_e}\right)\tilde{\alpha}\right]\cdot\theta\left(x_e - \frac{m_w^2}{m_t^2}\right) \\
\tilde{X} &\equiv X\Big/\frac{g_t^2}{16\pi^2} \\
&= \int_0^1\int_0^1 dx\,dy\,y\log\left[\hat{D}_3^{(h)}\hat{D}_3^{(z)}/\hat{F}(1-y)\right] - Re\,\hat{E} \\
\tilde{\alpha} &= \int_0^1\int_0^1 dx\,dy\,y(1-y)\left[\frac{(xy-y-1)}{\hat{D}_3^{(h)}} + \frac{(xy-y+1)}{\hat{D}_3^{(z)}}\right] \\
Re\tilde{E} &= \int_0^1 x(1-x)\left[\frac{2-x}{D_2(1,1,\hat{m}_h^2)} + \frac{-x}{D_2(1,1,\hat{m}_z^2)}\right] \\
&\quad -\frac{1}{2} + \hat{m}_w^2 + \hat{m}_w^2(\hat{m}_w^2-1)\log(1-\hat{m}_w^{-2}) \\
\hat{D}_3^{(s)} &= (1-y) + y^2(1-x) - y^2x(1-x)\hat{q}_w^2 \\
&\quad + xy\hat{m}_w^2 + y(1-x)(\hat{m}_s^2-1) \\
F(x) &= \left[D_2(1,1,\hat{m}_h^2)D_2(1,1,\hat{m}_z^2)\right]^{1/2}D_2(0,1,\hat{m}_w^2) \\
D_2(a,b,c;x) &= ax + b(1-x) - cx(1-x)
\end{aligned}
\qquad (3.84)
$$

To obtain the answer, we now require the value of $g_{e\nu}^2$. We will use the tree level relation $g = e/\sin\theta_w$, since the deviations in this relation show up as deviations to our deviation, and thus are unimportant

What remains is to evaluate the integrals, which I have done numerically, with the results shown in figure 3 13 and figure 3 14. We see the corrections are typically about about a tenth of a percent for a Higgs of mass greater than 100 GeV. The case of a 25-GeV Higgs is also included to illustrate that the 1/2% order of magnitude estimate we made in section 3 1 was essentially correct, of course, this value of m_h is ruled out by experiment

The above expressions take a simple form when m_t becomes large: Case 1. $m_t > m_h$:

$$
\begin{aligned}
\tilde{X}(m_t^2 > m_h^2, m_w^2) &= \frac{13}{4} - \log\left(\frac{m_t^2}{m_h^2}\right) \\
\tilde{\alpha}(m_t^2 > m_h^2, m_w^2) &= 1 \\
\Delta\Gamma/\Gamma &= \frac{\alpha_{em}}{8\pi s_w^2}\frac{m_t^2}{m_w^2}\left[\frac{17}{4} - \log\left(\frac{m_t^2}{m_h^2}\right)\right]
\end{aligned}
\qquad (3.85)
$$

Case 2: $m_h > m_t$

$$
\begin{aligned}
\tilde{X}(m_t^2 > m_h^2, m_w^2) &= \frac{9}{8} - \frac{1}{4}\log\left(\frac{m_t^2}{m_h^2}\right) \\
\tilde{\alpha}(m_t^2 > m_h^2, m_w^2) &= -\frac{1}{2}
\end{aligned}
$$

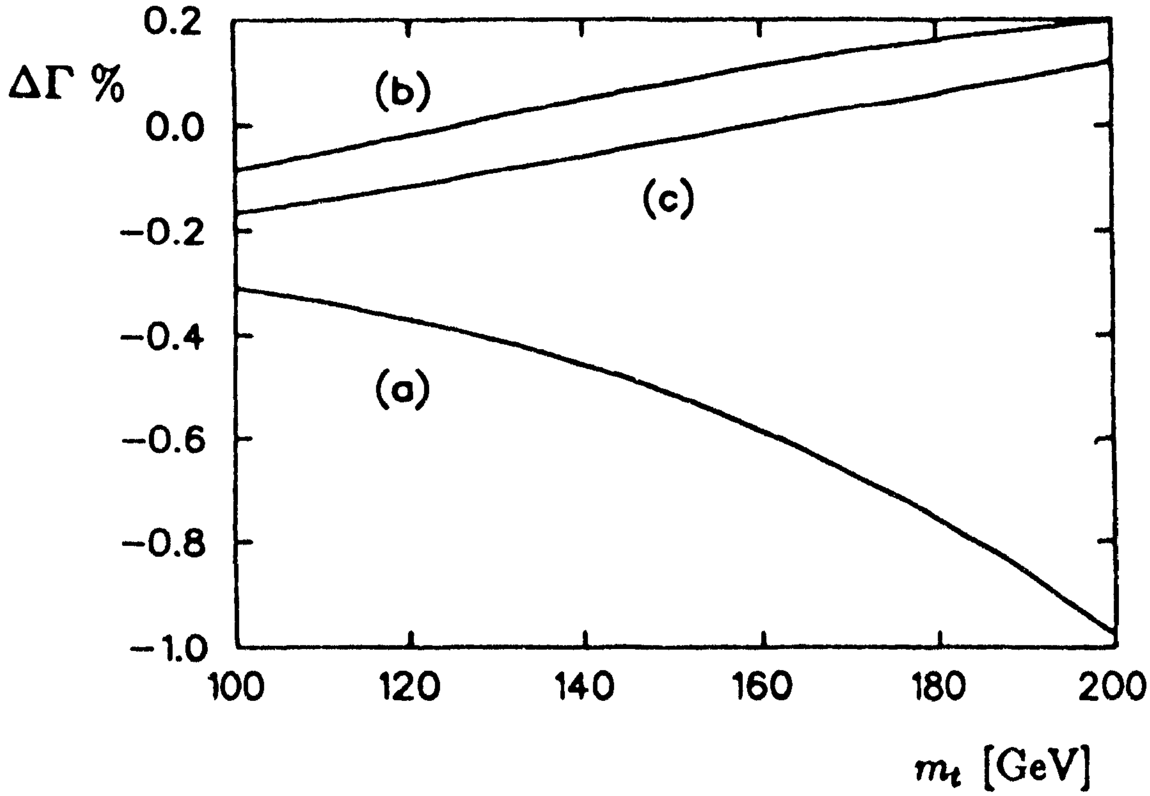

Figure 3.13: m_t^2 corrections to the tree level $t \rightarrow bW^+$ width as a function of m_t, for various values of m_h: (a) m_h=25 GeV, (b) = 1 TeV, (c) = 100 GeV.

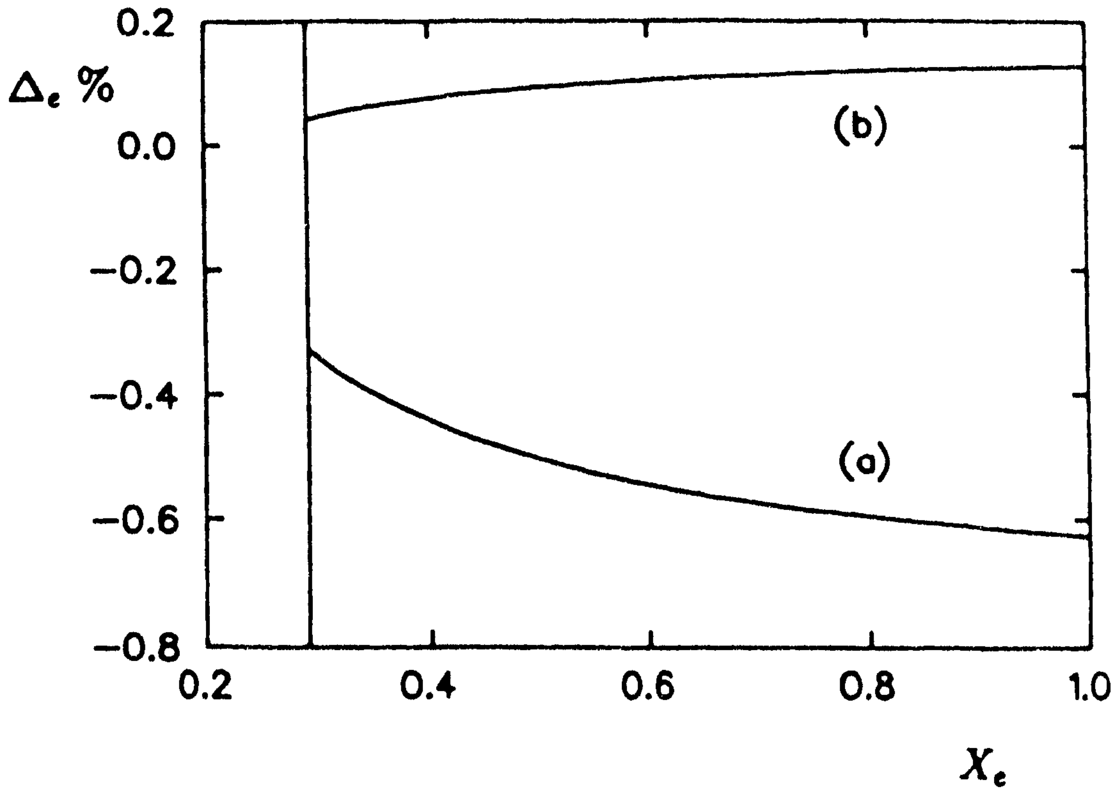

Figure 3.14: m_t^2 corrections to the lepton energy spectrum for the decay $t \to be^+\nu$ of a 150 GeV top quark, for various values of m_h: (a) $m_h = 25$ GeV, (b) $= 500$ GeV. ($\Delta_e \equiv d\Delta\Gamma/dX_e$, $X_e \equiv 2E_e/m_t$ where E_e is the electron energy).

$$\Delta\Gamma/\Gamma \quad = \quad \frac{\alpha_{em}}{8\pi s_w^2}\frac{m_t^2}{m_w^2}\left[\frac{5}{8} - \frac{1}{4}\log\left(\frac{m_t^2}{m_h^2}\right)\right] \tag{3.86}$$

It turns out that this approximation is valid only for a very heavy top, $m_t \sim 1\, TeV$, as was determined by computer. Thus the the non-leading terms implicitly contained in the integrals are making significant contributions for $m_t < 240\, GeV$.

3.6.3 Comparison with Other Work

The first-order Q.C.D. corrections to the $t \to bW^+$ decay have been known for some time [51] and are about -10%.

Subsequent to publication of this work, two groups [52, 53] have performed a complete calculation of all electro-weak corrections. Their results are in agreement. They perform the computation in two on-shell schemes:

1. Using α_{em}, s_w^2, M_Z, and fermion and Higgs masses as input. ("α-scheme")

2. Using G_F, M_W, M_Z, and fermion and Higgs masses as input. ("G_F-scheme")

The results are given in figure 3.15 taken from Denner and Sack [53]. In the case $m_t > m_h$, Denner and Sack also provide the leading order behaviour in m_t and $m_t m_h$. Their expression agrees with the one we have derived in 3.85, except for the $m_t m_h$ terms which we do not consider.

α-scheme

In the first scheme, there is large variation with m_t. This comes not from the type of m_t^2 corrections that we have computed, but from another m_t^2 contribution which was not present in our renormalization scheme (which is more like the second scheme). This extra effect is associated with the running of the gauge coupling from the low scale at which α_{em} is measured to the W^+ scale. This would shift our results by the amount:

$$\Delta r = \frac{\alpha}{4\pi s_w^2}\left(-\frac{N_c c_w^2}{4 s_w^2}\frac{m_t^2}{m_w^2}\right) \tag{3.87}$$

Note that the original definition of Δr comes from:

$$M_W^2\left(1 - \frac{M_W^2}{M_Z^2}\right) \quad = \quad \frac{\pi\alpha}{\sqrt{2}G_\mu}\frac{1}{1-\Delta r} \tag{3.88}$$

This contribution is essentially the ubiquitous m_t^2 effect discussed in section 2.4.2.

The authors in references [53, 54] find that these new formulae for the leading order m_t^2 corrections in scheme 1 approximates the full electro-weak corrections

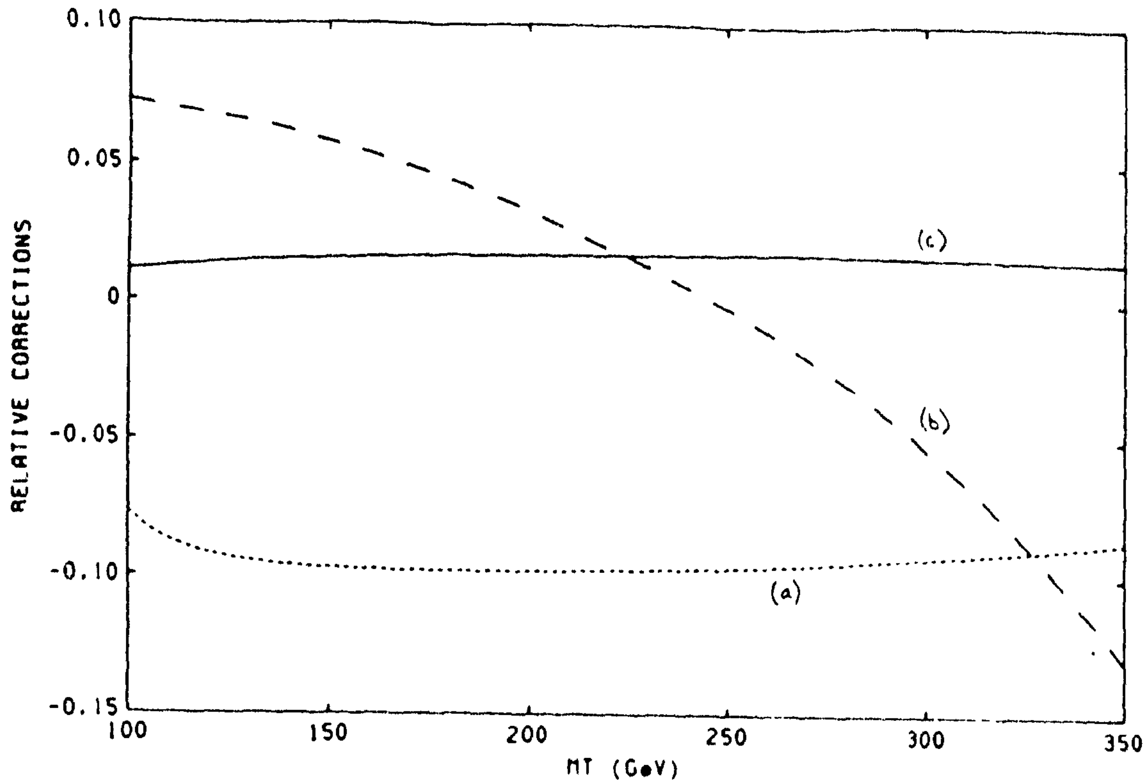

Figure 3.15: Results of a complete calculation of all first order Q.C.D. and electro-weak corrections to the top width: (a) Q.C.D. contributions, (b) electro-weak contributions in the "α" scheme, and (c) in the "G_F" scheme. Taken from reference [53].

(which are of order several per cent, see figure 3.15) to within a factor of two. However, the reason for such good agreement is due to the fact that the "boring" correction Δr itself dominates all the electro-weak corrections.

G_f-scheme

The second scheme corresponds most closely to the scheme we have used, because the coupling constant information essentially comes from the W^+ mass input, which is at the same scale that our SU(2) coupling $g^{e\nu}$ is measured at. Inspection of figure 3.15 indicates the complete result is 4-5 times larger than ours, and changes little over the indicated region of top quark mass. By contrast, our results in figure 3.13 vary significantly. Thus we must conclude that though we have computed the leading order contributions to the top width, within the interval of top quark mass allowed by experiment they in fact do not dominate.

Recently, Yuan and Yuan [54] have also computed the leading m_t^2 term in the top width, using the equivalence theorem from the outset. They work in both the α and G_F schemes, and obtain the same results as us in the latter scheme.

After submission of this work for publication, we became aware of a similar analysis by Liu and Yao [55]. However their quoted asymptotic limit differs from ours, that of Yuan and Yuan, and of Denner and Sack.

3.7 Appendix: Effects of Like-Charge Quark Mixing

Till now we have neglected the effects of the KM mechanism [24] of the standard model, in essence assuming that $V_{tb} = 1$. In fact, V_{tb} is a completely free parameter of the theory, with some bounds on its values coming from the observation of V_{cb} and V_{ub} and the unitarity of the charged current coupling matrix in the KM scenario.

The introduction of this extra parameter, however, strips our study of its predictiveness. Previously, after measuring the SU(2) coupling constant in the W^+-e-ν vertex, we could predict the top width at tree level, and any difference between this tree level prediction and the observed value could be converted into information about the Higgs mass (perhaps poorly, given the logarithmic dependence of the formulae). However, now we do not know how much of the deviation of the top width from its tree level prediction is due to radiative corrections and how much is due to mixing between the quarks.

The best way to get around our ignorance of V_{tb} is to consider the inclusive decay rate:

$$\Gamma(t \to W^+X) \equiv \Gamma(t \to bW^+) + \Gamma(t \to sW^+) + \Gamma(t \to dW^+) \qquad (3.89)$$

Let $\tilde{\Gamma}(t \to bW^+)$ denote the rate prediction under the assumption that the KM matrix is the unit. We have:

$$\Gamma^{(0)}(t \to W^+ b_i) = |V_{ti}|^2 \tilde{\Gamma}^{(0)}(t \to W^+ b_i) \qquad (3.90)$$

where b_i represents b, s, d. Now note that

$$\tilde{\Gamma}^{(0)}(t \to W^+ b_i) - \tilde{\Gamma}^{(0)}(t \to W^+ b_j) \propto \frac{m_i^2 - m_j^2}{m_t^2} \qquad (3.91)$$

where the mass dependence enters through the fact that the volume of phase space is different for the different quarks. We are everywhere neglecting such mass effects, so that:

$$\begin{aligned} \Gamma^{(0)}(t \to W^+ X) &= \left[\sum_i |V_{ti}|^2\right] \tilde{\Gamma}^{(0)}(t \to W^+ b) \quad + O(m_i^2) \\ &= \tilde{\Gamma}^{(0)}(t \to bW^+) \end{aligned} \qquad (3.92)$$

It is just $\tilde{\Gamma}(t \to bW^+)$ that we have computed. Thus our calculation is really relevant to the prediction of the deviation of the inclusive width. From a phenomenological point of view this is a much better situation anyway, because it is that quantity which is all that we will probably ever be able to know about the top.

The results here can be understood generally. If all three quarks were degenerate in mass, the standard model Lagrangian would have a larger symmetry which would allow us to absorb the KM matrix into the defintion of the quark fields. The charge current coupling matrix would become the unit. This is entirely analogous to the situation in the leptonic sector, where the degeneracy of the neutrino masses (they are all zero) makes a KM matrix there meaningless. Now allowing the quarks to have mass, the change in our predictions from the case of a unit KM matrix must be proportional to the quark masses, since they are functioning as order parameters for the symmetry. This is what we found above.

Part II

Υ Decay

Chapter 4

Introduction

4.1 The Decay $\Upsilon \to J/\psi X$

Recently [56] the "semi-inclusive" decay:

$$\Upsilon \to J/\psi X$$

has been observed, with the branching ratio:

$$Br(\Upsilon \to J/\psi X) = (1.1 \pm .4 \pm .2) \times 10^{-3}$$

where the first error is statistical and the second systematic. In this second part of the thesis I compute the perturbative Q.C.D. prediction for this process. The results are presented in chapter 8.

We will work to lowest order in the strong coupling α_s, which we will extract from the perturbative Q.C.D. predictions of the hadronic widths of the various mesons. This approach yields [57] a typical value $\alpha_s \sim 0.2$ and has the feature that α_s is deduced in an consistent fashion with respect to our model.

The perturbative Q.C.D. estimate of transition rates for mesons relies on the assumption that the constituent quarks move non-relativistically. This allows us to perform an expansion in the average relative quark momentum, so that in the end we need only know the value of the wave function or its derivative at the origin. These in turn can be deduced consistently from a leptonic width of the meson. Given the validity of the non-relativistic assumption, this expansion makes just as much sense as the expansion in α_s: the typical momentum particles bound by a coloumb type force of strength α_s is $|\vec{p}| \sim \alpha_s m$.

One attractive feature of the process $\Upsilon \to J/\psi X$ is that we expect the assumption of non-relativistic motion to be reasonably well satisfied for each of the mesons in the transition. A sign of this is the relatively small level splittings between the different quark anti-quark bound states in the Υ and J/ψ systems. Many of these states differ [58] from each other only in the way that the total quark spin and the orbital angular momentum are combined to produce the total meson spin. Thus we can interpret the level splittings between such states as being produced by spin-orbit coupling, such effects are proportional to the relative momentum of the constituents and various powers of the coupling constant.

Another attractive feature about the $\Upsilon \to J/\psi X$ rate is that it involves quark-onia of two different types. All previous uses of perturbative Q.C.D. to describe heavy meson physics have involved inclusive decay widths of only a single type of meson, or do not yet have experimental data to compare the predictions with. Examples of these two situations are the decays $\Upsilon \to \gamma X$ and $\Upsilon \to J/\psi \eta_c$ respectively. The predicted branching ratio for the latter decay is $\sim 10^{-6}$ [59]. A survey of single meson inclusive rates may be found in reference [57].

The research to be reported herein constitutes the first study of a transition between two different species of quark-onia, for which there exists experimental data to compare the prediction with, and for which both systems can be reasonably approximated as non-relativistic.

A related point of interest in this process concerns the possibility [60] that the $\Upsilon(4S)$ state decays to J/ψ's an anomalously large number of times, in comparison to the decay $\Upsilon(1S) \to J/\psi X$. One [61] proposed explanation of this (possible) anomaly postulates that the $\Upsilon(4S)$ has a large width for decay to some other $b\bar{b}$ bound state, which in turn has a large J/ψ width. If perturbative Q.C.D. is successful in describing the measured $\Upsilon(1S) \to J/\psi X$ decay, then we could trust it to make a host of predictions about the J/ψ widths of the other b-quark states, and thus confirm or refute this important aspect of the proposed explanation.

I will not attempt to review the extensive literature that exists on the subject of perturbative description of transitions between non-relativistic bound states. Some particularly good references are:

- [62] and [16] apply the method to the decay of positronium to two or three photons, which was the original context in which it was developed. [63] was the first paper to apply the method to mesons, computing the leptonic widths of vector states.

- [58] and [64] contain more sophisticated discussions of the conditio under which we can expect the technique to be reliable.

- [65] contains many useful formulae applicable to transitions involving P-wave mesons.

- [66], [67] apply the method to compute the decay of heavy mesons to electro-weak particles like the Higgs, etc.

However, in appendix B I do derive the covariant form of a non-relativistic bound state wave function, which should suffice to justify the Feynman rules for vertex functions associated with mesons in Feynman diagrams

This decay was considered using perturbative Q C D about a decade ago [68]. However, in those studies no attempt was made to correlate the final charm quarks into definite meson states. Rather the rate for $\Upsilon \to (c\bar{c})gg$ was computed, under the constraint that the invariant mass of the charm quark anti quark pair lie between M_J and the threshold for $D\overline{D}$ production. The authors argue that this method yields the complete branching ratio for $\Upsilon \to J/\psi$, including the effects of cascade production through the χ, etc. states. A branching fraction of about 1% is obtained, with no error estimate, to be compared with the recently obtained experimental result of 0.1%.

The discussion of the $\Upsilon \to J/\psi X$ width is organized as follows. First I will discuss how inclusive hadronic widths are computed in general using perturbative Q C D. I will next review the rules for calculating the S matrix and invariant amplitude for transitions involving mesons, and I will discuss how the conservation of charge-parity in Q C D leads to a reduction in the number of Feynman diagrams that describe such amplitudes. Chapters 5, 6, 7 then constitute the bulk of the calculation, wherein the Feynman diagrams are computed. Lastly I will summarize the results of the study in chapter 8.

4.2 Decays Contributing to the Inclusive Rate

Herein I discuss the general plan of attack for our problem.

The inclusive rate $\Gamma(\Upsilon \to J/\psi X)$ is computed by summing up the partial widths for *all* decay modes that eventually contain a J/ψ. This summation may be broken into two parts:

1. Decays directly to J/ψ plus anything.

2. Decays directly to narrow resonances "Y" plus anything, where the state Y subsequently decays to a J/ψ .

Pictorially, this is described in figure 4.1. The mode labeled 1 corresponds to case 1, while the modes labeled 2 and 3 are examples of case 2.

4.2.1 Direct Decays to J/ψ

The rate for Υ to decay to J/ψ plus any light hadron is the sum of the squares of the projections of state $< \Upsilon|$ against any hadronic state containing J/ψ :

$$\Gamma_{par} = \sum_{h \equiv had} |< \Upsilon|\psi h >|^2 = < \Upsilon| \left\{ \sum_{had} |\psi h >< \psi h| \right\} |\Upsilon > \qquad (4.1)$$

where the sum is over the *complete* set of hadronic states in the part of the Hilbert space that is energetically allowed. Perturbative Q.C D. enters in the

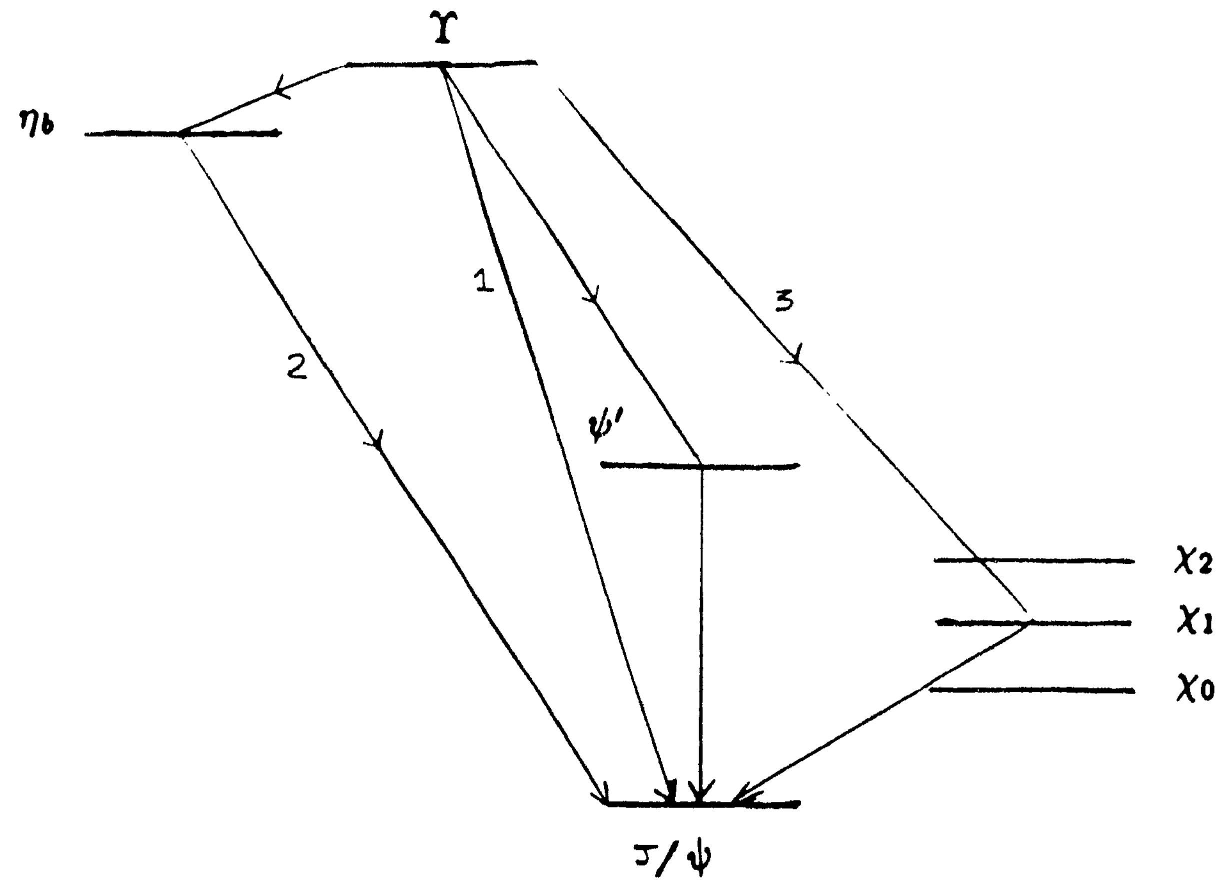

Figure 4.1: Decays contributing to inclusive J/ψ production

following way There is an equally good basis for this subspace of hadronic states, namely the set colour-neutral many-quark and -gluon states

$$\sum_{had} |\psi h><\psi h| = \sum_{q\,g} |\psi; q, g><\psi; q, g|$$
$$= |\psi gg><\psi gg| + |\psi ggg><\psi ggg| + |\psi q\bar{q}><\psi q\bar{q}|$$
$$+ |\psi q\bar{q}g><\psi q\bar{q}g| + |\psi gggg><\psi gggg| + \ldots \qquad (4.2)$$

Note that no *particular* hadronic mass eigenstate is necessarily well approximated by any one multi-quark and -gluon state, the above identity follows because we are considering an *inclusive* rate

The important point is that now the projection of $<\Upsilon|$ against each of these new states is easily characterized by a unique power of the strong coupling constant α_s. We can re-organize the sum into an ascending series in α_s. Finally, to the extent to which perturbative Q.C.D. is valid, we can obtain a good approximation to the sum of overlaps in 4.1 by truncating the reorganized series at the lowest order term

$$\Gamma_{par} = \sum_{X-had} |<\Upsilon|\psi X_{had}>|^2$$
$$= |<\Upsilon|\psi gg>|^2 + |<\Upsilon|\psi gggg>|^2 + O(\alpha_s^7) \qquad (4.3)$$

Here we have anticipated future results, that the dominant terms are of order α_s^6, and consist of the $|\psi gg>$ and $|\psi gggg>$ states. The evaluation of the overlap of $|\Upsilon>$ with these two states will constitute the bulk of this study

Note that at the scale of the Υ, $\alpha_s \sim 0.2$ [57]. Thus we should not expect our prediction to agree with experiment to any better than 20%.

4.2.2 Indirect Decays to J/ψ

If the Υ decay proceeds through a narrow intermediate resonance "Y", then to a very good approximation:

$$\Gamma(\Upsilon \to YX' \to \psi X) = \frac{\Gamma(\Upsilon \to YX') \cdot \Gamma(Y \to \psi X)}{\Gamma_Y} \qquad (4.4)$$

and thus:

$$Br(\Upsilon \to Y \to \psi X) = Br(\Upsilon \to YX') \cdot Br(Y \to \psi X) \qquad (4.5)$$

where "Br" denotes the branching ratio

I have made a survey of all the intermediate resonances through which the Υ could reach the J/ψ. We will only be interested in those modes that could compete with or dominate the "direct" decay to J/ψ discussed in the previous section The following decay sequences all warrant discussion:

$$\begin{aligned}
\Upsilon \quad &\rightarrow \quad \eta_b'\gamma \rightarrow J/\psi X && (4.6)\\
&\rightarrow \quad \eta_c' X' \rightarrow J/\psi X && (4.7)\\
&\rightarrow \quad \psi' X' \rightarrow J/\psi X \qquad * && (4.8)\\
&\rightarrow \quad \chi_0 X' \rightarrow J/\psi X && (4.9)\\
&\rightarrow \quad \chi_1 X' \rightarrow J/\psi X \qquad * && (4.10)\\
&\rightarrow \quad \chi_2 X' \rightarrow J/\psi X && (4.11)\\
&\rightarrow \quad h_c X' \rightarrow J/\psi X && (4.12)
\end{aligned}$$

"h_c" is the 1^{-+}, L=1, S=0 c-$\bar{c}$ meson. This list has been arrived at by:

1. Ignoring all intermediate c-$\bar{c}$ states that lie above the threshold for decay to open charm (eg. D-$\overline{D}$). These have infinitesimal branching ratios to J/ψ
2. Noting that the only b-$\bar{b}$ state lying below the Υ is the η_b. (States containing a single b-quark can only be reached from Υ via weak decay, and thus have tiny branching ratios.)
3. Ignoring possible D or higher wave c-$\bar{c}$ bound states, due to our current ignorance of their nature.

It turns out that in perturbative Q.C.D., the transition of Υ to each of

$$\eta_c, \chi_0, \chi_1, \chi_2, h_c$$

is one order α_s *lower* than the Υ to J/ψ transition This is essentially because the former mesons all have positive charge parity and can couple to just two gluons, as we will discuss in section 4.4. Thus their potentially larger rates could offset the suppression coming from the branching ratio factor in 4.5 A rule of thumb is that their branching fraction to J/ψ's should be larger than α_s, which is about 0.2 at this scale [57]

In this thesis, we shall only consider the contributions of the indirect decays 4.8 and 4.10, marked with a "*", which have the following observed branching ratios to J/ψ [46]

$$\begin{aligned}
Br(\psi' \rightarrow J/\psi X) \quad &= \quad (55 \pm 7)\% && (4.13)\\
Br(\chi_1 \rightarrow J/\psi\gamma) \quad &= \quad (27.3 \pm 1.6)\% && (4.14)
\end{aligned}$$

The rate for the decay through the ψ' will be easily obtained from our calculation of $\Gamma(\Upsilon \rightarrow J/\psi X)$. The branching ratio 4.14 associated with the second mode 4.10 is actually larger than α_s, and thus this mode might be producing more J/ψ's than the direct decay. Detailed analysis (chapter 7) shows that the predicted branching fraction for Υ to χ_1 is in fact *not* enhanced with respect to the Υ to J/ψ mode, so that in the end this mechamsm is responsible for only about 10% of the signal

We have not considered the other decays here because

1. Modes 4 6, 4 7 and 4 12 Primarily I have not looked at these modes because none of the mesons η_b, η_c', or h_c have been observed Thus we have no way of knowing what their appropriate wave-function at the origin factor is, or their branching ratios for decay to J/ψ In principle, this information could be obtained from some potential model study, at the cost of expanding the underlying assumptions of the prediction Such considerations are reserved for later study. Also, there is no reason to expect that the η_c' or the h_c would have appreciably large J/ψ branching ratios

2. Mode 4 6: We can say more about the decay through the η_b Its non observation in Υ decays can be translated into an upper bound on $Br(\Upsilon \to \eta_b\gamma)$ [69].

$$Br(\Upsilon \to \eta_b\gamma) < 1/2\%$$

Thus to make more than a 10% contribution to the J/ψ signal, we would have to have: $Br(\eta_b \to J/\psi) \sim 2\%$. This would be 20 times as large as the observed $\Upsilon \to J/\psi$ branching ratio, which does not seem likely

3. Modes 4 9 and 4 11: The observed branching ratios are:

$$\begin{aligned} Br(\chi_0 \to \psi\gamma) &= 0.6\% \\ Br(\chi_2 \to \psi\gamma) &= 13.5\% \end{aligned}$$

On the one hand, these are both below the $\alpha_s \sim 2$ enhancement factor that $Br(\Upsilon \to \chi)$ might experience over $Br(\Upsilon \to J/\psi)$, certainly in the case of the χ_0 On the other hand, we will see in our study of the χ_1 mode that other factors eliminate such enhancements anyway Our calculation of $Br(\Upsilon \to \chi_1)$ will serve as a benchmark that justifies our neglect of these modes. Nevertheless, a study of the χ_2 process is currently being made

4.2.3 Summary

To summarize, we will use perturbative Q.C D. to compute the following decay widths:

1. $\Upsilon \to J/\psi gg$, the dominant (as we will see) part of the direct decay

2. $\Upsilon \to J/\psi gggg$, another part of the direct decay.

3. $\Upsilon \to \psi' gg$, $\psi' gggg$, trivially obtained from the results of 1 and 2.

4. $\Upsilon \to \chi_1 ggg$, the most promising indirect production mode.

The first three are computed in chapters 5 and 6 and the summary 8, and the last in chapter 7.

4.3 Matrix Elements of Weakly Bound States

4.3.1 Normal Feynman Rules

I will assume that the reader is familiar with all the rules for computing the S-matrix and invariant amplitude for processes involving free quarks and gluons. Reference [70] provides a thorough discussion of this subject

Here I just want to point out that I will everywhere suppress the factors of "i" and "-1" that typically appear in expressions for the particle propagators and vertex factors, with the exception of section 5.4.3 where the relative sign between two completely different types of Feynman diagrams must be carefully computed The rest of the time, the set of Feynman diagrams that must be added to obtain the amplitude will generate *exactly* the same overall combination of i's and -1's, and this combination will always disappear when we square the amplitude to obtain the rate. This approach is adopted in the interests of notational simplicity, to avoid a proliferation of such factors. It is only the relative phase between Feynman diagrams that I will make a point of writing.

For example, the vertex function for the coupling of a gluon to a quark I set equal to:

$$g_s T_a \gamma^\mu$$

where T_a are the **3** representation of SU(3). Similarly, for a fermion propagator I employ:

$$\frac{1}{\not p - m}$$

The precise rules including factors of "i" etc. are mentioned in sections 5.4.3 and 5.6.3.

4.3.2 Meson Wave Functions

The easiest way to understand the formulae for processes involving weakly bound states is to compare the equations for different particle wave functions.

Single Fermion: This is a one-lorentz-spinor-index object. Normalized such there is exactly one fermion in a box of volume "V" the wave function is:

$$\sqrt{\frac{1}{2EV}}\,\left[u(p,\sigma)\right]_\alpha e^{ip\cdot x}$$

where $\overline{u}u = 2m$, m the fermion mass.

Single Massless Vector Boson: This is a one-lorentz-vector-index object. Normalized such there is exactly one massless vector boson in a box of volume "V" the wave function is:

$$\sqrt{\frac{1}{2EV}}\,\epsilon^\mu(p,\lambda)e^{ip\cdot x}$$

where $\epsilon^\mu \epsilon_\mu = -1$.

Non-relativistic Vector Bound State: This is a two-lorentz-spinor-object, since it consists of two fermions. Normalized such there is exactly one vector bound state in a box of volume "V" the wave function is:

$$\frac{\psi(0)}{\sqrt{M}} \cdot \sqrt{\frac{1}{2EV}}\ [(\not p_q + m_q)\not\epsilon]_{\alpha\beta}\ e^{ip_q x_1} e^{ip_q x_2}$$

where p_q, m_q are the quark four-momenta and mass. This formula is valid only to lowest order in the quark relative momentum. To this same order:

$$p_q^\mu = \frac{1}{2} P^\mu \qquad m_q = \frac{1}{2} M \tag{4.15}$$

where P, M are the bound state four momentum and mass. The momentum and vector polarization label dependence of the vector bound state polarization vector has been suppressed:

$$\epsilon \equiv \epsilon(P, \lambda_v)$$

By working to lowest order in the relative quark momentum, the formulae no longer depends on the entire relative position wave function, only its value at the origin.

The latter formulae concerning the vector bound state are derived in appendix B.3. What is somewhat surprising is that there are no lorentz spinors to describe the two constituent fermions, only the object $(\not p_q + m_q)\not\epsilon$. This is a direct result of the fact that the two fermion spins in the bound state are *correlated*, and the correlation function is given by the Clebsch-Gordan coefficients in the bound state wave function.

A similar formula for an axial vector meson wave function is discussed in chapter 7, which is the only place we will use it.

4.3.3 S-Matrix and Transition Rate

Given these formulae, we can now deduce the equation for the S-matrix in the usual way:

$$S = (2\pi)^4 \delta^4(\Sigma p) \cdot \left[\prod_{all} \sqrt{\frac{1}{2EV}}\right] \left[\prod_{B.S.'s} \frac{\psi(0)}{\sqrt{M}}\right] A \tag{4.16}$$

where the invariant amplitude "A" is calculated according to the rules:

1. a factor of $u(p, \sigma)$ for each external fermion;
2. a factor of $\epsilon^\mu(p, \lambda)$ for each external massless vector;
3. a factor of $(\not p_q + m_q)\not\epsilon$ for each external vector bound state;

4 plus all the other rules concerning propagators, vertex functions, loop integrals etc. familiar from Q.E.D.

The formula for a "m" particle to "n" particle transition rate is thus:

$$
\begin{aligned}
|S|^2 dN &= VT \left[\prod_{k=1}^{m} \frac{1}{2E_k V} \right] \left[\prod_{B\,S's} \frac{|\psi(0)|^2}{M} \right] \cdot |A|^2 \cdot d_n(LIPS) \\
d_n(LIPS) &= (2\pi)^4 \delta(\Sigma p) \prod_{k=1}^{n} \frac{d^3 p_k}{(2\pi)^3 2E_k} \qquad (4.17)
\end{aligned}
$$

4.3.4 Color Rules

If we were only going to calculate transitions between *leptonic* bound states, the rules we have seen so far would be sufficient. Since we are investigating quark anti-quark bound states, we must also introduce the rules for handling the color part of amplitudes involving mesons. These rules are very simple

Suppose we have a Feynman diagram in which quark of color state "i" emits three gluons with color octet labels "a", "b", "c", thereby changing into a quark of color state "j". The total invariant amplitude for the process is:

$$
\mathcal{M}_{free} = \chi^{(j)\dagger} T_a T_b T_c \chi^{(i)} \mathcal{M}_{qed} \qquad (4.18)
$$

where $\mathcal{M}_{qed}$ corresponds to the usual "lorentz" part of the amplitude and is calculated according to the rules above, and the T_a are essentially the Gell-Mann matrices.

If these two quarks now belong to the same meson, the invariant amplitude becomes:

$$
\mathcal{M}_{bound} = \frac{1}{\sqrt{3}} \mathrm{Tr} \{T_a T_b T_c\} \mathcal{M}_{qed} \qquad (4.19)
$$

This new formula comes about because the color values of the quark and anti-quark in a meson are *correlated*. The correlation function is the color Clebsch-Gordan coefficient that combines a color triplet and anti-triplet into a color singlet, namely δ_{ij}. In fact, the entire meson color wave function, including normalization is.

$$
\frac{1}{\sqrt{3}} \delta_{ij}
$$

4.4 Implications of the C-Parity Symmetry

Both the strong and electro-magnetic interactions conserve C-parity (neglecting non-perturbative effects) We will make frequent use of this conservation principle in our study, and in this section I present a general discussion of why it proves so useful.

4.4.1 Meson C-Parities

A bound state with relative orbital angular momentum "L" and total quark spin "S" is automatically in a state of definite parity "P" and charge-parity, given by [64]:

$$P = (-1)^{L+1} \qquad C = (-1)^{L+S} \tag{4.20}$$

We will often employ the spectroscopic notation of atomic physics to describe a meson:

$$^{(2S+1)}L_J.$$

Thus, a $^3S_1$ state has J^{PC} values 1^{--}, while a $^3P_1$ state corresponds to 1^{++}, and transform as vectors and axial vectors respectively.

4.4.2 Implications for Feynman Diagram Construction

Let us first review the constraints that C-parity conservation puts on the number of photons that a vector meson can couple to. A photon is a "-1" C-parity eigenstate, and the total C-parity of a multi photon state is just the product of the individual photon C-parities. Thus, for an n-photon state

$$C_n = (-1)^n. \tag{4.21}$$

Since a vector meson has C-parity "-1", this means that it can only couple to an odd number of photons.

When we turn from photons to gluons, the situation becomes more complicated. This is because the gluons carry colour charge, and are not in general charge-conjugation eigenstates. The precise charge-parity of a colour-singlet multi-gluon state depends on *how* these gluons are combined into a singlet. The following rules apply:

- If n gluons are combined symmetrically in color space, their C-parity is $(-1)^n$ i.e. they behave as photons with respect to charge conjugation.
- If n gluons are combined anti symmetrically in color space, their C-parity is $(-1)^{n+1}$.

This has the following implications:

- A colour-singlet two-gluon state can only have positive C-parity. This is because there is only one two-index function to combine them into a colour-singlet (δ_{ab}) and it is symmetric.
- A colour-singlet three gluon state can have either positive or negative C-parity. In the former case, their colour space "wave function" is f_{abc}, and in the latter it is d_{abc}.

These three functions are discussed in appendix A. The above rules lead to:

1. A vector meson which is C-odd, cannot couple to two gluons.

2. Any C even meson (pseudo-scalar, scalar, axial-vector, ...) can couple to two or three gluons. In the latter case, the gluons must be combined into a singlet with the f_{abc} function.

3. A vector meson can couple to three gluons, which are combined into a singlet with the d_{abc} function.

Note that *no* meson can couple to one gluon, by colour conservation. This means that in all of our Feynman graphs, the vector meson must touch three or more gluons, and the C even mesons must touch two or more gluons.

Using these rules, an exhaustive survey was made of all possible Feynman diagrams containing an Υ and a J/ψ, and any number of radiated light quarks and gluons. I found that the lowest order diagrams of this sort were proportional to g_s^6 and correspond to the processes $\Upsilon \to J/\psi\, q\bar{q}$ and $\Upsilon \to J/\psi\, q\bar{q}q\bar{q}$. These two decays are computed in chapters 5 and 6.

4.4.3 Implications on Equality of Feynman Diagrams

We have seen the conservation of charge parity predicts that the amplitudes for some meson transitions are exactly zero. However, this does not mean that the *individual* Feynman diagrams for these processes are zero. The vanishing of the amplitude occurs because certain Feynman diagrams are equal and opposite to other Feynman diagrams. It turns out that it is the operation of charge conjugation which converts one Feynman diagram expression into another, times a negative sign. The demonstration of the equal and opposite nature of two Feynman diagrams for a forbidden process proceeds in fashion similar to the demonstration that the three photon vertex in Q.E.D. vanishes [16], due to a cancelation between one Feynman diagram with a fermion triangle and the other obtained from it by exchanging two of the photons.

In the case of amplitudes for allowed meson transitions, the charge conjugation operation will *still* convert the individual Feynman diagrams for the process into one another, *but now there is no relative negative sign*. In this way the general discussion of the precise amplitude zeroes implied by charge-conjugation symmetry has led to a further implication: that the number of distinct Feynman graphs that need to be evaluated can be significantly less than it naively appears. An example of this in Q.E.D. is the four-photon vertex. Many of the distinct Feynman diagrams can be shown to be equal to each other, and in the end there are only five diagrams that must be computed to lowest order [62].

I will demonstrate explicitly how this works in section 5.3.1, and employ the results in each of the other chapters 6 and 7.

Chapter 5

$\Upsilon \longrightarrow J/\psi gg$

5.1 Decay Rate and Spectrum

The formula for the spin averaged, and color and spin summed, decay rate of an Υ to a "J" plus two gluons follows from equation 4.17.

$$d\Gamma = \frac{1}{2}\frac{1}{2J_\Upsilon + 1}\frac{1}{2M_\Upsilon}\frac{|\psi_\Upsilon(0)|^2}{M_\Upsilon}\frac{|\psi_J(0)|^2}{M_J}\sum_{col,pol}|A_q|^2 d_3(LIPS) \qquad (5.1)$$

where the first factor takes account of the fact that there are two identical particles in the final state, and A_q is the quark level invariant amplitude calculated with the rules of section 4.3.3.

Labeling the two gluons with "1" and "2", the 3-body phase space is given by [71]:

$$\begin{aligned} \int d_3(LIPS) &= \frac{1}{(2\pi)^5}\int \frac{d^3k_J}{2E_J}\frac{d^3k_1}{2E_1}\frac{d^3k_2}{2E_2}\delta^4(k_\Upsilon - k_J - k_1 - k_2) \\ &= \frac{1}{32\pi^3}\int_{|\cos\theta_{12}|\leq 1} dE_1 dE_2 \end{aligned} \qquad (5.2)$$

Introducing:

$$\begin{aligned} m_0 &\equiv \frac{1}{2}M_\Upsilon \\ m_f &\equiv \frac{1}{2}M_J \\ c &\equiv 1 - \frac{m_f^2}{m_0^2} \\ E_{1/2} &\equiv x_{a/b} m_0 \end{aligned} \qquad (5.3)$$

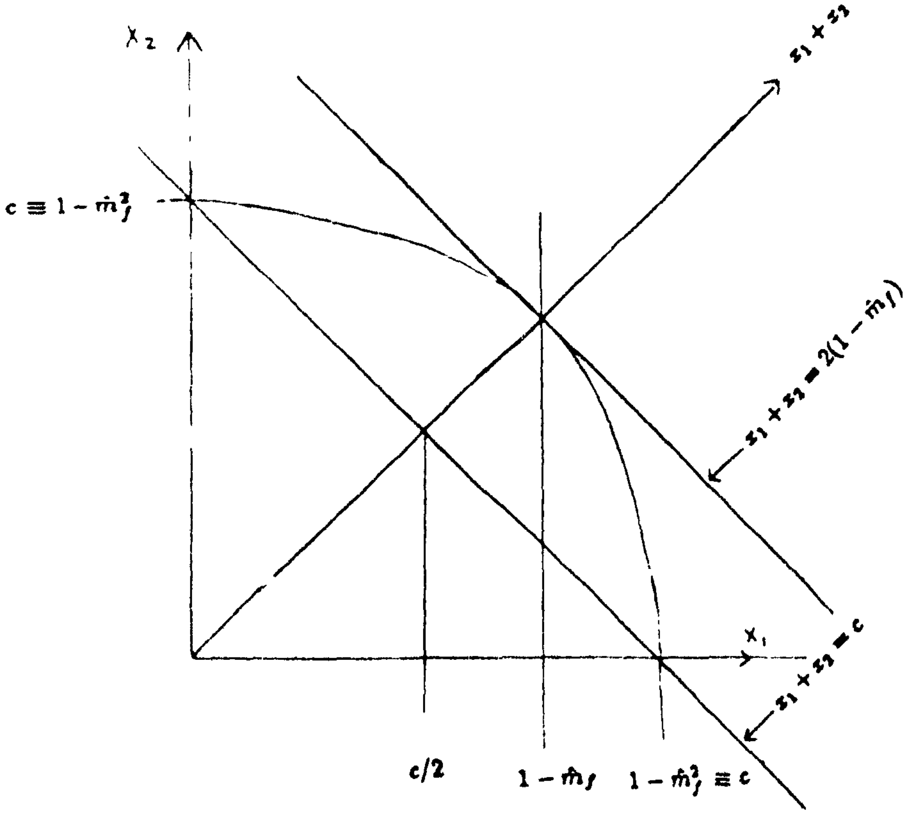

Figure 5.1: Allowed region of phase space for the $\Upsilon \to J/\psi gg$ decay

Then the constraint $|\cos\theta_{12}| \leq 1$ may be restated:

$$\begin{array}{rcl} 0 \leq & x_1 & \leq c \\ c - x_1 \leq & x_2 & \leq \dfrac{c - x_1}{1 - x_1} \end{array} \tag{5.4}$$

Thus we have finally:

$$d_3(LIPS) = \frac{1}{32\pi^3}\, m_0^2 \int_0^c dx_1 \int_{c-x_1}^{\frac{c-x_1}{1-x_1}} dx_2 \tag{5.5}$$

The integration region, i.e. the allowed region of phase space for a decay to one massive and two massless particles, is shown in figure 5.1.

This leads to the following formula for the decay rate:

$$\Gamma_J = \frac{1}{3}\frac{1}{512\pi^3}\frac{1}{M_J}|\psi_J(0)|^2|\psi_\Upsilon(0)|^2 \int dx_1 dx_2 \sum_{pol,col} |A_q|^2 \tag{5.6}$$

In the ensuing sections, we shall compute the invariant amplitude. We will find that the lowest order purely strong contributions are of order g_s^6, that they contain a loop, and that the color part of the amplitude is proportional to δ_{ab}, where "a, b" are color octet gluon labels. Thus I now introduce the dimensionless quantity $\hat{M}_q$

$$A_q \equiv \frac{g_s^6}{16\pi^2} F_c \delta_{ab} \frac{1}{m_0^2} \hat{M}_q \tag{5.7}$$

$$\begin{aligned} \sum_{col} |A_q|^2 &\equiv (4\pi)^2 \alpha_s^6 F_c^2 \left[\sum_{ab} \delta_{ab}\right] \frac{1}{m_0^4} |\hat{M}_q|^2 \\ &= 2^{11}\pi^2 \alpha_s^6 F_c^2 \frac{1}{M_\Upsilon^4} |\hat{M}_q|^2 \end{aligned} \tag{5.8}$$

The width becomes:

$$\Gamma_J = \frac{4}{3\pi} F_c^2 \alpha_s^6 \frac{|\psi_J(0)|^2 |\psi_\Upsilon(0)|^2}{M_J M_\Upsilon^4} \int dr_1 dr_2 \sum_{pol} |\hat{M}_q|^2 \tag{5.9}$$

The parameters α_s and $\psi(0)$ can be extracted from the total hadronic and leptonic widths of the mesons [57], as discussed in section B.5. For example, recall [64] the equation for the hadronic width of a vector meson to lowest order in α_s

$$\begin{aligned} \Gamma(V \to ggg) &= 2c_1 \alpha_s^3 |\psi_V(0)|^2 \frac{1}{M_V^2} \\ c_1 &= \frac{80(\pi^2 - 9)}{81} \approx 0.85 \end{aligned} \tag{5.10}$$

Rather than invert such formulae for α_s and $\psi(0)$, and then substitute the results into equation 5.9, we will express the J/ψ branching ratio in such a way that the unknown parameters drop out naturally:

$$\begin{aligned} \frac{\Gamma(\Upsilon \to Jgg)}{\Gamma_\Upsilon} &= \frac{\Gamma(\Upsilon \to Jgg)\Gamma_J}{\Gamma(\Upsilon \to ggg)\Gamma(J \to ggg)} \cdot \frac{\Gamma(\Upsilon \to ggg)}{\Gamma_\Upsilon} \cdot \frac{\Gamma(J \to ggg)}{\Gamma_J} \\ &= B_\Upsilon^{(had)} B_J^{(had)} \cdot \frac{F_c^2}{3\pi c_1^2} \cdot \frac{M_J \Gamma_J}{M_\Upsilon^2} \cdot \sum_{pol} \int dr_1 dr_2 |\hat{M}_q|^2 \end{aligned} \tag{5.11}$$

where:

$$B_X^{had} \equiv Br(X \to had) \tag{5.12}$$

The hadronic branching ratios "$Br(X \to had)$" are known from experiment. Thus we must now turn to the evaluation of the sum of the invariant amplitude squared over the polarizations of the vector fields.

5.2 Numerical Evaluation of Helicity Amplitudes

Let me begin this section by stating that the integral of the amplitude squared over phase space and another, loop, integral that we will encounter *will all be computed numerically*. The expressions we will obtain for the invariant amplitude are sufficiently complicated that analytic computation of either type of integral is essentially out of the question. With this in mind, we now turn to a discussion of the merits and method of working directly with the invariant amplitude of a transition, rather than the invariant amplitude squared.

The chief advantage lies in the fact that the number of terms in M is much smaller than the number of terms of $|M|^2$. In our case, M will typically be described as a sum of anywhere between 10 and 50 Feynman diagrams, so that the number of terms in $|M|^2$ becomes ridiculously large.

The main disadvantage to computing "M" directly is that we can no longer make use of the well known techniques for computing the spin summed rate. For example, in our case, the amplitude is a function of four helicity labels through the four polarization vectors

$$\epsilon_0, \epsilon_f, \epsilon_1, \epsilon_2$$

The usual method of summing the rate over any one of these labels,

$$\Gamma \propto \sum_{\lambda} \left|\epsilon_{\mu}^{(\lambda)} M^{\mu}\right|^2$$

is to employ the identity:

$$\begin{aligned} \sum_{\lambda} \epsilon_{\mu}^{(\lambda)} \epsilon_{\nu}^{(\lambda)*} &= -g_{\mu\nu} && \textit{for massless vectors} \\ &= -g_{\mu\nu} + \frac{k_\mu k_\nu}{M^2} && \textit{for massive vectors} \end{aligned}$$

One then contracts the above expressions into the quantity:

$$M_{\mu}^{\dagger} M_{\nu}$$

to obtain the spin summed rate.

Since we do not want to work with $M_{\mu}^{\dagger} M_{\nu}$, we must find a way to compute $M(\lambda_0, \lambda_f, \lambda_1, \lambda_2)$ for each possible set of vector meson and gluon helicity labels. Assuming we succeed in doing so, we will then separately compute M a total of

$$3 \times 3 \times 2 \times 2 = 36$$

times, as the mesons have three polarization states and the gluons two. With these 36 complex numbers in hand, we can then "manually" square and sum them to obtain $\Sigma|M|^2$. The problem of computing $M(\lambda_0, \lambda_f, \lambda_1, \lambda_2)$ for each set of helicity labels is solved if we can find a way of constructing a set of polarization four-vectors at each point in phase space for each combination $\{\lambda_0, \lambda_f, \lambda_1, \lambda_2\}$. To this we now turn.

Each point in phase space describes a particular configuration of particle four-momenta:

$$x_1, x_2 \Longrightarrow k_0, k_f, k_1, k_2$$

We always work in the decaying particle rest frame, so the final three decay product three-momenta lie in a plane. We can define this to be the "x-z" plane, and without loss of generality assume that $\vec{k}_f$ lies along the "z" axis, since we are averaging over all polarizations and there are no preferred directions. Then the four-momenta are all well defined functions of x_1 and x_2 (see figure 5.2):

$$\begin{aligned} k_0 &= (m_0, 0, 0, 0) \\ k_f &= (E_f, 0, 0, |\vec{k}_f|) \\ k_1 &= x_1(1, \cos\theta_1, 0, \sin\theta_1) \\ k_2 &= x_2(1, -\cos\theta_2, 0, \sin\theta_2) \end{aligned} \tag{5.13}$$

$$\begin{aligned} \frac{E_f}{m_0} &= 1 - \frac{1}{2}(x_1 + x_2) \\ |\vec{k}_f| &= +\sqrt{E_f^2 - m_f^2} \end{aligned}$$

$$\begin{aligned} x_1\left[E_f - |\vec{k}_f|\cos\theta_1\right] &= 1 - \hat{m}_f^2 - x_2 \\ x_2\left[E_f - |\vec{k}_f|\cos\theta_2\right] &= 1 - \hat{m}_f^2 - x_1 \end{aligned}$$

The negative sign in the formula for k_2 follows from the fact that we shall always take:

$$0 < \theta_k < \pi.$$

Thus, we see that at each point in phase space we can re-construct the particle four-momenta. We now wish to define a set of particle polarization vectors for each phase space point. Essentially, these may be chosen in any way consistent with the constraint of orthogonality: $\epsilon^{(\lambda)} \cdot k = 0$, with the further condition that $\vec{\epsilon} \cdot \vec{k} = 0$ in the case of the gluons. The latter condition actually constitutes a choice of gauge, so we are choosing a different gauge at each point in phase space. There is of course nothing wrong with this because the amplitude at each point in phase space is an in principle observable quantity and thus gauge independent. The following definitions are consistent with the

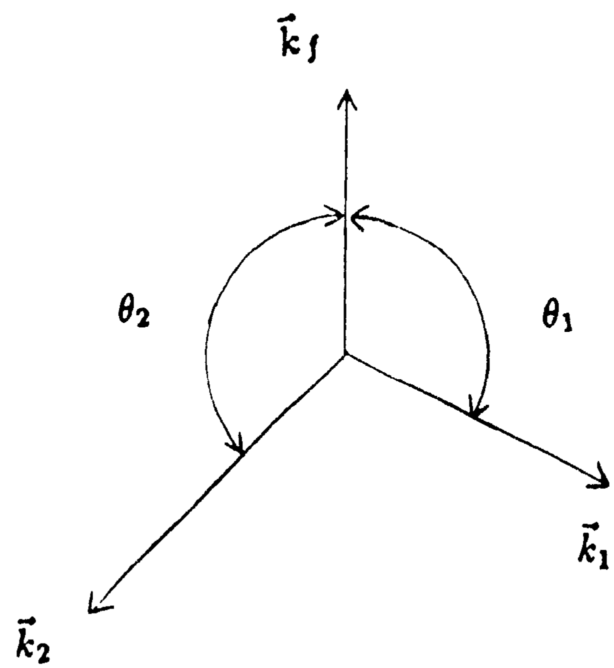

Figure 5.2. Three-momentum vectors of the final products in $\Upsilon \to J/\psi gg$

aforementioned constraints:

$$
\begin{array}{rcll}
\epsilon_0^{(\lambda)} & = & (0, \delta_{\lambda 1}, \delta_{\lambda 2}, \delta_{\lambda 3}) & \\
\epsilon_f^{(\lambda)} & = & (0, \delta_{\lambda 1}, \delta_{\lambda 2}, 0) & \lambda = 1, 2 \\
 & = & (|\vec{k}_f|, 0, 0, E_f)/m_f & \lambda = 3 \\
\epsilon_1^{(\lambda)} & = & (0, -\sin\theta_1, 0, \cos\theta_1) & \lambda = 1 \\
 & = & (0, 0, 1, 0) & \lambda = 2 \\
\epsilon_2^{(\lambda)} & = & (0, \sin\theta_2, 0, \cos\theta_2) & \lambda = 1 \\
 & = & (0, 0, 1, 0) & \lambda = 2
\end{array}
$$

Given the polarization vectors, the method of computing the spin-summed rate becomes:

- We will find an expression for the invariant amplitude, which is necessarily a function of $k_a \cdot k_b$, $k_a \cdot \epsilon_b$, and $\epsilon_a \cdot \epsilon_b$, "$a, b$" $\in \{0, f, 1, 2\}$.
- The numerical integrator that is doing the sum over phase space will generate a pair of phase space co-ordinates (x_1, x_2). These will in turn be used to generate the particle four-momenta and thus the $k_a \cdot k_b$
- For each possible set of helicity label values, the particle polarization vectors will be generated. The invariants $k_a \cdot \epsilon_b$ and $\epsilon_a \cdot \epsilon_b$ may then be computed, and thus the invariant amplitude, and thus the invariant amplitude squared.

- At this particular point in phase space, the program will sum the squares of the invariant amplitude over the possible sets of values for the helicity labels
- Lastly, the numerical integrator will move to a new point in phase space, repeat the above procedure, and sum the values of the spin summed invariant amplitude squared over the phase space

Thus we have a well defined algorithm for converting expressions for the invariant amplitude into a number for the integral of the sum of the invariant amplitude squared over polarizations, and thus for the partial width of the Υ into $J/\psi\, gg$

We now turn to deriving expressions for the invariant amplitude. The lowest order purely strong contribution to $\Upsilon \to Jgg$ is of order g_s^6, and contains a loop. The lowest order electromagnetic contribution is of order $e^2 g_s^4$, and is a tree diagram. Since loop diagrams are typically suppressed by a factor of $1/(16\pi^2)$ relative to tree diagrams, these two contributions may be comparable

5.3 Purely Strong Part

5.3.1 Feynman Diagrams

The lowest order Feynman diagrams contributing to $\Upsilon \to Jgg$ are of order g_s^6. This follows from the fact that vector mesons must couple to at least three gluons, as discussed in section 4.4.2. Nine of these are depicted in figure 5.3. The remaining diagrams are obtained from these by exchanging the two gluons in the loop, and by exchanging the two radiated gluons, for a total of $9 \times 4 = 36$.

Denote the nine amplitudes in figure 5.3 by A_k, and the amplitudes corresponding to the diagrams with crossed loop gluons by $\tilde{A}_k$. Formally, I will denote the sum of these 18 diagrams by:

$$
\begin{aligned}
A_{18} &\equiv A_1 + A_2 + \cdots + \tilde{A}_1 + \tilde{A}_2 + \cdots \\
&= \sum \begin{bmatrix} A_1 & A_2 & A_3 \\ A_4 & A_5 & A_6 \\ A_7 & A_8 & A_9 \end{bmatrix} + \sum \begin{bmatrix} \tilde{A}_1 & \tilde{A}_2 & \tilde{A}_3 \\ \tilde{A}_4 & \tilde{A}_5 & \tilde{A}_6 \\ \tilde{A}_7 & \tilde{A}_8 & \tilde{A}_9 \end{bmatrix}
\end{aligned}
\tag{5.14}
$$

Each amplitude in the first array describes the appropriately positioned diagram in figure 5.3.

Separate the amplitudes into a color and lorentz (normal Q.E.D.) parts:

$$A_k = F_k^{ab} M_k \tag{5.15}$$

where F_k^{ab} is one of the following two color traces:

$$F_1^{ab} = \left(\frac{1}{\sqrt{3}}\right)^2 \sum_{cd} tr\{T_a T_c T_d\}\, tr\{T_b T_c T_d\}$$

$$F_2^{ab} = \left(\frac{1}{\sqrt{3}}\right)^2 \sum_{cd} tr\,\{T_a T_c T_d\}\, tr\,\{T_b T_d T_c\} \tag{5.16}$$

As discussed in section 4.3 4 the trace arises because the quark color spinors are correlated in the color singlet mesons, and the $1/\sqrt{3}$ factor is the normalization factor for the meson color wave function For example, inspecting figure 5.4 where only the color labels have been shown, F_1^{ab} is the color portion of amplitude A_1, while F_2^{ab} is that of amplitude A_2.

The amplitudes A_k and $\tilde{A}_k$ necessarily have *opposite* color wave functions, due to the permutation of the loop gluons. Thus we have,

$$\begin{aligned}
\begin{bmatrix} A_1 & A_2 & A_3 \\ A_4 & A_5 & A_6 \\ A_7 & A_8 & A_9 \end{bmatrix}_{color} &= \begin{bmatrix} F_1 & F_2 & F_1 \\ F_2 & F_1 & F_2 \\ F_1 & F_2 & F_1 \end{bmatrix} \\
\begin{bmatrix} \tilde{A}_1 & \tilde{A}_2 & \tilde{A}_3 \\ \tilde{A}_4 & \tilde{A}_5 & \tilde{A}_6 \\ \tilde{A}_7 & \tilde{A}_8 & \tilde{A}_9 \end{bmatrix}_{color} &= \begin{bmatrix} F_2 & F_1 & F_2 \\ F_1 & F_2 & F_1 \\ F_2 & F_1 & F_2 \end{bmatrix}
\end{aligned} \tag{5.17}$$

I now demonstrate that the lorentz or Q.E.D parts of the amplitudes, the M_k, satisfy:

$$\begin{bmatrix} \tilde{M}_1 & \tilde{M}_2 & \tilde{M}_3 \\ \tilde{M}_4 & \tilde{M}_5 & \tilde{M}_6 \\ \tilde{M}_7 & \tilde{M}_8 & \tilde{M}_9 \end{bmatrix} = \begin{bmatrix} M_3 & M_2 & M_1 \\ M_6 & M_5 & M_4 \\ M_8 & M_8 & M_7 \end{bmatrix} \tag{5.18}$$

Proof: It will suffice to show that $\tilde{M}_1 = M_3$. The Feynman diagrams for these amplitudes are displayed in figure 5.5, where a particular routing for the loop momentum has been chosen Using the usual rules of Q.E D. and the rules of section 4 3 3 to account for the correlated spins of the quarks in the vector meson:

$$\begin{aligned}
M_3 &= K_{03} \cdot K_f / l^2 (l-t)^2 \\
\tilde{M}_1 &= \tilde{K}_{01} \cdot K_f / l^2 (l-t)^2 \\
K_{03}^{\alpha\beta} &= tr\,\{(\not k_0 + m_0)\not\epsilon_0 \gamma^\beta (\not k_0 - \not k_2 - \not l - m_0)^{-1} \gamma^\alpha (\not k_0 - \not k_2 - m_0)^{-1} \not\epsilon_2\} \\
\tilde{K}_{01}^{\alpha\beta} &= tr\,\{(\not k_0 + m_0)\not\epsilon_0 \not\epsilon_2 (\not k_2 - \not k_0 - m_0)^{-1} \gamma^\alpha (\not l + \not k_2 - \not k_0 - m_0)^{-1} \gamma^\beta\} \\
t &= 2k_1 + k_f = 2k_0 - k_2
\end{aligned} \tag{5.19}$$

I have suppressed the integral over the loop momentum "l", because it does not affect the equality. The precise form of the final current K_f does not concern us because it is the same in both diagrams The problem is now reduced to demonstrating the equality of $K_{03}^{\alpha\beta}$ and $\tilde{K}_{01}^{\alpha\beta}$. This is accomplished by charge

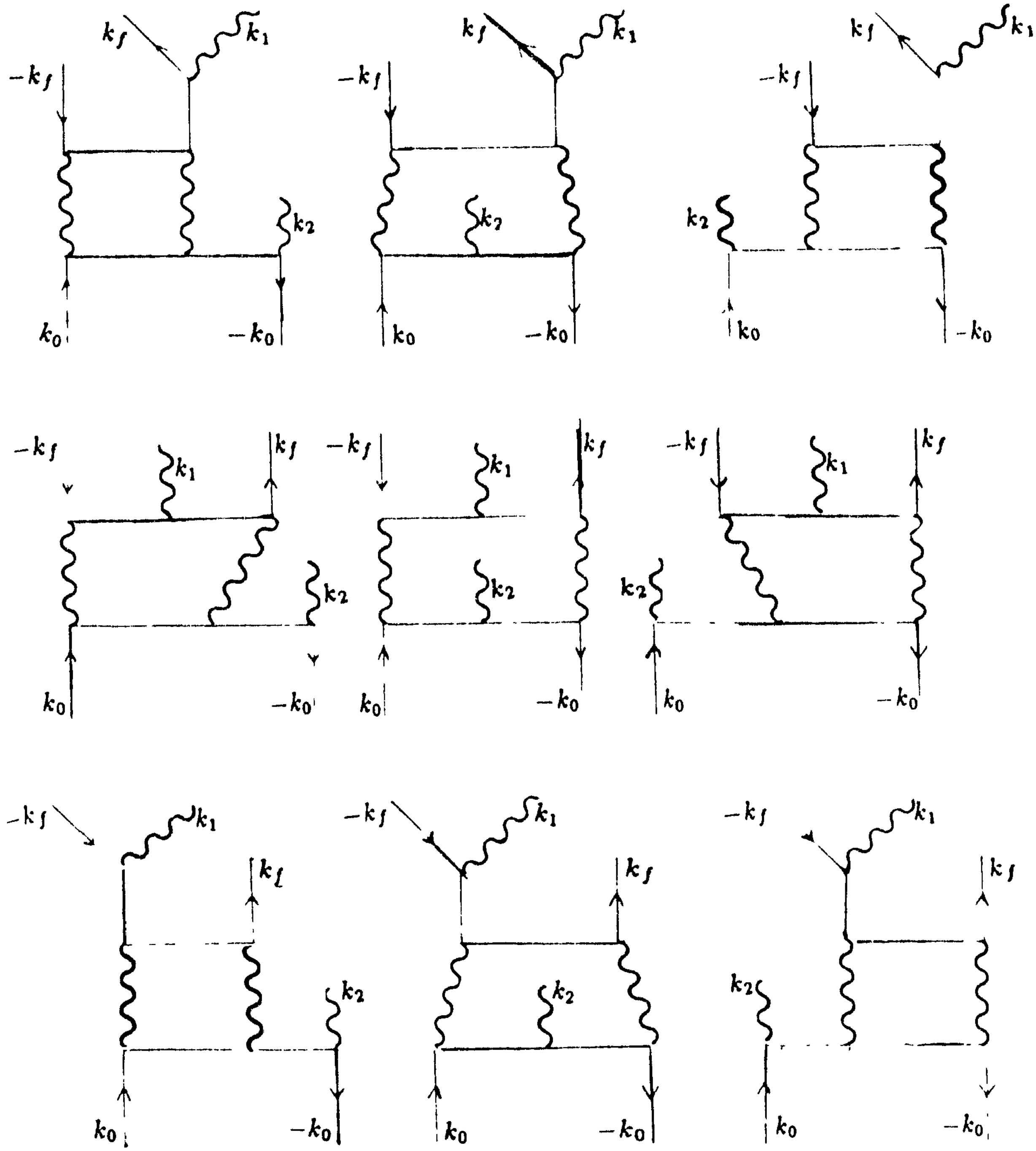

Figure 5.3: 9 of the 36 purely gluonic Feynman diagrams for $\Upsilon \to J/\psi gg$

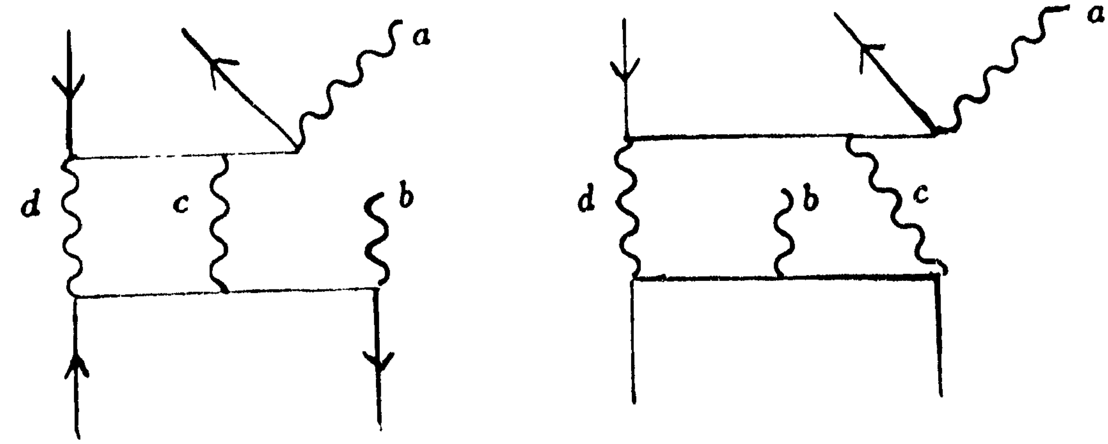

Figure 5.4: Colour labled diagrams for the amplitudes A_1 and A_2

conjugation, as discussed qualitatively in section 4.4.3. We will insert the following unit matrix:

$$CC^{-1} = C^{-1}C = 1$$

into the trace for $\tilde{K}_{01}$, where:

$$C\gamma_\mu = -\gamma_\mu^T C \tag{5.20}$$

We then use this last identity to push the "C" matrix from one end of the trace to the other, where it then recombines with C^{-1} and disappears:

$$\begin{aligned}
\tilde{K}_{01} &= tr\left\{(\not{k}_0 + m_0)\not{\epsilon}_0\not{\epsilon}_2(\not{k}_2 - \not{k}_0 - m_0)^{-1}\gamma^\alpha(\not{l} + \not{k}_2 - \not{k}_0 - m_0)^{-1}\gamma^\beta C C^{-1}\right\} \\
&= (-1)^4 \cdot tr\left\{(-\not{k}_0^T + m_0)\not{\epsilon}_0^T\not{\epsilon}_2^T(-\not{k}_2^T + \not{k}_0^T - m_0)^{-1}\gamma^{\alpha T}(-\not{l}^T - \not{k}_2^T + \not{k}_0^T - m_0)^{-1}\gamma^{\beta T} \right. \\
&= tr\left\{\gamma^\beta(\not{k}_0 - \not{k}_2 - \not{l} - m_0)^{-1}\gamma^\alpha(\not{k}_0 - \not{k}_2 - m_0)^{-1}\not{\epsilon}_2\not{\epsilon}_0(-\not{k}_0 + m_0)\right\} \\
&= K_{03}
\end{aligned} \tag{5.2}$$

The second last equality follows from the fact that $tr\{B\} = tr\{B^T\}$, and the last line relies on the cyclicity of the trace and the identity:

$$\not{k}_0\not{\epsilon}_0 = -\not{\epsilon}_0\not{k}_0$$

since $k_0 \cdot \epsilon_0 = 0$. Thus we have shown $\tilde{M}_3 = M_1$.

The proof of the other equalities involves similar manipulations, but ultimately relies on the charge conjugation invariance of Q.E.D. □

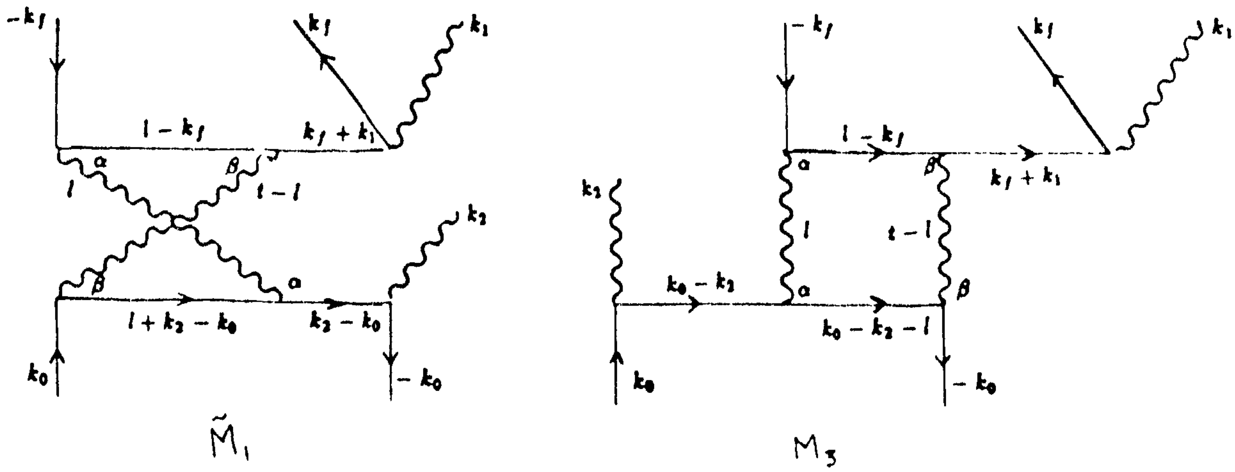

Figure 5.5: Momentum labeled diagrams for the amplitudes $\tilde{M}_1$ and M_3

Combining equations 5.14, 5.17, 5.18:

$$
\begin{aligned}
A_{18} &= \sum \begin{bmatrix} F_1 M_1 & F_2 M_2 & F_1 M_3 \\ F_2 M_4 & F_1 M_5 & F_2 M_6 \\ F_1 M_7 & F_2 M_8 & F_1 M_9 \end{bmatrix} + \sum \begin{bmatrix} F_2 M_3 & F_1 M_2 & F_2 M_1 \\ F_1 M_6 & F_2 M_5 & F_1 M_4 \\ F_2 M_9 & F_1 M_8 & F_2 M_7 \end{bmatrix} \\
&= (F_1 + F_2)^{ab} \sum \begin{bmatrix} M_1 & M_2 & M_3 \\ M_4 & M_5 & M_6 \\ M_7 & M_8 & M_9 \end{bmatrix} \qquad (5.22)
\end{aligned}
$$

Since the two radiated gluons must be in a total color singlet, $(F_1 + F_2)^{ab}$ must be proportional to δ^{ab}. In fact:

$$
\begin{aligned}
(F_1 + F_2)^{ab} &= \frac{1}{24} \sum_{ce} d_{ace} d_{bce} = F_c \delta^{ab} \\
F_c &= \frac{1}{8 \cdot 24} \sum_{acd} d_{acd} d_{acd} = \frac{5}{2^3 3^2} \qquad (5.23)
\end{aligned}
$$

as I derive in appendix A.

We have so far reduced the number of Feynman diagrams we need to compute by a factor of 2. Of the initial 36, only 18 remain: the nine amplitudes $M_1, \ldots, M_9$, and those obtained from them by exchanging the radiated gluon labels. This was accomplished by charge conjugating the initial quark current

We have one more operation to exploit, namely charge conjugation of the final quark current. This will further reduce the number of terms in the sum by essentially another factor of 2.

The lorentz parts of the first nine amplitudes satisfy:

$$\begin{bmatrix} M_1 & M_2 & M_3 \\ M_4 & M_5 & M_6 \\ M_7 & M_8 & M_9 \end{bmatrix} = \begin{bmatrix} M_1 & M_2 & M_3 \\ M_4 & M_5 & M_4 \\ M_3 & M_2 & M_1 \end{bmatrix} \qquad (5.24)$$

Proof: I will demonstrate that $M_7 = M_3$. The Feynman diagram for M_7 including momentum labels is given in figure 5.6, and M_3 we have already seen in figure 5.5. Using the same techniques of inserting CC^{-1}, transposition, and cyclicity of the trace, we obtain:

$$\begin{aligned}
M_3 &= K_{03} \cdot K_{f3}/l^2(l-t)^2 \\
M_7 &= K_{07} \cdot K_{f7}/l^2(l-t)^2 \\
K_{07} &= tr\left\{(\not{k}_0 + m_0)\not{\epsilon}_0\not{\epsilon}_2(\not{k}_2 - \not{k}_0 - m_0)^{-1}\gamma^\alpha(\not{k}_2 - \not{k}_0 + \not{l} - m_0)^{-1}\gamma^\beta[CC^{-1}]\right\} \\
&= tr\left\{(-\not{k}_0^T + m_0)\not{\epsilon}_0^T\not{\epsilon}_2^T(-\not{k}_2^T + \not{k}_0^T - m_0)^{-1}\gamma^{\alpha T}(-\not{k}_2^T + \not{k}_0^T - \not{l}^T - m_0)^{-1}\gamma^{\beta T}\right\} \\
&= tr\left\{(\not{k}_0 + m_0)\not{\epsilon}_0\gamma^\beta(\not{k}_0 - \not{k}_2 - \not{l} - m_0)^{-1}\gamma^\alpha(\not{k}_0 - \not{k}_2 - m_0)^{1}\not{\epsilon}_2\right\} \\
&= K_{03} \\
K_{f7} &= tr\left\{(-\not{k}_f + m_f)\not{\epsilon}_f\gamma^\alpha(\not{k}_f - \not{l} - m_f)^{-1}\gamma^\beta(-\not{k}_f - \not{k}_1 - m_f)^{-1}\not{\epsilon}_1[CC^{-1}]\right\} \\
&= tr\left\{(-\not{k}_f + m_f)\not{\epsilon}_f\not{\epsilon}_1(\not{k}_f + \not{k}_1 - m_f)^{-1}\gamma^\beta(\not{l} - \not{k}_f l - m_f)^{-1}\gamma^\alpha\right\} \\
&= K_{f3}
\end{aligned} \qquad (5.25)$$

Thus we are done. The other equalities follow similarly. □

Combining 5.22 and 5.24 we now have for the purely strong invariant amplitude "A_q^s":

$$\begin{aligned}
A_q^s &= A_{18} \quad + \quad 1 \leftrightarrow 2 \\
&= 2F^{ab}\left[M_1 + M_2 + M_3 + M_4 + M_5/2 \quad + \; 1 \leftrightarrow 2\,\right]
\end{aligned} \qquad (5.26)$$

and thus $\hat{M}_q^s$ as defined in equation 5.7 is:

$$\hat{M}_q^s = 2\left[\hat{M}_1 + \hat{M}_2 + \hat{M}_3 + \hat{M}_4 + \hat{M}_5/2 \quad + \; 1 \leftrightarrow 2\right] \qquad (5.27)$$

$$\hat{M}_k = \frac{m_0^2 \cdot 16\pi^2}{g_s^6} M_k \qquad (5.28)$$

Note that the extra terms represented by "$1 \leftrightarrow 2$" will not lead to any extra work for us. The sum of the first five amplitudes constitute a function

$$G(k_1, \epsilon_1; k_2, \epsilon_2) \equiv \hat{M}_1 + \hat{M}_2 + \hat{M}_3 + \hat{M}_4 + \hat{M}_5/2 \qquad (5.29)$$

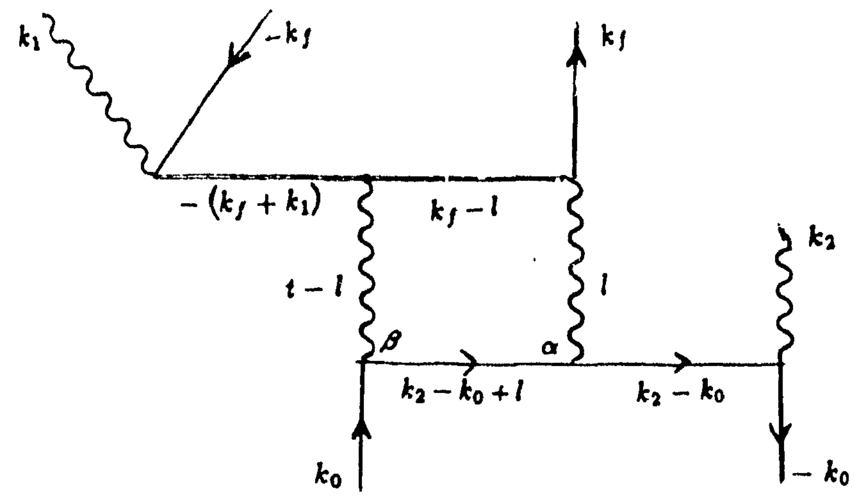

Figure 5.6: Momentum labeled diagram for amplitude M_7

of the gluonic momenta and polarizations. Once we have a general formula for "G", the terms "$1 \leftrightarrow 2$" can be easily computed from this one function:

$$"1 \leftrightarrow 2" = G(k_2, \epsilon_2; k_1, \epsilon_1)$$

Thus our problem is reduced to finding a procedure for calculating "G" as a function of the four vectors $k_1, k_2, \epsilon_1, \epsilon_2$.

Expressions for Five Amplitudes

The momentum labeled Feynman diagrams for the first five amplitudes are shown in figure 5.7. I have used "k_a, k_b " and "ϵ_a, ϵ_b" to denote the final gluon momenta and spin, rather than "k_1, k_2" and "ϵ_1, ϵ_2", to facilitate the exchange "$1 \leftrightarrow 2$" discussed in the last section. We obtain:

$$\begin{aligned}
\hat{M}_1 &= m_0^2 \int \frac{d^4 l}{\pi^2} \frac{f_1}{p_a p_b \cdot ABDF} \\
\hat{M}_2 &= m_0^2 \int \frac{d^4 l}{\pi^2} \frac{f_2}{p_a p_b \cdot ABCF} \\
\hat{M}_3 &= m_0^2 \int \frac{d^4 l}{\pi^2} \frac{f_3}{p_a \cdot ABCDF} \\
\hat{M}_4 &= m_0^2 \int \frac{d^4 l}{\pi^2} \frac{f_4}{p_b \cdot ABDEF}
\end{aligned}$$

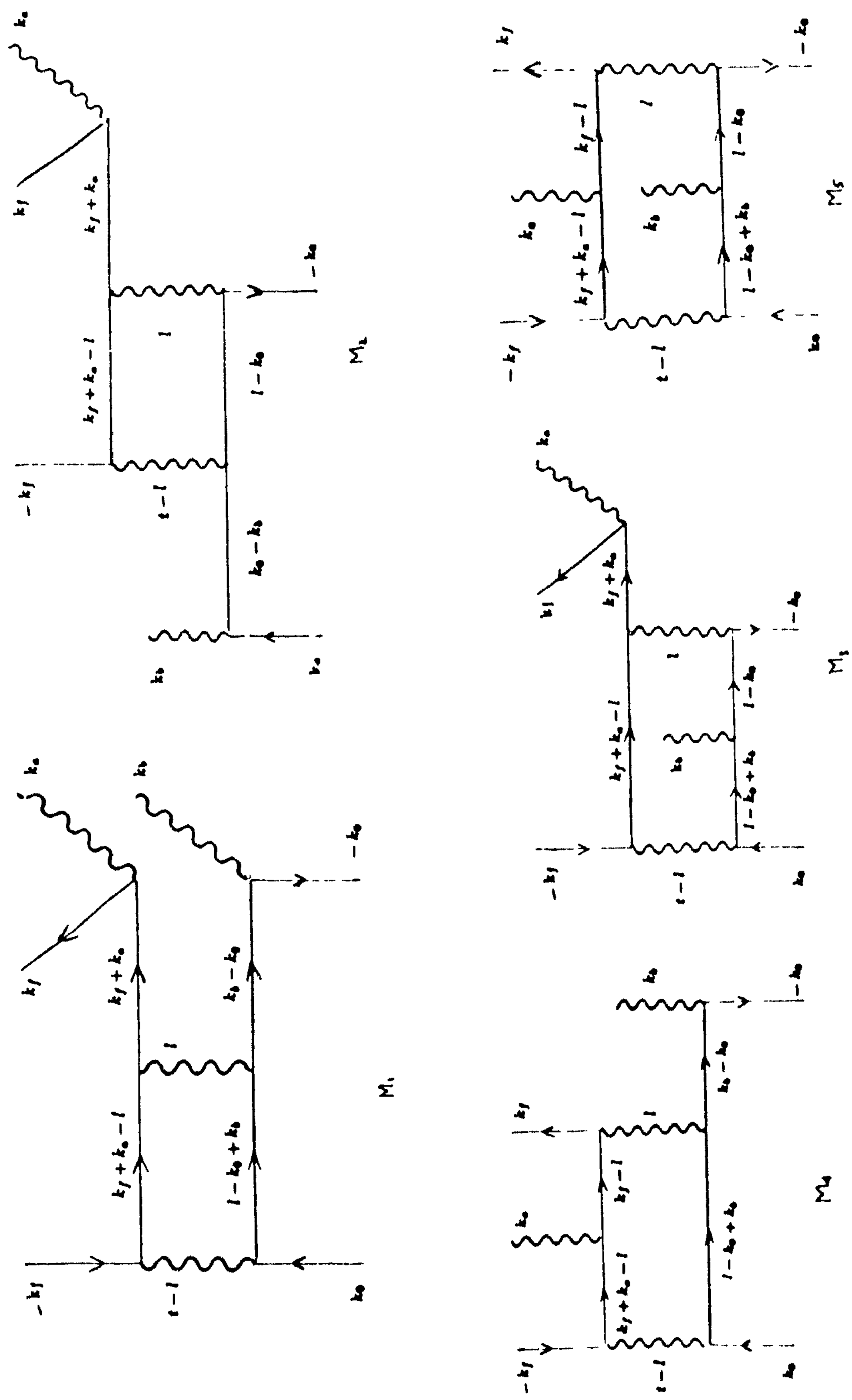

Figure 5.7: Momentum labeled diagrams for the first five ampitudes

$$
\begin{aligned}
\hat{M}_5 &= m_0^2 \int \frac{d^4 l}{\pi^2} \frac{f_5}{ABCDEF} \qquad (5.30) \\
f_1 &\equiv J_{01} \cdot J_{f1} \\
f_2 &\equiv J_{02} \cdot J_{f1} \\
f_3 &\equiv J_{03} \cdot J_{f1} \\
f_4 &\equiv J_{01} \cdot J_{f3} \\
f_5 &\equiv J_{03} \cdot J_{f3} \\
J_{01}^{\alpha\beta} &\equiv tr\left\{(\not{k}_0 + m_0)\not{\epsilon}_0\not{\epsilon}_b(\not{k}_b - \not{k}_0 + m_0)\gamma^\alpha(\not{l} - \not{k}_0 + \not{k}_b + m_0)\gamma^\beta\right\} \\
J_{02}^{\alpha\beta} &\equiv tr\left\{(\not{k}_0 + m_0)\not{\epsilon}_0\gamma^\alpha(\not{l} - \not{k}_0 + m_0)\gamma^\beta(\not{k}_0 - \not{k}_b + m_0)\not{\epsilon}_b\right\} \\
J_{03}^{\alpha\beta} &\equiv tr\left\{(\not{k}_0 + m_0)\not{\epsilon}_0\gamma^\alpha(\not{l} - \not{k}_0 + m_0)\not{\epsilon}_b(\not{l} - \not{k}_0 + \not{k}_b + m_0)\gamma^\beta\right\} \\
J_{f1}^{\alpha\beta} &\equiv tr\left\{(-\not{k}_f + m_f)\not{\epsilon}_f\not{\epsilon}_a(\not{k}_f + \not{k}_a + m_f)\gamma^\alpha(\not{k}_f + \not{k}_a - \not{l} + m_f)\gamma^\beta\right\} \\
J_{f3}^{\alpha\beta} &\equiv tr\left\{(-\not{k}_f + m_f)\not{\epsilon}_f\gamma^\alpha(\not{k}_f - \not{l} + m_f)\not{\epsilon}_a(\not{k}_f + \not{k}_a - \not{l} + m_f)\gamma^\beta\right\} \\
t &\equiv 2k_f + k_a = 2k_0 - k_b \\
A &\equiv l^2 - i\epsilon \\
B &\equiv (l-t)^2 - i\epsilon \\
C &\equiv (l-k_0)^2 - m_0^2 - i\epsilon \\
D &\equiv (l - k_0 + k_b)^2 - m_0^2 - i\epsilon \\
E &\equiv (l-k_f)^2 - m_f^2 - i\epsilon \\
F &\equiv (l - k_f - k_a)^2 - m_f^2 - i\epsilon \\
p_a &\equiv (k_f + k_a)^2 - m_f^2 = 2k_f \cdot k_a \\
p_b &\equiv (k_0 - k_b)^2 - m_0^2 = -2k_0 \cdot k_b
\end{aligned}
$$

I will not present the formulae for the f_k, obtained by evaluating the above traces. These expressions are quite long and not particularly illuminating (see figure 5.8). They have been computed using the symbol manipulation program called REDUCE [72] The expressions obtained from this program were directly substituted into a numerical integration program that computed the loop integrals, which were converted into integrals over a unit hypercube using Feynman parameter techniques discussed extensively in the section 5.6.

5.3.2 Infrared and Ultraviolet Finiteness

There are no ultraviolet divergences in this problem. All the loop integrals are finite by power counting.

I now discuss possible infrared divergences in the loop integrals. Naively, the presence of the massless gluons in the loop would lead us to expect an infrared divergence. However, a general argument implies that there can be none. The result is easily established from an intermediate step in the proof

```
16*U03*JF1
- 32*MF*MO*(L L*L E2*E1 EF*EO K1 - L L*L E2*E1 EO*EF K1 + 2*L L*L E2*E1 KF*EF EO + L L*L EO*E2 E1
  *EF K1 - 2*L L*L EO*E2 EF*E1 KF - L L*L EO*E2 K1*E1 EF - L L*E2 E1*EF K1*EO K1 - L L*E2 E1*EF
  K1*EO KF + 2*L L*E2 EF*E1 KF*EO K1 + 2*L L*E2 EF*E1 KF*EO KF + L L*E2 EO*E1 EF*K1 KF - L L*E2
  EO*E1 KF*EF K1 + 2*L L*E2 K1*E1 EF*EO K1 + L L*E2 K1*E1 EF*EO KF - L L*E2 K1*E1 EO*EF K1 + 2*L
  L*E2 K1*E1 KF*EF EO + L L*E2 KF*E1 EF*EO K1 - L L*E2 KF*E1 EO*EF K1 + 2*L L*E2 KF*E1 KF*EF EO -
  2*L L*E2 KO*E1 EF*EO K1 + 2*L L*E2 KO*E1 EO*EF K1 - 4*L L*E2 KO*E1 KF*EF EO - 2*L E2*L E1*L EO
  *EF K1 - 2*L E2*L E1*EF EO*K1 KO + 2*L E2*L E1*EF K1*EO K1 + 4*L E2*L E1*EF K1*EO KF + 2*L E2*L
  E1*EF KO*EO K1 + 4*L E2*L EF*L EO*E1 KF + 2*L E2*L EF*E1 EO*K1 KO - 4*L E2*L EF*E1 KF*EO K1 -
  4*L E2*L EF*E1 KF*EO KF - 2*L E2*L EF*E1 KF*EO K1 + 2*L E2*L EO*L K1*E1 EF + L E2*L EO*E1 EF*K2
  K1 - 2*L E2*L EO*E1 EF*K1 KF - 2*L E2*L E1*E1 EF*K1 KO - L E2*L EO*E1 K2*EF K1 + 2*L E2*L EO*
  E1 KF*EF K2 + 2*L E2*L EO*E1 KF*EF K1 - 4*L E2*L E1*E1 KF*EF KO + 2*L E2*L EO*E1 KO*EF K1 - 4*L
  E2*L K1*E1 EF*EO K1 - 2*L E2*L K1*E1 EF*EO KF + 2*L E2*L K1*E1 EO*EF K1 - 2*L E2*L K1*E1 EO*EF
  KO - 4*L E2*L K1*E1 KF*EF EO + 2*L E2*L K1*E1 K2*EF EO - 2*L E2*L KF*E1 EF*EO K1 + 2*L E2*L KF
  *E1 EO*EF K1 - 4*L E2*L KF*E1 KF*EF EO - L E2*E1 EF*EO K2*K1 KF + L E2*E1 EF*EO K2*K1 KO - 2*L
  E2*E1 EF*EO K1*K2 K1 - L E2*E1 EF*EO K1*K2 KF + 4*L E2*E1 EF*EO K1*K1 KO + 4*L E2*E1 EF*EO K1*
  KF KO - L E2*E1 EF*EO KF*K2 K1 + L E2*E1 E1*EF K1*K2 K1 + L E2*E1 EO*EF K1*K2 KF - 4*L E2*E1 EO
  *EF K1*K1 KO - 4*L E2*E1 EO*EF K1*KF KO + 4*L E2*E1 EO*EF KO*K1 KF + L E2*E1 K2*EF K1*EO K1 + L
  E2*E1 K2*EF K1*EO KF - 2*L E2*E1 KF*EF EO*K2 K1 - 2*L E2*E1 KF*EF E*K2 KF - 8*L E2*E1 KF*EF
  EO*K1 KO + 8*L E2*E1 KF*EF EO*KF KO - 2*L E2*E1 KF*EF K2*EO K1 - 2*L E2*E1 KF*EF K2*EO KF + L
  E2*E1 KF*EF K1*EO K2 + 2*L E2*E1 KF*EF KO*EO K2 - 4*L E2*E1 K*EF EO*K1 KF - L E2*E1 KO*EF K1*
  EO K2 + L E1*L EO*E2 EF*K2 K1 - L E1*L EO*E2 K1*EF K2 + 2*L E1*L EO*E2 KO*EF K1 - 2*L E1*E2 EF*
  EO K2*K1 KF + L E1*E2 EF*EO K2*K1 KO + 2*L E*E2 EO*EF K2*K1 KF - L E1*E2 EO*EF K2*K1 KO - L E1
  *E2 EO*EF K1*K2 K1 - L E1*E2 EO*EF K1*K2 KF - L E1*E2 EF*EF K1*K2 KO + L E1*E2 E*EF K1*K2 K1 +
  L E1*E2 K1*EF K1*EO K2 - L E1*E2 K1*EF KO*EO K2 + L E1*E2 KF*EF K1*EO K2 + 2*L E1*E2 KO*EF EO*
  K1 KO + L E1*E2 KO*EF K1*EO K2 - 2*L E1*E2 KO*EF K1*EO K1 - 2*L E1*E2 KO*EF K1*EO KF - 2*L E1*
  E2 KO*EF KO*EO K1 - L EF*L EO*E2 E1*K2 K1 + L EF*L EO*E2 K1*E1 K2 - 4*L EF*L EO*E2 KO*E1 KF + 2
  *L EF*E2 E1*EO K2*K1 KF - L EF*E2 E1*EO K2*K1 KO - 2*L EF*E2 EO*E1 K2*K1 KF + L EF*E2 EO*E1 K2*
  K1 KO + 2*L EF*E2 EO*E1 KF*K2 K1 + 2*L EF*E2 EO*E1 KF*K2 KF + 2*L EF*E2 EO*E1 KF*K2 KO - L EF*
  E2 EO*E1 KO*K2 K1 - 2*L EF*E2 K1*E1 KF*EO K2 + L EF*E2 K1*E1 KO*EO K2 - 2*L EF*E2 KF*E1 KF*EO
  K2 - 2*L EF*E2 KO*E1 EO*K1 KO - 2*L EF*E2 K*E1 KF*EO K2 + 4*L EF*E2 KO*E1 KF*EO K1 + 4*L EF*E2
  KO*E1 KF*EO KF + 2*L EF*E2 KO*E1 KO*EO K1 + L EO*L K2*E2 E1*EF K1 - 2*L EO*L K2*E2 EF*E1 KF -
  L EO*L K2*E2 K1*E1 EF + L EO*L K1*E2 E1*EF K2 - L EO*L K1*E2 EF*E1 K2 - 2*L EO*L K1*E2 KO*E1 EF
  - 2*L EO*L KO*E2 E1*EF K1 + 4*L EO*L KO*E2 EF*E1 KF + 2*L E*L KO*E2 K1*E1 EF - 2*L EO*E2 E1*
  EF K2*K1 KF + L EO*E2 E1*EF K1*K2 K1 + L EO*E2 E*EF K1*K2 KF + 2*L E*E2 E1*E1 K2*K1 KF - 2*L
  EO*E2 EF*E1 KF*K2 K1 - 2*L EO*E2 EF*E1 KF*K2 KF - L EO*E2 K1*E1 EF*K2 KF - L EO*E2 K1*E1 K2*EF
  K1 + 2*L EO*E2 K1*E1 KF*EF K2 + L EO*E2 KF*E1 EF*K2 K1 - L EO*E2 KF*E1 K2*EF K1 + 2*L EO*E2 KF*
  E1 KF*EF K2 + 2*L EO*E2 KO*E1 EF*K1 KF + 2*L E*E2 KO*E1 EF*K1 KO - 2*L EO*E2 KO*E1 KF*EF K1 +
  4*L EO*E2 KO*E1 KF*EF KO - 2*L EO*E2 KO*E1 K*EF K1 - L K2*E2 E1*EF K1*EO K1 - L K2*E2 E1*EF K1
  *EO KF + 2*L K2*E2 EF*E1 KF*EO K1 + 2*L K2*E2 EF*E1 KF*EO KF + L K2*E2 EO*E1 EF*K1 KF - L K2*E2
  EO*E1 EF*K1 KO - L K2*E2 EO*E1 KF*EF K1 - 2*L K2*E2 EO*E1 KF*EF KO + L K2*E2 EO*E1 KO*EF K1 +
  2*L K2*E2 K1*E1 EF*EO K1 + L K2*E2 K1*E1 EF*EO KF - L K2*E2 K1*E1 EO*EF K1 + 2*L K2*E2 K1*E1 KF
  *EF EO + L K2*E2 KF*E1 EF*EO K1 - L K2*E2 KF*E1 EO*EF K1 + 2*L K2*E2 KF*E1 KF*EF EO - L K1*E2
  E1*EF K1*EO K2 + L K1*E2 E1*EF KO*EO K2 + 2*L K1*E2 EF*E1 KF*EO K2 - L K1*E2 EF*E1 KO*EO K2 + L
  K1*E2 EO*E1 EF*K2 KF + L K1*E2 EO*E1 EF*K2 KO + L K1*E2 EO*E1 K2*EF K1 - L K1*E2 E*E1 K2*EF
  KO - 2*L K1*E2 EO*E1 KF*EF K2 + L K1*E2 EO*E1 KO*EF K2 - L K1*E2 KF*E1 EF*EO K2 - L K1*E2 KO*E1
  EF*EO K2 + 4*L K1*E2 KO*E1 EF*EO K1 + 2*L K1*E2 K*E1 EF*EO KF - 2*L K1*E2 KO*E1 EO*EF K1 + 2*
  L K1*E2 KO*E1 EO*EF KO + 4*L K1*E2 KO*E KF*EF EO - 2*L K1*E2 K*E1 KO*EF EO - L KF*E2 E1*EF K1
  *EO K2 + 2*L KF*E2 EF*E1 KF*EO K2 - L KF*E2 EO*E1 EF*K2 K1 + L KF*E2 EO*E1 K2*EF K1 - 2*L KF*E2
  EO*E1 KF*EF K2 + L KF*E2 K1*E1 EF*EO K2 + 2*L KF*E2 KO*E1 EF*EO K1 - 2*L KF*E2 KO*E1 EO*EF K1
  + 4*L KF*E2 KO*E1 KF*EF EO - L KO*E2 E1*EF K1*EO K2 + 2*L KO*E2 E1*EF K1*EO K1 + 2*L KO*E2 E1*
  EF K1*EO KF + 2*L KO*E2 EF*E1 KF*EO K2 - 4*L KO*E2 EF*E1 KF*EO K1 - 4*L KO*E2 EF*E1 KF*EO KF -
  L KO*E2 EO*E1 EF*K2 K1 - 2*L KO*E2 EO*E1 EF*K1 KF + L KO*E2 EO*E1 K2*EF K1 - 2*L K*E2 EO*E1 KF
  *EF K2 + 2*L KO*E2 EO*E1 KF*EF K1 + L KO*E2 K1*E1 EF*EO K2 - 4*L KO*E2 K1*E1 EF*EO K1 - 2*L KO*
  E2 K1*E1 EF*EO KF + 2*L KO*E2 K1*E1 EO*EF K1 - 4*L KO*E2 K1*E1 KF*EF EO - 2*L KO*E2 KF*E1 EF*EO
  K1 + 2*L KO*E2 KF*E1 EO*EF K1 - 4*L KO*E2 KF*E1 KF*EF EO + 2*L KO*E2 KF*E1 EF*EO K1 - 2*L KO*
  E2 KO*E1 E1*EF K1 + 4*L KO*E2 KO*E1 KF*EF EO + 2*E2 E1*EF K1*EO K2*K1 KO + 4*E2 E1*EF K1*EO K2*
  KF KO - 2*E2 E1*EF KO*EO K2*K1 KF - 4*E2 EF*E1 KF*EO K2*K1 KO - 4*E2 EF*E1 KF*EO K2*KF KO + 2*
  E2 EF*E1 KO*EO K2*K1 KF + 2*E2 EO*E1 EF*K2 K1*K1 KO + 2*E2 EO*E1 EF*K2 K*KF KO - 4*E2 EO*E1 EF
  *K2 KO*K1 KF - 2*E2 EO*E1 K2*EF K1*K1 KO - 2*E2 EO*E1 K2*EF K1*KF KO + 2*E2 EO*E1 K2*EF KO*K1
  KF + 4*E2 EO*E1 KF*EF K2*K1 KO + 4*E2 EO*E1 KF*EF K2*KF KO - 2*E2 EO*E1 KO*EF K2*K1 KF - 2*E2
  K1*E1 EF*EO K2*K1 KO - 2*E2 K1*E1 EF*EO K2*KF KO + 2*E2 KO*E1 EF*EO K2*K1 KF - 4*E2 KO*E1 EF*EO
  K1*K1 KO - 4*E2 KO*E1 EF*EO K1*KF KO + 4*E2 KO*E1 EO*EF K1*K1 KO + 4*E2 KO*E1 EO*EF K1*KF KO -
  4*E2 KO*E1 EO*EF KO*K1 KF - 8*E2 KO*E1 KF*EF EO*K1 KO - 8*E2 KO*E1 KF*EF EO*KF KO + 4*E2 KO*E1
  KO*EF EO*K1 KF)
```

Figure 5.8: The function "f_3" as computed by REDUCE

of the cancellation of infrared divergences between radiative corrections and bremsstrahlung [62].

The point is that the $O(\alpha_s^3)$ loop diagrams for $\Upsilon \to Jgg$ can be thought of as radiative corrections to an $O(\alpha_s^2)$ amplitude; but this just happens to vanish because of the rule that each vector meson must couple to at least three gluons, a consequence of C-parity invariance. Let us use $M_{[3]}^{IR}$ to denote the *infrared divergent* part of the $O(\alpha_s^3)$ amplitude, and $M_{[2]}$ to denote the amplitude at $O(\alpha_s^2)$. One can show [62] that $M_{[3]}^{IR}$ is given by an infinite factor (which can be regulated by a suitable infrared cutoff, such as a gluon mass λ) times $M_{[2]}$. On the other hand, $M_{[2]}$ is identically zero, as discussed. Hence

$$M_{[3]}^{IR} \propto \alpha_s \log \lambda \cdot M_{[2]} \equiv 0 \tag{5.31}$$

However, while the entire amplitude is infrared finite the individual Feynman diagrams usually are not. This is because typically several diagrams have to be combined to put the intermediate, loop, gluons in a state of definite C-parity, which was an important ingredient in the preceding proof of finiteness. Specifically, note that each of the amplitudes (except M_2) contain the three propagators B, D, and F, which can be expressed as:

$$\begin{aligned} B &= (l-t)^2 \\ D &= (l-t+k_0)^2 - m_0^2 \\ &= 2k_0\cdot(l-t) + (l-t)^2 \\ F &= 2k_f\cdot(l-t) + (l-t)^2 \end{aligned} \tag{5.32}$$

Note that the other propagators A, C, E are non-zero at $l = t$. Thus near $l = t$, the integrals behave as:

$$\int \frac{d^4 l}{BDF} \sim \int \frac{d^4 l}{(t-l)^4} \tag{5.33}$$

which is logarithmically divergent. This is an infrared divergence that we know must not exist.

This bad behaviour only disappears when several of the amplitudes are summed, and then it depends most crucially on a "zero" that a certain combination of the currents has:

$$(J_{01} + J_{03})^{\alpha\beta}(l=t) = 0 \tag{5.34}$$

$$(J_{f1} + J_{f3})^{\alpha\beta}(l=t) = 0 \tag{5.35}$$

Proof: First we substitute $l = t$ into the above formulae for the currents:

$$(J_{01} + J_{03})^{\alpha\beta}(l=t) = \\ tr\left\{(\not k_0 + m_0)\not\epsilon_0\left[\not\epsilon_b(\not k_b - \not k_0 + m_0)\gamma^\alpha + \gamma^\alpha(\not k_0 - \not k_b + m_0)\not\epsilon_b\right](\not k_0 + m_0)\gamma^\beta\right\} \tag{5.36}$$

Now note that:

$$
\begin{aligned}
(\not{k}_0 + m_0)\gamma^\beta(\not{k}_0 + m_0) &= \delta^{\beta 0}(\not{k}_0 + m_0)\gamma^0(\not{k}_0 + m_0) \\
&= 2m_0\delta^{\beta 0}(\not{k}_0 + m_0) \equiv a(\not{k}_0 + m_0) \qquad (5.37)
\end{aligned}
$$

since $k_0 = (m_0, 0)$. Using this and inserting $1 = CC^{-1}$:

$$
\begin{aligned}
&(J_{01} + J_{03})^{\alpha\beta}(l = t) = \qquad (5.38) \\
&\quad a \cdot tr\left\{(\not{k}_0 + m_0)\not{\epsilon}_0\left[\not{\epsilon}_b(\not{k}_b - \not{k}_0 + m_0)\gamma^\alpha + \gamma^\alpha(\not{k}_0 - \not{k}_b + m_0)\not{\epsilon}_b\right]CC^{-1}\right\} \\
&\quad = a(-1)^3 tr\left\{(-\not{k}_0^T + m_0)\not{\epsilon}_0^T\left[\not{\epsilon}_b^T(-\not{k}_b^T + \not{k}_0^T + m_0)\gamma^{\alpha T} + \gamma^{\alpha T}(-\not{k}_0^T + \not{k}_b^T + m_0)\not{\epsilon}_b^T\right]\right\} \\
&\quad = -a \cdot tr\left\{\left[\gamma^\alpha(\not{k}_0 - \not{k}_b + m_0)\not{\epsilon}_b + \not{\epsilon}_b(\not{k}_b - \not{k}_0 + m_0)\gamma^\alpha\right]\not{\epsilon}_0(-\not{k}_0 + m_0)\right\} \\
&\quad = -(J_{01} + J_{03})^{\alpha\beta}(l = t) \qquad (5.39)
\end{aligned}
$$

Thus $(J_{01} + J_{03})^{\alpha\beta}(l = t) \equiv 0$ as claimed. Here we used the same techniques as in section 5.3.1, where we were concerned with demonstrating the equality of diagrams. As there, this identity is a consequence of C-parity invariance of the theory. The other identity is proved via similar manipulations. □

This proof is demonstrated pictorially in figure 5.9. We will use this identity in the later sections to motivate the construction of manifestly infrared finite combinations of the amplitudes.

5.3.3 Reduction to Four Propagators

To compute the loop integrals in 5.30, we will introduce Feynman parameters according to the usual methods [16, 45]. An amplitude with "n" propagators in the denominator will be converted into an integral over an "n-1" dimensional unit hypercube. Obviously, it is desirable to keep the dimension of this cube as low as possible. This may be accomplished by multiplying amplitudes containing 5 or more propagators in the denominator by one of the following factors of "1"

$$
\begin{aligned}
1 &= \frac{A + B - C - D}{t^2 - p_b} \qquad (5.40) \\
&= \frac{A + B - E - F}{t^2 - p_a} \qquad (5.41) \\
&= \frac{C + D - E - F}{p_b - p_a} \qquad (5.42)
\end{aligned}
$$

These may be verified by direct computation; for example:

$$
\begin{aligned}
A + B - C - D &\equiv l^2 + (l - t)^2 - \left[(l - k_0)^2 - m_0^2 + (l - k_0 + k_b)^2 - m_0^2\right] \\
&= -2l \cdot (t - k_0 - k_0 + k_b) + t^2 - \left[(k_0 - k_b)^2 - m_0^2\right] \\
&= t^2 - p_b \qquad (5.43)
\end{aligned}
$$

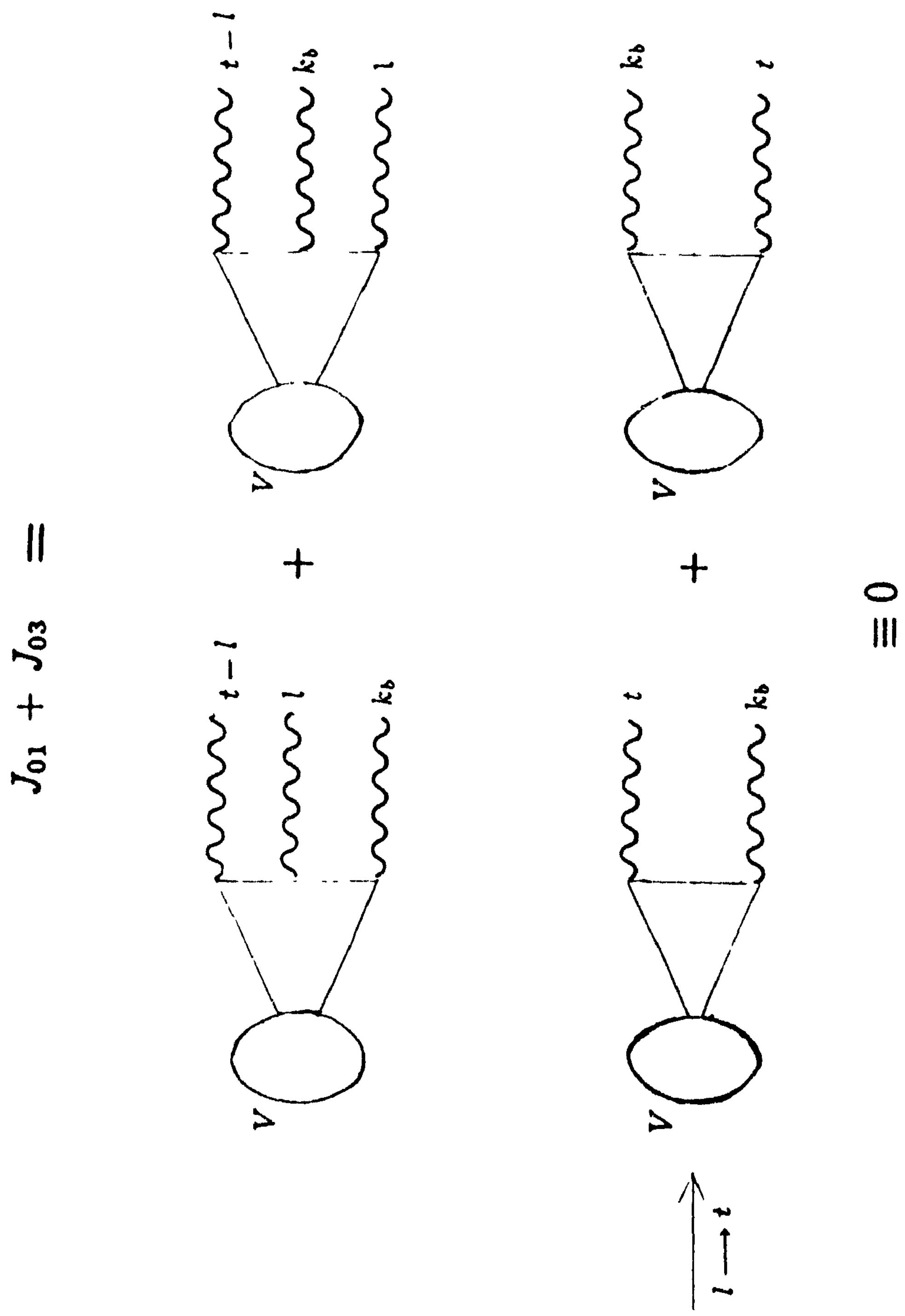

Figure 5.9: Pictorial demonstration that $J_{01} + J_{03}$ has a zero at $l = t$.

We now use these identities to express the sum of the amplitudes in terms of four-propagator integrals. Note that under the operation:

$$l \longrightarrow t - l$$

we have,

$$\begin{aligned} A &\leftrightarrow B \\ C &\leftrightarrow D \\ E &\leftrightarrow F \\ J_{03}^{\alpha\beta} &\leftrightarrow J_{03}^{\beta\alpha} \\ J_{f3}^{\alpha\beta} &\leftrightarrow J_{f3}^{\beta\alpha} \end{aligned} \tag{5.44}$$

These last two imply that:

$$f_5(l) = f_5(t-l)$$

Thus the integrand of $\hat{M}_5$ is invariant under the change of variable $l' = t - l$, and we have:

$$\begin{aligned} \frac{\pi^2}{m_0^2}\frac{1}{2}\hat{M}_5 &= \int \frac{d^4 l}{ABDF}\frac{f_5}{2CE} \\ &= \int \frac{d^4 l}{ABDF}\frac{f_5}{2CE}\frac{C + D - E - F}{p_b - p_a} \\ &= \int \frac{d^4 l}{ABDF}\frac{f_5}{CE}\frac{C - E}{p_b - p_a} \end{aligned}$$

Therefore:

$$\begin{aligned} (G - \hat{M}_2) &\equiv \hat{M}_1 + \hat{M}_3 + \hat{M}_4 + \frac{1}{2}\hat{M}_5 \\ &= m_0^2 \int \frac{\pi^{-2} d^4 l}{ABDF}\left\{\frac{f_1}{p_a p_b} + \frac{f_3}{p_a C} + \frac{f_4}{E p_b} + \frac{f_5}{C(p_a - p_b)} - \frac{f_5}{E(p_a - p_b)}\right\} \\ &= \frac{m_0^2}{p_a - p_b}\int \frac{\pi^{-2} d^4 l}{ABDF}\left\{\frac{f_1}{p_b} - \frac{f_1}{p_a} + \frac{f_3}{C}(1 - \frac{p_b}{p_a}) + \frac{f_4}{E}(1 - \frac{p_a}{p_b}) + \frac{f_5}{C} - \frac{f_5}{E}\right\} \\ &\equiv \frac{m_0^2}{p_a - p_b}\int \frac{\pi^{-2} d^4 l}{ABDF}\left\{\frac{F_1}{C} - \frac{F_2}{E}\right\} \end{aligned} \tag{5.45}$$

$$\begin{aligned} F_1 &= f_5 + f_3 - (p_b f_3 + C f_1)/p_a \\ F_2 &= f_5 + f_4 - (p_a f_4 + E f_1)/p_b \end{aligned} \tag{5.46}$$

Thus at $l = t$ we have:

$$C\big|_t = (t - k_0)^2 - m_0^2 = p_b$$

$$
\begin{aligned}
E_{1_t} &= (t-k_f)^2 - m_0^2 = p_a \\
F_1(t) &= \left[f_5 + f_3 - \frac{p_b}{p_a}(f_3 + f_1)\right]_t \\
&= J_{03} \cdot [J_{f1} + J_{f3}](l=t) - \frac{p_b}{p_a} J_{f1} \cdot [J_{01} + J_{03}](l=t) \\
&= 0 \\
F_2(t) &= \left[f_5 + f_4 - \frac{p_a}{p_b}(f_4 + f_1)\right]_t \\
&= J_{f3} \cdot [J_{01} + J_{03}](l=t) - \frac{p_a}{p_b} J_{01} \cdot [J_{f1} + J_{f3}](l=t) \\
&= 0
\end{aligned}
$$

where we have used 5.35. Thus each of the two terms in equation 5.45 is separately infrared finite.

The expression 5.45 for "G" contains 5 propagators in the denominator. Further use of the identities 5.42 leads to a formula with just four propagators in the denominator

$$
\begin{aligned}
\frac{\pi^2}{m_0^2}(p_a - p_b)G &= \int \frac{d^4l \cdot h_1}{ABCE} + \int \frac{d^4l \cdot h_2}{ADEF} + \int \frac{d^4l \cdot h_3}{ACDF} \\
&\quad + \int \frac{d^4l \cdot h_4}{ABCF} + \int \frac{d^4l \cdot h_5}{ACEF} + \int \frac{d^4l \cdot h_6}{ACDE}
\end{aligned}
\tag{5.47}
$$

$$
\begin{aligned}
h_1 &= -(h_5 + h_6) \\
h_2 &= \frac{-F_2}{t^2 - p_a} \\
h_3 &= \frac{F_1}{t^2 - p_b} \\
h_4 &= -(h_3 + h_5) + \frac{p_a - p_b}{p_a p_b} f_2 \\
h_5 &= \frac{-\tilde{F}_2}{t^2 - p_a} \\
h_6 &= \frac{\tilde{F}_1}{t^2 - p_b} \\
\tilde{F}_k(l) &\equiv F_k(t-l)
\end{aligned}
\tag{5.48}
$$

Note that I have made the the change of variable $l' = t - l$ where necessary to ensure that one of the four propagators in each integrand is:

$$
A = l^2 - i\epsilon
$$

The evaluation of such integrals will is discussed in section 5.6.

5.4 Electromagnetic Part

5.4.1 Feynman Diagrams

The twelve leading Feynman diagrams for this process are of order $e^2 g_s^2$, and are depicted in figure 5.10. These are all the diagrams consistent with the rule that a vector meson must couple to either an odd number of photons or at least three gluons (see section 4.4.2). We see that inclusion of a single photon lowers the total number of vertices and thus coupling constants in the Feynman diagram, with respect to the purely gluonic contributions of section 5.3.

The electromagnetic amplitude is the sum of the twelve diagrams

$$A_q^{em} = \sum \begin{bmatrix} A_1^{em} & A_2^{em} & A_3^{em} \\ \tilde{A}_1^{em} & \tilde{A}_2^{em} & \tilde{A}_3^{em} \\ A_4^{em} & A_5^{em} & A_6^{em} \\ \tilde{A}_4^{em} & \tilde{A}_5^{em} & \tilde{A}_6^{em} \end{bmatrix} \tag{5.49}$$

Each amplitude in the array corresponds to the appropriately positioned diagram in figure 5.10. Separating the amplitudes into color and lorentz parts

$$\begin{aligned} A_k^{em} &= F_{em}^{ab} M_k^{em} \\ F_{em}^{ab} &= \left(\frac{1}{\sqrt{3}}\right)^2 tr\left\{1_{3\times 3}\right\}\ tr\left\{T_a T_b\right\} \quad = F_{em}\delta^{ab} \\ F_{em} &= \frac{1}{2} \end{aligned} \tag{5.50}$$

where I have used the identities of appendix A. Each of the diagrams have the same color factor.

By charge conjugating the single fermion current, it is possible to show that:

$$\tilde{M}_k^{em} = M_k^{em} \tag{5.51}$$

The proof is exactly analogous to what we did in section 5.3.1, with the purely strong amplitudes. In fact, the demonstration in that section that "$K_{03} = \tilde{K}_{01}$" constitutes the essence of the proof. Thus the amplitude becomes.

$$A_q^{em} = 2F_{em}\delta^{ab}\left[M_1^{em} + M_2^{em} + M_3^{em} + M_4^{em} + M_5^{em} + M_6^{em}\right] \tag{5.52}$$

Define the unitless quantitiy $\hat{M}_q^{em}$ (the analogue of $\hat{M}_q^{s}$ in equation 5.7), by extracting the coupling constants, color factor, and powers of mass:

$$\begin{aligned} A_q^{em} &= g_s^2 e^2 Q_c Q_b \cdot F_{em}\delta^{ab} \cdot \frac{1}{m_0^2}\ \hat{M}_q^{em} \\ Q_c &= 2/3 \\ Q_b &= -1/3 \end{aligned} \tag{5.53}$$

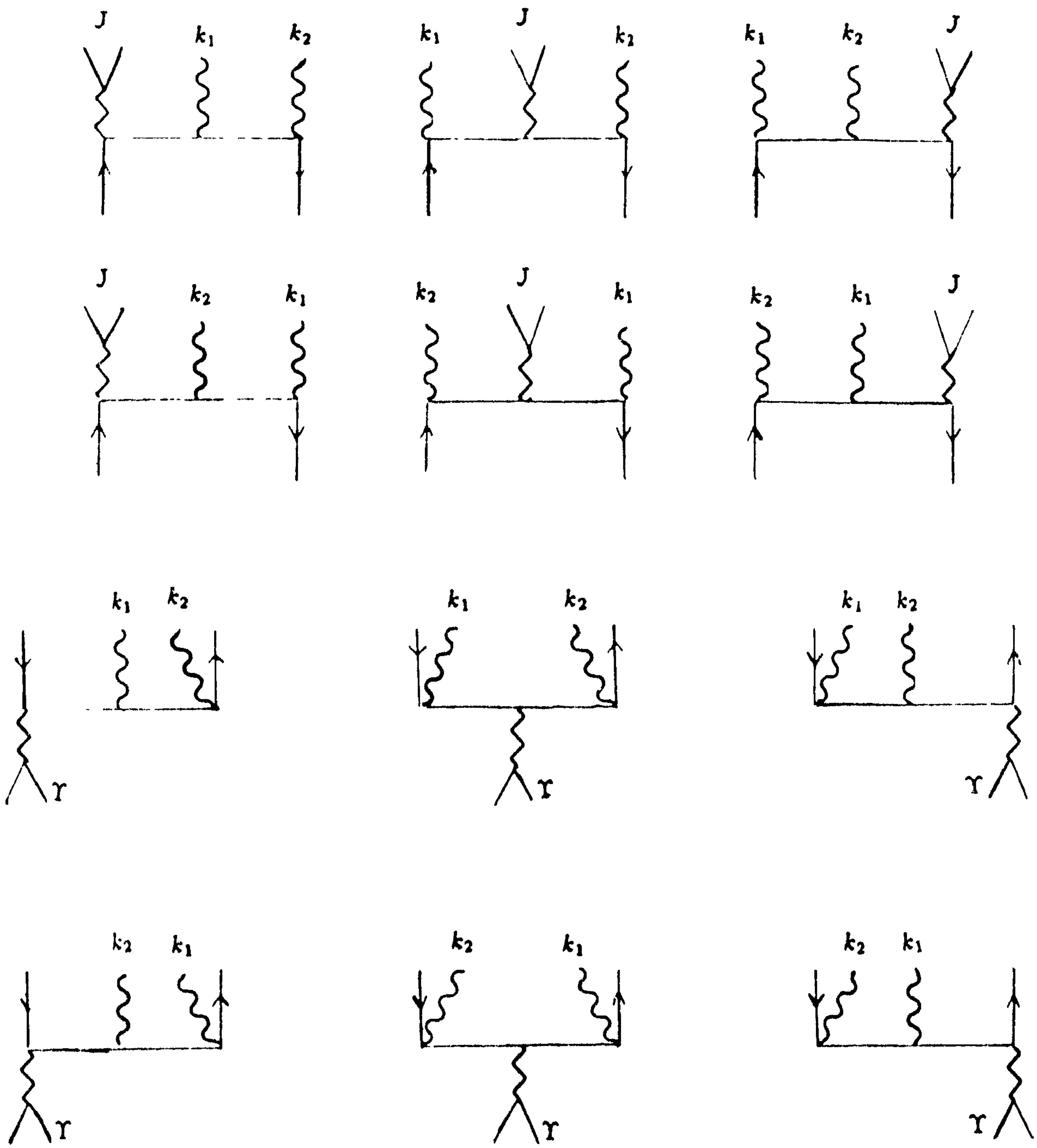

Figure 5.10: The twelve Feynman diagrams for the electromagnetic contribution to $\Upsilon \to J/\psi gg$

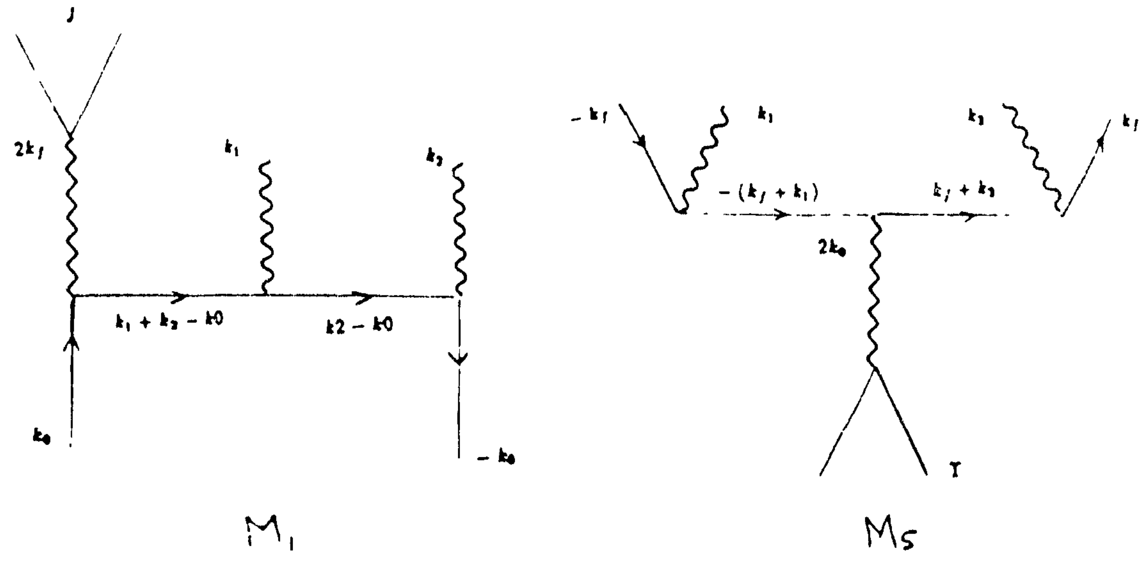

Figure 5.11. Momentum labeled diagrams for M_1^{em} and M_5^{em}

Figure 5 11 depicts the momentum-labeled form of the Feynman diagrams corresponding to amplitudes M_1^{em} and M_5^{em} These are tree diagrams, and there is no ambiguity in the momentum which flows through each line Similar diagrams for the other amplitudes yields the formulae (note that definitions of the "J" are local to this section; similarly labeled objects in other sections will generally describe different currents):

$$
\begin{aligned}
\hat{M}_q^{em} &= 2\left[\hat{M}_1^{em} + \hat{M}_2^{em} + \hat{M}_3^{em} + \hat{M}_4^{em} + \hat{M}_5^{em} + \hat{M}_6^{em}\right] \\
\hat{M}_1^{em} &= m_0^2 \cdot J_{01} \quad J_{f0}/(q_0 p_2 p_3) \\
\hat{M}_2^{em} &= m_0^2 \cdot J_{02} \cdot J_{f0}/(q_0 p_1 p_2) \\
\hat{M}_3^{em} &= m_0^2 \cdot J_{03} \cdot J_{f0}/(q_0 p_1 p_3) \\
\hat{M}_4^{em} &= m_0^2 \cdot J_{00} \quad J_{f1}/(p_0 q_2 q_3) \\
\hat{M}_5^{em} &= m_0^2 \cdot J_{00} \cdot J_{f2}/(p_0 q_1 q_2) \\
\hat{M}_6^{em} &= m_0^2 \cdot J_{00} \quad J_{f3}/(p_0 q_1 q_3) \qquad (5\ 54) \\
J_{00}^{\alpha} &= tr\left\{(\not{k}_0 + m_0)\not{\epsilon}_0 \gamma^{\alpha}\right\} = 4 m_0 \epsilon_0^{\alpha} \\
J_{01}^{\alpha} &= tr\left\{(\not{k}_0 + m_0)\not{\epsilon}_0 \not{\epsilon}_2 (\not{k}_2 - k_0 + m_0)\not{\epsilon}_1 (\not{k}_1 + \not{k}_2 - \not{k}_0 + m_0)\gamma^{\alpha}\right\} \\
J_{02}^{\alpha} &= tr\left\{(\not{k}_0 + m_0)\not{\epsilon}_0 \not{\epsilon}_2 (\not{k}_2 - k_0 + m_0)\gamma^{\alpha}(\not{k}_0 - \not{k}_1 + m_0)\not{\epsilon}_1\right\} \\
J_{03}^{\alpha} &= tr\left\{(\not{k}_0 + m_0)\not{\epsilon}_0 \gamma^{\alpha}(\not{k}_0 - k_1 - k_2 + m_0)\not{\epsilon}_2 (\not{k}_0 - \not{k}_1 + m_0)\not{\epsilon}_1\right\} \\
J_{f0}^{\alpha} &= tr\left\{(-\not{k}_f + m_0)\not{\epsilon}_f \gamma^{\alpha}\right\} = 4 m_f \epsilon_f^{\alpha}
\end{aligned}
$$

$$
\begin{aligned}
J^{\alpha}_{f1} &= tr\,\{(-\not{k}_f + m_f)\not{\epsilon}_f\not{\epsilon}_2(\not{k}_f + \not{k}_2 + m_f)\not{\epsilon}_1(\not{k}_f + \not{k}_1 + \not{k}_2 + m_f)\gamma^{\alpha}\} \\
J^{\alpha}_{f2} &= tr\,\{(-\not{k}_f + m_f)\not{\epsilon}_f\not{\epsilon}_2(\not{k}_f + \not{k}_2 + m_f)\gamma^{\alpha}(-\not{k}_f - \not{k}_1 + m_f)\not{\epsilon}_1\} \\
J^{\alpha}_{f3} &= tr\,\{(-\not{k}_f + m_f)\not{\epsilon}_f\not{\epsilon}_2\not{\epsilon}_0(-\not{k}_f - \not{k}_1 - \not{k}_2 + m_f)\not{\epsilon}_2(-\not{k}_f - \not{k}_1 + m_f)\not{\epsilon}_1\} \\
p_0 &= (2k_0)^2 \;=\; 4m_0^2 \\
p_1 &= (k_0 - k_1)^2 - m_0^2 \;=\; -2x_1 \\
p_2 &= (k_0 - k_2)^2 - m_0^2 \;=\; -2x_2 \\
p_3 &= (k_0 - k_1 - k_2)^2 - m_0^2 \\
q_0 &= (2k_f)^2 \;=\; 4m_f^2 \\
q_1 &= (k_f + k_1)^2 - m_f^2 \;=\; 2(c - x_1) \\
q_2 &= (k_f + k_2)^2 - m_f^2 \;=\; 2(c - x_2) \\
q_3 &= (k_f + k_1 + k_2)^2 - m_f^2
\end{aligned}
\tag{5.55}
$$

The above expressions are in a form appropriate for numerical calculation as they stand. Proceeding as in the purely strong case, the traces are evaluated with the symbol manipulation program REDUCE [72]. The amplitudes may then be readily evaluated for each set of helicity labels at each point in phase space, as discussed in section 5.2.

This electromagnetic *amplitude* must be added to the purely strong amplitude of section 5.3, after which we can square the sum and integrate it over phase space. Thus the relative sign between these the two contributions must be carefully computed; this is the topic of section 5.4.3. Further, in the next section we will roughly estimate the relative magnitude of the purely strong and electromagnetic contributions, and find that they are comparable; this makes the task of computing the relative phase of the two parts all the more important.

5.4.2 Relative Size of Strong and Electromagnetic Parts

The invariant amplitude for the process $\Upsilon \to J/\psi gg$ is the sum of the strong and electromagnetic contributions (see 5.7 and 5.27):

$$
\begin{aligned}
A_q &= A_q^s + A_q^{em} \\
&= \frac{g_s^6}{16\pi^2}\cdot F_s\delta^{ab}\cdot\frac{1}{m_0^2}\cdot\hat{M}_q^s + \eta g_s^2 e^2 Q_c Q_b\cdot F_{em}\delta^{ab}\cdot\frac{1}{m_0^2}\cdot\hat{M}_q^{em} \\
&\equiv \frac{g_s^6}{16\pi^2}\; F_s\delta^{ab}\cdot\frac{1}{m_0^2}\left[\hat{M}_q^s + \eta\rho M_q^{em}\right]
\end{aligned}
\tag{5.56}
$$

$$
\rho = 4\pi\left[\frac{\alpha_{em}}{\alpha_s^2}\right][Q_c Q_b]\left[\frac{F_{em}}{F_c}\right] \tag{5.57}
$$

"η" is the relative phase between the two amplitudes. We saw in appendix 5.6.2 that all Feynman diagrams yield the same number of explicit factors of "i". (i.e.

those coming from vertices, propagators, and loops) Thus it is only the sign of "η" which is currently uncertain. In the next section we will see that in fact:

$$\mathrm{sgn}(\eta) \;=\; +1.$$

We estimate "ρ" by setting:

$$\alpha_s \approx 0.2, \quad \alpha_{em} \approx 1/(100\sqrt{2}), \quad \pi \approx 3 \tag{5.58}$$

and recalling equations 5.23, 5.50 for F_s and F_{em}:

$$\begin{aligned} \rho \;&\approx\; 12\left[\frac{1}{100\sqrt{2}}\frac{1}{(0.2)^2}\right]\left[\frac{-2}{9}\right]\left[\frac{1}{2}\frac{2^3 3^2}{5}\right] \\ &=\; \frac{12}{5}\sqrt{2} \;\approx\; 3 \end{aligned} \tag{5.59}$$

Thus the electromagnetic contribution seems to make the larger effect. On the other hand, there are more diagrams contributing to the purely strong amplitude than to the electromagnetic. Thus we should expect these two mechanisms for the transition to make roughly equal contributions In section 5 5 I will present the results of the full numerical calculation and we will see that this is roughly the case.

5.4.3 Relative Phase of Strong and Electromagnetic Parts

The fermion and massless vector boson propagators are:

$$\begin{aligned} \textit{gauge boson}: &\quad \frac{-ig^{\mu\nu}}{p^2} \\ \textit{fermion}: &\quad \frac{i}{\not{p} - m} \end{aligned}$$

The negative sign in the numerator of the gauge boson propagator originates in our use of the metric $diag(+1, -1, -1, -1)$. It causes the residue of the propagator for the spatial modes of the vector field to be "i", just like the fermion, and consistent with the rule that all physical degrees of freedom of a field must have a propagator residue of "i". The time-like mode of the gauge boson is un-physical and has residue "$-i$".

Previously I have everywhere neglected these explicit factors of "i" and those coming from vertex functions (see section 4.3.1). Now we must count them carefully to ensure that we get the relative sign of the strong and electromagnetic contributions correct. We could ignore such considerations before because the relative phase between the amplitudes in each type of contribution was just "+1", and the overall phase of the amplitude disappeared in the rate. Since all diagrams in each group have the same phase, it will suffice to determine

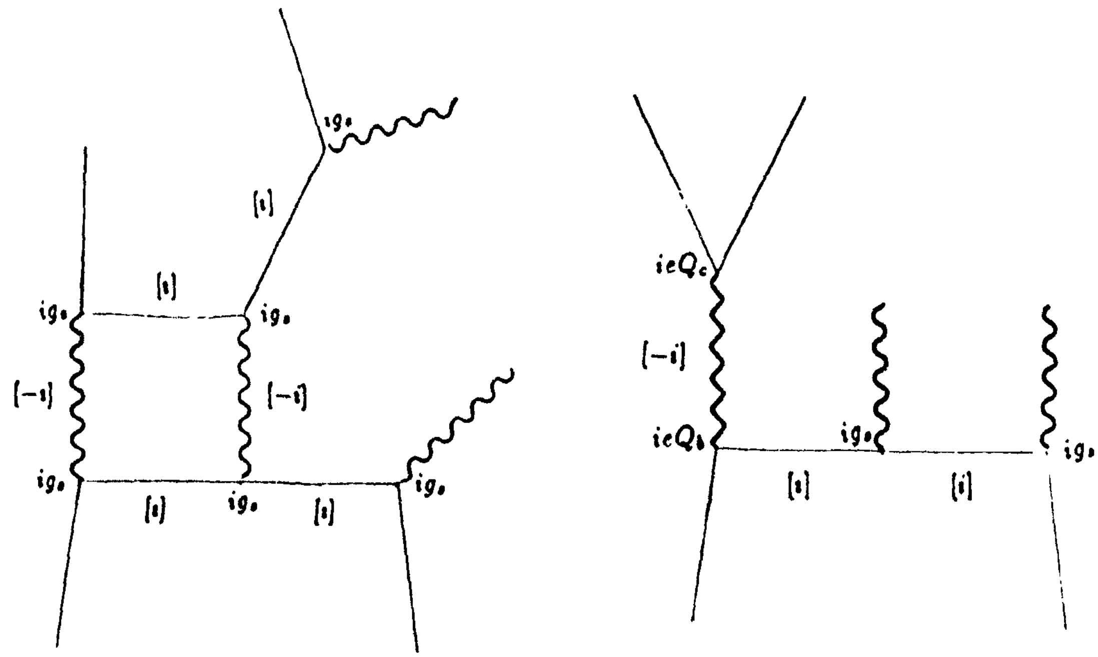

Figure 5.12: Typical purely gluonic and electromagnetic diagrams indicating sources of "i"

the relative phase between two randomly chosen diagrams from the strong and electromagnetic parts.

These explicit factors of "i" are labeled on two such diagrams in figure 5.12. Using the notation:

$$(i)^{(\# vertices)} \cdot (i)^{(\# ferm\ props)} \cdot (-i)^{(\# bos\ props)} \cdot (i)^{(\# loops)} \tag{5.60}$$

we obtain:

$$\begin{aligned} strong: &\quad (i)^6 \cdot (i)^4 \cdot (-i)^2 \cdot (i)^1 &= -i \\ electromagnetic: &\quad (i)^4 \cdot (i)^2 \cdot (-i)^1 \cdot (i)^0 &= -i \end{aligned}$$

Note that each Feynman diagram is proportional to "i", as discussed in appendix 5.6.2.

Thus the strong and electromagnetic contributions have the same phase, and the formulae as presented in sections 5.3 and 5.4 should be simply added.

5.5 Results

Recall equations 5.11, 5.56, 5.57:

$$
\begin{aligned}
Br(\Upsilon \to J/\psi gg) &= B_\Upsilon^{(had)} B_J^{(had)} \cdot \frac{F_c^2}{3\pi c_1^2} \cdot \frac{M_J \Gamma_J}{M_\Upsilon^2} < \hat{M}_q^2 > \\
< \hat{M}_q^2 > &\equiv \sum_{pol} \int dx_1 dx_2 |\hat{M}_q|^2 \\
\hat{M}_q &= \hat{M}_q^s + \rho \hat{M}_q^{em} \\
\rho &= 4\pi \left[\frac{\alpha_{em}}{\alpha_s^2}\right] [Q_c Q_b] \left[\frac{F_{em}}{F_c}\right]
\end{aligned}
$$

$\hat{M}_q^s$ is given in equations 5.27, 5.29, 5.47, and 5.30; $\hat{M}_q^{em}$ is given in equation 5.54.

We require the following data:

$$
\begin{aligned}
M_J &= 3.10\,GeV \\
\Gamma_J &= (68 \pm 10) \times 10^{-6}\,GeV \\
B_J^{(had)} &= 0.622 \pm 0.044 \\
M_\Upsilon &= 9.46\,GeV \\
B_\Upsilon^{(had)} &= 0.794 \pm 0.014
\end{aligned}
$$

The hadronic widths are taken from an analysis in reference [57], and the other numbers are from the Particle Data Book [46]. Thus:

$$
Br(\Upsilon \to J/\psi gg) = (0.824 \pm 0.194) < \hat{M}_q^2 > \times 10^{-9}
$$

The error here is mostly from uncertainty in the J/ψ width.

The parameter integrals contained in the formula for $\hat{M}_q^s$ were computed using the IMSL numerical integration program DQUAND [73], and the subsequent integration over phase space was done using the program VEGAS [74]. To get an idea for the relative size of the electromagnetic, dispersive strong, and absorptive strong contributions, consider the value of the matrix element $\hat{M}_q$ at a typical point in phase space for a typical set of helicity labels

$$
\begin{aligned}
x_1 &= 0.5 \\
x_2 &= 0.6 \\
\{\lambda_0, \lambda_f, \lambda_1, \lambda_2\} &= \{1, 1, 1, 1\}
\end{aligned}
$$

using the notation of section 5.2. The result:

$$
\begin{aligned}
\hat{M}_q(x_1, x_2) &= 31.1 + 87.4i \\
&\equiv \rho M_q^{em} + Re\, M_q^s + i\, Im\, M_q^s \\
\rho M_q^{em} &= -16.3 \\
Re\, M_q^s &= 47.4
\end{aligned}
$$

Upon integration over phase space and summation over the 36 helicity configurations, the result is:

$$< \hat{M}_q^2 > \quad = \quad (2.06 \pm 0.06) \times 10^5$$

The source of error here originates in the quantity α_s contained in ρ above. The value of α_s used was:

$$\alpha_s = 0.175 \pm 0.015 \tag{5.61}$$

as determined in reference [57] from a survey of inclusive decay widths of the Υ. (Thus it is determined within the same model as we have used.) The errors on the result for $< \hat{M}_q^2 >$ were obtained by running the program at the two extreme values of α_s. There is also a small error of about 1% in this result, which was the accuracy to which the numerical integrator was asked to evaluate the integrals. This parameter was chosen such that the computation could be performed in a reasonable amount of time.

Further, I have performed the following check of the computer program. Instead of the gluon polarization vectors given in section 5.2, I had the program use the four-momenta of the corresponding gluons. Current conservation means that the answer should be zero. The results were:

$$\begin{aligned} (\epsilon_1 = k_1) \quad &: \quad < \hat{M}_q^2 > = 0.82 \times 10^3 \\ (\epsilon_1 = k_1) \;\&\; (\epsilon_2 = k_2) \quad &: \quad < \hat{M}_q^2 > = 3.12 \times 10^3 \end{aligned}$$

which are consistent with zero given the 1% accuracy to which the numerical integrator was working.

Thus we finally obtain:

$$Br(\Upsilon \to J/\psi gg) \quad = \quad (0.170 \pm 0.045) \times 10^{-3} \tag{5.62}$$

5.6 Appendix: Evaluation of Four Propagator Integrals

We now require expressions for integrals of the form:

$$
\begin{aligned}
I &\equiv \int \frac{f(l)d^4 l}{l^2 \cdot P_1 \cdot P_2 \cdot P_3} \\
P_i &= (l-p_i)^2 - m_i^2 - i\epsilon \\
&= l^2 - 2l \cdot p_i + (p_i^2 - m_i^2) - i\epsilon
\end{aligned} \tag{5.63}
$$

"I" can be converted into an integral over a unit hypercube in the usual way [62, 16]. The four propagators are combined using the identity.

$$
\frac{1}{P^n Q} = n \int_0^1 du \frac{u^{n-1}}{[Pu + Q(1-u)]^{n+1}}
$$

Then the integrals over loop-momenta for a general numerator function may then be performed by shifting the origin, symmetrizing the numerator, and using the two results:

$$
\int \frac{d^4 l}{(l^2+a)^4} = \frac{i\pi^2}{6a^2}, \qquad \int \frac{d^4 l}{(l^2+a)^3} = \frac{i\pi^2}{2a} \tag{5.64}
$$

My goal in this section is *not* to obtain analytic expressions for the general four-propagator integral; rather, I wish to manipulate the basic formula for "I" until I reach a form that is easily computed numerically. One might think that once the loop integral has been converted into a parameter integral over a hypercube, that our goal has been achieved. For example, this approach suffice in the calculations of multi-loop contributions to the electron anomalous magnetic moment [75]. However, it will *not* work in our case, due to the presence of *non-removable* singularities that exist in the parameter integrals. The origin of these "divergences" lies in the fact that all of our diagrams contain a so-called "absorptive cut", wherein some of the fields in the loop become on shell in certain regions of the integration variable. (Such cuts are necessarily absent in the electron magnetic moment calculations, stemming from the fact that the electron is the lightest charged lepton and that the calculations are performed at $q_\gamma^2 = 0$.) The best way I have found to handle such poles of the integrands is to perform the integral over one of the parameters analytically. The resulting expressions are then amenable to numerical integration.

5.6.1 "Singularities" in the Parameter Integrals

Start by converting "I" into parameter integral form:

$$
\begin{aligned}
I &= 2\int_0^1 dx \int_0^1 y\,dy \int \frac{f(l)\,d^4l}{(l^2 - \imath\epsilon)(l^2 - 2l\cdot d + \epsilon^2)^3} \equiv \int dx\,dy\,y I(x,y) \\
d &= [xp_1 + (1-x)p_2]\,y + (1-y)p_3 \\
\epsilon^2 &= \left[x(p_1^2 - m_1^2) + (1-x)(p_2^2 - m_2^2)\right] y + (1-y)(p_3^2 - m_3^2) - \imath\epsilon
\end{aligned}
$$

Now, for the simple case of:

$$
f(l) \equiv f_0 + f_1^\mu l_\mu
$$

consider the integrand of the "x, y" integral, in parameter form:

$$
\begin{aligned}
I(x,y) &= 6\int_0^1 dz\, z^2 \int \frac{d^4l(f_0 + f_1^\mu l_\mu)}{[l^2 - 2l\cdot(zd) + z\epsilon^2]^4} \\
&= 6\int_0^1 dz\, z^2 \int \frac{d^4l(f_0 + zf_1^\mu d_\mu)}{[l^2 + z\epsilon^2 - z^2d^2]^4} \\
&= \imath\pi^2 \int_0^1 dz\, z^2 \frac{f_0 + f_1^\mu d_\mu z}{[z\epsilon^2 - z^2d^2]^2} \\
&= i\pi^2 \int_0^1 dz \frac{f_0 + f_1^\mu d_\mu z}{[d^2 z - \epsilon^2]^2}
\end{aligned}
$$

It is at this point that the problem is evident. It is quite possible that:

$$
0 < \frac{e^2(x,y)}{d^2(x,y)} < 1
$$

for some value(s) of "x" and "y". Thus the "z" integral appears to have non-removable singularities in the form of double and single poles. The resolution of this problem stems from the presence of the "$\imath\epsilon$" in "ϵ^2". This pushes the poles off the real axis so that the integral is well defined. In the process, the integral picks up an imaginary part, via the identity:

$$
\frac{1}{z - \imath\epsilon} = P\left(\frac{1}{z}\right) + i\pi\delta(z) \tag{5.65}
$$

$$
\begin{aligned}
\int_0^1 dz \frac{1}{[d^2z - \epsilon^2 - \imath\epsilon]^2} &= \frac{1}{d^2}\left[\frac{1}{d^2 - \epsilon^2 - \imath\epsilon} + \frac{1}{e^2 - \imath\epsilon}\right] \\
\int_0^1 dz \frac{1}{[d^2z - e^2 - \imath\epsilon]} &= \frac{1}{d^2}\left[\log\left|\frac{e^2 - d^2}{\epsilon^2}\right| + \imath\pi\,\mathrm{sgn}(d^2)\Theta(\frac{e^2}{d^2})\Theta(1 - \frac{\epsilon^2}{d^2})\right]
\end{aligned}
$$

Thus:

$$
\begin{aligned}
I(x,y) &= \imath\pi^2 \frac{f_0 + f_1^\mu d_\mu}{d^2}\left[\frac{1}{d^2 - \epsilon^2 - \imath\epsilon} + \frac{1}{\epsilon^2 - \imath\epsilon}\right] \\
&\quad + i\pi^2 \frac{f_1^\mu d_\mu}{d^4}\left[\log\left|\frac{\epsilon^2 - d^2}{\epsilon^2}\right| + i\pi\,\mathrm{sgn}(d^2)\Theta(\frac{\epsilon^2}{d^2})\Theta(1 - \frac{\epsilon^2}{d^2})\right]
\end{aligned}
$$

Though we have now performed the "z" integral, and the "singularity" is no longer a problem, the point is that we had to resort to analytic methods to do so. Had we simply requested a numerical integrator to perform the integral over all three variables "x, y, z", the program would have returned nonsense. It is unfortunate that this latter approach is insufficient, because it is preferable to the analytic method from the standpoint of simplicity. We will find the analytic formulae associated with a more general function "$f(l)$" somewhat daunting.

Note that I have retained the "$i\epsilon$" in the expressions for the "x" and "y" integrand; this is because there may exist further "divergences" of exactly the sort that we just encountered. Specifically, the terms,

$$\frac{1}{d^2 - \epsilon^2 - i\epsilon}, \qquad \frac{1}{\epsilon^2 - i\epsilon} \tag{5.66}$$

are singular if either:

$$d^2 - \epsilon^2 = 0 \qquad or \qquad \epsilon^2 = 0. \tag{5.67}$$

I will introduce a different method for handling such problems when they occur in the "x" and "y" integrations. This is discussed below in section 5.6.4.

Also, note that the vanishing of ϵ^2 or $d^2 - \epsilon^2$ in

$$\log\left|\frac{\epsilon^2 - d^2}{\epsilon^2}\right|$$

constitutes an *integrable* singularity. A good numerical integrator can compute this integral as it stands.

Lastly, note that there is a method that would allow us to perform the integral over all three variables numerically. Using Cauchy's theorem, we can deform the contour of integration for the "z" variable off of the real axis (in a direction determined by the "$i\epsilon$") such that there are no longer any poles lying on it. This contour integral in the complex plane could then be performed numerically. In fact, this is the method we shall use (see section 5.6.4) to handle further singularities of this type when they occur in the "y" integral, because analytic methods become prohibitively complicated for the type of non-trivial integrands that appear in the "x" and "y" integrals. And it is just because we will sometimes have to analytically continue the "y" variable into the complex plane that we may *not* employ this same method to to handle the singularities in the "z" integral. The actual contour in the complex "z" plane would necessarily become a function of "x" and the complex variable "y", it then becomes difficult to ensure that this contour is not passing over any poles of the integrand when both the contour and integrand are functions of a complex parameter. Such considerations are the domain of the theory of complex functions of several complex variables.

5.6.2 Origin of Imaginary Parts in Feynman Diagrams

In the previous section we found that the loop integrals yielded both real and imaginary parts. Here I recall the decision criteria which allows one to tell from a glance at the associated Feynman diagram if parameter integral "singularities" will arise.

First recall that for each vertex, propagator (fermion or boson), and loop (see 5.6.1) in a Q E D/Q C D Feynman diagram there is associated an explicit factor of "i". Thus the amplitude corresponding to a Feynman diagram with "V" vertices, "E" internal lines (propagators), and "L" loops is proportional to:

$$i^{E+V+L}$$

Further recalling Euler's equation for planar graphs,

$$V - E + L = 1$$

this proportionality factor becomes:

$$i^{2E+1} \propto i.$$

The S-matrix is related to the invariant amplitude by a another factor of "i". Should we conclude that the S-matrix is always purely real? We know this cannot be the case because general arguments [16] based on unitarity relate the imaginary part of "S" to observable quantities which we know do not vanish in all cases:

$$Im\, S \propto \sum_n < f|n >< n|i >$$

Here "$|n >$" is any energetically allowed "real" state (i.e. consisting of on-shell particles). In perturbation theory, the imaginary part of "S" thus first arises at order g^{i+j}, if "$< f|n >$" and "$< i|n >$" are of order g^i and g^j.

What then have we overlooked that could produce a non-trivial phase in the S-matrix? The answer is the type of parameter integral singularities that we encountered in the last section. We saw there that the value of the loop integral acquires both real and imaginary parts in such a situation. Since this is the only such source of non-trivial phase in the amplitude, it must be linked to the presence of the energetically allowed states "$|n >$" discussed in the last paragraph.

Now, inspection of the Feynman diagrams can tell us if such states exist. If a line can be drawn through the Feynman diagram such that:

1. a cut along the line would split the diagram into two disjoint parts, and

2. it is possible for both the initial and final states to make a transition to the set of fields that the "cutting" line intersects

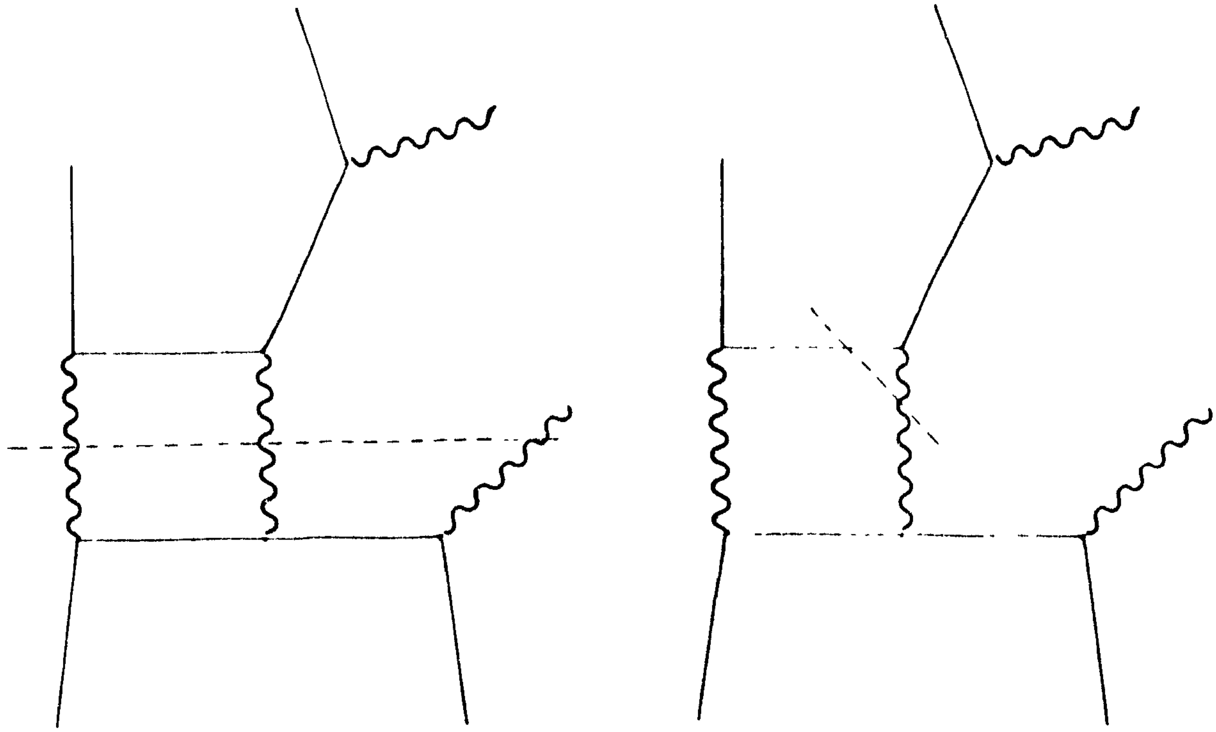

Figure 5.13: Absorptive cuts in the $\Upsilon \rightarrow J/\psi gg$ diagrams

then this latter set of fields is just the intermediate state "$|n>$" mentioned above. Certainly the product of the perturbative orders of "$< f|n >$" and "$< i|n >$" must equal the order to which we are calculating the amplitude and thus the S-matrix. There exist two such cuts in the case of our process, shown in figure 5.13. The intermediate state is the three gluon state "$|ggg>$" in the left diagram, and the state "$|c\bar{c}gg>$" in the right.

In summary, if there exists such a cut in a Feynman diagram, then the S-matrix must have a non-trivial phase at the order we are working to in perturbation theory, and thus the parameter integrands must have poles, since this is the only way to introduce non-trivial phases into the expression for a Feynman diagram.

Conversely, if the Feynman diagrams have no such cuts, and we have properly identified *all* of the relevant diagrams for the transition, then there can be none of the states "$|n>$" described above, and the S-matrix must be purely real; thus the parameter integrals cannot have any poles.

5.6.3 Formulae for the Four Propagator Integral

Herein I present a parameter integral formula for a loop integral of the form:

$$\int d^4 l \, \frac{f(l)}{l^2 \cdot P_1 \cdot P_2 \cdot P_3} \tag{5.68}$$

$$P_k \;=\; l^2 - 2l \cdot p_k + (p_k^2 - m_k^2) - i\epsilon \tag{5.69}$$

The numerator has the general form:

$$f(l) \;\equiv\; f_0 + f_1^{\mu} l_\mu + f_{2a} l^2 + f_{2b}^{\mu\nu} l_\mu l_\nu + f_{3a}^{\mu} l^2 l_\mu + f_{3a}^{\mu\nu\lambda} l_\mu l_\nu l_\lambda + f_4(l)$$

where $f_4(l)$ represents a possible quartic piece. Note that if $f_4(l)$ behaves as l^4 for large "l", $\int d^4 l f_4(l)/[l^2 P_1 P_2 P_3]$ diverges logarithmically. We are thus faced with a slight paradox, since on the one hand we know that each of our Feynman diagrams generated an amplitude that was on its own ultraviolet finite by power counting, but nevertheless some of the numerator functions in equation 5.30 (specifically f_5) certainly *do* contain quartic parts.

In fact, the appearance of these naively divergent expressions is an artifact of our reduction of the multi-propagator integrals to four-propagator integrals. A small amount of analytic manipulation of the final results shows that the quartic pieces of each of the numerator functions really only increase as "l^3" for large "l". That is, $f_4(l)$ always has the form:

$$f_4(l) \;=\; f_{4a}^{\mu\nu} \, l^2 \left[l_\mu l_\nu\right]_r + f_{4b}^{\mu\nu\alpha\beta} \left[l_\mu l_\nu l_\alpha l_\beta\right]_r$$

where I have introduced the notation:

$$\begin{aligned}
\left[l^\mu l^\nu\right]_r &\equiv l^\mu l^\nu - l^2 \frac{g^{\mu\nu}}{4} \\
\left[l^\mu l^\nu l^\alpha l^\beta\right]_r &\equiv l^\mu l^\nu l^\alpha l^\beta - l^4 \frac{g^{\mu\nu\alpha\beta}}{24} \\
g^{\mu\nu\alpha\beta} &\equiv g^{\mu\nu} g^{\alpha\beta} + g^{\mu\alpha} g^{\nu\beta} + g^{\mu\beta} g^{\nu\alpha}
\end{aligned}$$

Thus, it will suffice to now present formulae for the following integrals:

$$\int \frac{d^4 l}{l^2 \cdot P_1 \cdot P_2 \cdot P_3} \left\{1, l^\mu, l^2, l^\mu l^\nu, l^2 l^\mu, l^\mu l^\nu l^\lambda, l^2 \left[l^\mu l^\nu\right]_r, \left[l^\mu l^\nu l^\alpha l^\beta\right]_r \right\} \tag{5.70}$$

As in section 5.6.1, I first convert each into parameter integral form, and then analytically perform the integration corresponding to the parameter which is used to combine the propagator "l^2" with the other three propagators. (This is the "last" parameter introduced.) The derivation of each equation proceeds in a fashion completely analogous to the derivation of the equations in section 5.6.1

for the simple numerator function $f_0 + f_1^\mu l_\mu$. Lastly, it should be understood that a factor of

$$i\pi^2 \int dx dy\, y$$

must multiply the left hand side of each of the integral formulae

$$\begin{aligned}
\int d^4 l \, \frac{1}{P_1 \cdot P_2 \cdot P_3} &= \frac{1}{\epsilon^2 - d^2} \\
\int d^4 l \, \frac{l^\mu}{P_1 \cdot P_2 \cdot P_3} &= \frac{d^\mu}{\epsilon^2 - d^2} \\
\int d^4 l \, \frac{[l^\mu l^\nu]_r}{P_1 \cdot P_2 \cdot P_3} &= \frac{[d^\mu d^\nu]_r}{\epsilon^2 - d^2} \\
\int d^4 l \, \frac{1}{l^2 \cdot P_1 \cdot P_2 \cdot P_3} &= \frac{1}{\epsilon^2(\epsilon^2 - d^2)} = \frac{1}{d^2}\left[\frac{1}{d^2 - \epsilon^2} + \frac{1}{\epsilon^2}\right] \\
\int d^4 l \, \frac{l^\mu}{l^2 \cdot P_1 \cdot P_2 \cdot P_3} &= d^\mu \left[\frac{1}{\epsilon^2(\epsilon^2 - d^2)} + \frac{1}{d^4}\log_1\left(\frac{1}{a}\right)\right] \\
\int d^4 l \, \frac{l^\mu l^\nu}{l^2 \cdot P_1 \cdot P_2 \cdot P_3} &= D_2^{\mu\nu} \left[\frac{1}{\epsilon^2(\epsilon^2 - d^2)} + \frac{2a}{d^4}\log_2\left(\frac{1}{a}\right)\right] + \frac{g^{\mu\nu}/4}{\epsilon^2 - d^2} \\
\int d^4 l \, \frac{l^\mu l^\nu l^\lambda}{l^2 \cdot P_1 \cdot P_2 \cdot P_3} &= D_3^{\mu\nu\lambda} \left[\frac{1}{\epsilon^2(\epsilon^2 - d^2)} + \frac{3a^2}{d^4}\log_3\left(\frac{1}{a}\right)\right] + \frac{\Omega^{\mu\nu\lambda}/6}{\epsilon^2 - d^2} \\
\int d^4 l \, \frac{[l^\mu l^\nu l^\alpha l^\beta]_r}{l^2 \cdot P_1 \cdot P_2 \cdot P_3} &= D_4^{\mu\nu\alpha\beta} \left[\frac{1}{\epsilon^2(\epsilon^2 - d^2)} + \frac{4a^3}{d^4}\log_4\left(\frac{1}{a}\right)\right] + \frac{\Omega^{\mu\nu\alpha\beta}/8}{\epsilon^2 - d^2}
\end{aligned} \tag{5.71}$$

$$\begin{aligned}
d^\mu &= [xp_1 + (1-x)p_2]^\mu y + (1-y)p_3^\mu \\
\epsilon^2 &= \left[x(p_1^2 - m_1^2) + (1-x)(p_2^2 - m_2^2\right] y + (1-y)(p_3^2 - m_3^2) \quad i\epsilon \\
a &\equiv \epsilon^2/d^2 \\
D_2^{\mu\nu} &= d^\mu d^\nu - d^2 g^{\mu\nu}/4 = [d^\mu d^\nu]_r \\
D_3^{\mu\nu\lambda} &= d^\mu d^\nu d^\lambda - d^2\Omega^{\mu\nu\lambda}/6 \\
D_4^{\mu\nu\alpha\beta} &= \left[d^\mu d^\nu d^\alpha d^\beta\right]_r - d^2\Omega^{\mu\nu\alpha\beta}/8 \\
\Omega^{\mu\nu\lambda} &= g^{\mu\nu}d^\lambda + g^{\mu\lambda}d^\nu + g^{\nu\lambda}d^\mu \\
\Omega^{\mu\nu\alpha\beta} &= g^{\mu\nu}D_2^{\alpha\beta} + g^{\mu\alpha}D_2^{\nu\beta} + g^{\mu\beta}D_2^{\nu\alpha} + g^{\nu\alpha}D_2^{\mu\beta} + g^{\nu\beta}D_2^{\mu\alpha} + g^{\alpha\beta}D_2^{\mu\nu} \\
\log_k(x) &= \log(1-x) + x + \frac{1}{2}x^2 + \cdots + \frac{1}{k}x^k + i\pi\Theta(x-1) \\
&= -\sum_{n=k+1} \frac{x^n}{n} \qquad for\ |x| < 1
\end{aligned} \tag{5.72}$$

In summary, I have reduced the loop-integral of four propagators and a general momentum dependent numerator function, to a set of two-dimensional integrals that can be readily evaluated numerically, and such that the correct absorptive contribution to the integral will be obtained (See also the next section for a discussion of further singularities in the "y" integral.)

5.6.4 Further Singularities in the "x" and "y" Integrals

The formulae of the last section contains three potential "divergence" problems, associated with the following expressions:

1. $\dfrac{1}{d^2}$
2. $\dfrac{1}{\epsilon^2}$
3. $\dfrac{1}{\epsilon^2 - d^2}$

$d^2 = 0$ "Divergences"

Recall that "d" is given by the expression:

$$d^\mu = [xp_1 + (1-x)p_2]^\mu y + (1-y)p_3^\mu. \tag{5.73}$$

As "x" and "y" vary from 0 to 1, the tip of the four-vector "d" traces out a two dimensional triangle in Minkowski space, whose vertices are p_1, p_2, and p_3. Hence if one of the p_k is space-like, while the other two are time-like (or visa-versa), there must exist some value of "x" and "y" for which "d" is time-like, i.e. for which.

$$d^2 = 0.$$

Note that d^2 does not contain an $i\epsilon$ term to push any such singularities off the real axis and keep the integrals well defined. Thus $d^2 = 0$ cannot really be a singularity of the integrand.

To see this, note that the only terms proportional to $\frac{1}{d^2}$ are:

$$\frac{(k+1)a^k}{d^4} \log_k\left(\frac{1}{a}\right)$$

As $d^2 \to 0$,

$$\frac{1}{a} = \frac{d^2}{\epsilon^2} \to 0$$

(we will see below that for all our diagrams we can always choose the routing of the loop momenta such that $e^2 - d^2 \neq 0$ over the integration region.) and thus:

$$\begin{aligned}
\frac{(k+1)a^k}{d^4}\log_k\left(\frac{1}{a}\right) &\rightarrow \frac{(k+1)a^k}{d^4}\left[\frac{-1}{(k+1)a^{k+1}} + O\left(\frac{1}{a^{k+2}}\right)\right] \\
&= \frac{1}{a} + O\left(\frac{1}{a^2}\right) \\
&\rightarrow 0
\end{aligned}$$

using equation 5.72.

Next, consider the other two sources of singularity. It is quite possible that either e^2 or $e^2 - d^2$ vanishes for some values of "x" and "y". However, since e^2 contains the $i\epsilon$ factor, these poles will just lead to the type of "divergences" discussed in section 5.6.1, which there lead us to perform one of the parameter integrals analytically.

$e^2 - d^2 = 0$ "Divergences"

I present here a criteria to tell immediately if $e^2 - d^2$ vanishes or not. Recall equation 5.71.

$$A \equiv \int d^4 l \frac{1}{P_1 \cdot P_2 \cdot P_3} = i\pi^2 \int dx dy\, y \frac{1}{e^2 - d^2}$$

The left-hand side is the expression associated with a triangular loop of scalars in a Feynman diagram. Recalling section 5.6.2, the parameter integral form of "A" has singularities if and only if this associated Feynman diagram has a "cut". Thus we need only inspect the associated Feynman diagram to determine if $e^2 - d^2$ vanishes in the integration region or not.

This rule can be used to choose momentum routings in Feynman diagram loops which eliminate these types of poles in the "x-y" integrals. This is illustrated in figures 5.14, 5.15. Figure 5.14a depicts the Feynman diagram for the amplitude M_1, with the same routing of momentum in the loop that we used in section 5.3.1. Figure 5.14b depicts the Feynman diagram associated with the three propagators P_1, P_2, P_3. It is clear that this latter diagram has no cuts ($(k_0 - k_1)^2 < (m_0 + m_f)^2$, always), so that we need never worry that $e^2 - d^2$ vanish in our "x-y" integral. If we had routed the loop momenta for amplitude M_1 as in figure 5.15a the associated Feynman triangle diagram (figure 5.15b) *would* admit a cut, as shown in figure 5.15b. Thus our "x-y" integrand would have a pole that would have to be dealt with somehow, perhaps analytically. Since $e^2 - d^2$ is a general quadratic in both "x" and "y", this would constitute a very complex, tedious exercise.

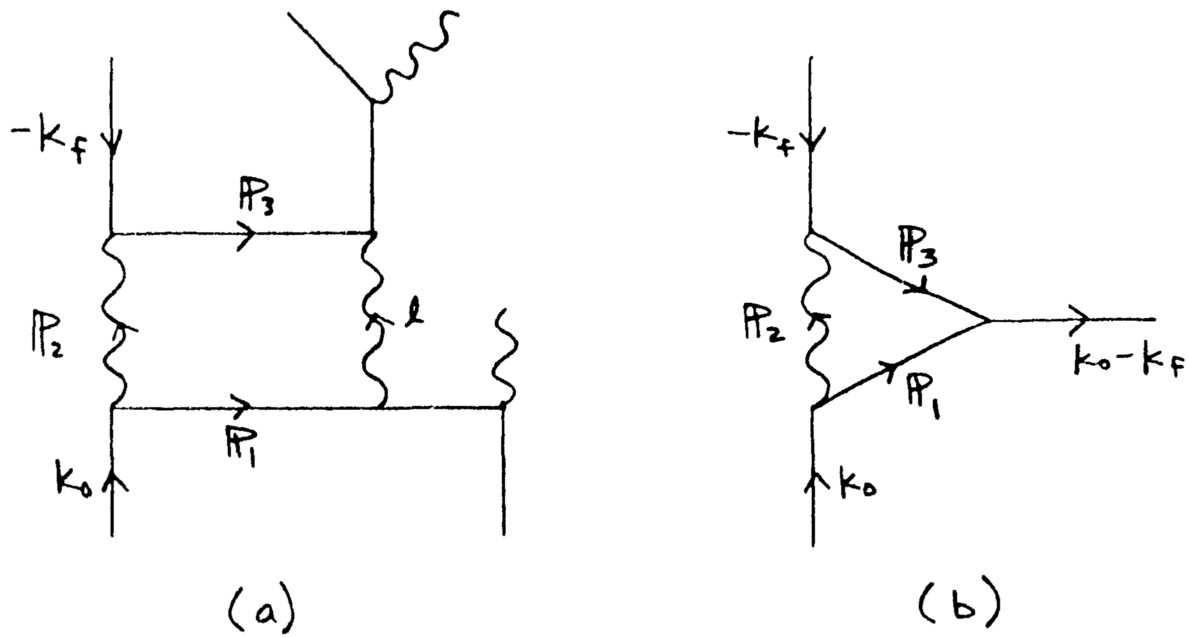

Figure 5 14: (a) Feynman diagram M_1 with the momentum routing we have used, and (b) its associated triangle diagram

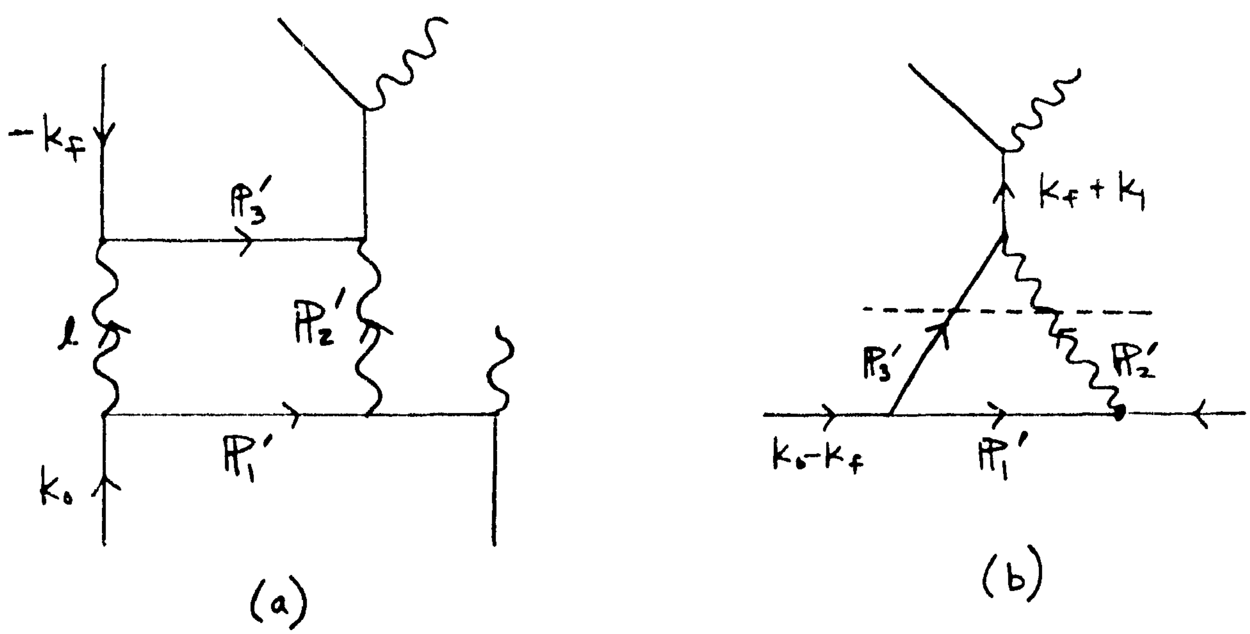

Figure 5.15: (a) Feynman diagram M_1 with an alternate momentum routing, and (b) its associated triangle diagram with absorptive cut

$\epsilon^2 = 0$ "Divergences"

ϵ^2 will in general vanish at some point in the "x-y" integral. As stated, this does not mean the integral diverges, because the $i\epsilon$ pushes the position of the pole off the real axis, which is the current integration contour for the "y" integral. We have:

$$\begin{aligned}
\epsilon^2 &= \alpha(x)\, y \;+\; \beta \;-\; i\epsilon \\
\alpha(x) &= x(p_1^2 - m_1^2) + (1-x)(p_2^2 - m_2^2) - (p_3^2 - m_3^2) \\
\beta(x) &= (p_3^2 - m_3^2) \\
\frac{1}{\epsilon^2} &= \frac{1}{\alpha(x)}\,\frac{1}{y - u(x) - i\epsilon/\mathrm{sgn}(\alpha)} \\
u(x) &= \frac{\beta}{\alpha(x)}
\end{aligned}$$

Doing the "y" integral analytically, using the formula:

$$\frac{1}{y - i\epsilon} = P(\frac{1}{y}) + i\pi\delta(y),$$

similar to the way we did the "z" integral in sections 5.6.1 and 5.6.3 is prohibitively complicated now. This is because the $\frac{1}{\epsilon^2}$ terms in our formulae are multiplied by quite complicated functions of "x" and "y", such as $\frac{1}{d^2}$ (see equation 5.71).

To handle this problem, the following method was employed. By Cauchy's theorem, the integral of y along the two paths in figure 5.16 must yield the same answer, if there are no further poles lying between them (this is easily verified). Note that the direction we must deform the contour is determined by "$i\epsilon/\mathrm{sgn}(\alpha)$". The integration may now be performed numerically by simply choosing some convenient parameterization of the contour. For example, I used a semi-circular path parameterized by the angle θ:

$$y(\theta) = \frac{1}{2} - \frac{1}{2}e^{-i\theta} \qquad \theta \in [0, \pi]$$

Singularities in the "x" Integral

The badly behaved terms in the "z" integral consisted of single and double poles. Those in the "y" integral were only single poles, which were derived from the integral of the double pole terms in the "z" integral. The remaining "x" integral contains no poles. All singularities associated with the vanishing of ϵ^2, etc. are at most integrable, logarithmic, singularities.

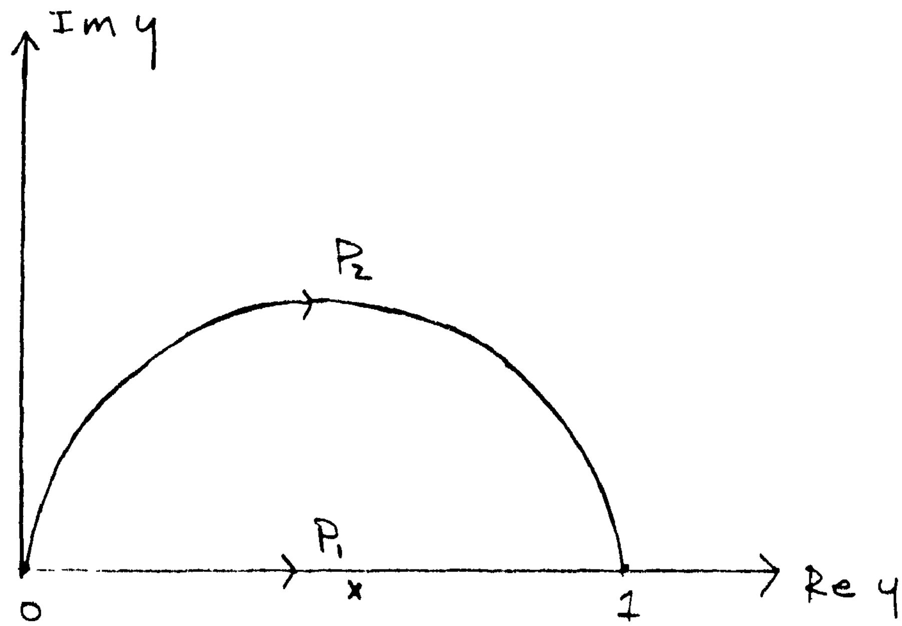

Figure 5.16: Contour used to perform the "y" integral

Chapter 6

$\Upsilon \longrightarrow J/\psi gggg$

6.1 Decay Rate, Helicity Amplitudes

6.1.1 Decay Rate

The formula for the spin averaged, and color and spin summed, decay rate of an Υ to a "J" plus four gluons follows from equation 4.17.

$$d\Gamma = \frac{1}{4!}\frac{1}{2J_\Upsilon + 1}\frac{1}{2M_\Upsilon}\frac{|\psi_\Upsilon(0)|^2}{M_\Upsilon}\frac{|\psi_J(0)|^2}{M_J}\sum_{col,pol}|A_q|^2 d_5(LIPS) \tag{6.1}$$

where the first factor is the symmetry factor associated with the four identical gluons, and A_q is the quark level invariant amplitude calculated with the rules of section 4.3.3.

In section 6.5 we discuss the 5-body phase space, and define a set of variables "$\vec{r}$" $\in R^8$ such that:

$$\begin{aligned} d_5(LIPS) &= \frac{1}{(2\pi)^{11}}\frac{d^3k_J}{2E_J}\frac{d^3k_1}{2E_1}\frac{d^3k_2}{2E_2}\frac{d^3k_3}{2E_3}\frac{d^3k_4}{2E_4}\delta^4\left(k_\Upsilon - k_J - \textstyle\sum_i k_i\right) \\ &= \frac{1}{(2\pi)^{11}}\left(\frac{\pi}{2}\right)^4 M_\Upsilon^6 \int d^8r \end{aligned} \tag{6.2}$$

The boundaries of the integration region are discussed there also.

We now extract the color factor, coupling constants, and powers of the quark mass to define the dimensionless quantity $\hat{M}_q$:

$$A_q = g_s^6 \cdot F_c^{abcd} \cdot \frac{1}{m_0^4} \cdot \hat{M}_q \tag{6.3}$$

Note that the color factor is now a function of four octet labels, one for each gluon. We will see that:

$$F_c^{abcd} = \frac{1}{12}\sum_e d_{abe}d_{cde}$$

and using the identities of appendix A:

$$F_c^2 \equiv \sum_{abcd}\left[F_c^{abcd}\right]^2 = \frac{5^2}{2\cdot 3^4} \tag{6.4}$$

Returning to the decay rate, we have:

$$\Gamma = \frac{2}{9\pi}F_c^2\alpha_s^6\frac{|\psi_\Upsilon(0)|^2|\psi_J(0)|^2}{M_J M_\Upsilon^4}\int d^8r\sum_{pol}|\hat{M}_q|^2 \tag{6.5}$$

Expressing the branching ratio in the same way that we did in the $\Upsilon \to J/\psi gg$ case (see equation 5.11) we finally obtain:

$$\frac{\Gamma(\Upsilon \to Jgggg)}{\Gamma_\Upsilon} = B_\Upsilon^{(had)}B_J^{(had)}\cdot\frac{F_c^2}{18\pi c_1^2}\cdot\frac{M_J\Gamma_J}{M_\Upsilon^2}\cdot\int d^8r\sum_{pol}|\hat{M}_q|^2 \tag{6.6}$$

where c_1 is given in equation 5.10.

6.1.2 Numerical Computation of Helicity Amplitudes

As in the $\Upsilon \to Jgg$ case we will compute the amplitudes directly, for each set of helicity labels. Note that there are:

$$3\times 3\times 2\times 2\times 2\times 2 = 144$$

such quantities. Both the summation over amplitudes and the integration over phase space will be done numerically. In section 6.5 where the 5-body phase space variables are defined, it is shown how to reconstruct the 5 particle's four-momenta from each set of phase space co-ordinates. Following the discussion of section 5.2 of the $\Upsilon \to Jgg$ decay, we must now give a prescription for the particle polarization four-vectors if we want our computer program to numerically compute the helicity amplitudes. I have used the following definitions:

$$\begin{aligned}
\epsilon_0^{(\lambda)} &= (0,\delta_{\lambda 1},\delta_{\lambda 2},\delta_{\lambda 3}) & \\
\epsilon_f^{(\lambda)} &= (0,\delta_{\lambda 1},\delta_{\lambda 2},0) & \lambda = 1,2\\
&= (|\vec{k}_f|,0,0,E_f)/m_f & \lambda = 3\\
\epsilon_i^{(\lambda_i)} &= (0,\vec{\epsilon}_i^{\,(\lambda_i)}) &
\end{aligned}$$

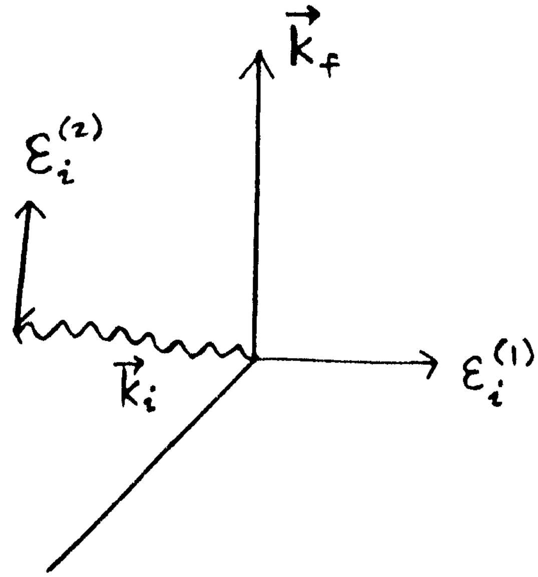

Figure 6.1: Polarization vectors for the gluons generated by the computer program

where:

$$\vec{\epsilon}_\imath^{(1)} \equiv \frac{\vec{k}_\imath \times \vec{k}_f}{|\vec{k}_\imath \times \vec{k}_f|}$$
$$\vec{\epsilon}_\imath^{(2)} \equiv \frac{\vec{k}_\imath \times (\vec{k}_\imath \times \vec{k}_f)}{|\vec{k}_\imath \times (\vec{k}_\imath \times \vec{k}_f)|}$$

According to these definitions, $\vec{\epsilon}_\imath^{(1)}$, $\vec{\epsilon}_\imath^{(2)}$ is respectively perpendicular, parallel to the plane defined by the momentum vectors of the J/ψ and gluon "$\imath$". (See figure 6.1).

Now that we have explicit expressions for each particle's momenta and polarization vector at each point in phase space, we may proceed with the numerical evaluation of the integral over phase space. All that remains is to derive the formulae for the invariant amplitude.

6.2 Feynman Diagrams

The lowest order Feynman diagrams contributing to $\Upsilon \to Jgggg$ are of order g_s^6. This follows from the fact that vector mesons must couple to at least three gluons, as discussed in section 4.4.2.

There are a total of 216 Feynman diagrams contributing to this process, 9 of which are depicted in figure 6.2. The label "a", for example, is short for "p_a, ϵ_a, a", respectively the particle momentum, polarization, and octet color label. To each of these 9 diagrams must be added the 23 graphs obtained by permuting the four labels $\{a, b, c, d\}$.

To these 9 diagrams correspond the 9 amplitudes:

$$\begin{bmatrix} A_1 & A_2 & A_3 \\ A_4 & A_5 & A_6 \\ A_7 & A_8 & A_9 \end{bmatrix}$$

I will use the notation:

$$A_k^{a \leftrightarrow b}$$

to denote the amplitude obtained from A_k by exchanging the labels "a" and "b" in A_k's Feynman diagram. Using the techniques of charge conjugation first employed in section 5.3.1, we can show that the amplitudes A_1, A_3, A_7, and A_9 all have the same lorentz (or Q.E.D.) parts. Thus:

$$\begin{aligned} A_1 + A_3 + A_7 + A_9 &= \\ &\left(\frac{1}{\sqrt{3}}\right)^2 [tr\{T_d T_c T_e\}\, tr\{T_b T_a T_e\} + tr\{T_e T_c T_d\}\, tr\{T_b T_a T_e\} \\ &\quad + tr\{T_d T_c T_e\}\, tr\{T_e T_a T_b\} + tr\{T_e T_c T_d\}\, tr\{T_e T_a T_b\}] M_1 \\ &= \frac{1}{12}\left[\sum_e d_{abe} d_{cde}\right] M_1 \quad \equiv \quad F_c^{abcd} M_1 \end{aligned}$$

Similarly:

$$\begin{aligned} A_2 + A_8 + (A_2 + A_8)^{c \leftrightarrow d} &= F_c^{abcd} M_2 \\ A_4 + A_6 + (A_4 + A_6)^{a \leftrightarrow b} &= F_c^{abcd} M_4 \\ A_5 + A_5^{a \leftrightarrow b} + A_5^{c \leftrightarrow d} + A_5^{\substack{a \leftrightarrow b \\ c \leftrightarrow d}} &= F_c^{abcd} M_5 \end{aligned}$$

I now define the quantity $M_{(ab)(cd)}$, which is the sum of the *lorentz* parts of:

1. the 9 Feynman diagrams in figure 6.2;
2. the 9 Feynman diagrams obtained from those in figure 6.2 by exchanging the labels "a" and "b",
3. the 9 Feynman diagrams obtained from those in figure 6.2 by exchanging the labels "c" and "d";
4. the 9 Feynman diagrams obtained from those in figure 6.2 by simultaneously exchanging the labels "a" and "b", and the labels "c" and "d".

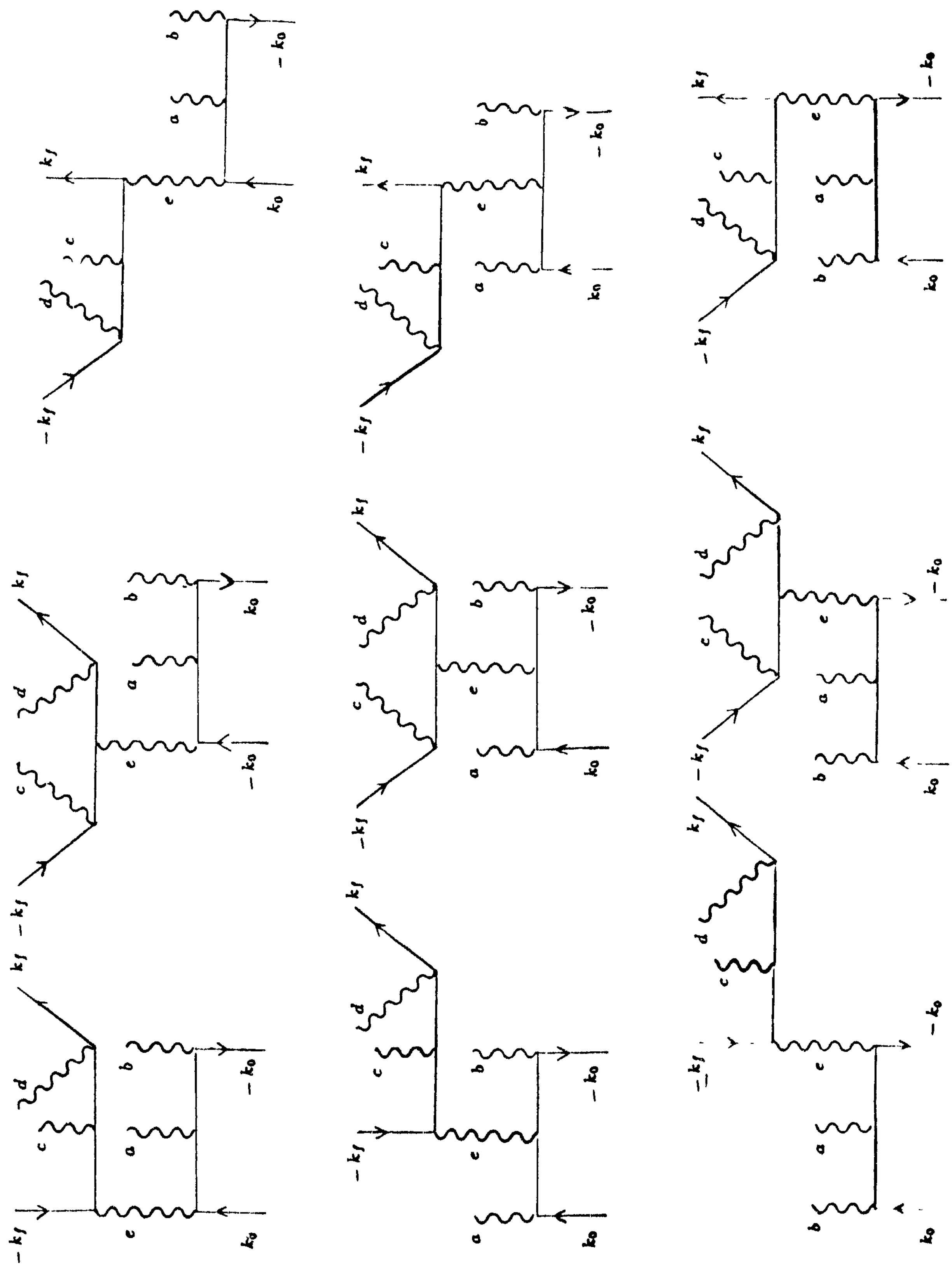

Figure 6.2: 9 of the 216 Feynman diagrams for the decay $\Upsilon \to J/\psi gggg$

$$
\begin{aligned}
M_{(ab)(cd)} &= \Big[M_1 + M_1^{a\leftrightarrow b} + M_1^{c\leftrightarrow d} + M_1^{\substack{a\leftrightarrow b \\ c\leftrightarrow c}} + M_2 + M_2^{a\leftrightarrow b} \\
&\qquad + M_4 + M_4^{c\leftrightarrow d} + M_5 \Big] \\
&= g_s^6 \Big[(J_{01} + \tilde{J}_{01})^\mu (J_{f1} + \tilde{J}_{f1})_\mu + (J_{01} + \tilde{J}_{01})^\mu J_{f2\,\mu} \\
&\qquad + J_{02}^\mu (J_{f1} + \tilde{J}_{f1})_\mu + J_{02}^\mu J_{f2\,\mu} \Big] / s_{ab} \\
&= g_s^6 \Big[J_{01} + \tilde{J}_{01} + J_{02} \Big]^\mu \Big[J_{f1} + \tilde{J}_{f1} + J_{f2} \Big]_\mu / s_{ab}
\end{aligned}
\tag{6.7}
$$

where:

$$
\begin{aligned}
\tilde{J}_{01}^\mu &\equiv J_{01}^{\mu\, a\leftrightarrow b} \\
\tilde{J}_{f1}^\mu &\equiv J_{f1}^{\mu\, c\leftrightarrow d}
\end{aligned}
$$

and:

$$
\begin{aligned}
J_{01}^\mu &= tr\left\{ (\not{k}_0 + m_0)\not{\epsilon}_0 \not{\epsilon}_b (\not{k}_b - \not{k}_0 + m_0) \not{\epsilon}_a (\not{k}_a + \not{k}_b - \not{k}_0 + m_0)\gamma^\mu \right\} / (p_b p_{ab}) \\
\tilde{J}_{01}^\mu &= tr\left\{ (\not{k}_0 + m_0)\not{\epsilon}_0 \not{\epsilon}_a (\not{k}_a - \not{k}_0 + m_0) \not{\epsilon}_b (\not{k}_a + \not{k}_b - \not{k}_0 + m_0)\gamma^\mu \right\} / (p_a p_{ab}) \\
J_{02}^\mu &= tr\left\{ (\not{k}_0 + m_0)\not{\epsilon}_0 \not{\epsilon}_b (\not{k}_b - \not{k}_0 + m_0) \gamma^\mu (-\not{k}_a - \not{k}_0 + m_0) \not{\epsilon}_a \right\} / (p_a p_b) \\
J_{f1}^\mu &= tr\left\{ (-\not{k}_f + m_f)\not{\epsilon}_f \not{\epsilon}_d (\not{k}_d + \not{k}_f + m_f) \not{\epsilon}_c (\not{k}_c + \not{k}_d + \not{k}_f + m_f)\gamma^\mu \right\} / (q_d q_{cd}) \\
\tilde{J}_{f1}^\mu &= tr\left\{ (-\not{k}_f + m_f)\not{\epsilon}_f \not{\epsilon}_c (\not{k}_d + \not{k}_f + m_f) \not{\epsilon}_c (\not{k}_c + \not{k}_d + \not{k}_f + m_f)\gamma^\mu \right\} / (q_d q_{cd}) \\
J_{f2}^\mu &= tr\left\{ (-\not{k}_f + m_f)\not{\epsilon}_f \not{\epsilon}_d (\not{k}_d + \not{k}_f + m_f) \gamma^\mu (-\not{k}_c - \not{k}_f + m_f) \not{\epsilon}_c \right\} / (q_c q_d) \\
s_{ab} &= (2k_0 - k_a - k_b)^2 \\
p_a &= (k_0 - k_a)^2 - m_0^2 = 2k_0 \cdot k_a \\
p_b &= (k_0 - k_b)^2 - m_0^2 = 2k_0 \cdot k_b \\
p_{ab} &= (k_0 - k_a - k_b)^2 - m_0^2 \\
q_c &= (k_0 - k_c)^2 - m_0^2 = 2k_f \cdot k_c \\
q_c &= (k_0 - k_d)^2 - m_0^2 = 2k_f \cdot k_d \\
q_{cd} &= (k_0 - k_c - k_d)^2 - m_0^2
\end{aligned}
$$

Further defining:

$$
\hat{M}_{(ab)(cd)} \equiv m_0^4 \cdot \Big[J_{01} + \tilde{J}_{01} + J_{02} \Big]^\mu \Big[J_{f1} + \tilde{J}_{f1} + J_{f2} \Big]_\mu / s_{ab} \tag{6.8}
$$

we see that the expression:

$$
A_{q,36} = g_s^6 F^{abcd} \frac{1}{m_0^4} \cdot \hat{M}_{(ab)(cd)}
$$

represents the sum of 36 diagrams. To obtain all 216 diagrams, we must now distribute the gluon labels $\{1, 2, 3, 4\}$ over the labels $\{a, b, c, d\}$, taking care to note that $M_{(ab)(cd)}$ is symmetric in $\{a,b\}$ and $\{c,d\}$.

$$\begin{aligned}\hat{M}_q &= \Big[\hat{M}_{(12)(34)} + \hat{M}_{(13)(24)} + \hat{M}_{(14)(23)} \\ &\qquad + \hat{M}_{(23)(14)} + \hat{M}_{(24)(13)} + \hat{M}_{(34)(12)}\Big]\end{aligned} \tag{6.9}$$

This is now in a form readily computed numerically, and when combined with equation 6.3 yields the final result

6.3 Results

Recall the equation for the branching ratio 6.6:

$$Br(\Upsilon \to Jgggg) = B_{\Upsilon}^{(had)} B_J^{(had)} \cdot \frac{F_c^2}{18\pi c_1^2} \cdot \frac{M_J \Gamma_J}{M_{\Upsilon}^2} \int d^8 r \sum_{pol} |\hat{M}_q|^2 \tag{6.10}$$

The values of the parameters M_J, $B_{\Upsilon}^{(had)}$, etc. are given and were discussed in section 5.5. Inserting these into the above, and using equation 6.4, we obtain

$$Br(\Upsilon \to Jgggg) = \left[(4.39 \pm 1.03) \times 10^{-9}\right] \cdot \int d^8 r \sum_{pol} |\hat{M}_q|^2 \tag{6.11}$$

$\hat{M}_q$ is given in equation 6.3, 6.7, and 6.9. The phase space integral is performed using the program VEGAS [74]. The result is:

$$\int d^8 r \sum_{pol} |\hat{M}_q|^2 = 1.77 \times 10^4 \tag{6.12}$$

There is essentially no error in this number, since there are no parameters like α_s in $\hat{M}_q$. We finally obtain the prediction:

$$Br(\Upsilon \to Jgggg) = (0.0777 \pm 0.0206) \times 10^{-3} \tag{6.13}$$

This result is about 46% as large as the $Br(\Upsilon \to Jgg)$ (see section 5.5). The fact that these two numbers are comparable is discussed in the next section.

6.4 Estimate of Relative Size of Jgg and $Jgggg$ Decays

We have seen that the decay probability of the Υ to the Jgg state is of the same order as that for the decay to $Jgggg$. This is somewhat counter-intuitive since typically the many factors of $(2\pi)^{-3}$ associated with multi particle phase space tend to greatly suppress the effects of a decay to many particles. Herein I present a crude estimate of of the relative factors to see that in our case this rule of thumb does not apply.

The ratio of the decay widths for $\Upsilon \to Jgg$ and $\Upsilon \to Jgggg$ follows from equations 5 11 and 6.6:

$$\frac{\Gamma(\Upsilon \to Jgggg)}{\Gamma(\Upsilon \to Jgg)} = \frac{1}{6} \cdot \frac{F_{c5}^2}{F_{c3}^2} \cdot \frac{\sum_{pol} \int d^8 r |\hat{M}_{q,5}|^2}{\sum_{pol} \int dx_1 dx_2 |\hat{M}_{q,3}|^2} \tag{6.14}$$

where from equations 5 23 and 6.4:

$$F_{c3}^2 = \frac{5^2}{2^6 \cdot 3^2} \qquad F_{c5}^2 = \frac{5^2}{2 \cdot 3^2} \tag{6.15}$$

To make a crude estimate of the phase space integrals, first recall [71] the formula for the volume of the n-body phase space in the case that all the final particles are massless:

$$V_n(m_f = 0) = \left(\frac{\pi}{2}\right)^{n-1} \cdot \frac{1}{(n-1)!(n-2)!} \cdot M_0^{2n-4} \tag{6.16}$$

This should also hold reasonably well in the case of massive final particles if $\frac{m_f^2}{M_0^2} \ll 1$, which is the case here: $M_J^2/M_\Upsilon^2 \approx 1/9$.

Note that we have already extracted the $(\pi/2)$ and M_Υ factors in 6.16 from the general phase space expressions to arive at equations 5.11 and 6.6, and hence 6.14. Thus rather than 6.16 we must use:

$$\tilde{V}_n = \frac{1}{(n-1)!(n-2)!}$$

for our estimate of the size of the domains of each of the integrals in 6.14.

Next, let us assume that in both decays each Feynman diagram for each set of helicity labels is exactly equal to "1". Our crude estimate of each integral becomes:

$$\sum_{pol} \int_{PS} |\hat{M}_q|^2 \sim (\#\ helicity\ sets) \cdot (\#\ Feynman\ diagrams)^2 \cdot \tilde{V}_n$$

The Jgg decay has 36 helicity amplitudes and 36 Feynman diagrams; the $Jgggg$ decay has $4 \cdot 36$ helicity amplitudes and $6 \cdot 36$ Feynman diagrams. Thus we have:

$$\begin{aligned} \frac{\Gamma(\Upsilon \to Jgggg)}{\Gamma(\Upsilon \to Jgg)} &= \frac{1}{6} \cdot \frac{F_{c5}^2}{F_{c3}^2} \cdot \left[4 \cdot 6^2 \cdot \frac{\tilde{V}_5}{\tilde{V}_3}\right] \\ &= \frac{1}{6} \cdot 2^5 \cdot 4 \cdot 6^2 \cdot \frac{2}{4!3!} \\ &= \frac{2^5}{3} \end{aligned} \tag{6.17}$$

Thus the 5-body decay naively dominates over the 3-body decay. This estimate is admittedly extremely crude, but it serves to demonstrate that there is no reason to expect that the usual suppression that multi-body decays experience is at play here. Usually, it is the many factors of π that make a 5-body decay small in comparison to a 3-body decay; this mechanism is irrelevent here because the 3-body decay in our problem is described by a Feynman diagram with a *loop*, while the 5-body decay has none. Because of this, both the $\Upsilon \to Jqq$ and the $\Upsilon \to Jqqqq$ decay widths end up being proportional to the same power of π (see equations 5.11 and 6.6). In fact, we can deduce immediately that this must be so by noting that any two processes computed to the same order in pertubation theory will have the same number of overall factors of π in there final formulae: this is just the reason that it makes sense to use the combination $\alpha_s = g_s^2/(4\pi)$ as the perturbation parameter.

Given that there is no relative suppression coming from factors of π, we have seen that the further smallness of the multi body phase space volume (the V_n) is offset a larger color factor, and by the increased number of diagrams and helicity amplitudes for the $Jqqqq$ final state with respect to Jqq.

6.5 Appendix: Multi-Body Phase Space

Here I review one of the simplest possible recursion relations for multi-particle phase space. It is based on the physical picture of a sequential decay, exhibited in figure 6.3.

Specifically, suppose we have n-body phase space viewed as describing the a decay from state of momentum "k_0" to n particles of momentum "k_i", i = 1, ... n:

$$\begin{aligned} R_n\left[k_0 \to k_i\right] &= \frac{d^3k_1}{2E_1}\cdots\frac{d^3k_n}{2E_n}\delta\left[k_0 - \textstyle\sum_i k_i\right] \\ &= \frac{d^3k_n}{2E_n}\cdot\prod_{i=1}^{n-1}\frac{d^3k_i}{2E_i}\delta\left[(k_0 - k_n) - \textstyle\sum_i k_i\right] \\ &= \frac{d^3k_n}{2E_n}\cdot R_{n-1}\left[(k_0 - k_n) \to k_i\right] \end{aligned}$$

Now we introduce the quantities m_{n-1}^2 and p_{n-1}, defined by:

$$1 = \int dm_{n-1}^2\delta\left(m_{n-1}^2 - p_{n-1}^2\right)\cdot\int d^4p_{n-1}\delta^4\left(k_0 - k_n - p_{n-1}\right) \qquad (6.18)$$

Multiplying the phase space by this factor of "1":

$$R_n\left[k_0 \to k_i\right] = \int dm_{n-1}^2\frac{d^3k_n}{2E_n}\left[d^4p_{n-1}\delta\left(m_{n-1}^2 - p_{n-1}^2\right)\right]$$

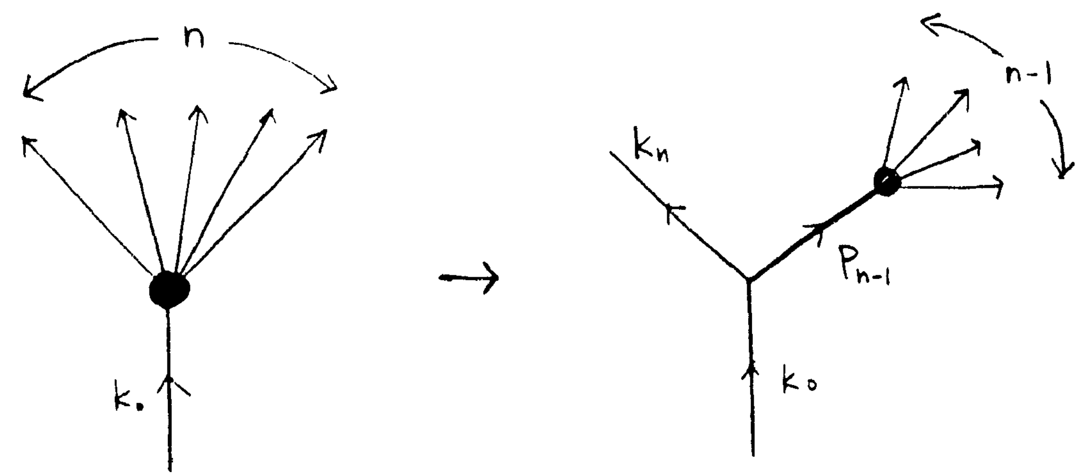

Figure 6 3: Sequential picture of an n-body decay used to generate the recursion formula

$$
\begin{aligned}
& \times\delta^4\left(k_0 - k_n - p_{n-1}\right) \cdot R_{n-1}\left[\left(k_0 - k_n\right) \to k_i\right] \\
= & \int dm_{n-1}^2 \frac{d^3 k_n}{2E_n}\left[\frac{d^3 p_{n-1}}{2E_{n-1}}\right] \delta^4\left(k_0 - k_n - p_{n-1}\right) \cdot R_{n-1}\left[p_{n-1} \to k_i\right] \\
= & \int dm_{n-1}^2 R_2\left[k_0 \to k_n, p_{n-1}\right] \cdot R_{n-1}\left[p_{n-1} \to k_i\right]
\end{aligned}
$$

The limits on m_{n-1} are easily deduced from physical considerations. On the one hand, the particle "0" is decaying to the particle "n" and the hypothetical particle of mass m_{n-1}; thus

$$m_{n-1} \leq M_0 - M_n$$

where equality corresponds to threshold production, with the particle "n" and the system described by m_{n-1} both at rest. On the other hand, the hypothetical particle is decaying to the collection of particles i = 1... n-1; thus:

$$M_1 + \cdots + M_{n-1} \leq m_{n-1}$$

where again equality corresponds to the situation where all the particles i = 1... n-1 are at rest.

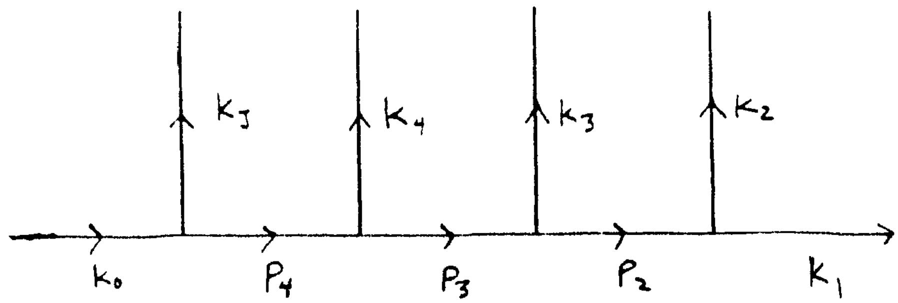

Figure 6.4: Equivalent sequential decay for 5 body phase space

Thus we have finally obtained the desired recursion formula.

$$R_n\left[k_0 \rightarrow k_1\right] = \int_{(M_1+\quad M_{n-1})^2}^{(M_0-M_n)^2} dm_{n-1}^2 R_2\left[k_0 \rightarrow k_n, p_{n-1}\right] \quad R_{n-1}\left[p_{n-1} \rightarrow k_1\right] \tag{6.19}$$

Now recall that:

$$\begin{aligned} R_2\left[p_a \rightarrow p_b, p_c\right] &= \frac{d^3 p_b}{E_b}\frac{d^3 p_c}{E_c}\delta^4\left(p_a - p_b - p_c\right) \\ &= \frac{\lambda^{1/2}(m_a^2, m_b^2, m_c^2)}{8m_a^2} d\Omega_{bc}^* \\ \lambda(x, y, z) &= x^2 + y^2 + z^2 - 2xy - 2xz - 2yz \end{aligned} \tag{6.20}$$

in the "a" particle rest frame. "$d\Omega_{bc}^*$" is the solid angle of the b-c particle axis in the a particle rest frame. Throughout this thesis, we shall always define this solid angle with respect to the direction we have to boost to return to the "actual" frame that the particle "a" is in. If we are already in the "a" particle rest frame, then there is no preferred direction and the solid angle may be replaced with "4π".

5 Body Phase Space

As an example, consider the decay of a scalar particle to 5 scalars, 4 of which are massless, with momenta k_J, k_1, k_2, k_3, k_4 respectively. (We are considering scalars so that there are no preferred directions except the relative orientation of the final particle momenta.) We chain the phase space in the order described in figure 6.4

$$
\begin{aligned}
R_5 &= \int_0^{(M_0-M_J)^2} dm_4^2 \int_0^{m_4^2} dm_3^2 \int_0^{m_3^2} dm_2^2 \times \\
&\qquad R_2\left[k_0 \to p_4 k_J\right] \cdot R_2\left[p_4 \to p_3 k_4\right] \cdot R_2\left[p_3 \to p_2 k_3\right] \cdot R_2\left[p_2 \to k_1 k_2\right] \\
&= \int_0^{(M_0-M_J)^2} dm_4^2 \int_0^{m_4^2} dm_3^2 \int_0^{m_3^2} dm_2^2 \, \frac{\lambda^{1/2}(M_0^2, m_4^2, M_J^2)}{8M_0^2} d\Omega_4^* \\
&\qquad \cdot \frac{\lambda^{1/2}(m_4^2, m_3^2, 0)}{8m_4^2} d\Omega_3^* \cdot \frac{\lambda^{1/2}(m_3^2, m_2^2, 0)}{8m_3^2} d\Omega_2^* \cdot \frac{\lambda^{1/2}(m_2^2, 0, 0)}{8m_2^2} d\Omega_1^*
\end{aligned}
$$

Now note that the angle Ω_4 just describes the overall orientation of the decay products in the initial particle rest frame. No physical quantity can depend on it. Similarly, writing:

$$
d\Omega_3 = d(\cos\theta_3) d\phi_3 \tag{6.21}
$$

we note that the angle "ϕ_3" describes the azimuthal orientation of all of the massless particles about the massive particle momentum axis; again no physical quantity can depend on this. Thus the three variables Ω_4^*, ϕ_3 may be integrated immediately, to obtain:

$$
\begin{aligned}
R_5 &= \left(\frac{4\pi}{8}\right)^4 \int_0^{(M_0-M_J)^2} dm_4^2 \int_0^{m_4^2} dm_3^2 \int_0^{m_3^2} dm_2^2 \, \lambda^{1/2}(M_0^2, m_4^2, M_J^2)/M_0^2 \\
&\qquad \left(1 - \frac{m_3^2}{m_4^2}\right)\left(1 - \frac{m_2^2}{m_3^2}\right) \frac{d(\cos\theta_3)}{2} \frac{d\Omega_2^*}{4\pi} \frac{d\Omega_1^*}{4\pi} \\
&= \left(\frac{\pi}{2}\right)^4 M_0^6 \int_0^{(1-M_J)^2} d\hat{m}_4^2 \int_0^{\hat{m}_4^2} d\hat{m}_3^2 \int_0^{\hat{m}_3^2} d\hat{m}_2^2 \, \lambda^{1/2}(1, \hat{m}_4^2, \hat{M}_J^2) \\
&\qquad \left(1 - \frac{\hat{m}_3^2}{\hat{m}_4^2}\right)\left(1 - \frac{\hat{m}_2^2}{\hat{m}_3^2}\right) \frac{d(\cos\theta_3)}{2} \cdot \frac{d\Omega_2^*}{4\pi} \cdot \frac{d\Omega_1^*}{4\pi}
\end{aligned} \tag{6.22}
$$

The 5 body phase space was initially an integral over $(3)^5 - 4 = 11$ variables, but three of the integrations were trivial, so that our final formula is an 8-dimensional integral. In general, n-body phase space is an integral over a set of dimension:

$$
\begin{aligned}
\textit{polarized to polarized}: &\quad 3^n - 4 &= 3^n - 4 \\
\textit{unpolarized to polarized}: &\quad 3^n - 4 - 2 &= 3^n - 6 \\
\textit{unpolarized to unpolarized}: &\quad 3^n - 4 - 3 &= 3^n - 7
\end{aligned}
$$

since the triviality of first solid angle integral follows from the un-polarized nature of the decaying particle, and the triviality of the azimuthal angle integral relies on the un-polarized nature of all the final particles.

Lastly, I present formulae to reconstruct the particle four-momenta from the integration variables:

$$m_2^2, m_3^2, m_4^2, \cos\theta_3, \Omega_2^*, \Omega_1^*$$

for the case of one massive and four massless particles in the final state. The method is to work along the decay chain from the initial particle to the final massless particles "1" and "2".

$$\begin{aligned}
k_0 &= M_0 \begin{pmatrix} 1 \\ 0 \\ 0 \\ 0 \end{pmatrix} \\
p_4 &= m_4 L(\varphi_4) \begin{pmatrix} 1 \\ 0 \\ 0 \\ 0 \end{pmatrix} \\
p_3 &= m_3 L(\varphi_4)\,[R_{xz}(\theta_3^*)L(\varphi_{43})] \begin{pmatrix} 1 \\ 0 \\ 0 \\ 0 \end{pmatrix} \\
p_2 &= m_2 L(\varphi_4)\,[R_{xz}(\theta_3^*)L(\varphi_{13})]\,[R_{xy}(\phi_2^*)R_{zx}(\theta_2^*)L(\varphi_{32})] \begin{pmatrix} 1 \\ 0 \\ 0 \\ 0 \end{pmatrix} \\
k_1 &= \frac{m_2}{2} L(\varphi_4)\,[R_{xz}(\theta_3^*)L(\varphi_{43})]\,[R_{xy}(\phi_2^*)R_{zx}(\theta_2^*)L(\varphi_{32})]\,[R_{xy}(\phi_1^*)R_{zx}(\theta_1^*)] \begin{pmatrix} 1 \\ 0 \\ 0 \\ 1 \end{pmatrix}
\end{aligned}$$

where:

$$\begin{aligned}
L(\varphi) &= \begin{bmatrix} \cosh\varphi & 0 & 0 & \sinh\varphi \\ 0 & 1 & 0 & 0 \\ 0 & 0 & 1 & 0 \\ \sinh\varphi & 0 & 0 & \cosh\varphi \end{bmatrix} \\
R_{xz}(\theta) &= \begin{bmatrix} 1 & 0 & 0 & 0 \\ 0 & \cos\theta & 0 & \sin\theta \\ 0 & 0 & 1 & 0 \\ 0 & -\sin\theta & 0 & \cos\theta \end{bmatrix} \\
R_{xy}(\theta) &= \begin{bmatrix} 1 & 0 & 0 & 0 \\ 0 & \cos\phi & \sin\phi & 0 \\ 0 & 0 & 1 & 0 \\ 0 & -\sin\phi & \cos\phi & 0 \\ 0 & 0 & 0 & 1 \end{bmatrix}
\end{aligned}$$

$$
\begin{aligned}
\cosh\varphi_4 &= \gamma_4 = \frac{M_0^2 + m_4^2 - M_J^2}{2M_0 m_4} \\
\cosh\varphi_{43} &= \frac{m_4^2 + m_3^2}{2m_4 m_3} \\
\cosh\varphi_{32} &= \frac{m_3^2 + m_2^2}{2m_3 m_2}
\end{aligned}
$$

These formulae correspond to the definitions:

- θ_k^* is the polar angle in the "$k+1$" rest frame between the momentum vector $\vec{p}_k$ and the axis along which we must boost this frame to reach the "true" "$k+1$" frame.

- ϕ_k^* is the azimuthal angle in the "$k+1$" rest frame of the momentum vector $\vec{p}_k$ with respect to the plane defined by the "$k+2$" momentum vector as viewed in this frame and the axis along which we must boost this frame to reach the "true" "$k+1$" frame.

Chapter 7

$\Upsilon \longrightarrow \chi_1 ggg$

We now turn to the calculation of inclusive rate $\Upsilon \rightarrow \chi_1 X$ as discussed in section 4.3.2, where χ_1 is the ${}^3P_1$ c-$\bar{c}$ bound state. We will find that the lowest order perturbative Q.C.D. description of this width is the decay $\Upsilon \rightarrow \chi_1 ggg$, and is of order α_s^5. This will follow from the fact that vector mesons must couple to at least 3 gluons, while the even charge parity χ_1 state can couple to two gluons (one of the gluons must be off-shell to avoid the constraint of Yangs theorem [76], discussed below).

Till now, I have only presented the rules for computing Feynman diagrams containing vector mesons. Below we shall first review the analogous rules for L=1, S=1 ${}^3P_1$ states. We shall then discuss the hadronic widths of such states, for which the situation is complicated somewhat due to an infra-red type logarithmic divergence of the width for the process ${}^3P_1 \rightarrow q\bar{q}g$ with respect to the quark binding energy. Finally, we will estimate the $\Upsilon \rightarrow \chi_1 ggg$ rate, and thus the width for J/ψ production in Υ decay through this channel.

7.1 Feynman Rules for ${}^3P_1$ States

Following the discussion of section 4.3.2, we first present the wave function of an axial vector, ${}^3P_1$, state, derived in appendix B.4:

$$\Upsilon(x_1, x_2) = \sqrt{\frac{1}{2EV}} \cdot \frac{\psi'(0)}{\sqrt{M}} \cdot \left[2iM\not{\epsilon}\gamma_5 + P_\alpha \epsilon_\beta \varepsilon^{\alpha\beta\mu\nu} \cdot (\not{p}_q + m_q)\gamma^\nu \cdot \frac{\partial}{\partial t^\mu}\right]_{t=0} \times e^{-i(P/2+t)\, x_1} e^{-i(P/2-t)\, x_2} \tag{7.1}$$

where I have made the definitions:

$$\psi'(0) \equiv \sqrt{\frac{3}{8\pi}}\frac{1}{M}\left.\frac{dR(r)}{dr}\right|_{r=0}$$
$$p_q = \frac{1}{2}P$$
$$m_q = \frac{1}{2}M$$

where "P", "ϵ"and "M" are the meson four-momentum, polarization, and mass, and "t" is an arbitrary four-vector. Processes involving P-wave mesons are proportional to the derivative of the radial wave function at the origin, for reasons discussed in the appendix B, chiefly stemming from the fact that the wave function of $L = 1$ states vanishes at the origin.

The analogue of equation 4.16 for the S-matrix becomes:

$$S = (2\pi)^4\delta^4(\Sigma p)\cdot\left[\prod_{all}\sqrt{\frac{1}{2EV}}\right]\cdot\left[\prod_{^3S_1}\frac{\psi(0)}{\sqrt{M}}\right]\cdot\left[\prod_{^3P_1}\frac{\psi'(0)}{\sqrt{M}}\right]\cdot A_q \quad (7.2)$$

where the invariant amplitude "A_q" is calculated according to the previous rules of section 4.3.3, with the following additional rules for the $^3P_1$ vertices:

1. The quark and anti-quark comprising the axial vector bound state are given momentum $\frac{1}{2}P \pm t$.

2. The amplitude "$M_q(t)$" for the process is calculated by applying the usual Feynman diagram rules, with the exception that no "u" or "v" spinors are written for the quark and anti-quark coming from the axial vector meson.

3. $M_q(0)$ and $\partial M_q(0)/\partial t^\mu$ are computed; the amplitude is then given by:

$$A = 2iM\cdot tr\{M_q(0)\not{\epsilon}\gamma_5\} + P_\alpha\epsilon_\beta\varepsilon^{\alpha\beta\mu\nu}\cdot tr\{\frac{\partial M_q(0)}{\partial t^\mu}(\not{p}_q + m_q)\gamma_\nu\}$$

$^3P_1$ Decay to Two Gluons

I illustrate this process with the example of an axial vector meson decaying to two possibly off-shell photons (to avoid the complications of color factors for the moment). This is discussed in reference [65]. We will use the results of this analysis later in sections 7 2, 7.3.

The two diagrams for the decay are shown in figure 7.1. We have:

$$M_q(t) = e^2\left[\gamma^\rho\frac{1}{\not{p}_q + \not{t} - \not{k}_a - m_q}\gamma^\eta + \gamma^\eta\frac{1}{-\not{p}_q + \not{t} + \not{k}_a - m_q}\gamma^\rho\right]$$

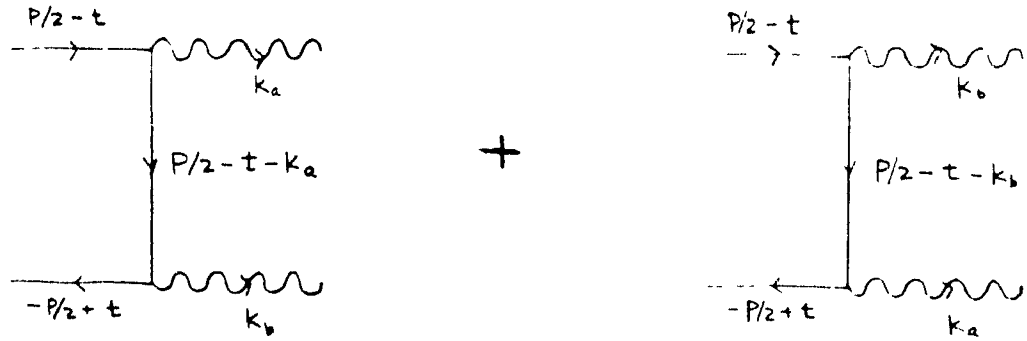

Figure 7.1: Coupling of a $^3P_1$ state to two photons

After lengthy manipulation, and by discarding pieces with a $(-\not{p}_q + m_q)$ factor on the left or a $(\not{p}_q + m_q)$ factor on the right (which it is readily seen vanish in the above trace):

$$
\begin{aligned}
M_q(0) &= e^2 \cdot \left[\gamma^\rho \gamma^\eta \not{k}_a - \not{k}_a \gamma^\rho \gamma^\eta\right] / p_1 \\
\left.\frac{\partial M_q(t)}{\partial t^\mu}\right|_{t=0} &= e^2 \cdot \left[\gamma^\rho \frac{1}{\not{p}_q - \not{k}_a - m_q} \gamma^\mu \frac{1}{\not{p}_q - \not{k}_a - m_q} \gamma^\eta \right. \\
&\quad \left. + \gamma^\eta \frac{1}{-\not{p}_q + \not{k}_a - m_q} \gamma^\mu \frac{1}{-\not{p}_q + \not{k}_a - m_q} \gamma^\rho \right] \\
&= e^2 \cdot \left[(k_a \cdot k_b) g^{\mu\rho} \gamma^\eta - k_a^\mu \left(g^{\rho\eta} \not{p}_b + k_b^\rho \gamma^\eta - k_a^\eta \gamma^\rho\right)\right] / p_1^2 \\
p_1 &= (P/2 - k_a)^2 - m_q^2
\end{aligned}
$$

Inserting this into the formula for the complete amplitude, we obtain the simple expression:

$$A = 4e^2 \cdot \epsilon_\alpha \varepsilon^{\rho\eta\alpha\beta} \left[k_a^2 k_b + k_b^2 k_a\right]^\beta / p_1^2 \tag{7.3}$$

Note that the part proportional to $1/p_1$ has disappeared. We see that the for both gluons on-shell, i.e. for $k_a^2 = k_b^2 = 0$, the amplitude vanishes This is an example on Yang's theorem [76]: a spin-one particle cannot decay to two identical massless spin-one particles.

7.2 Hadronic Width of the χ_1

As discussed in section 4.2 1, the inclusive hadronic width is estimated in perturbative Q.C.D by computing the transition rate of the χ_1 to the color singlet quark and gluon state to which it couples at lowest order. Were it not for Yang's theorem, this would be the $|gg>$ state at order α_s^2. The transition of a χ_1 to two gluons does not violate charge parity Indeed, we saw in the last section that if one or both of the gluons is off shell, the transition rate is non-zero. However, both the gluons in the $|gg>$ state are *on-shell* so we must proceed to states coupling at higher order

The χ_1 can couple to both the $|ggg>$ and $|q\bar{q}g>$ state, at order α_s^3. Now it turns out that the transition to the $|q\bar{q}g>$ state has a problem: it diverges if we assume, as we have all along, that the mass of the quarks in the χ_1 is one half of the χ_1 mass. The origin of this divergence lies in the fact that the formula 7.3 for the χ_1-g^*-g amplitude is proportional to:

$$\frac{1}{\left[(P/2-k_g)^2-m_q^2\right]^2} = \frac{4}{M^2}\cdot\frac{1}{[E_g-b/2]^2}$$

$$b = M-2m_q$$

where k_g is the four-momentum of the radiated gluon in the $|q\bar{q}g>$ state, and "b" is essentially the binding energy of the meson. In the integral over the three body phase space, this factor generates a whopping infra-red type divergence at the point $E_g=0$, if we set $b=0$. Quark current symmetries and charge-parity identities soften this divergence, but the final result is that the decay rate is proportional to:

$$\int\frac{dE_g}{E_g-b} \sim \log(b)$$

The arguments of section 5.3 2 that rule out such infra-red divergences break down here because the next lowest order amplitude is *not* zero because of charge symmetry arguments, but instead because of Yang's theorem. For similar reasons, this divergence does not disappear when the contributions of soft bremstrahlung diagrams is included The logarithmic dependence on the binding energy has a physical origin, which is similar to that of the lamb shift in the hydrogen atom [77].

This problem was first noted in reference [77], where the contribution to the χ_1 width from both the $|ggg>$ and $|q\bar{q}g>$ states was computed. The authors found that the decay to the $|ggg>$ does not have a similar divergence problem. They also found, speaking in the context of an expansion in the binding energy "b", that the leading contribution to the decay width is given by:

$$\Gamma(\chi_1\to q\bar{q}g) = \frac{n_f}{3}\frac{2^{10}}{9}\cdot\alpha_s^3|\psi'(0)|^2\cdot\frac{1}{M_\chi^2}\cdot\log\left[\frac{M_\chi}{2b}\right] \qquad (7.4)$$

where "n_f" is the number of light quark flavours. The non-leading parts of the decay to $|q\bar{q}g>$ and the contribution of the decay to $|ggg>$ are presumably negligible, though no precise statement of their size is given in reference [77]

We will find, numerically, a similar divergence in our estimate of the the $\Upsilon \to \chi_1 ggg$ rate. When we normalize the branching ratio to the χ_1 width, however, the dependence on the binding energy "b" will essentially disappear, the logarithmic dependence in our rate and that in the hadronic width will cancel. We now turn to the estimate of $\Gamma(\Upsilon \to \chi_1 ggg)$.

7.3 Decay Rate

The formula for the spin averaged, and color and spin summed, decay rate of an Υ to a χ_1 plus three gluons follows from equation 7.2:

$$d\Gamma = \frac{1}{3!}\frac{1}{2J_\Upsilon + 1}\frac{1}{2M_\Upsilon}\frac{|\psi_\Upsilon(0)|^2}{M_\Upsilon}\frac{|\psi'_\chi(0)|^2}{M_\chi}\sum_{col,pol}|A_q|^2 d_4(LIPS) \tag{7.5}$$

where the first factor is the symmetry factor associated with the three identical gluons, and A_q is the quark level invariant amplitude calculated with the rules of section 7.1.

In appendix 6.5 we discussed multi-body phase space. Four body phase space has dimension 5, and may be co-ordinatized with a subset of the variables we used in the five body decay of chapter 6. Doing so, we obtain:

$$d_4(LIPS) \;=\; \frac{1}{(2\pi)^8}\left(\frac{\pi}{2}\right)^3 M_\Upsilon^4 \int d^5r \tag{7.6}$$

The boundaries of the integration region may also be taken explicitly from the five body formulae.

We now extract the color factor, coupling constants, and powers of the quark mass to define the dimensionless quantity $\hat{M}_q$:

$$A_q \;=\; g_s^5 \cdot F_c^{abc} \cdot \frac{1}{m_0^3} \cdot \hat{M}_q \tag{7.7}$$

Note that the color factor is now a function of three octet labels, one for each gluon. We will see that:

$$F_c^{abc} \;=\; \frac{1}{6}d_{abc} \tag{7.8}$$

and using the identities of appendix A:

$$F_c^2 \;\equiv\; \sum_{abc}\left[F_c^{abc}\right]^2 \;=\; \frac{2\cdot 5}{3^3} \tag{7.9}$$

Returning to the decay rate, we have:

$$\Gamma = \frac{8}{9} \cdot F_c^2 \alpha_s^5 \cdot \frac{|\psi_\Upsilon(0)|^2 |\psi'_\chi(0)|^2}{M_J M_\Upsilon^4} \int d^5 r \sum_{pol} |\hat{M}_q|^2 \tag{7.10}$$

We now express the branching ratio in a fashion similar to that in sections 5.1 and 6.1.1, towards the goal of eliminating the unknown parameters. However, in this case "α_s" will appear in our final formula, due to the fact that the χ_1 hadronic width is proportional to an extra power of α_s with respect to the $\chi_1 \to gg^*$ rate:

$$\begin{aligned}\frac{\Gamma(\Upsilon \to \chi_1 ggg)}{\Gamma_\Upsilon} &= \frac{\Gamma(\Upsilon \to \chi_1 ggg)\Gamma_\chi}{\Gamma(\Upsilon \to ggg)\Gamma(\chi_1 \to q\bar{q}g)} \cdot \frac{\Gamma(\Upsilon \to ggg)}{\Gamma_\Upsilon} \cdot \frac{\Gamma(\chi_1 \to q\bar{q}g)}{\Gamma_\chi} \\ &= B_\Upsilon^{(had)} B_{\chi_1}^{(had)} \cdot \frac{F_c^2}{2^8 c_1 \alpha_s} \cdot \frac{M_\chi \Gamma_\chi}{M_\Upsilon^2} \cdot \int d^5 r \sum_{pol} |\hat{M}_q|^2 \Big/ \log\left[\frac{M_\chi}{2b}\right]\end{aligned} \tag{7.11}$$

where c_1 is given in equation 5.10. The amplitudes A_q are computed numerically for each helicity set as described in section 6.1.2 of the $\Upsilon \to J/\psi gggg$ decay.

7.4 Feynman Diagrams

The lowest order Feynman diagrams contributing to $\Upsilon \to \chi_1 ggg$ are of order g_s^5. This follows from the fact that vector mesons must couple to at least three gluons, while the axial vector can couple to just two if one or more of them is off-shell, as discussed in sections 4.4.2 and 7.2.

There are a total of 36 Feynman diagrams contributing to this process. 6 of these are depicted in figure 7.2. The label "a", for example, is short for "p_a, ϵ_a, a", respectively the particle momentum, polarization, and octet color label. To each of these 6 diagrams must be added the 5 graphs obtained by permuting the three labels $\{a, b, c\}$.

To these 6 diagrams correspond the 6 amplitudes:

$$\begin{bmatrix} A_1 & A_2 & A_3 \\ A_4 & A_5 & A_6 \end{bmatrix}$$

Using the notation $A_k^{a\leftrightarrow b}$ as in section 6.2, and the usual techniques of charge conjugation, we obtain:

$$\begin{aligned} A_1 + A_3 + A_4 + A_6 &= \\ \left(\frac{1}{\sqrt{3}}\right)^2 &\sum_e \left[tr\{T_c T_e\} + tr\{T_e T_c\}\right] \cdot \left[tr\{T_b T_a T_e\} + tr\{T_e T_a T_b\}\right] \cdot M_1 \\ &= \frac{1}{6} d_{abc} M_1 \quad \equiv \quad F_c^{abc} M_1 \end{aligned} \tag{7.12}$$

and:

$$A_2 + A_4 + (A_2 + A_4)^{a\leftrightarrow b} = F_c^{abc} M_2$$

$$\begin{aligned}
M_1 &= g_s^5 J_{01\,\mu} J_f^\mu / s_{ab} \\
M_2 &= g_s^5 J_{02\,\mu} J_f^\mu / s_{ab} \\
s_{ab} &= (2k_0 - k_a - k_b)^2 = (2k_f + k_c)^2 \\
J_f^\mu &= \frac{2s_{ab} \cdot \varepsilon^\mu_{\ \nu\alpha\beta} \epsilon_f^\nu k_c^\alpha \epsilon_c^\beta}{[2k_f \cdot k_c - m_f b/2]^2}
\end{aligned}$$

where J_f comes essentially from equation 7.3, and J_{01} and J_{02} are given exactly as in section 6.2 (Usually this is not the case — though similarly denoted, the currents "J" differ from section to section.) Introducing the quantity:

$$\begin{aligned}
M_{(ab)c} &= M_1 + M_1^{a\leftrightarrow b} + M_2 \\
&= g_s^5 \left(J_{01} + \tilde{J}_{01} + J_{02} \right)^\mu J_{f\,\mu} / s_{ab} \qquad (7.13)
\end{aligned}$$

and distributing the numbers $\{1,2,3\}$ over the labels $\{a,b,c\}$ we finally obtain:

$$A_q = F_c^{abc} \left[M_{(12)3} + M_{(23)1} + M_{(31)2} \right] \qquad (7.14)$$

7.5 Results

Recall equation 7.11 for the branching ratio:

$$\begin{aligned}
Br(\Upsilon \to \chi_1 ggg) &= B_\Upsilon^{(had)} B_{\chi_1}^{(had)} \cdot \frac{F_c^2}{2^8 c_1 \alpha_s} \cdot \frac{M_{\chi_1}\Gamma_{\chi_1}}{M_\Upsilon^2} < |\hat{M}_q^2| > \\
< |\hat{M}_q^2| > &\equiv \sum_{pol} \int d^5 r |\hat{M}_q|^2 \Big/ \log\left[\frac{M_\chi}{2b}\right] \qquad (7.15)
\end{aligned}$$

$\hat{M}_q$ is given in equations 7.7 and 7.14, and the color factor in equation 7.9. We require the following data:

$$\begin{aligned}
M_{\chi_1} &= 3.51\,GeV \\
\Gamma_{\chi_1} &\leq (1.3 \times 10^{-3})\,GeV \\
B_{\chi_1}^{(had)} &= 0.73 \pm 0.02
\end{aligned}$$

All this data is from reference [46]. $B_{\chi_1}^{(had)}$ is obtained by subtracting the branching ratio for the mode $\chi_1 \to J/\psi\gamma$ from "1" and neglecting all other observed decay modes, whose branching ratios are of order 10^{-3}. As we can see, Γ_{χ_1} is

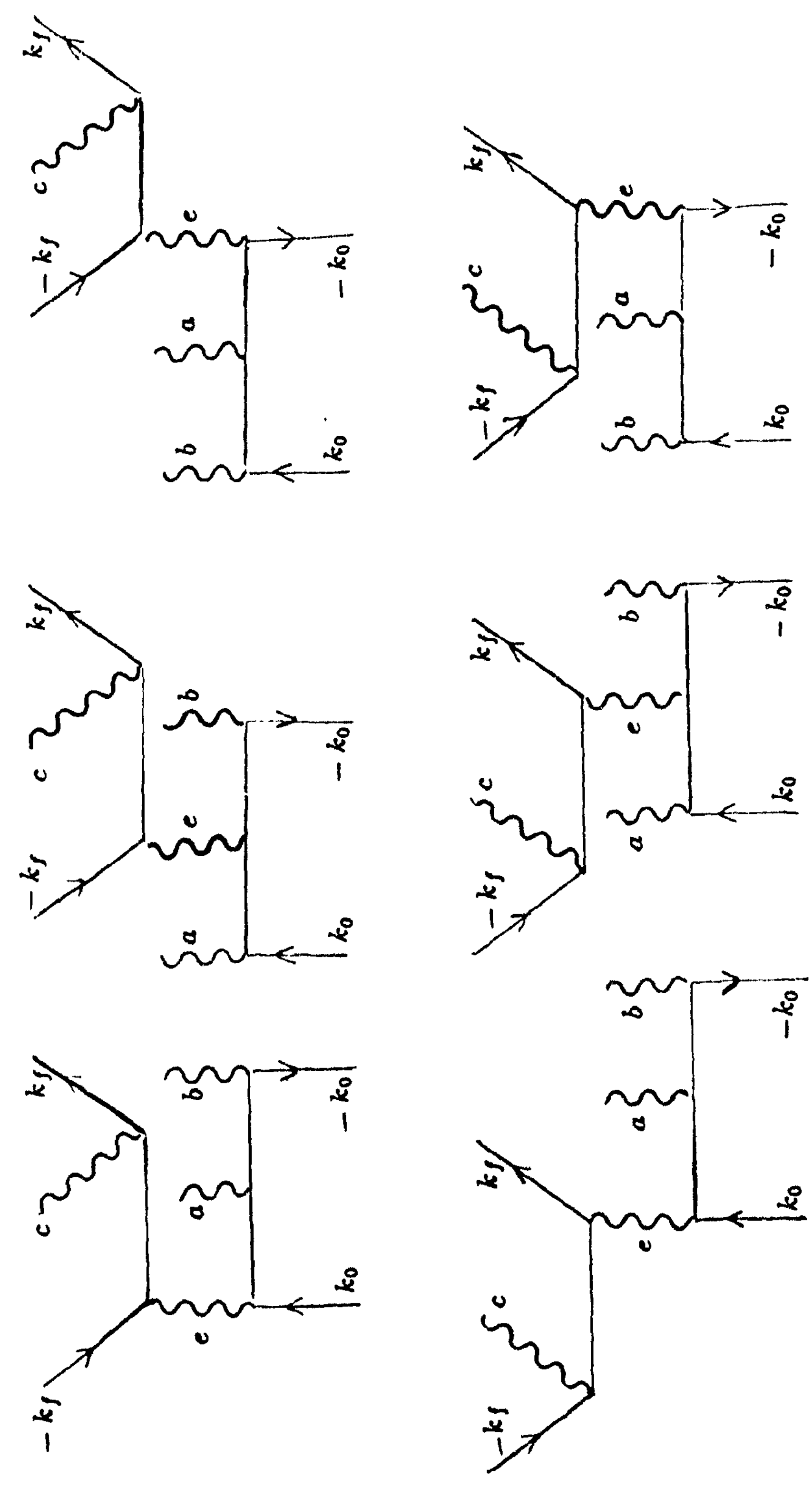

Figure 7.2: 6 of the 36 diagrams for the decay $\Upsilon \to \chi_1 ggg$

not known. However, we expect it to be of the order of the upper limit quoted, since the widths of χ_0 and χ_2 are $14\,MeV$ and $2.6\,MeV$ respectively. The other information necessary for the evaluation of the branching ratio may be found in section 5.5. We obtain:

$$Br(\Upsilon \rightarrow \chi_1 ggg) \;\; \leq \;\; (0.278 \times 10^{-8}) \; < |\hat{M}_q^2| >$$

where I have not included errors, since the dominant source of error is in the χ_1 total width which is not yet known. The phase space integral is performed using VEGAS [74], with the result:

$$< |\hat{M}_q^2| > = \; 5.93 \times 10^4 \tag{7.16}$$

Note that this is a function of the binding energy $b = M_{\chi_1} - 2m_q$ both through $\hat{M}_q$ and through the explicit logarithmic factor in the definition 7.15. The quoted number was obtained by using the naive, Bohr model, estimate for the binding energy:

$$b \; = \; \alpha_s^2 m_q$$

In fact the value of $< |\hat{M}_q^2| >$, and thus the branching ratio, is essentially independent of the value of "b". This may be seen from figure 7.3, where the ratio $Br(\Upsilon \rightarrow \chi_1)(b)/Br(\Upsilon \rightarrow \chi_1)(\alpha_s^2 m_q)$ has been plotted. Note that we expect "b" to be small if our assumption of non relativistic motion is to be valid, and we can see that for $(b/m_q) < .2$ the plot is essentially flat.

In fact, the "b" independence of the branching ratio was one of the reasons that the form 7.11 was employed, despite present ignorance of the total χ_1 width. This independence tells us that our decay rate, $\Gamma(\Upsilon \rightarrow \chi_1 ggg)$, contains the same logarithmic divergence with respect to "b" that $\Gamma(\chi_1 \rightarrow q\bar{q}g)$ has. This in turns leads us to expect that an analytic formula in the small "b" limit might be easily obtained. Such considerations are topics for further study.

Finally, we have:

$$Br(\Upsilon \rightarrow \chi_1 ggg) \;\; \leq \;\; 0.165 \times 10^{-3} \tag{7.17}$$

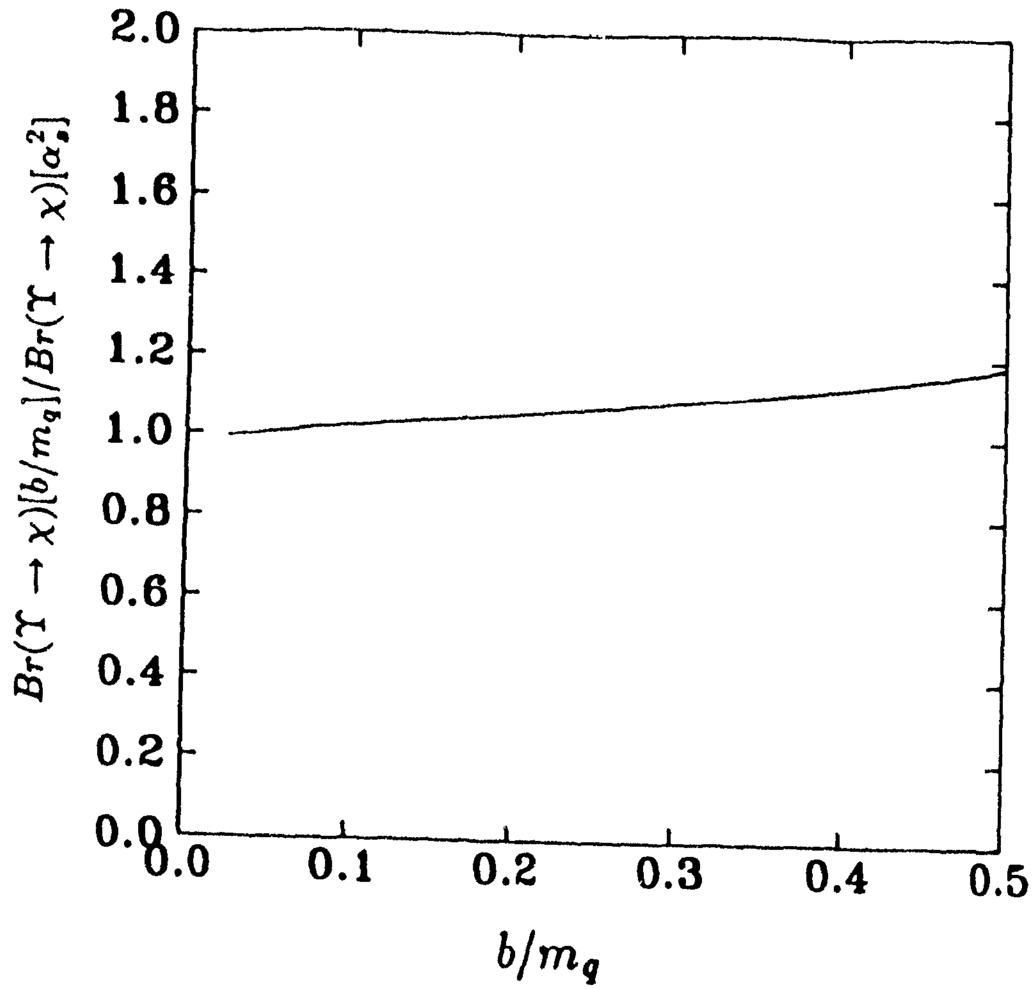

Figure 7.3: $Br(\Upsilon \to \chi_1 ggg)$ as a function of b, normalized to its value at $b = \alpha_s^2$

Chapter 8

Summary

8.1 Direct $\Upsilon \to J/\psi X$ Decay Width

The branching ratio for the "direct" transition (i.e. not through a resonance) of the Υ to J/ψ is obtained simply by adding the results of sections 5.5 and 6.3.

$$\begin{aligned} Br(\Upsilon \to J/\psi X)\Big|_{dir} &\equiv Br(\Upsilon \to J/\psi gg) + Br(\Upsilon \to J/\psi gggg) \\ &= (0.248 \pm 0.065) \pm 10^{-3} \end{aligned} \tag{8.1}$$

To obtain the quoted error, we do not add the errors of the individual results. This is because the error in the separate results originates from uncertainty in the same combination of experimental observables.

$$Br_{\Upsilon}^{(had)} \cdot Br_{J}^{(had)} \cdot \Gamma_J$$

Consider the following approach for computing the decay width. We could have worked directly from equation 5.9, manually inserting the values for the wave-functions-at-the-origin and the strong coupling, as determined from the leptonic widths (see section B.5) and the hadronic widths respectively. The error in the leptonic width (and thus $|\psi(0)|^2$) is typically 10%, while from reference [57] we have.

$$\alpha_s = 0.175 \pm 0.015$$

from various Υ inclusive decay widths, so that the error on α_s is about 8%. (Actually, this reference compared α_s as determined from many sources, so that the error on α_s as computed purely from the hadronic width is slightly smaller, about 4%.) Since our rate is proportional to α_s^6, the final error obtained using this method ends up being about the same as that quoted above.

When we turn to the decay to ψ' in the next section, we will see that the latter approach is in fact the preferable one, due to the uncertainty to which its width, etc. is known.

8.2 $\Gamma(\Upsilon \to \psi' X)$

We now use the results of chapters 5 and 6 to compute the rate of ψ' production in Υ decay. The formulae of those chapters are valid for any final vector meson, not just the J/ψ. Thus no further Feynman diagrams need to be evaluated to compute $\Gamma(\Upsilon \to \psi' gg)$ and $\Gamma(\Upsilon \to \psi' gggg)$. We only need to replace the parameters M_J, Γ_J, and $Br_J^{(had)}$ with their appropriate values for the ψ'. Recall equations 5.11 and 6.6 for decays to J/ψ:

$$
\begin{aligned}
Br(\Upsilon \to J/\psi gg) &= B_\Upsilon^{(had)} B_J^{(had)} \cdot \frac{F_c^2}{3\pi c_1^2} \cdot \frac{M_J \Gamma_J}{M_\Upsilon^2} \cdot \int dx_1\, dx_2 \sum_{pol} |\hat{M}_{q,3}|^2 \\
Br(\Upsilon \to J gggg) &= B_\Upsilon^{(had)} B_J^{(had)} \cdot \frac{F_c^2}{18\pi c_1^2} \cdot \frac{M_J \Gamma_J}{M_\Upsilon^2} \cdot \int d^8 r \sum_{pol} |\hat{M}_{q,5}|^2 \quad (8.2)
\end{aligned}
$$

The two integrals change by only small amounts under the replacement $M_J \to M_{\psi'}$. Thus the branching ratio for ψ' production in Υ decay may be simply obtained from the J/ψ results:

$$
Br(\Upsilon \to \psi' X) = \frac{M_{\psi'}}{M_J} \cdot \frac{\Gamma_{\psi'}}{\Gamma_J} \cdot \frac{Br_{\psi'}^{(had)}}{Br_J^{(had)}} \cdot Br(\Upsilon \to J/\psi X)\Big|_{dir} \qquad (8.3)
$$

The branching ratio $Br_{\psi'}^{(had)}$ may be deduced from information in the Particle Data Book by subtracting from "1" the branching fractions for the following modes:

- $\psi' \to J/\psi\gamma$;
- $\psi' \to \chi_k\gamma$, $k = 1, 2, 3$;
- $\psi' \to \gamma^* \to X$

which are the dominant decay modes not proceeding through three gluons. Using this method, and quoting the values of the other parameters:

$$
\begin{aligned}
M_{\psi'} &= 3.69\, GeV \\
\Gamma_{\psi'} &= (243 \pm 43) \times 10^{-6}\, GeV \\
Br_{\psi'}^{(had)} &= 0.163 \pm 0.098 \qquad (8.4)
\end{aligned}
$$

we obtain:

$$
Br(\Upsilon \to \psi' gg + \psi' gggg) = 1.11 \cdot Br(\Upsilon \to J/\psi X)\Big|_{dir}
$$

Note that I do not include the error on the proportionality factor, because they are quite large, and because when I present the final result it will have been computed working directly from expressions like 5.9 as discussed at the end of the last section. The preceeding discussion was included to point out that we can conclude fairly generally that there are about as many ψ' mesons being produced in Υ decays as there are J/ψ mesons, as one would expect.

Finally, working directly from the formulae 5.9 and 6.5, using α_s from [57] and $|\psi(0)|^2$ as determined from $\psi' \to l^+l^-$ (see section B.5) and recomputing the above integrals at the ψ' mass, we have:

$$Br(\Upsilon \to \psi' gg + \psi' gggg) = (0.263 \pm 0.126) \times 10^{-3} \tag{8.5}$$

8.3 Final Results

In sections 7.5 and 8.2 we have seen:

$$\begin{aligned} Br(\Upsilon \to \chi_1 ggg) &\leq 0.165 \times 10^{-3} \\ Br(\Upsilon \to \psi' gg + \psi' gggg) &= (0.263 \pm 0.126) \times 10^{-3} \end{aligned}$$

Recalling the equations 4.13 and 4.14:

$$\begin{aligned} Br(\psi' \to J/\psi X) &= (55 \pm 7)\% \\ Br(\chi_1 \to J/\psi \gamma) &= (27.3 \pm 1.6)\% \end{aligned}$$

and equation 4.5 we finally obtain:

$$\begin{aligned} Br(\Upsilon \to J/\psi X)\Big|_{dir} &= (0.248 \pm 0.065) \times 10^{-3} \\ Br(\Upsilon \to \psi' \to J/\psi X) &= (0.145 \pm 0.088) \times 10^{-3} \\ Br(\Upsilon \to \chi_1 \to J/\psi X) &\leq 0.045 \times 10^{-3} \end{aligned} \tag{8.6}$$

Thus, for a χ_1 width equal to its upper bound, we obtain for the production of J/ψ via these 3 mechanisms:

$$Br(\Upsilon \to J/\psi X) = (0.438 \pm 0.153) \times 10^{-3}$$

Note that there is also an additional uncertainty of 20% in this predicted result, coming from the fact that the above number only represents the first term in a perturbation series in $\alpha_s \sim 0.2$

This is to be compared with the experimental result [56]:

$$Br(\Upsilon \to J/\psi X) = (1.1 \pm 0.4 \pm 0.2) \times 10^{-3}$$

where the first error is statistical and the second is systematic

Evidently, these two numbers agree to within one standard deviation, if we add the statistical and systematic in the experimental result. If instead we combine the two errors in quadrature, obtaining an effective error of ± 0.45, then the prediction lies below the one sigma limit by 0.06. This is within the uncertainty of the perturbation expansion. Alternately, a combination of other modes such as $\Upsilon \to \chi_2 \to J/\psi X$ or $\Upsilon \to \eta_b \to J/\psi X$ might make up this small (10%) amount.

8.4 Comments

The agreement between the theory and experiment is reasonable but not overwhelming: if we consider only the central values of these results, the perturbative Q.C D prediction is too small by over a factor of two We expected agreement to within $\alpha_s \approx 20\%$. Never the less, as discussed above, the errors on both the experimental and theoretical results are still too large to draw any definitive conclusions concerning the inadequacy of applying perturbative Q C D. to meson transitions at this scale. Interpreting the result optimistically, we could conclude that in fact this calculation represents another sucess of the model.

The approach I have adopted of working with the ratios like 5 11 and 7 11 has the following advantage. Intuitively, these combinations may be less sensitive to radiative corrections than if we had worked directly with the quantities α_s and $|\psi(0)|^2$ as discussed in section 8 2 Looking at the various Feynman diagrams for our process, the effect of adding an extra gluon is often to produce a radiatively-corrected hadronic decay diagram for one of the external mesons in a part of the new diagram.

The central value of the result 8 7 corresponds to the value of α_s as determined from the inclusive hadronic width of the Υ, which is $\alpha_s = 0.175$. Now suppose we had worked directly with α_s and $|\psi(0)|^2$, as described above, and left α_s a free parameter, essentially using the J/ψ experimental result to *deduce* α_s. Since the dominant contributions to the theoretical prediction are proportional to α_s^6, this means that α_s is given by

$$\left(\frac{\alpha_s}{0\ 175}\right)^6 = \frac{1.1 \pm 0\ 4}{0.45} = 2.45 \pm 0.89$$

using only the statistical uncertainty in the experimental result. Thus:

$$0.188 < \alpha_s < 0.214$$

This is to be compared with α_s as determined in a general survey of many inclusive Υ decay widths [57]:

$$\alpha_s = 0.175 \pm 0.015$$

Again, these results just overlap, and more so if the systematic error is combined with the statistical error. Again, improvement in the accuracy of the experimental data is required to draw any definite conclusions about the validity of perturbative Q.C.D in this transition between mesons

Finally, the decay through the χ_2 should also be considered. Though its branching ratio to J/ψ is smaller than that of the χ_1, it has more helicity states to sum over, and its hadronic width is somewhat larger. Thus it could contribute as much as or more that the χ_1, which constituted a 10% effect. This and a more detailed error analysis is currently underway.

Appendix A

Color Identities

A.1 $\sum d^2 = 40/3$

The purpose of this section is to prove the identity.

$$\sum_{abc} d_{abc} d_{abc} = \frac{40}{3}$$

for the group SU(3).

I proceed generally. Let "T_a" denote the $N^2 - 1$ generators of SU(N) in the fundamental or defining representation. These matrices, plus the unit, form a basis for the space of $N \times N$ special unitary matrices. A statement of this property is:

$$(T_a)_{ij}(T_b)_{mn} = \frac{1}{2}\left[\delta_{in}\delta_{jm} - \frac{1}{N}\delta_{ij}\delta_{mn}\right] \tag{A.1}$$

This identity does not follow from the stucture contants of the group, it is valid only for the fundamental representation.

Note the following SU(N) relations and definitions:

$$\begin{aligned} tr\{T_a T_b\} &= \frac{1}{2}\delta_{ab} \\ [T_a, T_b] &\equiv i \sum_c f_{abc} T_c \\ [T_a, T_b]_+ &\equiv \frac{1}{N}\delta_{ab} + \sum_c d_{abc} T_c \end{aligned}$$

From these we obtain:

$$\begin{aligned} d_{abc} &= 2 \cdot tr\{T_a\,[T_b, T_c]_+\} \\ \sum_a T_a^2 &= \frac{N^2 - 1}{2N} \end{aligned}$$

Now we have:

$$\begin{aligned}
\sum_{abc}(d_{abc})^2 &= 4\sum_{abc} tr\{T_a[T_b,T_c]_+\}\cdot tr\{T_a[T_b,T_c]_+\} \\
&= 8\sum_{abc}(T_a)_{ij}(T_a)_{mn}\,[T_bT_c+T_cT_b]_{ji}\,(T_bT_c)_{nm} \\
&= 4\sum_{bc}\left[\delta_{in}\delta_{jm}-\frac{1}{N}\delta_{ij}\delta_{mn}\right][T_bT_c+T_cT_b]_{ji}\,(T_bT_c)_{nm} \\
&= 4\sum_{bc}\left[tr\{T_bT_cT_bT_c\}+tr\{T_b^2T_c^2\}-\frac{2}{N}tr\{T_bT_c\}^2\right] \\
&= 4\sum_{bc}tr\{T_bT_cT_bT_c\}+4N\left[\frac{N^2-1}{2N}\right]^2-2\frac{N^2-1}{N}
\end{aligned}$$

Note that:

$$\begin{aligned}
\sum_c tr\{T_bT_cT_bT_c\} &= \sum_c(T_b)_{ij}(T_c)_{jk}(T_b)_{kl}(T_c)_{li} \\
&= \frac{1}{2}\left[\delta_{ji}\delta_{kl}-\frac{1}{N}\delta_{jk}\delta_{li}\right](T_b)_{ij}(T_b)_{kl} \\
&= \frac{-1}{2N}tr\{T_b^2\} = \frac{-1}{4N}
\end{aligned}$$

Thus:

$$\begin{aligned}
\sum_{abc}(d_{abc})^2 &= -\frac{N^2-1}{N}+\frac{(N^2-1)^2}{N}-2\frac{N^2-1}{N} \\
&= \frac{(N^2-1)(N^2-4)}{N}
\end{aligned}$$

Substituting N=3 in this yields the desired result.

Other results

From this basic identity follows:

$$\sum_{ef} d_{aef}d_{bef} = \frac{5}{3}\delta_{ab}$$

and:

$$\begin{aligned}
\sum_{abcd}\left[\sum_e d_{abe}d_{cde}\right]^2 &= \sum_{abcdef} d_{abe}d_{cde}d_{abf}d_{cdf} \\
&= \left[\frac{5}{3}\right]^2\sum_{ef}\delta_{ef} = \frac{8\cdot 5^2}{3^2}
\end{aligned}$$

Appendix B

Appendix: Bound State Wave Functions

Herein I will derive a covariant expression of the Schrödinger wave function of a non-relativistic bound-state, used in sections 4.3.3 and 7.1 to deduce the rules for the construction of the invariant amplitude and S-matrix. Note that we require such covariant formulae in our study because the J/ψ or χ_1 mesons are in general produced with with large velocities, it is only in their rest frame that they look non-relativistic.

Throughout this section we will be using "Bjorken-Drell" spinors $u(p,\sigma)$ which satisfy.

$$\overline{u}u = 1 \qquad u^{\dagger}u = \gamma \tag{B.1}$$

These are the most convenient here because of their simple form in the particle rest frame:

$$u \longrightarrow \begin{pmatrix} \chi \\ 0 \end{pmatrix}$$

in the Dirac representation.

B.1 Normalization

Recall one [45] description of a single fermion state:

$$\psi = N\, u(p,\sigma)e^{ip\cdot x}. \tag{B.2}$$

I wish to discuss the normalization of this state carefully, to establish a method for the more complicated task of normalizing the bound state later.

Suppose the fermion is part of some process taking place in a box of volume "V". The probability of finding the electron somewhere in the box must be unity:

$$\int d^3x\psi^\dagger\psi = N^2 \cdot V \cdot \gamma = N^2 \cdot V \frac{E}{m}$$

$$\psi = \sqrt{\frac{m}{EV}}\, u(p,\sigma)\, e^{ip\,x} \qquad \text{(B.3)}$$

Let us now deduce that same formula by first going to a frame where the electron is at rest. The wave function there reads:

$$\psi_r = N_r \begin{pmatrix} \chi \\ 0 \end{pmatrix} e^{ip\,x} \qquad \text{(B.4)}$$

since $(\chi, 0)$ is the non-relativistic limit of a Bjorken-Drell normalized spinor. To what size box should we confine the fermion in its rest frame, such that it is naturally confined to a box of volume "V" when we return to the frame in which the whole experiment is taking place? The answer is "$V_r = \gamma V$", in order to offset the contraction the volume will experience in the boost to the lab frame. Thus:

$$\int d^3x\psi_r^\dagger\psi_r = N_r^2 \cdot V_r = N_r^2 \cdot V\gamma \qquad \text{(B.5)}$$

which yields the same answer as we obtained before.

Next, suppose we have a fermion – anti-fermion bound state (meson) moving at some velocity in the same box of volume "V". We want the probability of observing this object in this box to be exactly one. In contrast to the single particle case, we will proceed immediately to the bound state rest frame, where as above we must choose the confinement volume V_r to be.

$$V_r = \gamma V$$

Now I will present the Schrödinger wave function of two non-relativistic fermions in a box of volume V_r. For the moment, we will ignore the details of how the orbital and spin parts of the wave function are combined to produce a state of total angular momentum. However, we *will* combine the fermion and anti-fermion spins into a state of total spin 1. This is because the two cases we are going to consider, vector and axial-vector mesons, both are $S = 1$ states. The properly normalized bound state wave function is:

$$\Upsilon(\vec{x}_1, \vec{x}_2, t) = \sqrt{\frac{1}{V_r}}\psi(\vec{r}) \cdot e^{-i(2m-E_B)} \cdot S^{1,k} \qquad \text{(B.6)}$$

$$S^{1,k} = (1,k|\sigma_1,\sigma_2)\,\chi^{(\sigma_1)} \otimes \chi^{(\sigma_2)}$$

$$\int d\vec{r}|\psi(\vec{r})|^2 = 1$$

where $E_B \ll m$ is the binding energy and $\chi^{(\sigma)}$ is a Pauli two-spinor. Note also that we are using "cartesian" labels for the different spin one polarization states: $k = 1, 2, 3$.

This formula has only one factor of $V^{-1/2}$ (as opposed to the two that a generic two fermion wave packet type state would have). This is just what we need to make the S-matrix scale with the volume as if the meson where a single particle. In essence, scaling up the volume only changes the probability density of one of the fermions, because the position of the other is correlated to the first by the wave function.

B.2 Covariant Wave Function

Introducing "$\vec{t}$", the relative momentum of the constituents, and $\phi(\vec{t})$, the associated probability amplitude distribution function:

$$\begin{aligned} \psi(\vec{r}) &\equiv \int \frac{d\vec{t}}{(2\pi)^{3/2}} \phi(\vec{t}) e^{-i\vec{t}\cdot\vec{r}} \\ \int d\vec{t} |\phi(\vec{t})|^2 &= \int d\vec{r} |\psi(\vec{r})|^2 = 1 \end{aligned} \quad \text{(B.7)}$$

we have the following identity ($f(\vec{t})$ arbitrary):

$$\begin{aligned} \int \frac{d\vec{t}}{(2\pi)^{3/2}} \phi(\vec{t}) f(\vec{t}) &= \int \frac{d\vec{t}}{(2\pi)^{3/2}} \phi(\vec{t}) \left\{ f(0) + t_m \frac{\partial}{\partial t_m} f \bigg|_{\vec{t}=0} + \ldots \right\} \\ &= \psi(0) \cdot f(0) + \frac{\partial \psi}{\partial r_m}\bigg|_{\vec{r}=0} \cdot \frac{\partial f}{\partial t_m}\bigg|_{\vec{t}=0} + O\left(\frac{< t^2 >}{m_q^2} \right) \end{aligned} \quad \text{(B.8)}$$

This expansion is a good approximation to the extent that $\phi(\vec{t})$ is small for large $|\vec{t}|$. In fact, the assertion that the bound state is non relativistic is equivalent to the statement:

$$\sqrt{< \vec{t}^2 >} \ll m_q$$

For non-relativistic bound states the average momentum is typically αm, where "α" is the fine structure constant characterizing the strength of the binding interaction. Thus this approximation is just as valid as those we make in the our perturbative evaluations of the transition amplitudes.

Equation B.6 becomes:

$$\begin{aligned} \Upsilon(\vec{x}_1, \vec{x}_2, t) &= \sqrt{\frac{1}{V_r}} \cdot e^{-i(2m-E_B)t} \int \frac{d\vec{t}}{(2\pi)^{3/2}} \phi(\vec{t}) e^{-i\vec{t}\cdot\vec{r}} \cdot S^{1,\lambda} \\ &= \sqrt{\frac{1}{\gamma V}} \cdot e^{-iP\cdot(x_1+x_2)} \int \frac{d\vec{t}}{(2\pi)^{3/2}} \phi(\vec{t}) \cdot e^{-it\cdot(x_1-x_2)} \cdot S^{1,\lambda} \\ &= \sqrt{\frac{1}{\gamma V}} \int \frac{d\vec{t}}{(2\pi)^{3/2}} \phi(\vec{t}) \cdot e^{-i(P/2+t)\cdot x_1} e^{-i(P/2-t)\cdot x_2} \cdot S^{1,\lambda} \end{aligned} \quad \text{(B.9)}$$

where I have defined:

$$
\begin{aligned}
x_k &= (t, \vec{x}_k) \\
P &= (2m_0 - E_b, 0) \\
t^\mu &= (0, \vec{t})^\mu
\end{aligned}
$$

This is almost a covariant expression describing two particles with four-momenta $P/2 \pm t$. What remains is to identify which lorentz covariant will reduce to the Pauli-spinor factor $S^{1,k}$. The Pauli-spinor corresponding to the fermion we replace in the fashion:

$$
\chi^{(\sigma_1)} \longrightarrow u(P/2 + t, \sigma_1) \tag{B.10}
$$

The other two-spinor describes an anti-fermion which is leaving the interaction region (and entering the bound-state) so we set:

$$
\chi^{(\sigma_2)} \longrightarrow \overline{v}(P/2 - t, \sigma_2) \tag{B.11}
$$

Note that we now have relative momentum dependence $\vec{t}$ in the spinor part of the wave function. Thus we have embodied some of the effects of spin-orbit coupling (more accurately spin dependence of the Hamiltonian) which are typically put in "by hand" in the non-relativistic theory. These are also the same effects that arise naturally in the Foldy-Wouthuysan momentum expansion of the Dirac equation in a background field. We will see the effects of this dependence when study the axial vector, P-wave states.

Now recall the identities [78]:

$$
\begin{aligned}
u(p) &= e^{-\varphi v \cdot \vec{\alpha}/2} u(0) = \frac{\not{p} + m}{\sqrt{2m(E+m)}} u(0) \\
\overline{v}(p) &= \overline{v}(0) \frac{-\not{p} + m}{\sqrt{2m(E+m)}} \\
u(0) &= \begin{pmatrix} \chi \\ 0 \end{pmatrix} \qquad v(0) = \begin{pmatrix} 0 \\ \chi \end{pmatrix}
\end{aligned}
$$

Thus $S^{1,k}$ can be written as the limit of the covariant:

$$
\begin{aligned}
S^{1,k} \quad \rightarrow \quad \tilde{S}^{1,k} &= (1, k|\sigma_1, \sigma_2)\, u(P/2 + t, \sigma_1) \overline{v}(P/2 - t, \sigma_2) \\
&= (1, k|\sigma_1, \sigma_2) \frac{\left(\frac{1}{2}\not{P} + \not{t} + m_q\right) u(0, \sigma_1) \overline{v}(0, \sigma_2) \left(-\frac{1}{2}\not{P} + \not{t} + m_q\right)}{2m_q(E_q + m_q)} \\
E_q &= \sqrt{m_q^2 + \vec{t}^2} = m_q + O(\vec{t}^2) \\
m_q &= \frac{1}{2} M
\end{aligned} \tag{B.12}
$$

The Clebsch-Gordon sum is most easily reduced by momentarily using the Dirac representation for "γ^μ" matrices:

$$\begin{aligned}
(1,k|\sigma_1,\sigma_2)u(0,\sigma_1)\bar{v}(0,\sigma_2) &= (1,k|\sigma_1,\sigma_2)\begin{pmatrix}\chi^{(\sigma_1)}\\ 0\end{pmatrix}\begin{pmatrix}\chi^{(\sigma_2)\dagger} & 0\end{pmatrix} \\
&= (1,k|\sigma_1,\sigma_2)\begin{pmatrix}0 & \chi^{(\sigma_1)}\chi^{(\sigma_2)\dagger}\\ 0 & 0\end{pmatrix} \\
&= \frac{1}{\sqrt{2}}\begin{pmatrix}0 & \sigma^k\\ 0 & 0\end{pmatrix} \\
&= \frac{1}{\sqrt{2}}\begin{pmatrix}1 & 0\\ 0 & 0\end{pmatrix}\begin{pmatrix}0 & \sigma_k\\ -\sigma^k & 0\end{pmatrix} \\
&= \frac{1+\gamma^0}{2\sqrt{2}}\gamma^k \qquad k = 1,2,3 \qquad \text{(B.13)}
\end{aligned}$$

Thus $\tilde{S}^{1,k}$ becomes, to order "$\vec{t}$":

$$\begin{aligned}
\tilde{S}^{1,k} &= \frac{1}{4}\left(1+\gamma^0+\not{t}/m_q\right)\left[\frac{1+\gamma^0}{2\sqrt{2}}\gamma^k\right]\left(1-\gamma^0+\not{t}/m_q\right) \\
&= \left[\frac{1+\gamma^0}{2\sqrt{2}}\gamma^k\right] + \frac{1}{M}\left[\not{t}\frac{1+\gamma^0}{2\sqrt{2}}\gamma^k + \frac{1+\gamma^0}{2\sqrt{2}}\gamma^k\not{t}\right] + O(\vec{t}^2) \\
&= \left[\frac{1+\gamma^0}{2\sqrt{2}}\gamma^k\right] + \frac{1}{\sqrt{2}M}\left[t^k+\gamma^0\sigma^{k\mu}t_\mu\right] + O(\vec{t}^2) \\
\sigma^{\mu\nu} &\equiv \frac{1}{2}\left[\gamma^\mu,\gamma^\nu\right] \qquad \text{(B.14)}
\end{aligned}$$

We now return to formula B.9 for the wave function:

$$\begin{aligned}
\Upsilon(x_1,x_2) = {} & \sqrt{\frac{1}{2EV}}\cdot\frac{1}{\sqrt{M}}\int\frac{d\vec{t}}{(2\pi)^{3/2}}\phi(\vec{t}) \\
& \times\left\{\left[(\not{p}_q+m_q)\gamma^k + t^k + \gamma^0\sigma^{k\mu}t_\mu\right]\cdot e^{-i(P/2+t)\cdot x_1}e^{-i(P/2-t)\cdot x_2}\right\}
\end{aligned}$$

up to terms or order $< \vec{t}^2 > /m_q^2$

Till now we have been ignoring the Clebsch-Gordan factors that couple any orbital angular momentum the state might have with its total spin to put the bound state in an eigenstate of total angular momentum. Introducing such labels on the relative position wave function:

$$\begin{aligned}
\psi(\vec{r}) &\equiv \psi_{L,\jmath}(\vec{r}) \\
\phi_{L,\jmath}(\vec{t}) &\equiv \int\frac{d\vec{t}}{(2\pi)^{3/2}}\psi_{L,\jmath}(\vec{r})e^{i\vec{t}\cdot\vec{r}}
\end{aligned}$$

the final formula for the bound state wave function becomes:

$$\Upsilon^{J,\imath}(x_1,x_2) = \sqrt{\frac{1}{2EV}}\cdot\frac{1}{\sqrt{M}}\cdot(J,\imath|L,\jmath;1,k)\int\frac{d\vec{t}}{(2\pi)^{3/2}}\phi_{L,\jmath}(\vec{t})$$

$$\times\left\{\left[(\not{p}_q + m_q)\gamma^k + t^k + \gamma^0\sigma^{k\mu}t_\mu\right]\cdot e^{-i(P/2+t)\cdot x_1}e^{-i(P/2-t)\cdot x_2}\right\} \quad (B.15)$$

We now turn to using equation B.8 to simplify this formula, eliminating the relative momentum wave function of which we have no knowledge, by expanding it to lowest order in $\vec{t}$.

B.3 Vector Bound States

The vector mesons are total spin S=1, relative orbital angular momentum L=0, total angular momentum J=1 bound states, denoted in spectroscopic notation by $^3S_1$. The Clebsch-Gordan factors which combine the orbital and total quark spin are trivial. The relative position wave function of such states does not vanish at the origin. Thus the leading term of formula B.8 will suffice to expand and simplify equation B.15 for the bound state wave function (Note that we introduce a (cartesian) three-vector ϵ_m to specify the polarization state of the total angular momentum of the meson):

$$\Upsilon(x_1, x_2) = \sqrt{\frac{1}{2EV}}\cdot\frac{\psi(0)}{\sqrt{M}}\cdot(\not{p}_q + m_q)\not{\epsilon}\cdot e^{-iP\cdot x_1/2}e^{-iP\cdot x_2/2} \quad (B.16)$$

where:

$$\epsilon^\mu = (0, \vec{\epsilon}) \quad (B.17)$$

This expression is fully covariant and, though we have been working exclusively in the bound state rest frame, its form in any other frame is now trivially obtained.

B.4 Axial Vector Bound States

Axial vector mesons are total spin S=1, relative orbital angular momentum L=1, total angular momentum J=1 bound states, denoted in spectroscopic notation by $^3P_1$ The Clebsch-Gordon factor which combines two spin-1's into another spin-1 is essentially the three-index Levi-Civita tensor:

$$\varepsilon^{ijk} = \varepsilon^{0ijk} = \frac{1}{M}P_\mu\varepsilon^{\mu ijk} \quad (B.18)$$

where the last equality follows because we are still in the meson rest frame. The relative position wave function of these L=1 states vanishes at the origin. Thus we must go beyond the leading term of formula B.8 to simplify equation B.15. To this end consider:

$$\left.\frac{\partial\psi_{1,j}}{\partial r_m}\right|_{\vec{r}=0} = \left.\frac{\partial}{\partial r_m}\right|_{\vec{r}=0}\left\{\sqrt{\frac{3}{8\pi}}Y_{1j}(\theta,\phi)R(r)\right\}$$

$$
\begin{aligned}
&= \sqrt{\frac{3}{8\pi}}\frac{\partial}{\partial r_m}\left\{r_j\frac{R(r)}{r}\right\}_{\vec{r}=0} \\
&= \sqrt{\frac{3}{8\pi}}\left\{\delta_{jm}\frac{R(r)}{r} + r_j\left[\frac{R'(r)}{r} - \frac{R(r)}{r^2}\right]\frac{\partial r}{\partial r_m}\right\}_{\vec{r}=0} \\
&= \sqrt{\frac{3}{8\pi}}R'(0)\cdot\delta_{jm} + 0
\end{aligned}
\tag{B 19}
$$

Thus, using ϵ as in equation B 17 to denote the meson polarization:

$$
\begin{aligned}
\Upsilon(x_1, x_2) = & \sqrt{\frac{1}{2EV}}\cdot\sqrt{\frac{3}{8\pi}}\frac{R'(0)}{M\sqrt{M}}\cdot P_\alpha\epsilon_\beta\varepsilon^{\alpha\beta\mu\nu}\left.\frac{\partial}{\partial t_\mu}\right|_{t=0}\cdot \\
& \left\{e^{-i(P/2+t)\cdot x_1}e^{-i(P/2-t)\cdot x_2}\left[(\not{p}_q + m_q)\gamma_\nu + t_\nu + \gamma^0\sigma_{\nu\eta}t^\eta\right]\right\}
\end{aligned}
$$

Noting that:

$$
\begin{aligned}
P_\alpha\epsilon_\beta\varepsilon^{\alpha\beta\mu\nu}\gamma^0\sigma_{\nu\mu} &= 2i P_\alpha\epsilon_\beta\gamma^0\sigma^{\alpha\beta}\gamma_5 \\
&= 2i\gamma^0\not{P}\not{\epsilon}\gamma_5 = 2iM\not{\epsilon}\gamma_5
\end{aligned}
\tag{B 20}
$$

We finally obtain the standard form for the wave function of a ${}^3P_1$ state:

$$
\begin{aligned}
\Upsilon(x_1, x_2) = & \sqrt{\frac{1}{2EV}}\cdot\sqrt{\frac{3}{8\pi}}\frac{R'(0)}{M\sqrt{M}}\cdot \\
& \left[2iM\not{\epsilon}\gamma_5 + P_\alpha\epsilon_\beta\varepsilon^{\alpha\beta\mu\nu}\cdot(\not{p}_q + m_q)\gamma^\nu\cdot\frac{\partial}{\partial t^\mu}\right]_{t=0}\times e^{-i(P/2+t)\cdot x_1}e^{-i(P/2-t)\cdot x_2}
\end{aligned}
\tag{B 21}
$$

This is now in a fully covariant form.

B.5 Wave Functions at the Origin

The final formulae each contain an unknown: $\psi(0)$ or $R'(0)$, respectively the value of the relative position wave function of the two quarks and the derivative of its radial part, evaluated at the origin. We must specify the values of these to complete our discussion of the meson wave function.

It is in principle possible to calculate $\psi(0)$ and $R'(0)$ using some potential model. However, rather than introduce the new set of assumptions associated with a another model, what is usually done is to think of $\psi(0)$ and $R'(0)$ as free parameters. Each parameter is then chosen such that the perturbative Q.C.D prediction of one meson transition agrees with experiment. The lowest order perturbative Q.C.D prediction of the leptonic widths of mesons contains no unknown parameters other than the wave-function-at-origin factors, so these are the transitions usually used. For example, the decay of a vector to a lepton-anti-lepton pair is given by [63]:

$$\Gamma(V \to l^+l^-) \;=\; 16\pi \cdot Q^2\alpha_{em}^2 \cdot \frac{|\psi(0)|^2}{M_V^2} \tag{B.22}$$

where "Q" is the quark charge in units of "ϵ". Similar formulae can be derived for the decay of pseudoscalar or P-wave states into two photons.

Bibliography

[1] S.Weinberg, Phys. Rev. Lett. **19**, 1264 (1967); A. Salam, in Elementary Particle Theory: Relativistic Groups and Analyticity (Nobel Symposium 8), ed. N. Svartholm (Almqvist and Wiksell, Stockholm, 1968), S Glashow, J. Iliopoulos and L Maiani, Phys. Rev. **D2**, 1285 (1970).

[2] D. Gross and F. Wilczek, Phys Rev. Lett. **30**,, 1343 (1973); H D Politzer Phys. Rev. Lett. **30**, 1346 (1973), S. Weinberg, Phys Rev Lett. **31**, 494 (1973).

[3] C.N. Yang and R.L. Mills, Phys Rev. **96**, 191 (1954).

[4] P.W. Higgs, Phys. Lett. **12**, 132 (1964), and Phys. Rev. Lett **13**, 508 (1964), and Phys. Rev. **145**, 1156 (1966); F. Englert and R. Brout, Phys Rev. Lett. **13**, 321 (1964), G S. Guralnik, C.R Hagan, and T.W B Kibble, Phys. Rev. Lett **13**, 585 (1964).

[5] S. L. Adler and W. A. Bardeen, Phys. Rev. **182**, 1517 (1969).

[6] H. Georgi and S. Glashow, Phys. Rev. **D6**, 429, (1972); D. J. Gross and R. Jackiw Phys. Rev **D6**, 477 (1972); C Bouchiat, J. Iliopoulos and P Meyer, Phys. Lett. **38B**, (1972).

[7] G.L. Kane, in Proceedings of the Eighteenth SLAC Summer Institute on Particle Physics (July 1990), ed. E. Brennan, SLAC Report No. 378 (1990)

[8] V. Barger, W.Y Keung, R.N. and Phillips, Phys. Rev. **D24**, 1328 (1981)

[9] H. Georgi, Weak Interactions and Modern Particle Theory (The Benjamin/Cummings Publishing Company, Inc., Don Mills, Ontario, 1984).

[10] V. Barger and S Pakvasa, Phys. Lett. **81B**, 195 (1979), G L Kane and M. Peskin. Nucl. Phys. **B195**, 29 (1982).

[11] Cleo Collaboration, Phys. Rev. **D35**, 3733 (1987).

[12] D.Horn and and G.G. Ross, Phys. Lett. **67B**, 460 (1977); M. Perl et al , Phys. Lett. **70B**, 487 (1977).

[13] S. Glashow and S. Weinberg, Phys. Rev. **D15**, 1958 (1977).

[14] E. Ma, Phys. Rev. Lett. **57**, 535 (1986).

[15] S. Pakvasa, D Roy, and S U.Sankar, Phys. Rev. **D42**, 3160 (1990).

[16] C. Itzykson and J. Zuber, Quantum Field Theory (McGraw-Hill Inc., Montreal, 1980).

[17] G. G. Ross, Grand Unified Theories, (Benjamin/Cummings Publishing Co., Inc., New York 1984).

[18] M. Dine and J. Sapirstein, Phys. Rev. Lett. **43**, 668 (1979).

[19] ALEPH Collaboration, D.Decamp *et al.*, Phys. Lett. **B244**, 551 (1990).

[20] F. Halzen and A D. Martin, Quarks and Leptons (John Wiley & Sons, Toronto 1984).

[21] J. H. Kühn and P.M. Zerwas, Phys. Rep. **167**, 321 (1988).

[22] L3 Collaboration, B. Adeva *et al.*, Phys. Lett. **B241**, 416 (1990).

[23] AMY Collaboration, KEK preprint 89-38, AMY 89-04, July 1989; TASSO Collaboration, DESY 90-047, May 1990; JADE Collaboration, DESY 89-127, Oct. 1989; CELLO Collaboration, DESY 89-125, Oct. 1989. Quoted result is from the last reference.

[24] M. Kobayashi and T. Maskawa, Prog. Theor. Phys. **49**, 652 (1973).

[25] S. Dawson, K. Ellis, and P. Naso, Nucl. Phys. **B237**, 49 (1989); Errata Nucl. Phys. **B335**, 260, (1990)

[26] CDF Collaboration, L. Pondrom, in Proceedings of the 25th *International Conference on High Energy Physics*, Singapore, August 1990 (to be published)

[27] G. L. Kane, Proceedings of the Madison Workshop, "Could Higgs Bosons Be Found Before LEP", 1979.

[28] A.D. Martin, W.J. Stirling, and R.G Roberts, Phys. Lett. **207B**, 205 (1988).

[29] B. W. Lee, C. Quigg, and H. Thacker, Phys. Rev. **D16**, 1519 (1977).

[30] T. Appelquist and J. Carazzone, Phys. Rev. **D11**, 2856 (1975).

[31] J. Bernabéu, A. Pich and A. Santamaria, Phys. Lett **200B**, 569 (1988), A.A. Akhundov, D.Yu Bardin and T Riemann, Nucl Phys **B276**, 1 (1986), W. Beenakker and W. Hollik, Z. Phys **C40**, 141 (1988); B W. Lynn and R.G. Stuart Phys Lett **252B**, 676 (1990), J Bernabéu, A Pich and A Santamaria, Nucl. Phys **B363**, 326 (1991);

[32] M. B. Einhorn, D. R T. Jones, and M. Veltman, Nucl. Phys **B191**, 146 (1981).

[33] P. Sikivie, L. Susskind, M. Voloshin, H.Zakharov, Nucl. Phys. **B173**,, 189 (1980).

[34] K. Fujikawa, B. W. Lee, and A. I. Sanda, Phys. Rev **D6**, 2923 (1972)

[35] G. 't Hooft Nucl. Phys **B33**, 173 (1971).

[36] L3 Collarboration, CERN PPE 91-32 (1991).

[37] M. Veltman, Acta Physica Polonica, **B8**, 475 (1977), M. Veltman, Nucl. Phys. **B123**,, 89 (1977).

[38] J. L. Rosner, Phys. Rev. **D42**, 3107 (1990).

[39] J. Ellis and G. L. Fogli Phys. Lett **249B**, 543 (1990).

[40] B A. Irwin, B. Margolis, and H. Trottier, Phys. Lett **256B**, 533 (1991).

[41] E. Eichten, I. Hinchliffe, K. Lane, C. Quigg, Rev. Mod. Phys. **56**, 579 (1984).

[42] M. Strassler and M. Peskin, Phys. Rev. **D43**, 1500 (1991)

[43] A. Sirlin, Phys. Rev. **D22**, 971 (1980).

[44] K. Inoue, A. Kakuto, H. Komatsu, and S. Takeshita, Prog Theor. Phys **64**, 1008 (1980); D. Albert, W. J. Marciano, D. Wyler, and Z Parsa, Nucl Phys **B166**, 460 (1980).

[45] J. D. Bjorken and S. D. Drell, Relativistic Quantum Mechanics (McGraw Hill, New York 1964).

[46] Particle Data Group, Phys. Lett. **239B**, (1990).

[47] M.E. Peskin, in Proceedings of the Seventeenth SLAC Summer Institute on Particle Physics (July 1989), ed J. Hawthorne, SLAC Report No 361 (1989).

[48] M. Chanowitz and M.K.Gaillard, Nucl. Phys **B261**, 379 (1985), Z. Kunszt and D. E. Soper, Nucl. Phys. **B296**, 253 (1988).

[49] T. Cheng and L. Li, Gauge Theory of Elementary Particle Physics (Oxford University Press, New York 1984).

[50] K. Aoki, Z. Hioki, R. Kawabe, M. Konuma, and T. Muta, Sup. of the Prog. Theor. Phys., No. **73** (1982).

[51] M. Jezabek and J. H. Kuhn, Nucl. Phys. **B314**, 1 (1989); Nucl. Phys. **B320**, 20 (1989).

[52] G. Eilam, R. R. Mendel, R. R. Migneron, and A. Soni, Phys. Rev. Lett. **66**, 3105 (1991).

[53] A. Denner and T. Sack, Nucl. Phys. **B358,**, 46 (1991).

[54] C.-P. Yuan and T. C. Yuan, University of California at Santa Cruz preprint, SCIPP-91-10 (June 1991).

[55] J. Liu and Y.-P. Yao, University of Michigan preprint, UM-TH-90-11 (1990).

[56] CLEO Collaboration, Phys. Lett. **224B**, 445 (1989).

[57] W. Kwong, P. Mackenzie, R. Rosenfeld, and J. L. Rosner, Phys. Rev. **D37**, 3210 (1988).

[58] V. A. Novikov, L. B. Okun, M. A. Shifman, A.I. Vainshtein, M. B. Voloshin, and V. I. Zakharov, Phys. Rep. **41C** 1 (1978).

[59] B. A. Irwin, B. Margolis, and H. D. Trottier, Phys. Rev. **D42**, 1577 (1990).

[60] J. Alexander et al., Phys. Rev. Lett. **64**, 2226 (1990).

[61] D. Atwood, A. Soni, and D. Wyler, Phys. Rev. Lett. **65**, 2335 (1990).

[62] J. M. Jauch and F. Rohrlich, The Theory of Photons and Electrons (Springer-Verlag, Ney York 1956).

[63] R. Van Royen and V. F. Weisskopf, Il Nuovo Cimento **50A**, 617 (1967).

[64] F. E. Close, An Introduction to Quarks and Partons (Academic Press, New York 1979).

[65] J. H. Kuhn, J. Kaplan, and E. G. O. Safiani, Nucl. Phys. **B157**, 125 (1979).

[66] F. Wilczek, Phys. Rev. Lett. **39**, 1304 (1977).

[67] V. Barger, E. Glover, K. Hikasa, W. Keung, M. Olssen, C. Suchyta III, and X. Tata, Phys. Rev. **D35**, 3366 (1987).

[68] H. Fritzsch and K. H. Streng, Phys. Lett. **77B**, 299 (1978); I. I. Y. Bigi and S. Nussinov, Phys. Lett. **82B** 281 (1979).

[69] P. Franzini, et. al., Phys Rev. **35**, 2883 (1987).

[70] T. Muta, Foundations of Quantum Chromodynamics: An Introduction to Perturbative Methods in Gauge Theories (World Scientific, Singapore, 1987).

[71] E Byckling and K Kajantie, Particle Kinematics (John Wiley & Sons, New York 1973).

[72] REDUCE Users Manual, Version 3.3, Anthony C. Hearn, The Rand Corporation, Santa Monica CA (1987).

[73] K. Atkinson, An Introduction to Numerical Analysis (John Wiley & Sons, New York 1978).

[74] G. P. Lepage, J. Comput. Phys. **27**, 192 (1978).

[75] T. Kinoshita, ed., Quantum Electrodynamics (World Scientific, Singapore 1990).

[76] C.N. Yang Phys. Rev. **77**, 242 (1950).

[77] R. Barbieri, R. Gatto, and E. Remiddi, Phys. Lett. **61B**, 465 (1976).

[78] R. P. Feynman, Theory of Fundamental Processes: a Lecture Note Volume (Benjamin/Cummings Publishing Co., Inc , New York 1961)